**Charles University**

**Faculty of Science**

Study programme: Analytical chemistry

**Mgr. Jaroslava Zavázalová**

# Boron doped diamond and its utilization in electroanalysis of derivatives of aromatic compounds

Borem dopovaný diamant a jeho využití v elektroanalýze derivátů aromatických sloučenin

Doctoral Thesis

Supervisor: RNDr. Karolina Schwarzová, Ph.D.

Consultant: Prof. RNDr. Jiří Barek, CSc.

Prague, 2019

Prohlašuji, že jsem tuto závěrečnou práci zpracovala samostatně a že jsem uvedla všechny použité informační zdroje a literaturu. Tato práce ani její podstatná část nebyla předložena k získání jiného nebo stejného akademického titulu.

Jsem si vědoma toho, že případné využití výsledků, získaných v této práci, mimo Univerzitu Karlovu je možné pouze po písemném souhlasu této univerzity.

I declare that all the results used and published in this doctoral Thesis have been obtained by my own experimental work, and that all the ideas taken from work of others are properly referred to in the text and the literature survey. I am conscious that the prospective use of the results, published in this Thesis, outside the Charles University is possible only with a written agreement of the university.

I also declare that neither this Thesis nor its significant part has been submitted in any form for another degree or diploma at any university or other institution of tertiary education.

Praha

Mgr. Jaroslava Zavázalová

This doctoral Thesis was experimentally carried out at the Charles University, Faculty of Science, Department of Analytical Chemistry, UNESCO Laboratory of Environmental Electrochemistry. The research fellowship in the laboratory of Prof. Dr. Christopher M. A. Brett at the University of Coimbra, Faculty of Science and Technology, Department of Chemistry, Coimbra, Portugal, and in the laboratory of Prof. Dr. Josino Costa Moreira at the National School of Public Health, FIOCRUZ, Rio de Janeiro, Brazil, was also experienced.

Supervisor: RNDr. Karolina Schwarzová, Ph.D.
Department of Analytical Chemistry
Faculty of Science, Charles University

Consultant: Prof. RNDr. Jiří Barek, CSc.
Department of Analytical Chemistry
Faculty of Science, Charles University

# Content

## Abstract

This work is devoted to the study of boron doped diamond as electrode material, its properties and use in electroanalytical methods – in voltammetric and subsequently amperometric methods in combination with high performance liquid chromatography.

The series of boron doped diamond films was tested with respect to the effect of boron concentration on their morphology, quality, electrochemical and spectral properties using scanning electron microscopy, atomic force microscopy, Raman spectroscopy, and cyclic voltammetry and differential pulse voltammetry. Further, the effect of boron concentration on the determination of selected substances was investigated, both for their oxidation (2-aminobiphenyl, benzophenone-3) and for their reduction (5-nitroquinoline).

Furthermore, a voltammetric and amperometric method was developed for the determination of a mixture of aminobiphenyls and aminonaphthalenes using a boron doped diamond electrode.

The effects of activation cleaning programs on the signal of benzophenone-3 were investigated using a boron doped diamond electrode, and the determination of benzophenone-3 on boron doped diamond electrode in the presence of the selected surfactant was studied.

Boron doped diamond as carbon-based material was compared with other selected carbon materials such as glassy carbon and carbon film and their modifications. Their use has been tested for the determination of 1-aminonaphthalene and 2-aminonaphthalene.

## Abstrakt

Tato práce je věnována studiu borem dopovaného diamantu jako elektrodového materiálu, jeho vlastnostem a použití v elektroanalytických metodách – ve voltametrii a následně amperometrii v kombinaci s průtokovou metodou vysokoúčinné kapalinové chromatografie.

Série borem dopovaných diamantových filmů byla testována s ohledem na vliv koncentrace boru na jejich morfologii, kvalitu, elektrochemické a spektrální vlastnosti s použitím skenovací elektronové mikroskopie, mikroskopie atomárních sil, Ramanovy spektroskopie, cyklické voltametrie a diferenční pulsní voltametrie. Dále byl zkoumán vliv koncentrace boru na stanovení vybraných látek, jak jejich oxidací (2-aminobifenyl, benzofenon-3), tak jejich redukcí (5-nitrochinolin).

Dále byla vyvinuta voltametrická a amperometrická metoda pro stanovení směsi aminobifenylů a aminonaftalenů s použitím borem dopované diamantové elektrody.

Byly zkoumány účinky aktivačních čistících programů na signál benzofenonu-3 při použití borem dopované diamantové elektrody a dále stanovení benzofenonu-3 na borem dopované diamantové elektrodě v přítomnosti vybraného surfaktantu.

Borem dopovaný diamant jako materiál na bázi uhlíku byl porovnán s dalšími vybranými uhlíkovými materiály jako skelný uhlík a uhlíkový film a jejich modifikacemi. Jejich použití bylo testováno na stanovení 1-aminonaftalenu a 2-aminonaftalenu.

## Acknowledgement

I would like to acknowledge the support and help of my supervisor RNDr. Karolina Schwarzová, Ph.D., my consultant Prof. RNDr. Jiří Barek, CSc., and all the colleagues from the Department of the analytical chemistry, my partner Martin Horvát, my parents Jiřina and Jaroslav, and all my family.

The financial support of my work was provided by the following sources:

- Charles University (Specific University Research projects SVV);
- Czech Science Foundation (project P206/12/G151);
- European Commission (grant under the Erasmus student exchange programme);
- Fundacao para a Ciencia e a Tecnologia, Portugal (PTDC/QUI-QUI/116091/2009, POCH, POFC-QREN);
- Grant Agency of Charles University (Project GAUK 684213);
- KONTAKT (AMVIS Project YME10004);
- Ministry of Education, Youth, and Sports of the Czech Republic (Project MSM 0021620857).

## Key words

amperometric detection
boron-doped diamond
genotoxic organic compounds
modification of electrode
voltammetry

## Klíčová slova

ampérometrická detekce
borem dopovaný diamant
genotoxické organické sloučeniny
modifikace elektrody
voltametrie

## List of symbols and abbreviations

| | |
|---|---|
| 2-AB | 2-aminobiphenyl |
| 4-AB | 4-aminobiphenyl |
| AFM | atomic force microscopy |
| 1-AN | 1-aminonaphthalene |
| 2-AN | 2-aminonaphthalene |
| BDD | boron doped diamond |
| BP-3 | benzophenone-3 |
| CTAB | cetyltrimethylammonium bromide |
| CVD | chemical vapor deposition |
| $\Delta E_p$ | difference between the anodic and cathodic peak potentials |
| H-terminated | hydrogen-terminated |
| HF-CVD | hot filament chemical vapor deposition |
| HPLC | high performance liquid chromatography |
| HPLC-ED/UV | high performance liquid chromatography with electrochemical detection/UV spectrophotometric detection |
| MP-CVD | microwave plasma chemical vapor deposition |
| 5-NQ | 5-nitroquinoline |
| O-terminated | oxygen-terminated |
| SEM | scanning electron microscopy |

# 1. Introduction

This doctoral Thesis was elaborated at the UNESCO Laboratory of Environmental Electrochemistry, Department of Analytical Chemistry, Faculty of Science, Charles University, where scientific aims are focused on a long-term research in the field of development of highly sensitive and selective electrochemical methods for monitoring and determination of genotoxic organic compounds, different pollutants or biologically active organic compounds important from the environmental, medicinal, pharmaceutical, and toxicological point of view, with a special emphasis on the development of new types of electrochemical sensors and materials for their preparation. The attention of this work is devoted mainly to boron doped diamond (BDD) as an electrode material and his properties, suitable for the preparation of new electrochemical sensors. Other electrode materials used in this work are glassy carbon and carbon film.

The presented Thesis is based on the following seven scientific publications [1-7] which are attached as Appendix parts I – VII. Chapter 3 of this Thesis is divided according to these publications.

[1] **Zavázalová J.**, Barek J., Pecková K.: Boron doped diamond electrodes in voltammetry: New designs and applications. An overview. In *Sensing in Electroanalysis*. Kalcher K., Metelka R., Švancara I., Vytřas K. (Eds.), **8** (2014) pp. 21-34, University Press Centre, Pardubice, Czech Republic.

[2] Schwarzová-Pecková K., Vosáhlová J., Barek J., Šloufová I., Pavlova E., Petrák V., **Zavázalová J.**: Influence of boron content on the morphological, spectral, and electroanalytical characteristic of anodically oxidized boron-doped diamond electrodes. *Electrochimica Acta* **243** (2017) 170-182.

[3] Vosáhlová J., **Zavázalová J.**, Schwarzová-Pecková K.: Boron doped diamond electrodes: Effect of boron concentration on the determination of 2-aminobiphenyl. *Chemické Listy* **108** (2014) s270-s273.

[4] **Zavázalová J.**, Dejmková H., Barek J., Pecková K.: Voltammetric and amperometric determination of mixtures of aminobiphenyls and aminonaphthalenes using boron doped diamond electrode. *Electroanalysis* **25** (2013) 253-262.

[5] **Zavazalova J.**, Ghica M. E., Schwarzova-Peckova K., Barek J., Brett C. M. A.: Carbon-based electrodes for sensitive electroanalytical determination of aminonaphthalenes. *Electroanalysis* **27** (2015) 1556-1564.

[6] **Zavazalova J.**, Prochazkova K., Schwarzova-Peckova K.: Boron-doped diamond electrodes for voltammetric determination of benzophenone-3. *Analytical Letters* **49** (2015) 80-91.

[7] Vosáhlová J., **Zavázalová J.**, Petrák V., Schwarzová-Pecková K.: Factors influencing voltammetric reduction of 5-nitroquinoline at boron-doped diamond electrodes. *Monatshefte für Chemie* **147** (2016) 21-29.

Electroanalytical methods are widely used in scientific studies and in monitoring of industrial materials, pharmaceutical compounds, biological samples, and the environment. The most widespread methods are voltammetry using various electrode materials, and amperometry as detection method in liquid flow techniques. These methods permit the screening and determination of a great number of organic compounds with detection limits typically in the concentration range $\sim 10^{-6}$ mol $L^{-1}$ – $\sim 10^{-7}$ mol $L^{-1}$. Among the greatest advantages of electrochemical methods belong the rapidity and low operating costs.

There is a never-ending search for new electrode materials for voltammetric or amperometric determination of mentioned substances. For new electrode materials, the attention is paid to following basic requirements: broad potential range, high signal-to-noise ratio, mechanical robustness enabling measurements in flowing systems, compatibility with organic solvents making them compatible with high performance liquid chromatography (HPLC), flow injection analysis or capillary electrophoresis with electrochemical detection and resistance towards surface passivation. The last

requirement is especially important because electrode fouling is a serious complication limiting applications of electroanalytical methods in practice.

Further, the scientists' search for non-toxic electrode materials friendly to the environment, compatible with the concept of "green analytical chemistry". One of the newest electrode materials – boron doped diamond – is compatible with above mentioned requirements and thus investigation of its mechanical, physical and electrochemical properties and its implementation in practice is of big concern.

Electrochemistry of diamond as a new research field was opened by the first studies in the eighties. In 1983 Iwaki *et al.* suggested the ion-implanted diamond electrodes [8], in 1987 a current-potential curve was recorded and the differential capacitance at the polycrystalline-diamond/electrolyte interface was measured for the first time [9]. In 1992, research group of Fujishima introduced polycrystalline boron doped diamond thin films [10, 11]. In 1993, Tenne *et al*. reported the application of BDD for the electroreduction of nitrate to ammonia [12], Swain and Ramesham reported the suitability of BDD for analytical applications [13], and Ramesham *et al*. indicated the advantage of BDD for dimensionally stable anodes in electrochemical waste treatment [14].

In recent years, BDD electrodes have been receiving increasing attention for applications in electroanalytical methods, as summarized in several reviews [15-19]. Due to the number of advantages over traditionally employed electrodes (*e.g.*, glassy carbon or platinum electrodes), such as extreme hardness, high corrosion resistance, very low and stable background current, and a wide working potential window, microstructural stability at extreme cathodic and anodic potentials, chemical inertness, high thermal conductivity, low sensitivity to dissolved oxygen, electrochemical stability in both alkaline and acidic media, good responsiveness for many redox analytes without pretreatment, and resistance to electrode fouling, boron doped diamond electrodes are applicable to voltammetric or amperometric determination of both oxidizable and reducible substances with limit of determination down to $10^{-8}$ mol $L^{-1}$ without any preconcentration step [20].

Over the past twenty-five years, BDD research has developed in these five main directions: (1) use of BDD electrodes in electroanalysis for detection of organic and inorganic species in environmental, biological and pharmaceutical matrices [4, 16, 17,

19, 21-24]; (2) electrochemical disinfection of drinking and bathing water [25-28]; (3) electrochemical oxidation of environmental pollutants at BDD anodes proposed for their quantitative conversion or destruction in wastewaters [29-34]; (4) developing of BDD-based sensors and biosensors [35, 36]; and (5) electrochemical synthesis, in particular in the production of strong inorganic oxidizing agents (*e.g.* peroxodisulfuric acid [37, 38], hydrogen peroxide, ozone, chlorine [39], or ferrates [40]), or in electro organic synthesis [41-45]. More information on these topics can be found also in general review [18] and monographs [46, 47].

The properties of BDD films are fundamentally influenced by the quantity and kind of the doping agent, morphologic factors and defects in the film, presence of impurities ($sp^2$ carbon), crystallographic orientation, and surface termination (most frequently oxygen or hydrogen). While the former factors are given by the preparation method, the latter can be determined by post-preparation procedures including electrochemical pretreatment. [19, 48, 49]

Boron doped diamond electrode belongs among carbon-based electrodes. Carbon is one of the most abundant elements found on Earth. It is the basis of life and all organic chemistry and it occurs freely in crystalline forms such as diamond and graphite. Carbon-based electrodes are generally of low cost and they have wide useful potential range, and significantly lower background oxidation currents which are the important advantages over metallic electrodes. All common carbon-based electrode materials share the basic structure of a six-member aromatic ring and $sp^2$ bonding but differ in the relative density of the edge and basal plane toward electron transfer and adsorption. For electrochemistry, the edge plane exhibits considerably faster electrode kinetics in comparison with the basal plane. The high degree of delocalization of electrons together with weak Van der Waals forces provides good electrical conductivity. [50]

The best-known carbon-based electrodes are glassy carbon, carbon paste, carbon fiber, screen printed carbon strips, carbon films, pyrolytic graphite, fullerenes, wax impregnated graphite, Kelgraf, carbon nanotubes, reticulated vitreous carbon, and boron doped diamond. The analytical use of these electrode and examples are summarized in reviews [50-54].

Glassy carbon is frequently used as an inexpensive electrode material with excellent electrical and mechanical properties, wide potential range, extreme chemical inertness, high resistance to acid attack, impermeability to gases and relatively reproducible performance [55]. It is practically gas-tight and exhibits an extremely low porosity. Glassy carbon has a low density, low thermal expansion, high corrosion resistance and high thermal and electrical conductivities. It is easily mounted and compatible with all common solvents. It is prepared by subjecting the organic precursors to a series of heat treatments at temperatures up to 3000 °C [56-58]. The earliest structural models assumed that both $sp^2$- and $sp^3$-bonded carbon atoms were present [59]. This structure was suggested to be composed of tetrahedral domains, perhaps linked by short oxygen-containing bridges. After this earlier model, a lot of structural models were suggested. However, it is now known that glassy carbon contains only $sp^2$ carbon atoms [57, 60]. The structure of glassy carbon consists of graphitic planes randomly organized in a complexed topology. Nearly all glassy carbon electrodes are successively polished with smaller alumina particles (~0.05 μm) on a smooth polishing cloth or on filter paper to create active and reproducible surface and to enhance its analytical performance. Some additional activation steps have also been used such as electrochemical, chemical, vacuum heat, or laser treatment, *etc.* [57, 58]. Glassy carbon electrodes can be used in many different application areas. [50, 51]

## 2. Boron doped diamond

### *2.1 Preparation of BDD*

For almost five decades, chemical vapor deposition (CVD) has been the most commonly used technique to synthesize diamond films, as reviewed in [61]. Various CVD techniques have been invented and applied to fabricate diamond films, including hot filament CVD (HF-CVD) [62], microwave plasma CVD (MP-CVD) [49], plasma enhanced CVD [63], electron assisted CVD [64], and direct current plasma CVD [65].

The common BDD films used in electroanalysis can be grown on Si supports from dilute mixtures of a hydrocarbon gas in hydrogen using one of several energy-assisted chemical vapor deposition methods. These methods mainly differ in the way the gas activation is accomplished. A carbon containing gas, most frequently methane, is energetically activated to decompose its molecules into methyl-radicals and atomic hydrogen and followed by their deposition on a suitable substrate. The substrate, typically silica wafers (also Pt, Nb, Ta, W, Ti) is pretreated by cleaning with a series of solvents and seeded with small particles by polishing the substrate with diamond powder. The embedded particles serve as nucleation centers for film growth. [66]

Typical growth conditions are: 0.3 – 1.0 % $CH_4$ in $H_2$, pressures of 10 – 150 torr, substrate temperatures of 700 – 1000 °C, and microwave powers of 1000 – 1300 W, or filament temperatures up to ~ 2800 °C, depending on the methods used. The film grows by nucleation at rates in the 0.1 – 2 μm $h^{-1}$ range. For the substrates to be continuously coated with diamond, the nominal film thickness must be ~ 1 μm. Boron doping is accomplished from the gas phase by mixing boron-containing compounds such as $B_2H_6$, trimethylborane or $B_2O_3$ with the source gases, or from the solid state by gasifying a piece of hexagonal boron nitride. In the solid-state approach, diborane is produced by the interaction of atomic hydrogen with hexagonal boron nitride and is then incorporated into the gas flux to the substrate. The doping level can be as high as 10000 ppm of boron, resulting in film resistivity < 0.1 Ω cm [67, 68]. The resulting films differ in quality and morphology − microcrystalline films are characterized by crystallite size < 1 – 5 μm, nanocrystalline films 10 – 500 nm [69-71]. It is generally accepted that the quality of MP-CVD films, *i.e.* content of $sp^2$ impurities and structure defects is enhanced compared with HF-CVD films.

*2.2 Availability of BDD electrodes*

BDD electrodes are available from different sources: (i) from own laboratory-made systems; (ii) from commercial growth systems, *e.g.*, Seki Diamond Systems (USA) [72], PLASSYS Bestek (France) [73], Diamond Materials (Germany) [74], Microwave Enterprises (USA) [75]; (iii) from commercial companies (representative companies listed in Table 1).

**Table 1** List of representative commercial suppliers of BDD materials.

| BDD supplier | Material properties | Ref. |
|---|---|---|
| Condias (Germany) | BDD electrodes coated on Nb, Ta, Si, graphite, conductive ceramics (HF-CVD)<br>geometry: plates, mesh, pins and combinations thereof<br>areas up to 100 x 50 cm²<br>thickness up to 15µm | [76] |
| Element Six (UK) | "as grown" polycrystalline BDD in wafer form (CVD)<br>individual pieces 10 x 10 mm and 5 x 5 mm<br>thickness 0.6 and 0.45 mm | [77] |
| NeoCoat (Switzerland), previously Adamant Technologies | BDD electrodes coated on Si or metal substrates (HF-CVD)<br>geometry: rectangle, disc, square<br>thickness from less than 100 nm up to more than 25 µm | [78] |
| sp3 Diamond Technologies (USA) | BDD electrodes coated on graphite, Nb, Si, silicon carbide, Ti, and W (HF-CVD)<br>thickness from 3 to 50 µm | [79] |
| Windsor Scientific (UK), since 2019 BioLogic SAS (France) | 3mm diameter electrodes in an inert Teflon body or individual pieces (both sides polished, 10 x 10, 5 x 5 or 3 x 3 $mm^2$)<br>thickness ~0.5 mm | [80] |

*2.3 Characterization of BDD surface*

The main factors influencing the properties and quality of the BDD are the content of non-diamond carbon impurities, the structural defects in the diamond film, the boron doping level, the size of the diamond crystallites, the crystallographic orientation, and the surface termination. The analytical techniques commonly used to characterize these

morphological and spectral properties are for example scanning electron microscopy (SEM), atomic force microscopy (AFM) and Raman spectroscopy.

For the visualization of the surface, the scanning electron microscopy can be used. This method characterizes the morphologic features of BDD films*, e.g.*, grain size, orientation and surface coverage [81]. Morphology of diamond includes the cubic {100}, the dodecahedral {110}, the octahedral {111}, and more complicated shapes. It is known the crystallographic orientation affects boron uptake, with {111} > {110} > {100} [82]. Atomic force microscopy is often employed in conjunction with scanning electron microscopy in order to accurately determine grain size and define surface roughness [83]. Representative AFM and SEM micrographs of the surface of some of BDD films utilized in studies of the Author [2, 3, 6, 7] are depicted in Figure 1.

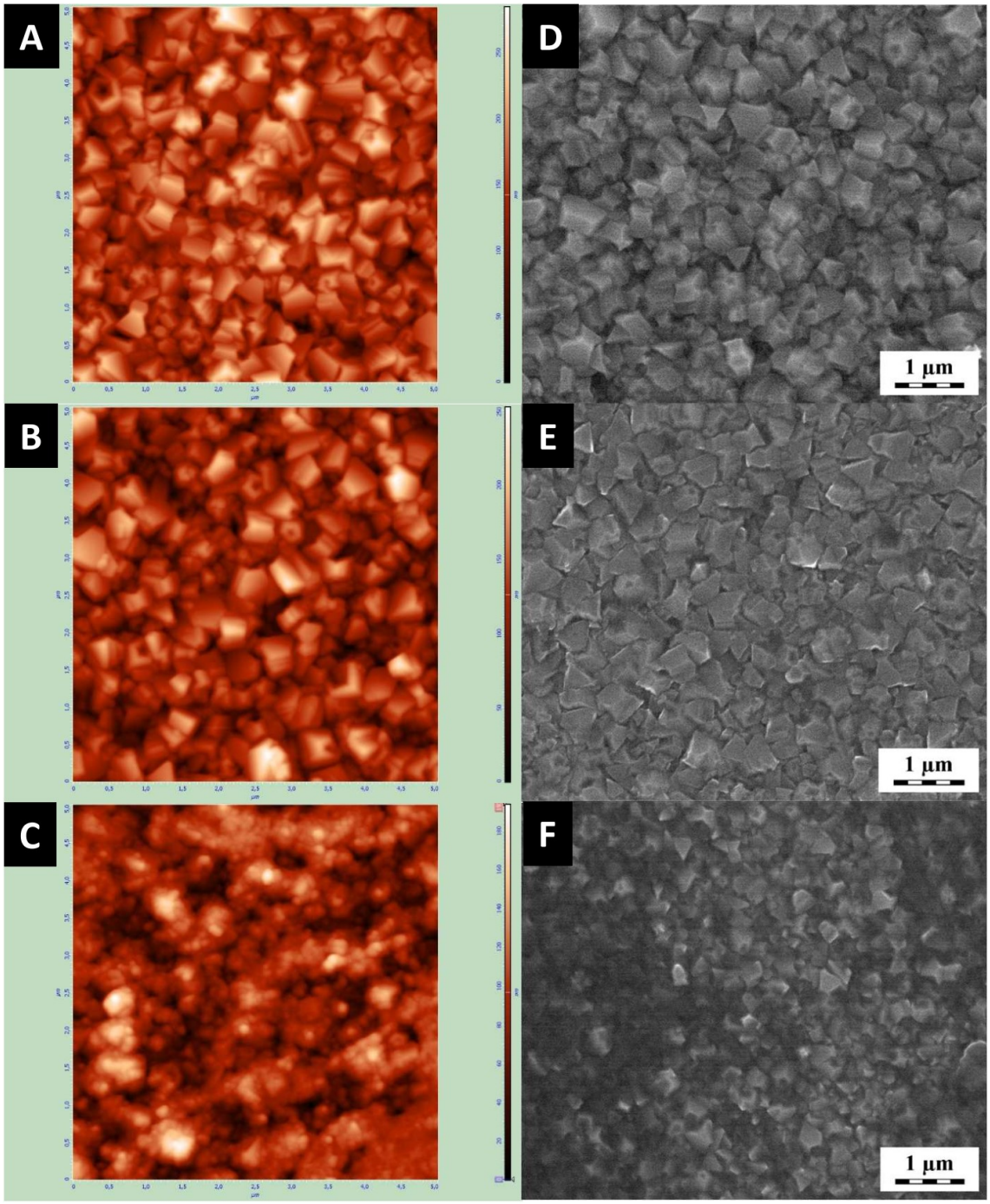


**Figure 1** Atomic force micrographs (A – C) and scanning electron micrographs (D – F) of the surface of BDD films with boron content 500 ppm (A + D), 2000 ppm (B + E), and 8000 ppm (C + F). The same magnification, adjusted from [2].

Raman spectroscopy is routinely used for the characterization of diamond films due to its sensitivity to $sp^3$ carbon and to the content of non-diamond $sp^2$ carbon impurities. The $sp^3$ carbon (in pure diamond) shows in Raman spectra a single sharp peak at 1332 $cm^{-1}$. At the metallic levels of doping, the diamond phonon line at 1332 $cm^{-1}$ exhibits asymmetry and a shift to lower wavenumbers, coming from the Fano interference of this one phonon band induced by quantum mechanical interference between the discrete phonon and electronic continuum. [83]

Cyclic voltammetry is often used to study the electrochemical response of BDD films, to evaluate kinetics of electron transfer and to give an insight into the condition of BDD surface. Several inner-sphere (*e.g.* $[Fe(CN)_6]^{3-/4-}$, dopamine, $Fe^{3+/2+}$) and outer-sphere (*e.g.* $[Ru(NH_3)_6]^{3+/2+}$, $[IrCl_6]^{2-/3-}$, $[IrCl_4]^{3-/4-}$, ferrocene$^{+/-}$) redox systems can serve as probes [52]. Cyclic voltammetric *I–E* curves can serve to evaluate character of the redox process (diffusion or adsorption controlled, value of apparent heterogenous electron-transfer rate constant $k^{\circ}_{app}$ from the peak potential difference between cathodic and anodic peak $\Delta E_p$ or $I_{pa}/I_{pc}$ ratio) [84].

### *2.4 Concentration of boron*

The boron doping level is one of the main factors influencing properties of BDD such as the film morphology, conductivity, and electrochemical properties [81, 85-87]. Depending on the boron content, the electrical conductivity of the BDD films ranges from insulating through semiconductive to metallic (details in [2]). Practically, the boundary boron content of about $(1 – 3) \times 10^{20}$ $cm^{-3}$ [88, 89] or higher ($4.5 \times 10^{20}$ $cm^{-3}$ [90]) were reported and it seems that these concentrations are sufficient to achieve fast electron transfer typical for metallic-type conductivity, which is preferred in electrochemical applications. Films with $[B] > 3 \times 10^{20}$ $cm^{-3}$ are denoted as heavily doped BDD films [91].

Some papers paid attention to the influence of boron content on the physical and electrochemical characteristics of BDD films [81, 85, 86, 92, 93], effectivity of electrocatalytic anodic oxidation of organic pollutants [65, 94-96], surface resistivity towards fouling [97], and analytical parameters of determination of selected inorganic ions [93, 98]. Only few of these studies deal with the influence of the boron content on electroanalytical characteristics of the BDD films, including the width of the potential

window [99-102] or voltammetric response for selected organic analytes such as 2-aminobiphenyl (2-AB) [2], benzophenone-3 (BP-3) [6], dopamine [97], 4-chloro-3-methylphenol [103], and 5-nitroquinoline [7].

*2.5 Surface termination, pretreatment and activation*

Pretreatment of the electrode surface determining attached chemical functionalities can be applied for its activation (preventing the passivation of electrode surface), and enhancement of voltammetric signals of studied compounds ensuring their repeatable and reproducible response. The surface of the BDD electrode can be hydrogen-terminated (H-terminated) and oxygen-terminated (O-terminated). The as-deposited diamond surface by CVD procedure is H-terminated, because the films are grown under hydrogen plasma or in a hydrogen atmosphere. The type of surface termination strongly influences the hydrophobicity/hydrophilicity and thus the wetting properties of the surface and further influences the polarity of the surface bonds resulting in electrostatic interactions which can raise or lower the energy levels of the valence and conduction bands of the BDD [83].

At the beginnings many studies were presented to be performed at "as-grown", H-terminated BDD electrodes [13, 104, 105]. This approach is outdated, because the maintenance of H-termination is complicated due to the easy electrochemical oxidation and even oxidation of BDD surface by air oxygen [102]. Also, the O-terminated surface can be easily formed by exposing the surface to oxygen plasma, boiling in strong acid or electrochemical exposure to the high anodic potential in the region of water decomposition, which is the most common approach in electrochemical studies [106, 107]. At BDD electrode, water decomposes according to the following equation:

$$H_2O(BDD) \rightarrow HO^{\bullet}(BDD) + H^+ + e^- \quad \text{(Eq. 1)}$$

Quasi-free $OH^{\bullet}$radicals are in close vicinity of the BDD surface and the subsequent reactions include their reactions with each other and/or reactions with intermediates, *e.g.* $H_2O_2$ and $O_2H^{\bullet}$ radicals including further electron transfers leading to $O_2$ (details in ref. [108, 109]). Technically, most frequently highly positive current densities (typically units to tens of mA $cm^{-2}$) or potentials (~ > +2.0 V) applied for few seconds to minutes are used to achieve sufficient O-termination (often directly in the analyte solution as

a surface renewal/activation step between individual measurements). It was reported that even tens of seconds may lead to almost complete oxidation when sufficiently high potentials are applied (~ > +3.0 V vs. a platinum counter electrode in 1mol $L^{-1}$ sulfuric acid or 0.5mol $L^{-1}$ nitric acid solution) [110].

The anodic pretreatments leads to incorporation of oxygen atoms on the BDD surface mostly through the carbon reaction with $OH^{\bullet}$ radicals generated according to the equation (1) in aqueous media (pH<9.0) [111]. Once the O-terminated surface is obtained, its re-hydrogenation is achievable either by hydrogen-flame annealing or hydrogen-plasma treatment, which requires adequate equipment, or more simply by cathodization of the surface. The type and distribution of oxygen-containing chemical functionalities on the polycrystalline BDD surface is dependent on the boron doping level [112], grain size, and proportion of different grain orientations [83]. The O-terminated BDD does not exhibit a measurable surface conductivity, in contrast to H-terminated surface [102] which can be utilized in studies of the BDD surface oxidation. As follows from studies with redox probes such as $[Fe(CN)_6]^{4-/3-}$ or various organic analytes [48, 83], O-terminated BDD exhibits slower heterogenous electron transfer compared to H-terminated BDD. [113]

Anodic activation is very effective in the case of passivation of the electrode surface by products of the analyte conversion, because OH radicals (eq. 1) are powerful oxidizing agents capable of oxidation of polymeric films formed at the electrode surface as results of electrochemical processes of analytes and their reaction by-products. The easiest way to activate the surface is to apply the positive potential directly in the measured solution. Examples of this strategy are the following studies on the development of electrochemical methods for determination of aromatic amines (aminonaphthalenes and aminobiphenyls [4]), and phenolic compounds (4-chloro-3-methylphenol [103], *m*-cresol [114], homovanillic and vanillylmandelic acid [115]). These species are generally considered as problematic surface-fouling substances (at any electrode) since their electrooxidation involves radical species that easily oligomerize or polymerize. Other compounds such as benzophenone-3 required *ex situ* activation in 0.5 mol $L^{-1}$ $H_2SO_4$ by switching between potentials +3, −3, +3, −3, +3 V, each for 10 s [6]. As an example, Figure 2 represents differential pulse voltammograms of 2-aminobiphenyl at BDD. The effectivity of anodic activation before

each scan preventing electrode passivation is clearly demonstrated in Figure 2C. The peak height repeatability characterized by relative standard deviation is 2.7 %, and anodic pretreatment is thus favorable compared with cathodic pretreatment, leading to instability of voltammetric responses (Figure 2B).

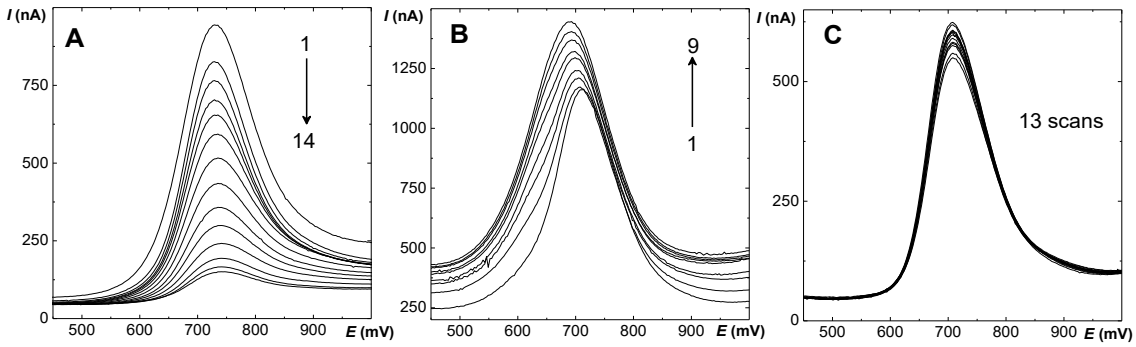


**Figure 2** Influence of the electrode pretreatment on the differential pulse voltammograms of 2-aminobiphenyl ($c$ = 5 × $10^{-5}$ mol $L^{-1}$) in Britton–Robinson buffer pH 7.0. Measured on BDD without pretreatment (**A**) and with pretreatment consisting of stirring and applying the potential of –2.4 V (**B**) or +2.4 V (**C**) for 15 s on working electrode in measured solution between individual measurements. The number of scans is indicated in individual figures. Adjusted from [1].

The H-termination can be achieved using high negative potentials (~ < –2.0 V) in the region of hydrogen evolution reaction or negative current densities. The H-terminated surfaces are more hydrophobic than the O-terminated ones, exhibiting measurable surface conductivity [83]. The cathodic pretreatment has to be applied just before the electrochemical experiments to ensure reliable and reproducible results, especially when the electrode has not been used for a long period of time due to its instability in air (thus from the practical point of view, the cathodic pretreatment is less user-friendly). For cathodically pretreated BDD exposed to air for 30 days, increase of superficial content of oxygen, accompanied by loss of the surface conductivity, was confirmed by X-ray photoelectron spectroscopy measurements [112]. Interestingly, it seems that increased boron content has stabilizing effect on the H-termination [81, 112]. Suffredini *et al.* presented faster heterogenous electron transfer for $[Fe(CN)_6]^{4-/3-}$, signal

increase and improved repeatability for selected chlorophenols on H-terminated electrode [48].

Cathodic pretreatment and/or activation of the electrode based on application of negative potentials is another way to modify BDD surface and/or to reactivate it when passivated. Examples may be the following studies on the comparison of voltammetric response after anodic and cathodic pretreatment: azo dyes tartrazine and allura red [116], phenolic compounds homovanillic and vanillylmandelic acid [117], and reducible nitro group containing 5-nitroquinoline [7]. Figure 3 represents its differential pulse voltammograms recorded at O-terminated BDD and H-terminated BDD. Cathodic activation has led to significant shift of peak potential to less negative values (indicating easier reduction of the analytes) and faster electron transfer recognizable by narrowing of voltammetric peaks recorded in the differential pulse mode.

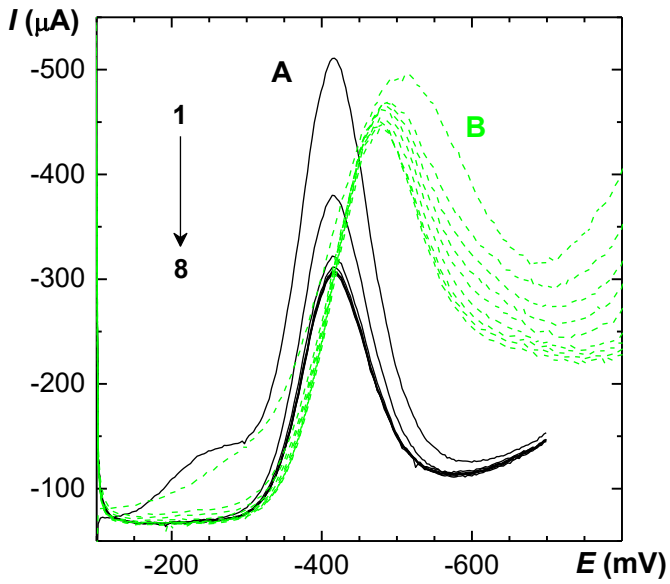


**Figure 3** Differential pulse voltammograms of 5-nitroquinoline ($c = 1 \times 10^{-4}$ mol $L^{-1}$) in 0.1 mol $L^{-1}$ acetate buffer pH 5.0 using different pretreatment of the BDD electrode in 0.5 mol $L^{-1}$ $H_2SO_4$: (**A**) anodic pretreatment ($E = +2.4$ V for 5 min), (**B**) cathodic pretreatment ($E = -2.4$ V for 10 min). BDD electrode B/C ratio 4000 ppm, scan rate 20 mV $s^{-1}$, adjusted from [7].

Another way to obtain a clean and defined BDD surface is mechanical polishing. The interest of analytical chemists in this possibility is decreased because of the devaluation of the main advantages of BDD electrodes – a possibility to omit the manual manipulation with the electrode by using solely electrochemical activation *in situ*. Already in 2002, reversible electron transfer for $Fe^{2+}/Fe^{3+}$ redox couple of the heme unit of cytochrome *c* at alumina polished BDD surface was reported [118]. Some later studies mentioned potential shifts and current increases of voltammetric signals at the same electrode [119]. Recently, the attention was paid to characterization of these surfaces and their rational utilization in electroanalysis. Results of X-ray photoelectron spectroscopy show a dramatic difference between the alumina polished surface and anodized surface, although both are reported to bear oxygenous groups [102].

For mechanical polishing of BDD electrodes alumina slurry and silk cloth is commonly used. Polishing is performed for few seconds to several minutes to efficiently remove films covering the electrode surface. Once it has been completed, the electrode surface must be carefully rinsed with distilled water to remove all traces of the polishing material. An example of mechanical polishing is the study of determination of benzophenone-3 on BDD in presence of surfactant cetyltrimethylammonium bromide [6]. Because fouling of the BDD electrode surface was observed, it was mechanically polished by alumina before each scan to provide good repeatability (relative standard deviation of peak height in differential pulse voltammetry was 5 % for $1 \times 10^{-4}$ mol $L^{-1}$ benzophenone-3). The positive effect of polishing on the kinetics of redox reactions on the BDD electrode is evident from cyclic voltammograms (Figure 4) of a surface-sensitive redox marker $[Fe(CN)_6]^{3-/4-}$. The difference between the anodic and cathodic peak potentials $\Delta E_p$ prior and after 3 min of polishing by alumina decreased from 397 mV to 206 mV. Further repetitive polishing (four times for three minutes) resulted in a further decrease of $\Delta E_p$ to 114 mV. This positive effect of polishing on the reversibility of $[Fe(CN)_6]^{3-/4-}$ has been reported previously [102, 120].

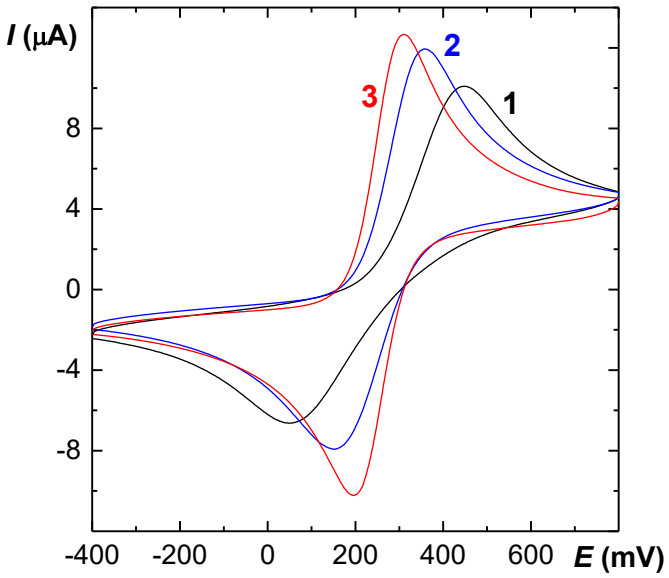


**Figure 4** Selected cyclic voltammograms of $1 \times 10^{-3}$ mol $L^{-1}$ $[Fe(CN)_6]^{3-/4-}$ in 1 mol $L^{-1}$ KCl measured at the BDD electrode at a scan rate of 100 mV $s^{-1}$. Alumina polishing for (**1**) zero minutes; (**2**) three minutes, and (**3**) fifteen minutes. The third cycle is depicted, adjusted from [6].

*2.6 Analytical applications*

Following Table 2 summarizes selected voltammetric methods developed for the detection of organic compounds on bare BDD electrodes. For each analyte, the table contains characterization of used BDD electrode, electroanalytical method, conditions, pretreatment/activation, achieved limit of detection, eventually matrix. The table enables an insight in the progress in applications of BDD electrodes in last few years. A wide range of oxidizable or reducible organic analytes was studied using BDD electrodes: neurotransmitters, their metabolites and precursors; monocyclic and polycyclic aromatic hydrocarbons or heterocycles; phenolic compounds and hydroxy derivatives of polycyclic aromatic hydrocarbons; pharmaceuticals and therapeutics; food and beverage components and additives and pesticides. BDD electrodes are used as-deposited, but more often anodic or cathodic electrochemical pretreatment or mechanical polishing is applied.

**Table 2** Selected examples of organic compounds using voltammetric methods on bare BDD electrodes.

| analyte | pretreatment/BDD electrode | electroanalytical method, conditions, activation program (ACT) | LOD (μmol $L^{-1}$) | determination in samples | Ref. |
|---|---|---|---|---|---|
| **Neurotransmitters, their metabolites and precursors** | | | | | |
| dopamine (DA)<br>pyridoxine (B6) | as-deposited/Ta substrate, EA-HFCVD porous BDD electrode | DPV in 0.1M phosphate buffer pH 7.0 | DA: 0.06[A]<br>B6: 0.22[A] | simultaneous in human serum | [121] |
| homovanillic acid (HVA)<br>vanillylmandelic acid (VMA) | AP/commercial BDD (Windsor Scientific, UK), B/C ratio 1000 ppm; AP: +2.4 V 20 min in 0.1M $H_2SO_4$ | DPV in 0.1M phosphate buffer pH 3.0;<br>ACT: +2.4 V 30 s in stirred analysed solution | HVA: 0.6[B]<br>VMA: 0.4[B] | --- | [115] |
| vanillylmandelic acid | CP/BDD film deposited on the tip of Ti wire by MW-PECVD, B/C 2000 ppm; CP: –1.0 V 15 s | DPV in 0.1M NaOH pH 13;<br>ACT: –1.0 V 15 s between each measurement | 2.2[C] | --- | [122] |
| **Monocyclic and polycyclic (substituted) aromatic hydrocarbons/heterocycles** | | | | | |
| 2-aminobiphenyl | AP/BDD films deposited on Si (100) wafer by MW-PECVD, variable B/C ratio 500, 1000, 2000, 4000, and 8000 ppm; AP: +2.4 V 180 s in 0.1M $H_2SO_4$ | DPV in 0.04M BR buffer pH 7.0;<br>ACT: +2.4 V 30 s in analysed solution | 500: 0.72[D]<br>1000: 0.48[D]<br>2000: 0.80[D]<br>4000: 0.48[D]<br>8000: 0.21[D] | | [2] |
| 1-aminonaphthalene | AP/microcrystalline BDD film deposited on *p*-Si (111) by MWCVD; AP: +2.4 V 15 s in stirred analysed solution | DPV in 0.04M BR buffer pH 2.0;<br>ACT: +2.4 V 15 s in stirred analysed solution | 1.4[D] | --- | [5] |

| | | | | | |
|---|---|---|---|---|---|
| anthranilic acid (2-aminobenzoic acid, AA) salicylic acid (2-hydroxybenzoic acid, SA) | PCP/commercial BDD (Windsor Scientific, UK), B/C ratio 1000 ppm; PCP: one cycle from +1.6 V to –1.0 V in 0.2M $H_2SO_4$ | LSV in 0.1M phosphate buffer pH 7.02 with 16% ethanol | AA:3.79<br>SA: 0.80 | commercial samples of plant growth stimulants | [123] |
| ethylone | PCP/commercial BDD film (NeoCoat SA, Switzerland), B/C ratio 8000 ppm, PCP: from +30 mA $cm^{-2}$ 30 s to –30 mA $cm^{-2}$ 150 s in 0.5M $H_2SO_4$ | SWV in 0.5M $H_2SO_4$; ACT: 20 cycles from +1.0 V to +1.6 V in 0.5M $H_2SO_4$ | $3.7^{E}$ | seized street drug samples | [124] |
| *N*-hydroxysuccinimide | AP/BDD films deposited on Si (100) wafers by MW-PECVD; AP: +3.0 V 30 min in 0.1M $HClO_4$ | LSV in 0.1M $NaHCO_3$ | $10.9^{A}$ | --- | [125] |
| 5-nitroquinoline | AP or CP/MW-PECVD BDD film, B/C ratio 4000 ppm; AP: +2.4 V 5 min in 0.5M $H_2SO_4$; CP: –2.4 V 10 min in 0.5M $H_2SO_4$ | DCV and DPV in 0.1M acetate buffer pH 5.0 | AP/CP<br>DCV: $2.7/4.7^{F}$<br>DPV: $0.20/0.50^{F}$ | --- | [7] |
| uric acid | as-deposited/lab-made BDD by HFCVD, B/C ratio 2000 ppm | DPV and SWV in 0.04M BR buffer pH 2.25 | $7.7^{E}$ | human urine samples | [126] |
| **Phenolic compounds and hydroxy derivatives of polycyclic aromatic hydrocarbons** | | | | | |
| benzophenone-3 | AP/commercial BDD (Windsor Scientific, UK), B/C ratio 1000 ppm; AP: +2.4 V 60 s in 0.5M $H_2SO_4$<br>AP/lab-made BDD films deposited on Si by MW-PECVD variable B/C ratio 2000, 4000, and 8000 ppm; AP: +2.4 V 60 s in 0.5M $H_2SO_4$ | DPV in 0.01M NaOH + surfactant 0.1 mM CTAB; ACT: polished with alumina before measurement;<br>DPV in 0.04M BR buffer pH 12.0; ACT: switching of potentials +3 V and –3 V each 10 s in 0.5M $H_2SO_4$ between each measurement | $0.1^{F}$<br>2000: $1.5^{F}$<br>4000: $1.9^{F}$<br>8000: $0.8^{F}$ | --- | [6] |

| | | | | | |
|---|---|---|---|---|---|
| catechol (CT)<br>hydroquinone (HQ)<br>resorcinol (RS) | AP/commercial BDD film (Adamant Technologies, Switzerland), B/C ratio 8000 ppm;<br>AP: +10 mA $cm^{-2}$ 30 min in 1M $HClO_4$ | DPV in 0.05M $H_2SO_4$ | CT: 16.34[G]<br>HQ: 15.47[G]<br>RS: 19.23[G] | --- | [127] |
| hydroquinone | as-deposited/lab-made BDD deposited on Ta substrate by EA-HFCVD | DPV in phosphate buffered saline pH 7.0 | 0.59[A] | --- | [128] |
| 1-naphthol (1NAP)<br>2-naphthol (2NAP) | CP/commercial BDD film (NeoCoat, Switzerland), B/C ratio 10000 ppm;<br>CP: –100 mA $cm^{-2}$ 180 s in 0.5M $H_2SO_4$) | DPV in 0.05M $H_2SO_4$ | 1NAP: 0.05[A]<br>2NAP: 0.10[A] | spiked lake water and synthetic urine samples | [129] |
| pyrogallol | as-deposited/commercial BDD (Windsor Scientific, UK), B/C ratio 1000 ppm | LSV in 0.18M $H_2SO_4$ | 0.85 | biofuels | [130] |
| quercetin | CP/commercial BDD (Windsor Scientific, UK), B/C ratio 1000 ppm;<br>CP: –1.4 V 180 s in 0.5M $H_2SO_4$ | SW-AdSV in 0.1M acetate buffer pH 4.7 + surfactant 300µM CTAB;<br>ACT: –1.4 V 60 s in 0.5M $H_2SO_4$ between each measurement | 0.00044[B] | apple juice | [131] |
| resveratrol | CP/commercial BDD (Windsor Scientific, UK), B/C ratio 1000 ppm,<br>CP: –1.5 V 180 s in 0.5M $H_2SO_4$ | SW-AdSV in 0.1M $HNO_3$ + surfactant 0.1 mM HDTMAB,<br>ACT: –1.5 V 60 s in 0.5M $H_2SO_4$ between each measurement | 0.0276[E] | dietary supplements | [132] |

| | | | | | |
|---|---|---|---|---|---|
| tetrabromobisphenol A | PCP/BDD film deposited on Si substrate by HFCVD, B/C ratio 1000 ppm; PCP: +3.0 V 100 s in 0.05M $H_2SO_4$ and –3.0 V 100 s in 0.05M $H_2SO_4$, then 15 cycles from +0.3 V to +0.8 V in 0.1M phosphate buffer pH 8.0 | CV in 0.1M phosphate buffer pH 8.0 | 0.027[A] | spiked river water samples | [133] |
| **Pharmaceuticals and therapeutics** | | | | | |
| acetaminophen (AC)<br>caffeine (CF)<br>carisoprodol (CR) | AP/commercial BDD film (Adamant Technologies, Switzerland), B/C ratio 8000 ppm;<br>AP: +0.5 A $cm^{-2}$ 30 s in 0.5M $H_2SO_4$ | DPV and SWV in 0.04M BR buffer pH 6.0 | DPV/SWV<br>AC:1.17/0.768[E]<br>CF:0.133/0.771[E]<br>CR:1.84/3.11[E] | simultaneous in pharmaceutical formulations | [134] |
| alprazolam | CP/commercial BDD (Windsor Scientific, UK), B/C ratio 1000 ppm; CP: softly rubbed with damp silk cloth, then +2.0 V 60 s and –2.0 V 30 s in 1M $H_2SO_4$ | DPV in 0.04M BR buffer pH 5.0 | 0.64 | pharmaceutical formulations | [135] |
| amiloride (AR)<br>amlodipine (AD)<br>atenolol (AT)<br>hydrochlorthiazide (HCT) | AP/commercial BDD film (Adamant Technologies, Switzerland), B/C ratio 8000 ppm;<br>AP: +0.5 A $cm^{-2}$ 30 s in 0.5M $H_2SO_4$ | SWV in 0.1M ammonium buffer pH 9.0 | AR: 0.09[E]<br>AD: 0.30[E]<br>AT: 0.06[E]<br>HCT: 0.08[E] | simultaneous in pharmaceutical formulations and spiked tap water samples | [136] |
| amlodipine (AD)<br>atorvastatin (AV) | AP/commercial BDD film (Adamant Technologies, Switzerland), B/C ratio 8000 ppm;<br>AP: +0.5 A $cm^{-2}$ 30 s in 0.5M $H_2SO_4$ | DPV and SWV in 0.04M BR buffer pH 4.0 with 10% methanol (v/v) | DPV/SWV<br>AD:0.078/0.028[E]<br>AV:0.904/0.383[E] | simultaneous in pharmaceutical formulations | [137] |

| | | | | | |
|---|---|---|---|---|---|
| ascorbic acid | PCP/BDD electrode, B/C ratio 8000 ppm; PCP: from –2.0 V to +2.0 V in 1.5M $H_2SO_4$ until stable signal was observed (cca 5 cycles) | DPV in 0.04M BR buffer pH 4.0 | 1.1[D] | pharmaceutical formulations | [138] |
| atenolol (AT)<br>nifedipine (NI) | AP/commercial BDD film (Adamant Technologies, Switzerland), B/C ratio 8000 ppm;<br>AP: +0.5 A $cm^{-2}$ 30 s in 0.5M $H_2SO_4$ | SWV and DPV in 0.1M TRIS buffer pH 8.0 | SWV/DPV<br>NI:0.685/0.612[E]<br>AT:0.370/0.999[E] | simultaneous in pharmaceutical formulations | [139] |
| benzocaine | AP/screen-printed BDD electrode (CBDD110, Dropsens, Spain), B/C ratio 2500 ppm;<br>AP: +2.0 V 40 s in 1M $HNO_3$ | DPV and SWV in 0.04M BR buffer pH 4.0 | DPV: 0.08[D]<br>SWV: 0.10[D] | pharmaceutical formulations and spiked human urine samples | [140] |
| bromazepam | CP/BDD film deposited on *n*-Si (100) wafer by HF-CVD, B/C ratio 1000 ppm; CP: softly rubber with damp silk cloth, then +2.0 V 60 s and –2.0 V 30 s in 1M $H_2SO_4$ | DPV in 0.04M BR buffer pH 11.0 | 0.31 | pharmaceutical formulations | [135] |
| caffeine (CAF)<br>paracetamol (PAR)<br>propyphenazone (PRO) | CP/commercial BDD film (NeoCoat, Switzerland), B/C ratio 8000 ppm;<br>CP: –0.01 A 1000 s in 0.1M $H_2SO_4$) | SWV in 0.1M $H_2SO_4$ | CAF: 0.031<br>PAR: 0.033<br>PRO: 0.039 | simultaneous in pharmaceutical formulations | [141] |
| cefalexin | PP/commercial BDD (Windsor Scientific, UK) with B/C of 1000 ppm; PP: polished with alumina before measurements | DPV in 0.2M acetate buffer pH 4.5, ACT: polished with alumina between each measurement | 0.10[H] | pharmaceutical formulations, spiked river water and human urine | [142] |

| | | | | | |
|---|---|---|---|---|---|
| cetirizine | CP/commercial BDD (Windsor Scientific, UK), B/C ratio 1000 ppm; CP: –3.0 V 300 s in 0.6M $H_2SO_4$) | DPV in 0.1M phosphate buffer pH 8.0 | 0.016[D] | pharmaceutical formulations and spiked human urine | [143] |
| ciprofloxacin | PCP/BDD film deposited on *n*-Si (100) wafer by HFCVD, B/C ratio 20000 ppm; PCP: 15 cycles from –2.0 V to +2.0 V 100 mV $s^{-1}$ in 1.5M $H_2SO_4$ | SWV in 0.1M ammonium acetate buffer pH 5.0 | 0.05[D] | spiked human urine samples | [144] |
| colchicine | CP/commercial BDD (Windsor Scientific, UK), B/C ratio 1000 ppm; CP: rubbed on a piece of damp silk cloth, then +2.0 V 180 s and –2.0 V 180 s in 1M $H_2SO_4$ | DPV in 0.04M BR buffer pH 7.5 | 0.26[D] | pharmaceutical formulations and human serum samples | [145] |
| enrofloxacin | AP/commercial BDD (Windsor Scientific, UK), B/C ratio 1000 ppm; AP: +1.8 V 180 s in 0.5M $H_2SO_4$ | SW-AdSV in 0.1M $HNO_3$ + surfactant 0.9mM SDS, ACT: +1.8 V 60 s in 0.5M $H_2SO_4$ between each measurement | 0.0159[B] | pharmaceutical formulations and spiked human urine samples | [146] |
| febuxostat | AP/commercial BDD (Windsor Scientific, UK), B/C ratio 1000 pm; AP: rubbed on a piece of paper, then +2.0 V 90 s in 0.5M $H_2SO_4$ | SWV in 0.04M BR buffer pH 5.0; ACT: rubbed on a piece of paper, then +2.0 V 90 s in 0.5M $H_2SO_4$ between each measurement | 0.095[E] | pharmaceutical formulations | [147] |
| flutamide | PP/commercial BDD (Windsor Scientific, UK), B/C ratio 1000 ppm; PP: rubbed with a piece of damp silk cloth | DPV and SWV in 0.1M $H_2SO_4$ | DPV: 0.42[D] SWV: 0.21[D] | pharmaceutical formulations, spiked human urine and water samples (river, well, tap) | [148] |

| | | | | | |
|---|---|---|---|---|---|
| hydrochlorthiazide (HYD)<br>ramipril (RAM) | CP/commercial BDD film (Adamant Technologies, Switzerland), B/C ratio 8000 ppm; CP: +0.5 A $cm^{-2}$ 30 s and –0.5 A $cm^{-2}$ 120 s in 0.5M $H_2SO_4$ | SWV in 0.04M BR buffer pH 2.0 | HYD: 0.0182[E]<br>RAM: 0.027[E] | simultaneous in pharmaceutical formulations | [149] |
| chlorpromazine (CPZ)<br>thioridazine (TDZ) | CP/commercial BDD (Windsor Scientific, UK), B/C ratio 1000 ppm; CP: +2.0 V 180 s and –2.0 V 180 s in 0.5M $H_2SO_4$ | DPV in BR buffer pH 4.0 (CPZ) and pH 6.0 (TDZ) | CPZ: 0.03[A]<br>TDZ: 0.12[A] | spiked human urine samples | [150] |
| ibuprofen | PP/commercial BDD (Windsor Scientific, UK), B/C ratio 1000 ppm;<br>PP: smoothed with a piece of wet silk | DPV and SWV in 1M $HClO_4$ | DPV: 0.41[D]<br>SWV: 0.93[D] | pharmaceutical formulations and spiked human urine samples | [151] |
| imipramine | PCP/BDD film deposited on *n*-Si (100) wafer by HFCVD, B/C ratio 4000 ppm; PCP: 30 cycles from –2.0 V to +2.0 V 500 mV $s^{-1}$ in 1.5M $H_2SO_4$ | DPV in 0.04M BR buffer pH 9.0 | 0.5[D] | pharmaceutical formulations | [152] |
| imipramine | CP/BDD film (CSEM, Switzerland), B/C ratio 8000 ppm; CP: +3.0 V 15 s and –3.0 V 30 s in 0.5M $H_2SO_4$ | SWV in 0.04M BR buffer pH 7.4 | 0.0435[E] | pharmaceutical formulations | [153] |
| indapamide | CP/commercial BDD film (Adamant Technologies, Switzerland), B/C ratio 8000 ppm; CP: –25 A $cm^{-2}$ 240 s in 0.5M $H_2SO_4$ | SWV in 0.01M $H_2SO_4$ | 0.056[D] | pharmaceutical formulations and spiked synthetic cerebrospinal fluid and tap water | [154] |

| | | | | | |
|---|---|---|---|---|---|
| isatin | as-deposited/BDD macroelectrode (MAC) and BDD microelectrode array (MEA) fabricated on Si wafer by MW-PECVD, B/C ratio 3000 ppm | SWV in 0.1M phosphate buffer pH 7.4 | MAC: 0.22[B]<br>MEA: 0.04[B] | urine simulant | [155] |
| leucovorin | AP/lab-made BDD films with B/C ratio 1000, 2000, 4000, 8000, 10000 and 20000 ppm;<br>AP: –2.0 V 60 s and +2.0 V 60 s, then 10 cycles from –1.0 V to +2.0 V in 0.5M $H_2SO_4$ | DPV in 0.4M BR buffer pH 3.0;<br>ACT: +2.0 V 5 s in 0.5M $H_2SO_4$ between each measurement | 1000: 0.067[D]<br>2000: 0.36[D]<br>4000: 0.12[D]<br>8000: 0.090[D]<br>10000: 0.10[D]<br>20000: 0.42[D] | pharmaceutical formulations | [156] |
| leucovorin | PCP/commercial BDD (Windsor Scientific, UK), B/C ratio 1000 ppm;<br>PCP: –1.0 V 60 s and +2.0 V 60 s, then 20 cycles from –1.0 V to +2.0 V in 0.5M $H_2SO_4$ | DPV in 0.04M BR buffer pH 3.0;<br>ACT: +2.0 V 5 s in 0.5M $H_2SO_4$ between each measurement | 0.015[E] | pharmaceutical formulations | [157] |
| levofloxacin | PCP/BDD film (CSEM, Switzerland), B/C ratio 3500 ppm;<br>PCP: cycling from –3.0 V to +3.0 V 120 s 5000 mV $s^{-1}$ | SWV and CV in 1.4 mM $Na_2SO_4$ pH 5.5 | SWV: 2.88[D]<br>CV: 10.01[D] | spiked human serum and synthethic urine samples | [158] |
| melatonin (M)<br>pyridoxine (P) | CP/commercial BDD (Windsor Scientific, UK), B/C ratio 1000 ppm;<br>CP: –1.7 V 180 s in 0.5M $H_2SO_4$ | SWV in 0.1M BR buffer pH 2.0;<br>ACT: –1.7 V 60 s 0.5M $H_2SO_4$ between each measurement | M: 0.60[B]<br>P: 6.6[B] | simultaneous in dietary supplements | [159] |

| | | | | | |
|---|---|---|---|---|---|
| mesalazine | CP/commercial BDD (Windsor Scientific, UK), B/C ratio 1000 ppm; CP: +3.0 V 60 s and –3.0 V 3000 s in 0.5M $H_2SO_4$ | SWV in 0.04M BR buffer pH 7.0 | 0.70[E] | pharmaceutical formulations and spiked human urine samples | [160] |
| omeprazole | AP/commercial BDD (Windsor Scientific, UK), B/C ratio 1000 ppm; AP: cleaned sonically and polished with alumina, then +5.0 V 60 s | DPV and SWV in 0.1M phosphate buffer pH 10.0; ACT: cleaned sonically and polished with alumina, then +5.0 V 60 s between each measurement | DPV: 0.91[I] SWV: 0.091[I] | pharmaceutical formulations and spiked human urine samples | [161] |
| oxacillin | PP/commercial BDD (Windsor Scientific, UK), B/C ratio 1000 ppm; PP: polished with alumina | DPV in 0.2M acetate buffer pH 4.5; ACT: polished with alumina between each measurement | 27.15[J] | pharmaceutical formulations, human urine samples and river water | [162] |
| pindolol | CP/BDD film (CSEM, Switzerland), B/C ratio 8000 ppm; CP: –3.0 V 30 s in 0.5M $H_2SO_4$ | DPV and SWV in 0.2M phosphate buffer pH 6.0 | DPV: 0.026 SWV: 0.043 | pharmaceutical formulations, spiked synthetic urine and serum | [163] |
| propofol | AP/rotating BDD disk (NeoCoat, Switzerland), B/C ratio 700 ppm; AP: +2.2 V 900 s in 0.1M $KNO_3$ | CV in 10mM phosphate buffer pH 7.4; ACT: 10 cycles from +0.75 V to +1.4 V in 0.1M NaOH | 2.40 ± 0.90[E] | spiked human serum samples | [164] |
| salbutamol | CP/commercial BDD (Windsor Scientific, UK), B/C ratio 1000 ppm; CP: –1.5 V 180 s in 0.5M $H_2SO_4$ | SW-AdSV in 0.04M BR buffer pH 9.0; ACT: –1.5 V 180 s in 0.5M $H_2SO_4$ between each measurement | 5.06[B] | pharmaceutical formulations | [165] |

| | | | | | |
|---|---|---|---|---|---|
| tadalafil | CP/commercial BDD film (Adamant Technologies, Switzerland), B/C ratio 8000 ppm;<br>CP: –0.5 A 120 s in 0.5M $H_2SO_4$ | SWV in 0.04M BR buffer pH 4.0 | 0.0423[A] | pharmaceutical formulations | [166] |
| tenofovir | PP/commercial BDD (Windsor Scientific, UK), B/C ratio 1000 ppm;<br>PP: polished with alumina slurry | SWV in 0.04M BR buffer pH 4.0 | 0.56[D] | pharmaceutical formulations | [167] |
| **Food and/or beverage components and additives** | | | | | |
| caffeine (CAF)<br>vanillin (VAN) | AP/commercial BDD (Windsor Scientific, UK), B/C ratio 1000 ppm;<br>AP: +1.8 V 180 s in 0.5M $H_2SO_4$ | SW-AdSV in 0.1M phosphate buffer pH 2.5;<br>ACT: +1.8 V 60 s in 0.5M $H_2SO_4$ between each measurement | CAF: 0.366[B]<br>VAN: 1.54[B] | simultaneous in food (vanilla sugar, foamy instant coffee) and drink (cola) samples | [168] |
| caffeine<br>5-*O*-caffeoylquinic acid<br>vanillin | CP/commercial BDD (Windsor Scientific, UK), B/C ratio 1000 ppm;<br>CP: –1.7 V 180 s in 0.5M $H_2SO_4$ | SW-AdSV in 0.1M $HNO_3$;<br>ACT: –1.7 V 180 s in 0.5M $H_2SO_4$ between each measurement | CAF: 0.15[B]<br>5-CQA: 0.40[B]<br>VAN: 0.38[B] | simultaneous in food (vanilla sugar, instant coffee) and drink (cola) samples | [169] |
| phlorizin | CP/commercial BDD (Windsor Scientific, UK), B/C ratio 1000 ppm; CP: +2.0 V 180 s and –2.0 V 180 s in 1M $H_2SO_4$ | SWV in 0.04M BR buffer pH 6.0 | 0.23[B] | apple root extracts and spiked urine samples | [170] |
| theobromine | as-received/screen-printed BDD electrode (CBDD110, Dropsens, Spain), B/C ratio 2500 ppm | DPV and SWV in 0.1M $H_2SO_4$;<br>ACT: rinsed with deionized water every ten measurements | DPV: 0.42[D]<br>SWV: 0.51[D] | chocolate products | [171] |

| **Pesticides** | | | | | |
|---|---|---|---|---|---|
| bentazone | CP/commercial BDD (Windsor Scientific, UK), B/C ratio 1000 ppm; CP: +2.0 V 180 s and –2.0 V 180 s in 0.5M $H_2SO_4$ | SWV and DPV in BR buffer pH 4.0 | SWV: 1.2[D]<br>DPV: 0.5[D] | spiked river water samples | [172] |
| carbaryl (CR)<br>carbendazim (CD) | CP/BDD film (CSEM, Switzerland), B/C ratio 8000 ppm;<br>CP: +3.0 V 10 min and –3.0 V 10 min | SWV in 0.1M BR buffer pH 6.0;<br>ACT: –3.0 V 30 s when necessary | CR: 1.5[E]<br>CD: 2.1[E] | simultaneous in plant infusions | [173] |
| clomazone | as-deposited/commercial BDD (Windsor Scientific, UK), B/C ratio 1000 ppm | SWV in 0.04M BR buffer pH 2.0 | 0.21[A] | spiked river water samples | [174] |
| 2,4-dichlorophenoxyacetic acid (2,4-D)<br>diuron (DI)<br>tebuthiuron (TB) | CP/commercial BDD film (Adamant Technologies, Switzerland), B/C ratio 8000 ppm,<br>CP: –2.0 V 120 s in 0.5M $H_2SO_4$ | DPV in 0.1M $H_2SO_4$;<br>SPE preconcentration | 2,4-D: 0.12[E]<br>DI: 0.035[E]<br>TB: 0.34[E] | simultaneous in spiked lake and well water samples | [175] |
| fenthion | CP/BDD film, B/C ratio 8000 ppm;<br>CP: +3.0 V 10 min and –3.0 V 10 min | SWV in 0.1M $Na_2HPO_4$ pH 4.0 | 0.080 | *Passiflora alata* herbal medicinal tinctures | [176] |
| formetanate | CP/BDD film (CSEM, Switzerland), B/C ratio 8000 ppm; CP: +3.0 V 30 s and –3.0 V 60 s in 0.5M $H_2SO_4$ | SWV in BR buffer pH 7.0;<br>ACT: 30 s mechanical stirring between measurements | 0.37[K] | fruits (mango, grape) | [177] |
| maneb | CP/commercial BDD (Windsor Scientific, UK), B/C ratio 1000 ppm;<br>CP: rubbed with a piece of damp silk sloth, then +2.0 V 180 s and –2.0 V 180 s 1.0M $H_2SO_4$ | DPV in 0.04M BR buffer pH 5.0 | 0.024[D] | river water samples | [178] |

| | | | | | |
|---|---|---|---|---|---|
| methomyl | CP/type of BDD not given; CP: +3.0 V 120 s and –3.0 V 240 s in 0.5M $H_2SO_4$ | SWV in 0.1M BR buffer pH 3.0, DPV in 0.1M BR buffer pH 2.0; ACT: +3.0 V 120 s and –3.0 V 240 s in 0.5M $H_2SO_4$ between measurement at different pH values | SWV: 19 DPV: 1.2 | pesticide formulation and spiked river and tap water samples | [179] |
| oxycarboxin | PCP/commercial BDD (Windsor Scientific, UK), B/C ratio 1000 ppm; PCP: sonicated for 5 min, then 10 cycles from –0.35 V to +1.85 V in 0.1M $H_2SO_4$ 100 mV $s^{-1}$ | SWV in 0.04M BR buffer pH 4.0 | 1.6[D] | spiked river water samples | [180] |
| pethoxamid | CP/commercial BDD (Windsor Scientific, UK), B/C ratio 1000 ppm; CP: +2.0 V 180 s and –2.0 V 180 s in 0.5M $H_2SO_4$ | SWV in BR buffer pH 4.0; ACT: slightly polished with cotton between each measurement | 1.37[E] | pesticide formulation and spiked river water samples | [181] |
| pirimicarb | CP/commercial BDD film (NeoCoat SA, Switzerland), B/C ratio 8000 ppm; CP: +3.0 V 5 s and –3.0 V 60 s in 0.5M $H_2SO_4$ | DPV in 1mM phosphate buffer pH 7.0 with 20% acetonitrile | 1.24[E] | spiked tap and weir water samples | [182] |
| **Others** | | | | | |
| ergosterol | CP/commercial BDD (Windsor Scientific, UK), B/C ratio 1000 ppm; CP: +2.0 V 180 s and –2.0 V 180 s in 1M $H_2SO_4$ | SWV in acetonitrile + 0.1M tetrabutylammonium hexafluorophosphate ACT: slightly clean with cotton between each measurement | 0.7[D] | fungi extract | [183] |

| | | | | | |
|---|---|---|---|---|---|
| indole (IND)<br>tryptophan (TRY) | PP/commercial BDD (Windsor Scientific, UK), B/C ratio 1000 ppm;<br>PP: polished with alumina slurry | DPV in 0.2M TBAH in acetonitrile | IND: 0.50[A]<br>TRY: 0.42[A] | simultaneous monitoring of their level during the bacterial growth | [184] |
| phenetylamines (25I-NBOMe, 25B-NBOMe, 25C-NBOMe, 2C-B) | CP/commercial BDD film (NeoCoat SA, Switzerland), B/C ratio 8000 ppm;<br>CP: +0.001 A 120 s and –0.03 A 360 s in 0.5M $H_2SO_4$ | SWV in 0.1M acetate buffer pH 4.0 with 10% methanol | 25I-NBOMe: 0.1<br>25B-NBOMe: 0.1<br>25C-NBOMe: 0.27<br>2C-B: 0.1 | blotting paper samples, no interference of LSD | [185] |
| ricin | CP/BDD film (CSEM, Switzerland), B/C ratio 8000 ppm; CP: +3.0 V 60 s and –3.0 V 120 s in 0.5M $H_2SO_4$ | SW-AdSV in 0.1M $H_2SO_4$ pH 1.0; ACT: +3.0 V 60 s and –3.0 V 120 s in 0.5M $H_2SO_4$ between each measurement | 0.00062 | castor seed cultivars | [186] |

BR buffer – Britton–Robinson buffer, CTAB – cetyltrimethylammonium bromide, HDTMAB – hexadecyltrimethylammonium bromide, SDS – sodium dodecyl sulfate, TBAH – tetrabutylammonium hexafluorophosphate, TRIS buffer – tris(hydroxymethyl)aminomethane hydrochloride;
BDD electrode pretreated anodically (AP), cathodically (CP), by polishing (PP), by potential cycling (PCP) or untreated (as-deposited/as-received);
ACT – activation program; EA-HFCVD – electron assisted hot filament chemical vapor deposition, MW-PECVD – microwave plasma enhanced chemical vapor deposition;
DCV – direct current voltammetry, DPV – differential pulse voltammetry, LSV – linear sweep voltammetry, SWV – square wave voltammetry, SW-AdSV – square wave adsorptive stripping voltammetry;

Limit of detection (LOD) calculated as: [A] – signal-to-noise ratio equal to three, [B] – three times standard deviation of the peak current of the lowest level concentration of the calibration curve divided by the slope of the related calibration equation, [C] – 3.3 times standard deviation of ten repetitive measurements of the lowest measurable concentration divided by slope of the calibration curve, [D] – three times standard deviation of intercept divided by slope of the linear calibration dependence, [E] – three times the standard deviation of the current response of the blank solution divided by the slope of the calibration curve, [F] – concentration of the analyte which gave a signal equal to three times the standard deviation of the peak height estimated from seven/ten consecutive measurements of the lowest measurable concentration, [G] – 3.3 times residual standard deviation $s_{y/x}$ divided by the slope of the calibration plot, [H] – lowest concentration giving rise to the signal $s_t$ satisfying the following equation $s_t \geq s_b + 3s$, where $s_t$ is the gross analyte signal, $s_b$ is the field blank signal and $s$ is standard deviation of five blank determinations, [I] – three times standard deviation of noise calculated from background response of BDD electrode divided by slope of the calibration curve, [J] – 3.2 times standard deviation of the regression line divided by slope of the regression line, [K] – standard deviation of y-residuals.

# 3. Results and discussion

This chapter describes a summary of the seven scientific publications that were mentioned at the beginning of this Thesis. The individual publications are enclosed in the Appendix part, where all the details of the experiments are specified.

## *3.1 Boron doped diamond electrodes in voltammetry: New designs and applications. An overview (Appendix I, ref. [1])*

The purpose of this publication [1] was to summarize the progress in the development and applications of bare BDD electrodes in voltammetry of organic compounds. It follows the review [15] where the development of electroanalysis by means of BDD electrodes since the beginnings in 1992 is summarized. The main topics are fouling and pretreatment of the BDD surface, influence of boron content on electrochemical properties of BDD electrodes and response of organic analytes, utilization of BDD electrodes in adsorptive stripping voltammetry. Examples of selected applications of bare BDD electrodes for voltammetric determination of organic analysis demonstrating the above mentioned topics are given. This publication was the basis for the introduction chapter of this Thesis. Selected figures and more detailed information are shown in Appendix I.

## *3.2 Influence of boron content on the morphological, spectral, and electroanalytical characteristic of anodically oxidized boron doped diamond electrodes (Appendix II and III, ref. [2, 3])*

The experiments presented in the publications [2, 3] represent a consistent study of the effect of boron content on the selected morphological, spectral and electrochemical characteristics. For this purpose, a set of anodically pretreated BDD films deposited by microwave plasma-assisted chemical vapor deposition with variable B/C ratio in gas phase 500 – 8000 ppm was employed.

Spectral properties were investigated using scanning electron microscopy, atomic force microscopy and Raman spectroscopy. The results of the first two methods are in good mutual agreement and reveal that the boron content obviously influences the morphology of the studied films. The results from Raman spectroscopy indicate that the

shift of maximum Lorentzian component of diamond phonon at ~1332 $cm^{-1}$ can be assessed as the function of boron concentration.

Cyclic voltammetry with the inner $[Fe(CN)_6]^{3-/4-}$ and outer $[Ru(NH_3)_6]^{3+/2+}$ sphere redox markers were measured (selected voltammograms depicted in Figure 5) and important parameters were evaluated. These include parameters of the linear dependences of the peak height $I_p$ of these markers on square root of the scan rate $v^{1/2}$, ratio of the anodic and cathodic peak heights $I_{pa}/I_{pc}$, dependence of the peak potential difference between cathodic and anodic peak $\Delta E_p$ on $v^{1/2}$, and values of apparent heterogenous electron-transfer rate constant $k^{\circ}_{app}$, calculated from $\Delta E_p$ at the scan rate 300 mV $s^{-1}$. These characteristics enable to differentiate among the semiconductive films (500 ppm and 1000 ppm) and films with metallic conductivity (2000 ppm, 4000 ppm and 8000 ppm). Nevertheless, only the inner sphere character of $[Fe(CN)_6]^{3-/4-}$ redox marker enables to visualize the differences between individual boron content for metallic films.

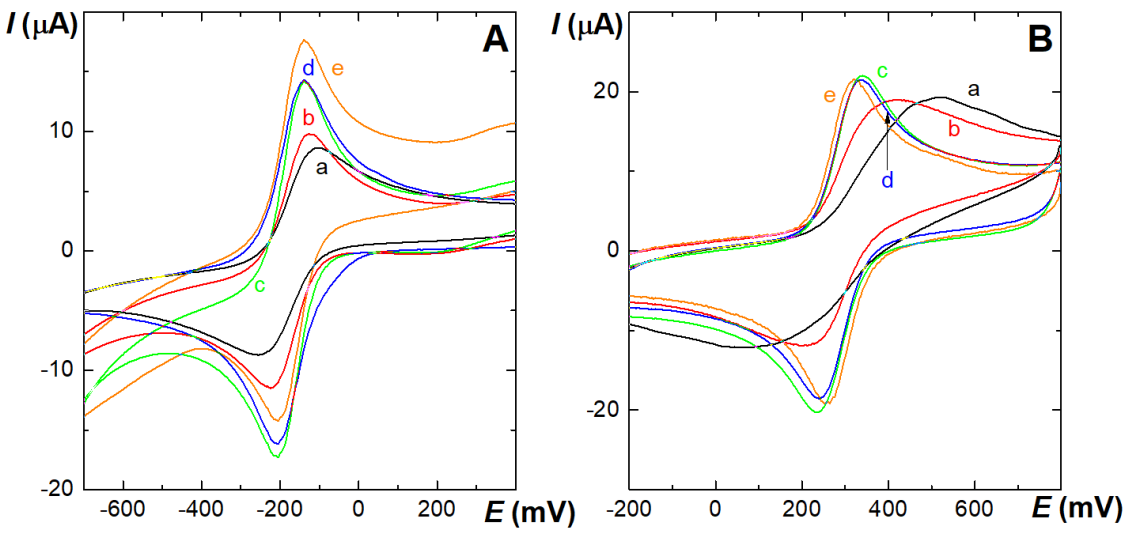


**Figure 5** Cyclic voltammograms of $[Ru(NH_3)_6]^{3+/2+}$ (A) and $[Fe(CN)_6]^{3-/4-}$ (B) (both $c$ = 1 mmol $L^{-1}$ in 1mol $L^{-1}$ KCl) measured at BDD electrode with different boron content: (a) 500 ppm, (b) 1000 ppm, (c) 2000 ppm, (d) 4000 ppm, (e) 8000 ppm. Scan rate $v$ = 300 mV $s^{-1}$. Adjusted from [2].

The width of the potential window in aqueous media of different pH values and in wide variety of supporting electrolytes commonly used in electroanalysis was investigated: 1 mmol $L^{-1}$ $Na_2SO_4$, 1 mol $L^{-1}$ KCl, 0.1 mol $L^{-1}$ $HClO_4$, 0.1 mol $L^{-1}$ acetate buffer pH 4.0, 0.1 mol $L^{-1}$ phosphate buffer pH 7.0, and 0.05 mol $L^{-1}$ borate buffer pH 9.0. It is obvious from the obtained voltammograms that, in general, the width of the potential window decreases with the increasing boron content, with independence of anodic potential limit for 2000 – 8000 ppm electrodes and more pronounced dependence of cathodic potential limit on boron content for all tested BDD films.

Next, we have studied electrochemical behavior and analytical parameters for the determination of 2-aminobiphenyl in Britton–Robinson buffer pH 7.0 (supporting electrolyte optimized in study [4]), so the comparison of linear sweep and differential pulse voltammetry at all tested BDD electrodes with boron doping level 500 – 8000 ppm was made. 2-aminobiphenyl was selected as a model analyte. Its amino group on aromatic skeleton is easily oxidizable within the potential window of BDD electrodes. Problems with electrode fouling had to be overcome by anodic pretreatment directly in the analyte solution by applying the potential +2.4 V (vs. Ag/AgCl/3 mol $L^{-1}$ KCl) for 30 s between individual measurements. Contrary to differential pulse voltammetry, where the height of symmetric peaks increases with increasing boron content, in linear sweep voltammetry the boron doping level influences the peak shape. Calibration dependences of 2-aminobiphenyl for all tested electrodes were obtained by differential pulse voltammetry in the concentration range of 0.25 – 50 μmol $L^{-1}$. An example representing differential pulse voltammograms obtained at 8000 ppm BDD film is given in Figure 6. The sensitivity is ca 2.5 times higher for the 8000 ppm electrode than for the 500 ppm electrode; the limits of detection being in the 0.21 – 0.80 μmol $L^{-1}$ concentration range for all tested electrodes.

To conclude, anodically oxidized BDD films deposited at B/C ratio 500 ppm – 8000 ppm were tested. Boron concentration was assessed as function of Raman shift at <1332 $cm^{-1}$. Cyclic voltammograms of $[Ru(NH_3)_6]^{3+/2+}$ and $[Fe(CN)_6]^{3-/4-}$ were used to assess the type of conductivity. Differential pulse voltammetric signal of 2-aminobiphenyl increases with boron doping level. More details can be found in Appendix II and III.

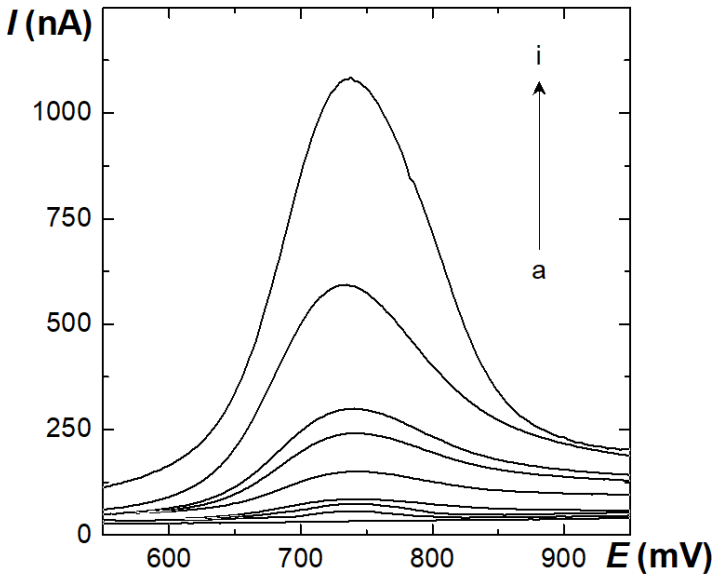


**Figure 6** Differential pulse voltammograms of calibration dependence of 2-aminobiphenyl in Britton–Robinson buffer pH 7.0, concentration of 2-aminobiphenyl (μmol $L^{-1}$): a) 0; b) 0.5; c) 1.0; d) 2.5; e) 5.0; f) 7.5; g) 10; h) 25; i) 50. Recorded at BDD film, B/C ration 8000 ppm. Adjusted from [2].

*3.3 Voltammetric and amperometric determination of mixtures of aminobiphenyls and aminonaphthalenes using boron doped diamond electrode (Appendix IV, ref. [4])*

In this work [4], an anodically pretreated BDD electrode was used for the voltammetric and amperometric determination of the genotoxic pollutants 1-aminonaphthalene (1-AN), 2-aminonaphthalene (2-AN), 2-aminobiphenyl (2-AB), and 4-aminobiphenyl (4-AB). For all electrochemical measurements, a microcrystalline BDD film deposited on silica wafers (preparation and characterization described in [84]) placed in a laboratory-made BDD disc electrode (active geometric area 12.6 $mm^2$) [123] was used.

Firstly, differential pulse voltammetry was used for the exploration of fouling of the electrode surface in the presence of 1-aminonaphthalene and 2-aminonaphthalene in analysed solution, because passivating films are formed as result of dimerization and further polymerization of nitrene cation radicals – products of initial one-electron oxidation of the amino group [124, 125]. Passivation of the electrode surface was visualized by the decrease of their peak heights at repetitive differential pulse

voltammograms of about 80 % and potential shift of ca 35 mV to more positive value during consecutive 10 scans (Figure 7). This problem was solved by an electrochemical activation program consisting of stirring and applying the potential of +2.4 V for 15 s on the BDD working electrode in analysed solution. As result, for ten repetitive differential pulse voltammograms of 1-aminonaphthalene ($c = 1 \times 10^{-5}$ mol $L^{-1}$ in Britton–Robinson buffer pH 5.0) reproducible peak heights with relative standard deviation 2.0 % were obtained.

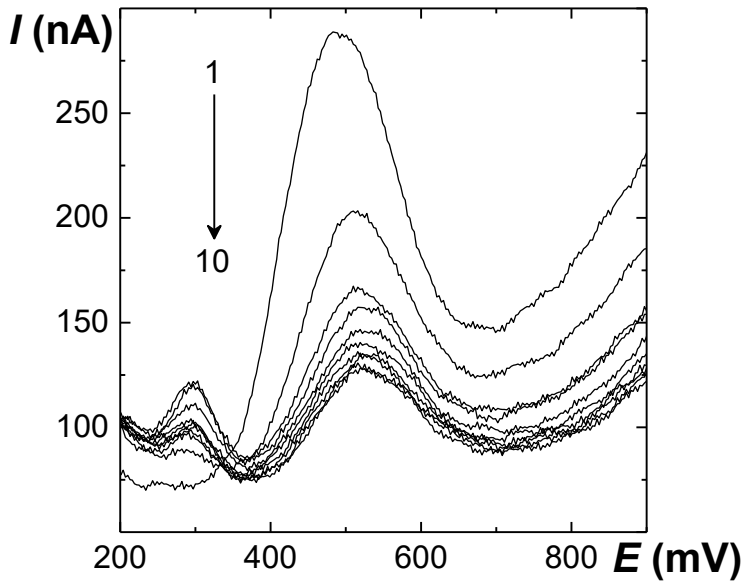


**Figure 7** Ten differential pulse voltammograms of 1-aminonaphthalene ($c = 1 \times 10^{-5}$ mol $L^{-1}$) in Britton–Robinson buffer pH 5.0 without treatment of BDD electrode surface between scans. Adjusted from [4].

Then, the influence of pH on signal of aminonaphthalenes ($c = 1 \times 10^{-5}$ mol $L^{-1}$) was investigated by differential pulse voltammetry in Britton–Robinson buffer in the range of pH 2.0 – 12.0. 1-aminonaphthalene gives four peaks in the range of pH 2.0 – 6.0 and one peak at pH 7.0 – 12.0. 2-aminonaphthalene offers four peaks in the region of pH 2.0 and 3.0, three peaks at pH 4.0, and only one peak at pH 5.0 – 12.0. More details are described in Appendix IV. For electroanalytical purposes, the pH 7.0

was chosen as optimal for both aminonaphthalenes based on the presence of one symmetric peak.

Calibration dependences of aminonaphthalenes were obtained by differential pulse voltammetry in the concentration range 1 – 100 μmol $L^{-1}$ under optimized condition (Britton–Robinson buffer pH 7.0, activation program between each measurement). Results of calibration dependences for other two compounds, 2-aminobiphenyl and 4-aminobiphenyl, are taken from our previous study [126]. The details about linearity and other parameters of all compounds are summarized in Appendix IV. Limits of determination were obtained in the range from 0.25 μmol $L^{-1}$ for 4-aminobiphenyl to 2.96 μmol $L^{-1}$ for 1-aminonaphthalene.

Also, an attempt to use differential pulse voltammetry for simultaneous determination of studied compounds, including fifth analyte 3-aminobiphenyl, was made. The simultaneous determination was possible only for the pair of 2-aminobiphenyl/4-aminobiphenyl or 3-aminobiphenyl/4-aminobiphenyl using Britton–Robinson buffer pH 12.0 as a supporting electrolyte. For pH 7.0 and pH 9.0, the optimum pH values for the individual determination of 2-aminobiphenyl and 4-aminobiphenyl, the differences of peak potentials are insufficient. 1-aminonaphthalene and 2-aminonaphthalene could not be determined in the mixtures, because the difference of the oxidation potential is too small with respect to each other and to all tested aminobiphenyls. Details of these simultaneous determinations are listed in Appendix IV.

Further, amperometric detection coupled with HPLC at BDD electrode in wall-jet arrangement was used to detect the mixture of 1-aminonaphthalene, 2-aminonaphthalene, 2-aminobiphenyl, and 4-aminobiphenyl after their separation using reversed phase system. To prevent the passivation of electrode surface, the activation program mentioned above was used on-line for all HPLC measurements. Based on the previous studies [127, 128], the optimization of the mobile phase (organic modifier acetonitrile and 0.01 mol $L^{-1}$ phosphate buffer) was carried out. Tested content of acetonitrile was 30 %, 35 % and 40 %, the buffer pH was changed in the range 2.0 – 5.0. Under all tested conditions the analytes were eluted in the order 2-aminonaphthalene, 1-aminonaphthalene, 4-aminobiphenyl, 2-aminobiphenyl. Optimum mobile phase consisting of acetonitrile and 0.01 mol $L^{-1}$ phosphate buffer pH 3.0 (40:60, v/v) and the flow rate of 1 mL $min^{-1}$ secured elution time of 9.8 min of the lastly eluted 2-aminobiphenyl and was used for further studies.

Next, the detection potential $E_{det}$ imposed on the working electrode was optimized in the range from +500 mV to +1500 mV in a step of 100 mV, and the peak heights of tested analytes and absolute value of the background current were evaluated. Detection potential +1000 mV was selected as optimum based on stable background current and satisfactory peak heights.

The calibration dependences were obtained in the concentration range from 0.02 to 10 μmol $L^{-1}$. The parameters of these dependences are summarized in Appendix IV. Limits of determination reached values 0.06 μmol $L^{-1}$ for 2-aminonaphthalene, 0.07 μmol $L^{-1}$ for 1-aminonaphthalene, 0.13 μmol $L^{-1}$ for 4-aminobiphenyl, and 0.20 μmol $L^{-1}$ for 2-aminobiphenyl. Selected chromatograms of calibration dependences are depicted in Figure 8A.

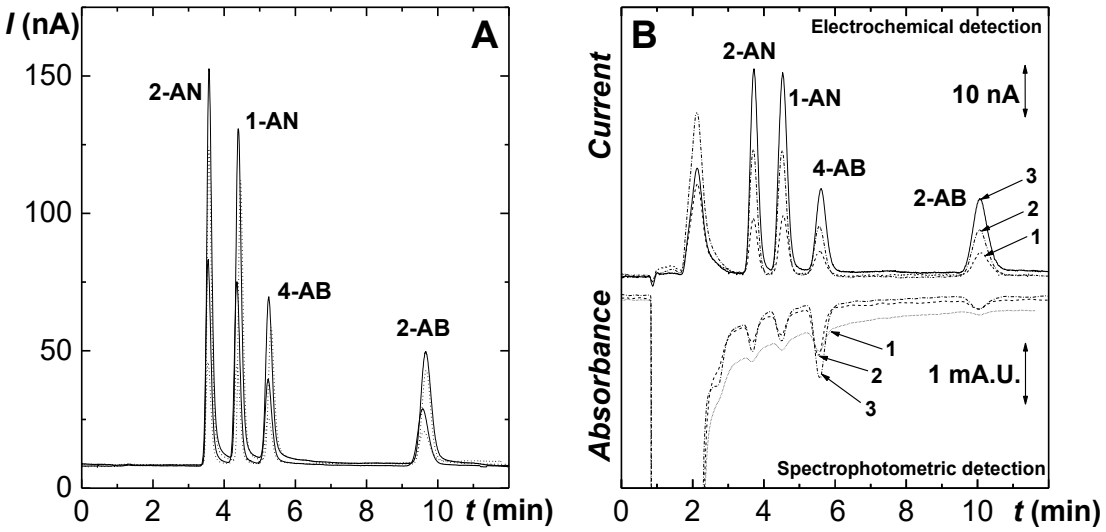


**Figure 8** (**A**) Chromatograms of the mixture of 2-AN, 1-AN, 4-AB, and 2-AB using HPLC with amperometric detection at BDD electrode, concentration of analytes 2, 4, 6, and 8 μmol $L^{-1}$. (**B**) Chromatograms of the mixture of 2-AN, 1-AN, 4-AB, and 2-AB after solid phase extraction from 10 mL of sunset yellow solution (0.1 g $mL^{-1}$) recorded using electrochemical detection at BDD electrode in wall-jet arrangement and UV detection. Concentrations of the analytes 0.25 (**1**), 0.5 (**2**), and 0.75 (**3**) μmol $L^{-1}$; eluent acetonitrile 2 mL. Measured by HPLC-ED/UV, column LichroCART® 125-4 Purospher®STAR RP-18e (5 μm), mobile phase acetonitrile and 0.01 mol $L^{-1}$ phosphate buffer pH 3.0 (40:60, v/v), injection volume 20 μL, $Q$ = 1.0 ml $min^{-1}$, $E_{det}$ = +1.0 V, $\lambda_{det}$ = 290 nm. Adjusted from [4].

The developed high performance liquid chromatography with electrochemical detection was used for the determination of mixture of aminonaphthalenes and aminobiphenyls in the synthetic colorant sunset yellow (E 110). Due to the large system peak that interfered with the evaluation after direct injection of dye, solid phase extraction was used to eliminate the influence of the dye matrix and to preconcentrate the tested compounds. Two different cartridges and procedures were applied (details in Appendix IV). Obtained calibration dependences are linear from 0.0075 to 1 μmol $L^{-1}$ and limits of determination reached values 4.62 nmol $L^{-1}$ for 2-aminonaphthalene, 4.98 nmol $L^{-1}$ for 1-aminonaphthalene, 11.3 nmol $L^{-1}$ for 4-aminobiphenyl, and 14.1 nmol $L^{-1}$ for 2-aminobiphenyl. Selected chromatograms of calibration dependences recorded using electrochemical and UV detection are depicted in Figure 8B.

This work presents a valuable contribution to the electroanalysis of amino derivatives of biphenyl and naphthalene with genotoxic and carcinogenic potential. The electrochemical methods represent an inexpensive, fast, and relatively selective independent alternative to the highly advanced methods such as high performance liquid chromatography with fluorescence detection. Details are shown in Appendix IV.

### *3.4 Carbon-based electrodes for sensitive electroanalytical determination of aminonaphthalenes (Appendix V, ref. [5])*

In the publication [5], the electroanalytical performance of bare BDD electrode for determination of 1-aminonaphthalene and 2-aminonaphthalene was compared with other types of carbon-based materials, specifically with glassy carbon (bare and modified by a Nafion permselective membrane or multiwalled carbon nanotubes) and carbon film.

Firstly, the electrochemical behavior of 1-aminonaphthalene and 2-aminonaphthalene at glassy carbon electrode was investigated by cyclic voltammetry. The linear dependence of current density on square root of scan rate indicates a diffusion-controlled electrochemical process for both compounds. A decrease of the oxidation peak currents of selected aromatic amines was observed after successive cycling without cleaning the electrode surface between individual scans. Because electrochemical pretreatment of glassy carbon electrode surface was inefficient, mechanical cleaning was done after each scan (details in Appendix V or [5]).

Afterwards, differential pulse voltammetry was applied to find out the effect of pH on the current and peak potential of aminonaphthalenes measured at glassy carbon electrode in Britton–Robinson buffer (pH from 2 to 11). Both aminonaphthalenes exhibit one peak at pH 2.0 and two peaks in the range 3.0 – 11.0. The influence of differential pulse voltammetry scan parameters on the response of 1-aminonaphthalene at bare glassy carbon electrode was also investigated. The parameters were pulse amplitude (50 mV), pulse time (25 and 50 ms), potential step (2 and 4 mV), and scan rate (5 and 10 mV $s^{-1}$). Based on the highest and best shaped peak, the pH 2.0, pulse amplitude 50 mV, pulse time 50 ms, potential step 2 mV, and scan rate 5 mV $s^{-1}$ were chosen as the optimum values.

Under the optimum conditions, the determination of both aminonaphthalenes was performed by differential pulse voltammetry at bare glassy carbon electrode. Further, the effect of the modification of the glassy carbon electrode surface with Nafion or multiwalled carbon nanotubes for 1-aminonaphthalene was tested and analytical parameters were compared with other bare carbon surfaces – BDD and carbon film electrode. A comparison of analytical figures of merit is given in Table 3 and differential pulse voltammograms of 20μmol $L^{-1}$ 1-aminonaphthalene for all investigated surfaces are depicted in Figure 9.

**Table 3** Analytical parameters of linear dependences for the determination of 1-aminonaphthalene and 2-aminonaphtahalene by differential pulse voltammetry at different types of electrodes in Britton–Robinson buffer pH 2.0. Adjusted from [5].

| Electrode | LDR (μmol $L^{-1}$) | Sensitivity (nA μmol$^{-1}$ L cm$^{-2}$) | LOD (μmol $L^{-1}$) | Pretreatment | RSD[a] (%) |
|---|---|---|---|---|---|
| ***1-aminonaphthalene*** | | | | | |
| BDD | 2 – 20 | 282 | 1.4 | electrochemical | 3.8 |
| CFE | 2 – 20 | 80 | 3.1 | without | 16.0 |
| GCE | 2 – 100 | 257 | 1.6 | mechanical | 4.3 |
| Nafion/GCE | 0.2 – 20 | 302 | 0.4 | without | 9.8 |
| MWCNT/GCE | 10 – 100 | 229 | 11.6 | without | 12.9 |
| ***2-aminonaphthalene*** | | | | | |
| GCE | 2 – 100 | 358 | 2.0 | mechanical | 4.4 |

CFE – carbon film electrode; GCE – glassy carbon electrode; LDR – linear dynamic range; LOD – limit of detection; MWCNT – multiwalled carbon nanotubes; [a] repeatability of peak height expressed by relative standard deviation for concentration $c$ = 20 μmol $L^{-1}$, $n$ = 4.

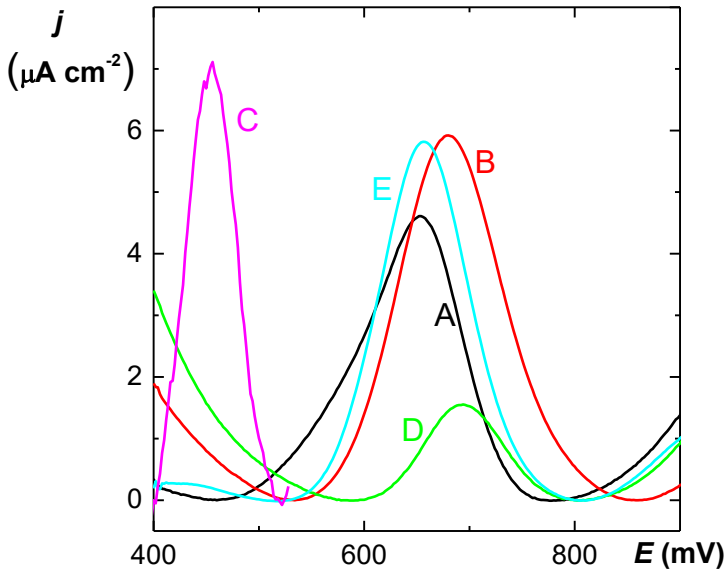


**Figure 9** Differential pulse voltammograms of 1-aminonaphthalene ($c$ = 20 μmol $L^{-1}$) at (**A**) bare glassy carbon electrode, (**B**) Nafion/glassy carbon electrode, (**C**) multiwalled carbon nanotubes/glassy carbon electrode, (**D**) carbon film electrode, and (**E**) BDD electrode in Britton–Robinson buffer pH 2.0, after baseline subtraction. Adjusted from [5].

Also, differential pulse voltammetry was used for the simultaneous determination of the two analytes in a mixture based on the presence of one peak and the difference of peak potentials of 1-aminonaphthalene ($E_p$ = +658 mV) and 2-aminonaphthalene ($E_p$ = +726 mV) at a glassy carbon electrode in Britton–Robinson buffer pH 2.0. The responses showed linear dependences in the range from 2 to 10 μmol $L^{-1}$ and micromolar limits of detection were obtained, namely 1.9 and 1.6 μmol $L^{-1}$ for 1-aminonaphthalene and 2-aminonaphthalene, respectively.

The practical applicability of the proposed method was tested by the determination of 1-aminonaphthalene and 2-aminonaphthalene in model samples of river water. For both analytes and both tested concentrations (50 and 100 μmol $L^{-1}$ for each analyte), high recoveries (91 – 102 %) with repeatability < 5 % (expressed by relative standard deviation, $n$ = 5) were obtained.

Blocking of the electrode surface was a problem for all types of bare electrode surface, but it could be eliminated by mechanical polishing of glassy carbon electrode or

by anodic pretreatment of BDD electrode. Modified electrodes do not require any cleaning.

It can be concluded that Nafion/glassy carbon electrode is the most sensitive electrode material of those tested, with the lowest limit of detection, and with simple handling. However, highly reproducible responses, with easy recovery of the electrode surface can be obtained at unmodified GCE and this electrode exhibited a wider linear range, which is more suitable for practical applications. [5]. For details see Appendix V.

### *3.5 Boron doped diamond electrodes for voltammetric determination of benzophenone-3 (Appendix VI, ref. [6])*

In this study [6], the influence of boron concentration in BDD films on electrochemical oxidation of benzophenone-3 and opportunities to influence its electroanalytical performance by the presence of surfactant were explored.

Benzophenone-3 is used as ultraviolet filter in sunscreens and various consumers' products. As an endocrine disruptor, benzophenone-3 can negatively influence living organisms by disturbing hormonal equilibrium [129-132].

Two types of boron doped diamond electrodes were used as working electrodes. For investigation of voltammetric behavior of benzophenone-3 in the absence of surfactant, BDD films (variable B/C ratio in the gas phase 500, 1000, 2000, 4000, and 8000 ppm) prepared at the Institute of Physics of the ASCR, v. v. i. in the Department of Functional Materials were used. Details of preparation are given in Appendix VI. These electrodes were marked as $BDD_A$ in this work with specification of boron content in the BDD film. For voltammetric determination of benzophenone-3 in the presence of surfactant, commercially available BDD electrode with B/C ratio 1000 ppm (Windsor Scientific, UK), further marked as $BDD_B$, were used. All working electrodes were activated at the beginning of each working day in 0.5 mol $L^{-1}$ sulfuric acid by oxidation at +2.4 V for 60 s.

For optimization, $BDD_A$ with B/C ratio 2000 ppm was utilized. The first experiments have shown the oxidation of benzophenone-3 caused passivation of the electrode surface. Different electrochemical activation programs (details in Appendix VI) were tested either directly in the measured solution or *ex situ* in 0.5 mol $L^{-1}$ sulfuric acid. Most of these programs were inefficient, only one was applicable: *ex situ*

activation in 0.5 mol $L^{-1}$ sulfuric acid by switching of potentials +3, –3, +3, –3, +3 V each for ten seconds.

Further, the effect of pH on the current and peak potential of benzophenone-3 was investigated at $BDD_A$ (2000 ppm) in Britton–Robinson buffer with pH values ranging from 2.0 to 12.0. With the increasing pH a gradual shift of the peak potential towards less positive values was observed. Substantially higher peak current was observed at pH 12.0, thus it was used for further electroanalytical measurements.

Considering that benzophenone-3 is practically water insoluble, but solubility in organic solvents is reasonable, and thus its determination in daily care products requires dilution or extraction with an organic solvent [133, 134], the influence of methanol and/or acetonitrile content in analysed solution on peak height and peak position of benzophenone-3 was studied. Two sets of benzophenone-3 solutions ($c = 1 \times 10^{-4}$ mol $L^{-1}$) in Britton–Robinson buffer pH 12.0 containing 1 %, 2 %, 10 %, 20 %, 50 %, 70 %, and 80 % (*v/v*) of methanol or acetonitrile, were prepared and analysed by differential pulse voltammetry at $BDD_A$ (2000 ppm). The shift of peak potential toward less positive values independent of the concentration of organic solvent in solution was observed. Simultaneously, the peak height of benzophenone-3 decreases with an increasing percentage of methanol or acetonitrile. Also, the background current increases. For further experiments, it was continued without presence of organic solvents in measured solution.

Then, a set of $BDD_A$ films with boron content of 500, 1000, 2000, 4000, and 8000 ppm were compared. The boron content, in BDD films given as number of boron atoms per $cm^3$, influences conductivity of $BDD_A$ electrode [81, 87]. Our previous study [2] revealed that for our set of electrodes the limit lies between films with boron content of 1000 ppm exhibiting semiconductive properties and 2000 ppm film with metallic type conductivity. This is confirmed by DP voltammograms of benzophenone-3 where the peak height of benzophenone-3 increases with increasing boron content. For 500 ppm and 1000 ppm $BDD_A$, *i.e.* semiconductive films, the peak of benzophenone-3 is not fully developed. Films with boron doping level 2000 ppm and higher provide symmetric and well-shaped peaks. Further, the peak potential of benzophenone-3 is moving toward less positive values as concentration of boron in films increases, similarly as in previous study with aminobiphenyls [2].

Further, the influence of presence of surfactant cetyltrimethylammonium bromide (CTAB) on benzophenone-3 peak height at $BDD_B$ electrode

in Britton–Robinson buffer pH 9.0 was studied. From cyclic voltammograms depicted in Figure 10A it is evident that the presence of surfactant markedly influences shape, height and position of oxidation peak as the result of electrostatic interaction of the cationic surfactant CTAB with anionic form of benzophenone-3 in pH 9.0 ($pK_{a,\ BP\text{-}3}$ value 7.56). The peak potential shift is also great advantage because the oxidation peak of benzophenone-3 in the absence of surfactant is relatively close to the onset of supporting electrolyte. As the next step, the dependence of benzophenone-3 peak height on concentration of CTAB was investigated. The dependence depicted in Figure 10B shows that the highest peak of benzophenone-3 ($c = 5 \times 10^{-5}$ mol $L^{-1}$) was achieved with the concentration of CTAB $1 \times 10^{-4}$ mol $L^{-1}$.

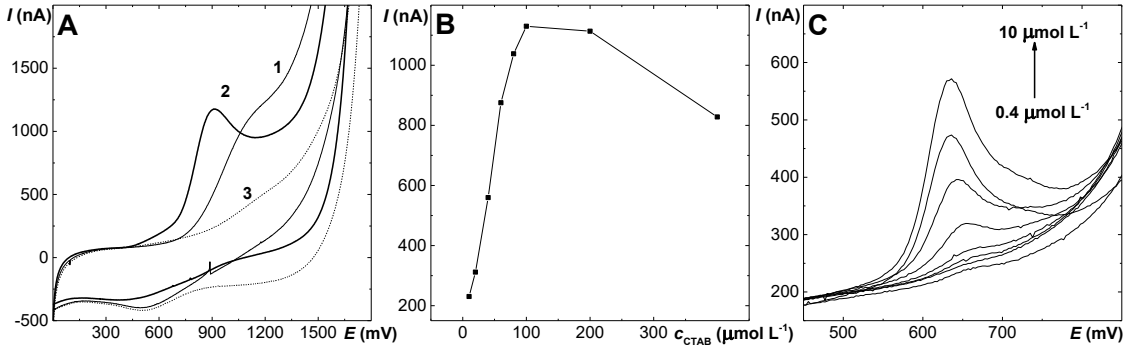


**Figure 10** **(A)** Cyclic voltammograms of benzophenone-3 ($c = 5 \times 10^{-5}$ mol $L^{-1}$) without presence of surfactant (thin line 1) and in the presence of surfactant (bold 2) CTAB ($c = 1 \times 10^{-3}$ mol $L^{-1}$) at $BDD_B$ electrode in Britton–Robinson buffer pH 9.0 (dashed 3). Scan rate 100 mV $s^{-1}$. **(B)** Dependence of peak height of benzophenone-3 ($c = 5 \times 10^{-5}$ mol $L^{-1}$) on the concentration of CTAB. Recorded by differential pulse voltammetry at $BDD_B$ electrode in 0.01mol $L^{-1}$ NaOH. The error bars are constructed as standard deviation of peak height of benzophenone-3. **(C)** Differential pulse voltammograms of benzophenone-3 measured at $BDD_B$ in 0.01mol $L^{-1}$ NaOH in the presence of surfactant CTAB ($c = 1 \times 10^{-4}$ mol $L^{-1}$). Concentration of benzophenone-3: 0.4, 0.6, 0.8, 1.0, 2.5, 5.0, 7.5, and 10 μmol $L^{-1}$. Adjusted from [6].

Calibration dependences of benzophenone-3 were obtained without the presence of surfactant at $BDD_A$ with boron content of 2000 ppm, 4000 ppm, and 8000 ppm, and with the presence of CTAB ($c = 1 \times 10^{-4}$ mol $L^{-1}$) at $BDD_B$. For 500 ppm and 1000 ppm BDD films, the lowest observable concentration was 100 μmol $L^{-1}$ and from the analytical point of view these measurements were not useful. Concentration dependences are linear practically in the whole concentration range. Selected differential pulse voltammograms are depicted in Figure 10C and parameters of calibration dependences are summarized in the Table 4. For details see Appendix VI.

**Table 4** Selected parameters of concentration dependences of benzophenone-3 at BDD electrodes measured by differential pulse voltammetry. Adjusted from [6].

| Electrode | LDR (μmol $L^{-1}$) | Slope (nA μmol$^{-1}$ L) | Intercept (nA) | LOD (μmol $L^{-1}$) |
|---|---|---|---|---|
| $BDD_A$ 2000 ppm | 1 – 100 | 13.48 | 20.57 | 1.5 |
| $BDD_A$ 4000 ppm | 1 – 100 | 5.90 | 12.28 | 1.9 |
| $BDD_A$ 8000 ppm | 2.5 – 100 | 9.34 | 6.19 | 0.8 |
| $BDD_B$ + CTAB | 10 – 75 | 18.98 | 129.65 | --- |
| | 0.8 – 10 | 29.85 | –19.44 | --- |
| | 0.4 – 0.8 | 13.29 | –1.35 | 0.1 |

LDR – linear dynamic range; LOD – limit of detection

*3.6 Factors influencing voltammetric reduction of 5-nitroquinoline at boron doped diamond electrodes (Appendix VII, ref. [7])*

In this work [7], 5-nitroquinoline with reducible aromatic nitro group and quinoline skeleton at boron doped diamond films with doping level 500, 1000, 2000, 4000 and 8000 ppm was studied by direct current and differential pulse voltammetry. The aim of this study was to extend the knowledge on the electroreduction of nitro and quinoline moieties at boron doped diamond electrodes. 5-nitroquinoline, an environmental pollutant, formed as product of incomplete combustion of fossil fuels, was selected as model compound [135, 136].

Firstly, the mechanism of reduction of 5-nitroquinoline was studied using pH dependence in Britton–Robinson buffer pH 2 – 12 by direct current, differential pulse, and cyclic voltammetry. The signal of the nitro group largely depends on the pH of the measured solution. This dependence is described in detail in section Appendix VII.

As optimum, 0.1 mol $L^{-1}$ acetate buffer pH 5.0 was selected and used for further experiments.

Next, the optimum condition for electrode pretreatment and activation between individual measurements was searched. Anodic and cathodic pretreatment at the potentials +2.4 V for 5 min and –2.4 V for 10 min, respectively, in 0.5 mol $L^{-1}$ sulfuric acid and activation (anodic, cathodic and stirring without applied potential) between individual scans directly in the measured solution were tested. Relatively stable electrode response was achieved for all activation modes, but as the application of anodic and cathodic potentials had no explicitly positive effect, only stirring of 20 s was used to assure repeatable signals. For direct current and differential pulse voltammetry the relative standard deviation values of peak height were 2.1 and 4.6 % for anodic pretreatment and 6.5 and 0.5 % for cathodic pretreatment ($c = 1 \times 10^{-4}$ mol $L^{-1}$, $n = 10$), respectively.

For direct current and differential pulse voltammetry and both types of pretreatment, the calibration dependences were constructed and limits of detection in the $10^{-6}$ and $10^{-7}$ mol $L^{-1}$ were obtained. Parameters of calibration straight lines and limits of detection are summarized in Appendix VII.

Also, boron doping level considerably affects the height of the peak and its potential as shown in Figure 11 (and summarized in Appendix VII). For electrodes 2000, 4000 and 8000 ppm (metallic type of conductivity), the peak heights are comparable and higher than for boron doped diamond electrodes with B/C ratio 500 and 1000 ppm (semiconductive type). The peak potential is shifted to more positive values using electrodes with metallic type of conductivity.

To conclude, boron doped diamond electrodes are good alternative for determination based on reduction of aromatic nitro group and highly doped films are recommended. For more detailed information see Appendix VII.

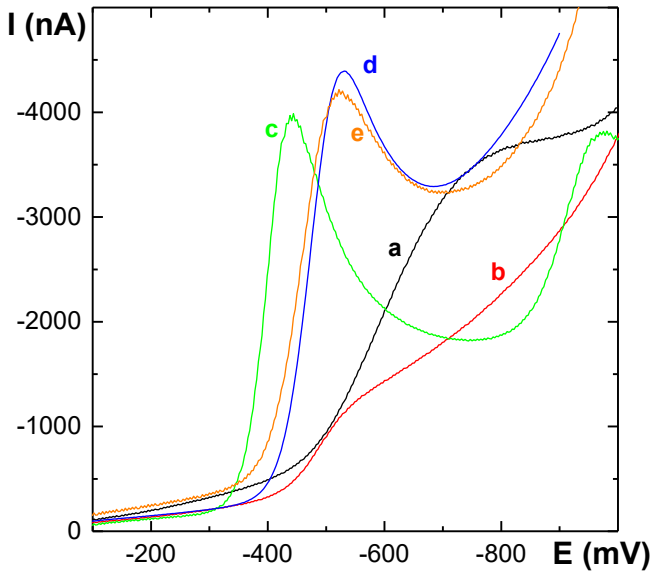


**Figure 11** Direct current voltammograms of 5-nitroquinoline ($c = 1 \times 10^{-4}$ mol $L^{-1}$) in 0.1 mol $L^{-1}$ acetate buffer pH 5.0 measured with boron doped diamond electrodes with different B/C ratio: (a) 500 ppm, (b) 1000 ppm, (c) 2000 ppm, (d) 4000 ppm, and (e) 8000 ppm. Scan rate is 50 mV $s^{-1}$. Adjusted from [7].

*3.7 List of analytes and their determination parameters*

**Table 5** Summary of studied compounds determined with different carbon-based electrodes and methods.

| Analyte | Pretreatment/Electrode | Method, conditions | Matrix | LDR (μmol $L^{-1}$) | LOD (μmol $L^{-1}$) | Ref. |
|---|---|---|---|---|---|---|
| **1-AN** | AP/microcrystalline BDD | DPV, BR buffer pH 7 | | 1 – 100 | 9.87[A] | [4] |
| | AP/microcrystalline BDD | HPLC-ED wall-jet arrangement | | 0.02 – 10 | 0.23[A] | [4] |
| | AP/microcrystalline BDD | HPLC-ED wall-jet arrangement, SPE extraction | sunset yellow dye | 0.0075 – 1 | 0.00498[A] | [4] |
| | AP/microcrystalline BDD | DPV, BR buffer pH 2 | | 2 – 20 | 1.4[B] | [5] |
| | ---/CFE | DPV, BR buffer pH 2 | | 2 – 20 | 3.1[B] | [5] |
| | PP/GCE | DPV, BR buffer pH 2 | river water | 2 – 100 | 1.6[B] | [5] |
| | ---/Nafion-GCE | DPV, BR buffer pH 2 | | 0.2 – 20 | 0.4[B] | [5] |
| | ---/MWCNT-GCE | DPV, BR buffer pH 2 | | 10 – 100 | 11.6[B] | [5] |
| **2-AN** | AP/microcrystalline BDD | DPV, BR buffer pH 7 | | 1 – 66 | 4.93[A] | [4] |
| | AP/microcrystalline BDD | HPLC-ED wall-jet arrangement | | 0.02 – 10 | 0.20[A] | [4] |
| | AP/microcrystalline BDD | HPLC-ED wall-jet arrangement, SPE extraction | sunset yellow dye | 0.0075 – 1 | 0.00462[A] | [4] |
| | PP/GCE | DPV, BR buffer pH 2 | river water | 2 – 100 | 2.0[B] | [5] |

| | | | | | | |
|---|---|---|---|---|---|---|
| **2-AB** | AP/BDD 500 ppm | DPV, BR buffer pH 7 | | 0.25 – 50 | 0.72[A] | [2] |
| | AP/BDD 1000 ppm | DPV, BR buffer pH 7 | | 0.25 – 50 | 0.48[A] | [2] |
| | AP/BDD 2000 ppm | DPV, BR buffer pH 7 | | 0.25 – 50 | 0.80[A] | [2] |
| | AP/BDD 4000 ppm | DPV, BR buffer pH 7 | | 0.25 – 50 | 0.48[A] | [2] |
| | AP/BDD 8000 ppm | DPV, BR buffer pH 7 | | 0.25 – 50 | 0.21[A] | [2] |
| | AP/microcrystalline BDD | HPLC-ED wall-jet arrangement | | 0.16 – 10 | 0.67[A] | [4] |
| | AP/microcrystalline BDD | HPLC-ED wall-jet arrangement, SPE extraction | sunset yellow dye | 0.0075 – 1 | 0.0141[A] | [4] |
| **4-AB** | AP/microcrystalline BDD | HPLC-ED wall-jet arrangement | | 0.09 – 10 | 0.43[A] | [4] |
| | AP/microcrystalline BDD | HPLC-ED wall-jet arrangement, SPE extraction | sunset yellow dye | 0.0075 – 1 | 0.0113[A] | [4] |
| **BP-3** | AP/BDD 2000 ppm | DPV, BR buffer pH 12 | | 1 – 100 | 1.5[C] | [6] |
| | AP/BDD 4000 ppm | DPV, BR buffer pH 12 | | 1 – 100 | 1.9[C] | [6] |
| | AP/BDD 8000 ppm | DPV, BR buffer pH 12 | | 2.5 – 100 | 0.8[C] | [6] |
| | PP/BDD* 1000 ppm | DPV, BR buffer pH 12 + CTAB | | 10 – 75 | | [6] |
| | | | | 0.8 – 10 | | |
| | | | | 0.4 – 0.8 | 0.1[C] | |

| | | | | | |
|---|---|---|---|---|---|
| **5-NQ** | CP/BDD 4000 ppm | DPV, 0.01 mol $L^{-1}$ acetate buffer pH 5 | 0.5 – 75 | 0.50[A] | [7] |
| | AP/BDD 4000 ppm | DPV, 0.01 mol $L^{-1}$ acetate buffer pH 5 | 0.5 – 100 | 0.20[A] | [7] |
| | CP/BDD 4000 ppm | DCV, 0.01 mol $L^{-1}$ acetate buffer pH 5 | 7.5 – 75 | 4.7[A] | [7] |
| | AP/BDD 4000 ppm | DCV, 0.01 mol $L^{-1}$ acetate buffer pH 5 | 10 – 100 | 2.7[A] | [7] |

BDD* – commercial electrode (Windsor Scientific, UK); AP/BDD – anodically pretreated BDD electrode, CP/BDD – cathodically pretreated BDD electrode, PP/BDD – BDD electrode pretreated by polishing, ---/BDD – "as-deposited" BDD electrode; CFE – carbon film electrode; GCE – glassy carbon electrode; MWCNT = multiwalled carbon nanotubes; DCV – direct current voltammetry, DPV – differential pulse voltammetry; SPE – solid phase extraction; BR buffer – Britton–Robinson buffer, CTAB – cetyltrimethylammonium bromide; LDR – linear dynamic range;

Limit of detection (LOD) was calculated as: [A]the concentration of the analyte, which gave the signal equal to three times the standard deviation of peak heights estimated from ten consecutive measurements of the lowest measurable concentration; [B]three times the standard deviation of intercept divided by the slope of the calibration curve; [C]the concentration of the analyte, which gave the signal equal to three times the standard deviation of peak heights estimated from seven consecutive measurements of the lowest measurable concentration.

## 4. Conclusion

The Thesis represents a contribution to the problematic related with electrochemical, spectral morphologic properties of boron doped diamond and its use in electroanalytical methods. Partially, it compares it with other carbon-based electrode materials. The following topics were investigated:

• the series of boron doped diamond films was tested with respect to the effect of boron concentration on their quality, selected morphologic, electrochemical and spectral properties using scanning electron microscopy, atomic force microscopy, Raman spectroscopy, and voltammetric cyclic and differential pulse voltammetry methods. The electrochemical data enable to differentiate between the semiconductive films (deposited at B/C ratio 500 and 1000 ppm) and films exhibiting metallic conductivity (2000, 4000 and 8000 ppm);

• the effect of boron concentration on the voltammetric signals of selected substances was investigated and methods for their determination were developed, both based on their oxidation (2-aminobiphenyl, benzophenone-3) and on reduction (5-nitroquinoline). In general, the electrochemical reactions on BDD films exhibiting metallic conductivity results in well-developed and narrow voltammetric signals positioned closer to zero potential in comparison to signals obtained on semiconductive films. This indicates easier oxidation/reduction and faster charge transfer kinetics for the former type of BDD films;

• the possibility of application of voltammetric and amperometric methods was tested for the simultaneous detection of a mixture of aminobiphenyls and aminonaphthalenes. Further, a method based on HPLC with amperometric detection was optimized for this mixture of analytes using a boron doped diamond electrode. For differential pulse voltammetry, limits of detection were obtained in micromolar concentration range under optimized conditions. The developed HPLC-ED method utilizing the boron doped diamond electrode in wall-jet arrangement enables in 14 minutes separation and simultaneous determination of 1-aminonaphthalene, 2-aminonaphthalene, 2-aminobiphenyl and 4-aminobiphenyl, position isomers with different genotoxic and carcinogenic potential, with limit of detection in $10^{-7}$ mol $L^{-1}$ concentration range. The applicability of the developed HPLC-ED method was successfully tested on the determination of the studied analytes in model solution of azo dye sunset yellow with recoveries around 100 % and nanomolar limits of detection;

• the effects of activation cleaning programs (*ex situ* anodic activation in acidic media or mechanical polishing by alumina) on the signal of benzophenone-3 were investigated using the boron doped diamond electrode. Oxidation of this compound causes fast fouling of the electrode surface and only switching of potentials in 0.5 mol $L^{-1}$ succeeded for its reactivation. Also, the possibility to influence its electroanalytical performance by the presence of cationic surfactant cetyltrimethylammonium bromide was investigated. Selected surfactant has a positive effect: the sensitivity is increased, the peak potential shifted to less positive values, and the limit of detection is 0.1 μmol $L^{-1}$ (about an order of magnitude lower than without a surfactant);

• boron doped diamond was compared with other selected bare carbon-based electrode materials including glassy carbon and carbon film and glassy carbon modified by Nafion permselective membrane and multiwalled carbon nanotubes for the determination of 1-aminonaphthalene and 2-aminonaphthalene. For 1-aminonaphthalene, similar detection limits were achieved for bare surfaces: at BDD electrode 1.4 μmol $L^{-1}$, at glassy carbon electrode 1.6 μmol $L^{-1}$ and at carbon film electrode 3.1 μmol $L^{-1}$, but for the last electrode the sensitivity was visibly lower than with the other electrode materials. No such effect on sensitivity was observed for the studied compounds at glassy carbon electrode modified by multiwalled carbon nanotubes. Glassy carbon electrode modified by Nafion offers the lowest limit of detection of 1-aminonaphthalene (0.4 μmol $L^{-1}$) but is useful only for lower concentrations range (0.2–20 μmol $L^{-1}$).

In this Thesis, applicability of boron doped diamond electrodes for detection of selected amino and nitro derivatives of aromatic organic compounds using voltammetric and amperometric methods was studied. Important factor, influencing signals of the compounds and demanding optimization include activation of electrode surface, boron concentration and parameters of the electroanalytical method used. Undoubtedly, boron doped diamond represents a user-friendly electrode material due to its robustness and easy maintenance of electrode surface, as presented also in this Thesis. Further studies on relation of the electrochemical behavior and factors estimating BDD quality and surface properties can be envisaged so that its advantageous properties estimating successful performance in electroanalysis are optimized.

## 5. References


[1] Zavázalová J., Barek J., Pecková K.: Boron doped diamond electrodes in voltammetry: New designs and applications. An overview. In *Sensing in Electroanalysis*. Kalcher K., Metelka R., Švancara I. and Vytřas K. (Eds.), **8** (2014) pp. 21-34, University Press Centre, Pardubice, Czech Republic.

[2] Schwarzova-Peckova K., Vosahlova J., Barek J., Sloufova I., Pavlova E., Petrak V., Zavazalova J.: Influence of boron content on the morphological, spectral, and electroanalytical characteristics of anodically oxidized boron-doped diamond electrodes. *Electrochimica Acta* **243** (2017) 170-182.

[3] Vosahlova J., Zavazalova J., Schwarzova-Peckova K.: Boron doped diamond electrodes: Effect of boron concentration on the determination of 2-aminobiphenyl. *Chemicke Listy* **108** (2014) S270-S273.

[4] Zavazalova J., Dejmkova H., Barek J., Peckova K.: Voltammetric and amperometric determination of mixtures of aminobiphenyls and aminonaphthalenes using boron doped diamond electrode. *Electroanalysis* **25** (2013) 253-262.

[5] Zavazalova J., Ghica M. E., Schwarzova-Peckova K., Barek J., Brett C. M. A.: Carbon-based electrodes for sensitive electroanalytical determination of aminonaphthalenes. *Electroanalysis* **27** (2015) 1556-1564.

[6] Zavazalova J., Prochazkova K., Schwarzova-Peckova K.: Boron-doped diamond electrodes for voltammetric determination of benzophenone-3. *Analytical Letters* **49** (2016) 80-91.

[7] Vosahlova J., Zavazalova J., Petrak V., Schwarzova-Peckova K.: Factors influencing voltammetric reduction of 5-nitroquinoline at boron-doped diamond electrodes. *Monatshefte Fur Chemie* **147** (2016) 21-29.

[8] Iwaki M., Sato S., Takahashi K., Sakairi H.: Electrical conductivity of nitrogen and argon implanted diamond. *Nuclear Instruments and Methods* **209** (1983) 1129-1133.

[9] Pleskov Y. V., Sakharova A. Y., Krotova M. D., Bouilov L. L., Spitsyn B. V.: Photoelectrochemical properties of semiconductor diamond. *Journal of Electroanalytical Chemistry and Interfacial Electrochemistry* **228** (1987) 19-27.

[10] Patel K., Hashimoto K., Fujishima A.: Photoelectrochemical investigations on boron-doped chemically vapor-deposited diamond electrodes. *Journal of Photochemistry and Photobiology a-Chemistry* **65** (1992) 419-429.

[11] Patel K., Hashimoto K., Fujishima A.: Application of boron-doped CVD-diamond film to photoelectrode. *Denki Kagaku* **60** (1992) 659-659.

[12] Tenne R., Patel K., Hashimoto K., Fujishima A.: Efficient electrochemical reduction of nitrate to ammonia using conductive diamond film electrodes. *Journal of Electroanalytical Chemistry* **347** (1993) 409-415.

[13] Swain G. M., Ramesham R.: The electrochemical activity of boron-doped polycrystalline diamond thin-film electrodes. *Analytical Chemistry* **65** (1993) 345-351.

[14] Ramesham R., Askew R. F., Rose M. F., Loo B. H.: Growth of polycrystalline diamond over glassy-carbon and graphite electrode materials. *Journal of the Electrochemical Society* **140** (1993) 3018-3020.

[15] Peckova K., Musilova J., Barek J.: Boron-doped diamond film electrodes – new tool for voltammetric determination of organic substances. *Critical Reviews in Analytical Chemistry* **39** (2009) 148-172.

[16] Freitas J. M., Oliveira T. D., Munoz R. A. A., Richter E. M.: Boron doped diamond electrodes in flow-based systems. *Frontiers in Chemistry* **7** (2019).

[17] Muzyka K., Sun J. R., Fereja T. H., Lan Y. X., Zhang W., Xu G. B.: Boron-doped diamond: current progress and challenges in view of electroanalytical applications. *Analytical Methods* **11** (2019) 397-414.

[18] Yang N. J., Yu S. Y., Macpherson J. V., Einaga Y., Zhao H. Y., Zhao G. H., Swain G. M., Jiang X.: Conductive diamond: synthesis, properties, and electrochemical applications. *Chemical Society Reviews* **48** (2019) 157-204.

[19] Baluchová S., Daňhel A., Dejmková H., Ostatná V., Fojta M., Schwarzová-Pecková K.: Recent progress in the applications of boron doped diamond electrodes in electroanalysis of organic compounds and biomolecules – A review. *Analytica Chimica Acta* **in press** (2019).

[20] Barek J., Fischer J., Navratil T., Peckova K., Yosypchuk B., Zima J.: Nontraditional electrode materials in environmental analysis of biologically active organic compounds. *Electroanalysis* **19** (2007) 2003-2014.

[21] Peckova K., Jandova K., Maixnerova L., Swain G. M., Barek J.: Amperometric determination of aminobiphenyls using HPLC-ED with boron-doped diamond electrode. *Electroanalysis* **21** (2009) 316-324.

[22] Lukacova-Chomistekova Z., Culkova E., Bellova R., Melichercikova D., Durdiak J., Beinrohr E., Rievaj M., Tomcik P.: Voltammetric detection of antimony in natural water on cathodically pretreated microcrystalline boron doped diamond electrode: A possibility how to eliminate interference of arsenic without surface modification. *Talanta* **178** (2018) 943-948.

[23] Maldonado V. Y., Espinoza-Montero P. J., Rusinek C. A., Swain G. M.: Analysis of Ag(I) biocide in water samples using anodic stripping voltammetry with a boron-doped diamond disk electrode. *Analytical Chemistry* **90** (2018) 6477-6485.

[24] Jarosova R., Sanchez S., Haubold L., Swain G. M.: Isatin analysis using flow injection analysis with amperometric detection – comparison of tetrahedral amorphous carbon and diamond electrode performance. *Electroanalysis* **29** (2017) 2147-2154.

[25] Panizza M., Cerisola G.: Application of diamond electrodes to electrochemical processes. *Electrochimica Acta* **51** (2005) 191-199.

[26] Martinez-Huitle C. A., Brillas E.: Electrochemical alternatives for drinking water disinfection. *Angewandte Chemie-International Edition* **47** (2008) 1998-2005.

[27] Simon R. G., Stockl M., Becker D., Steinkamp A. D., Abt C., Jungfer C., Weidlich C., Track T., Mangold K. M.: Current to clean water – electrochemical solutions for groundwater, water, and wastewater treatment. *Chemie Ingenieur Technik* **90** (2018) 1832-1854.

[28] Naji T., Dirany A., Carabin A., Drogui P.: Large-scale disinfection of real swimming pool water by electro-oxidation. *Environmental Chemistry Letters* **16** (2018) 545-551.

[29] Martinez-Huitle C. A., Brillas E.: Decontamination of wastewaters containing synthetic organic dyes by electrochemical methods: A general review. *Applied Catalysis B-Environmental* **87** (2009) 105-145.

[30] Kraft A.: Doped diamond: A compact review on a new, versatile electrode material. *International Journal of Electrochemical Science* **2** (2007) 355-385.

[31] Weiss E., Groenen-Serrano K., Savall A.: Electrochemical mineralization of sodium dodecylbenzenesulfonate at boron doped diamond anodes. *Journal of Applied Electrochemistry* **37** (2007) 1337-1344.

[32] Weiss E., Groenen-Serrano K., Savall A.: A comparison of electrochemical degradation of phenol on boron doped diamond and lead dioxide anodes. *Journal of Applied Electrochemistry* **38** (2008) 329-337.

[33] Rice D., Westerhoff P., Perreault F., Garcia-Segura S.: Electrochemical self-cleaning anodic surfaces for biofouling control during water treatment. *Electrochemistry Communications* **96** (2018) 83-87.

[34] He Y. P., Lin H. B., Guo Z. C., Zhang W. L., Li H. D., Huang W. M.: Recent developments and advances in boron-doped diamond electrodes for electrochemical oxidation of organic pollutants. *Separation and Purification Technology* **212** (2019) 802-821.

[35] Park J., Quaiserova-Mocko V., Peckova K., Galligan J. J., Fink G. D., Swain G. M.: Fabrication, characterization, and application of a diamond microelectrode for electrochemical measurement of norepinephrine release from the sympathetic nervous system. *Diamond and Related Materials* **15** (2006) 761-772.

[36] Patel B. A., Bian X. H., Quaiserova-Mocko V., Galligan J. J., Swain G. M.: In vitro continuous amperometric monitoring of 5-hydroxytryptamine release from enterochromaffin cells of the guinea pig ileum. *Analyst* **132** (2007) 41-47.

[37] Michaud P. A., Mahe E., Haenni W., Perret A., Comninellis C.: Preparation of peroxodisulfuric acid using boron-doped diamond thin film electrodes. *Electrochemical and Solid State Letters* **3** (2000) 77-79.

[38] Serrano K., Michaud P. A., Comninellis C., Savall A.: Electrochemical preparation of peroxodisulfuric acid using boron doped diamond thin film electrodes. *Electrochimica Acta* **48** (2002) 431-436.

[39] Ferro S., De Battisti A., Duo I., Comninellis C., Haenni W., Perret A.: Chlorine evolution at highly boron-doped diamond electrodes. *Journal of the Electrochemical Society* **147** (2000) 2614-2619.

[40] Canizares P., Arcis M., Saez C., Rodrigo M. A.: Electrochemical synthesis of ferrate using boron doped diamond anodes. *Electrochemistry Communications* **9** (2007) 2286-2290.

[41] Malkowsky I. M., Griesbach U., Putter H., Waldvogel S. R.: Unexpected highly chemselective anodic ortho-coupling reaction of 2,4-dimethylphenol on boron-doped diamond electrodes. *European Journal of Organic Chemistry* (2006) 4569-4572.

[42] Panizza M., Michaud P. A., Iniesta J., Comninellis C., Cerisola G.: Electrochemical oxidation of phenol at boron-doped diamond electrode. Application to electro-organic synthesis and wastewater treatment. *Annali Di Chimica* **92** (2002) 995-1006.

[43] Marselli B., Garcia-Gomez J., Michaud P. A., Rodrigo M. A., Comninellis C.: Electrogeneration of hydroxyl radicals on boron-doped diamond electrodes. *Journal of the Electrochemical Society* **150** (2003) D79-D83.

[44] Iniesta J., Michaud P. A., Panizza M., Comninellis C.: Electrochemical oxidation of 3-methylpyridine at a boron-doped diamond electrode: application to electroorganic synthesis and wastewater treatment. *Electrochemistry Communications* **3** (2001) 346-351.

[45] Lips S., Waldvogel S. R.: Use of boron-doped diamond electrodes in electro-organic synthesis. *Chemelectrochem* **6** (2019) 1649-1660.

[46] Brillas E., Martinez-Huitle C. A.: *Synthetic diamond films: Preparation, electrochemistry, characterization and applications*. John Wiley & Sons (2011), New Yersey, USA.

[47] Fujishima A., Einaga Y., Rao T. N., Tryk D. A.: *Diamond electrochemistry*. 1st ed., Elsevier (2005), Tokio, Japan.

[48] Suffredini H. B., Pedrosa V. A., Codognoto L., Machado S. A. S., Rocha R. C., Avaca L. A.: Enhanced electrochemical response of boron-doped diamond electrodes brought on by a cathodic surface pre-treatment. *Electrochimica Acta* **49** (2004) 4021-4026.

[49] Yang Q., Tang Y., Yang S. L., Li Y. S., Hirose A.: Simultaneous growth of diamond thin films and carbon nanotubes at temperatures <= 550 degrees C. *Carbon* **46** (2008) 589-595.

[50] Uslu B., Ozkan S. A.: Electroanalytical application of carbon based electrodes to the pharmaceuticals. *Analytical Letters* **40** (2007) 817-853.

[51] Uslu B., Ozkan S. A.: Solid electrodes in electroanalytical chemistry: Present applications and prospects for high throughput screening of drug compounds. *Combinatorial Chemistry & High Throughput Screening* **10** (2007) 495-513.

[52] McCreery R. L.: Advanced carbon electrode materials for molecular electrochemistry. *Chemical Reviews* **108** (2008) 2646-2687.

[53] Zhang W., Zhu S. Y., Luque R., Han S., Hu L. Z., Xu G. B.: Recent development of carbon electrode materials and their bioanalytical and environmental applications. *Chemical Society Reviews* **45** (2016) 715-752.

[54] Rana A., Baig N., Saleh T. A.: Electrochemically pretreated carbon electrodes and their electroanalytical applications - A review. *Journal of Electroanalytical Chemistry* **833** (2019) 313-332.

[55] Cavalheiro É. T. G., Brett C. M. A., Oliveira-Brett A. M., Fatibello-Filho O.: Bioelectroanalysis of pharmaceutical compounds. *Bioanalytical Reviews* **4** (2012) 31-53.

[56] Brett C. M. A., Brett A. M. O.: *Electrochemistry: principles, methods, and applications*. Oxford University Press (1993), Oxford.

[57] Kissinger P. T., Heineman W. R.: *Laboratory techniques in electroanalytical chemistry*. 2nd ed., Marcel Dekker (1996), New York.

[58] Wang J.: *Analytical Electrochemistry*. 3rd ed., Wiley-VCH (2006), New York.

[59] Jenkins G. M., Kawamura K.: Structure of glassy carbon. *Nature* **231** (1971) 175.

[60] Friedrich J. M., Ponce-De-Leon C., Reade G. W., Walsh F. C.: Reticulated vitreous carbon as an electrode material. *Journal of Electroanalytical Chemistry* **561** (2004) 203-217.

[61] Schwander M., Partes K.: A review of diamond synthesis by CVD processes. *Diamond and Related Materials* **20** (2011) 1287-1301.

[62] Liang X. B., Wang L., Zhu H. L., Yang D. R.: Effect of pressure on nanocrystalline diamond films deposition by hot filament CVD technique from $CH_4/H_2$ gas mixture. *Surface & Coatings Technology* **202** (2007) 261-267.

[63] Liang X. B., Wang L., Yang D. R.: The structural evolution of nanocrystalline diamond films synthesized by r.f. PECVD. *Materials Letters* **60** (2006) 730-733.

[64] Dong L. F., Ma B. Q., Dong G. Y.: Diamond deposition at low temperature by using $CH_4/H_2$ gas mixture. *Diamond and Related Materials* **11** (2002) 1697-1702.

[65] Feng Y. J., Lv J. W., Liu J. F., Gao N., Peng H. Y., Chen Y. Q.: Influence of boron concentration on growth characteristic and electro-catalytic performance of boron-doped diamond electrodes prepared by direct current plasma chemical vapor deposition. *Applied Surface Science* **257** (2011) 3433-3439.

[66] Peckova K., Musilova J., Barek J., Zima J.: Voltammetric and amperometric determination of organic pollutants in drinking water using boron-doped diamond

electrodes. In *Progress on Drinking Water Research*. Lefebvre M. H. and Roux M. M. (Eds.), (2008) pp. 103-141, Nova Science Publishers, Inc., New York, USA.

[67] Xu J. S., Granger M. C., Chen Q. Y., Strojek J. W., Lister T. E., Swain G. M.: Boron-doped diamond thin-film electrodes. *Analytical Chemistry* **69** (1997) A591-A597.

[68] Ivandini T. A., Einaga Y., Honda K., Fujishima A.: Preparation and characterization of polycrystalline chemical vapor deposited boron-doped diamond thin films. In *Diamond Electrochemistry*. Fujishima A., Einaga Y., Rao T. N. and Tryk D. A. (Eds.), (2005), Elsevier, Amsterdam, Netherland.

[69] May P. W., Ludlow W. J., Hannaway M., Heard P. J., Smith J. A., Rosser K. N.: Raman and conductivity studies of boron-doped micro crystalline diamond, facetted nanocrystalline diamond and cauliflower diamond films. *Diamond and Related Materials* **17** (2008) 105-117.

[70] Koizumi S., Nebel C., Nesladek M.: *Physics and applications of CVD diamond*. John Wiley & Sons (2008), Weinheim, Germany.

[71] de Barros R. C. M., Ferreira N. G., Azevedo A. F., Corat E. J., Sumodjo P. T. A., Serrano S. H. P.: Morphological and electrochemical studies of spherical boron doped diamond electrodes. *Thin Solid Films* **513** (2006) 364-368.

[72] www.sekidiamond.com, access date: 10. 10. 2018.

[73] www.plassys.com, access date: 10. 10. 2018.

[74] www.diamond-materials.com, access date: 10. 10. 2018.

[75] www.mwe-ltd.com, access date: 10. 10. 2018.

[76] www.condias.de, access date: 10. 10. 2018.

[77] www.e6.com, access date: 10. 10. 2018.

[78] www.neocoat.ch, access date: 10. 10. 2018.

[79] www.diamondtech.com, access date: 10. 10. 2018.

[80] www.windsorscientific.co.uk, access date: 10. 10. 2018.

[81] Holt K. B., Bard A. J., Show Y., Swain G. M.: Scanning electrochemical microscopy and conductive probe atomic force microscopy studies of hydrogen-terminated boron-doped diamond electrodes with different doping levels. *Journal of Physical Chemistry B* **108** (2004) 15117-15127.

[82] Janssen G., Vanenckevort W. J. P., Vollenberg W., Giling L. J.: Characterization of single-crystal diamond grown by chemical vapor-deposition processes. *Diamond and Related Materials* **1** (1992) 789-800.

[83] Macpherson J. V.: A practical guide to using boron doped diamond in electrochemical research. *Physical Chemistry Chemical Physics* **17** (2015) 2935-2949.

[84] Fischer A. E., Show Y., Swain G. M.: Electrochemical performance of diamond thin-film electrodes from different commercial sources. *Analytical Chemistry* **76** (2004) 2553-2560.

[85] Watanabe T., Shimizu T. K., Tateyama Y., Kim Y., Kawai M., Einaga Y.: Giant electric double-layer capacitance of heavily boron-doped diamond electrode. *Diamond and Related Materials* **19** (2010) 772-777.

[86] Wei J. J., Li C. M., Gao X. H., Hei L. F., Lvun F. X.: The influence of boron doping level on quality and stability of diamond film on Ti substrate. *Applied Surface Science* **258** (2012) 6909-6913.

[87] Zivcova Z. V., Frank O., Petrak V., Tarabkova H., Vacik J., Nesladek M., Kavan L.: Electrochemistry and in situ Raman spectroelectrochemistry of low and high quality boron doped diamond layers in aqueous electrolyte solution. *Electrochimica Acta* **87** (2013) 518-525.

[88] Bernard M., Deneuville A., Muret P.: Non-destructive determination of the boron concentration of heavily doped metallic diamond thin films from Raman spectroscopy. *Diamond and Related Materials* **13** (2004) 282-286.

[89] Pruvost F., Bustarret E., Deneuville A.: Characteristics of homoepitaxial heavily boron-doped diamond films from their Raman spectra. *Diamond and Related Materials* **9** (2000) 295-299.

[90] Levy-Clement C.: Semiconducting and metallic boron-doped diamond electrodes. In *Diamond Electrochemistry*. Fujishima A., Einaga Y., Rao T. N. and Tryk D. A. (Eds.), (2005) p. 80, Elsevier, Amsterdam, Netherland.

[91] Bernard M., Baron C., Deneuville A.: About the origin of the low wave number structures of the Raman spectra of heavily boron doped diamond films. *Diamond and Related Materials* **13** (2004) 896-899.

[92] Becker D., Juttner K.: The impedance of fast charge transfer reactions on boron doped diamond electrodes. *Electrochimica Acta* **49** (2003) 29-39.

[93] Jiang Y. Y., Liu D., Jiang Z. C., Mao B. J., Ma X., Li Q. B.: Investigation on electrochemically cathodic polarization of boron-doped diamond electrodes and its influence on lead ions analysis. *Journal of the Electrochemical Society* **161** (2014) H410-H415.

[94] Guinea E., Garrido J. A., Rodriguez R. M., Cabot P. L., Arias C., Centellas F., Brillas E.: Degradation of the fluoroquinolone enrofloxacin by electrochemical advanced oxidation processes based on hydrogen peroxide electrogeneration. *Electrochimica Acta* **55** (2010) 2101-2115.

[95] Bogdanowicz R., Fabianska A., Golunski L., Sobaszek M., Gnyba M., Ryl J., Darowicki K., Ossowski T., Janssens S. D., Haenen K., Siedlecka E. M.: Influence of the boron doping level on the electrochemical oxidation of the azo dyes at Si/BDD thin film electrodes. *Diamond and Related Materials* **39** (2013) 82-88.

[96] Fabianska A., Bogdanowicz R., Zieba P., Ossowski T., Gnyba M., Ryl J., Zielinski A., Janssens S. D., Haenen K., Siedlecka E. M.: Electrochemical oxidation of sulphamerazine at boron-doped diamond electrodes: Influence of boron concentration. *Physica Status Solidi a-Applications and Materials Science* **210** (2013) 2040-2047.

[97] Trouillon R., O'Hare D., Einaga Y.: Effect of the doping level on the biological stability of hydrogenated boron doped diamond electrodes. *Physical Chemistry Chemical Physics* **13** (2011) 5422-5429.

[98] Matsushima J. T., Silva W. M., Azevedo A. F., Baldan M. R., Ferreira N. G.: The influence of boron content on electroanalytical detection of nitrate using BDD electrodes. *Applied Surface Science* **256** (2009) 757-762.

[99] Salazar-Banda G. R., de Carvalho A. E., Andrade L. S., Rocha R. C., Avaca L. A.: On the activation and physical degradation of boron-doped diamond surfaces brought on by cathodic pretreatments. *Journal of Applied Electrochemistry* **40** (2010) 1817-1827.

[100] Muff J., Bennedsen L. R., Sogaard E. G.: Study of electrochemical bleaching of p-nitrosodimethylaniline and its role as hydroxyl radical probe compound. *Journal of Applied Electrochemistry* **41** (2011) 599-607.

[101] Dornellas R. M., Franchini R. A. A., da Silva A. R., Matos R. C., Aucelio R. Q.: Determination of the fungicide kresoxim-methyl in grape juices using square-wave voltammetry and a boron-doped diamond electrode. *Journal of Electroanalytical Chemistry* **708** (2013) 46-53.

[102] Hutton L. A., Iacobini J. G., Bitziou E., Channon R. B., Newton M. E., Macpherson J. V.: Examination of the factors affecting the electrochemical performance of oxygen-terminated polycrystalline boron-doped diamond electrodes. *Analytical Chemistry* **85** (2013) 7230-7240.

[103] Brycht M., Lochynski P., Barek J., Skrzypek S., Kuczewski K., Schwarzova-Peckova K.: Electrochemical study of 4-chloro-3-methylphenol on anodically pretreated boron-doped diamond electrode in the absence and presence of a cationic surfactant. *Journal of Electroanalytical Chemistry* **771** (2016) 1-9.

[104] Alehashem S., Chambers F., Strojek J. W., Swain G. M., Ramesham R.: Cyclic voltammetric studies of charge-transfer reactions at highly boron-doped polycrystalline diamond thin-film electrodes. *Analytical Chemistry* **67** (1995) 2812-2821.

[105] Xu J. S., Chen Q. Y., Swain G. M.: Anthraqunionedisulfonate electrochemistry: A comparison of glassy carbon, hydrogenated glassy carbon, highly oriented pyrolytic graphite, and diamond electrodes. *Analytical Chemistry* **70** (1998) 3146-3154.

[106] Duo I., Levy-Clement C., Fujishima A., Comninellis C.: Electron transfer kinetics on boron-doped diamond Part I: Influence of anodic treatment. *Journal of Applied Electrochemistry* **34** (2004) 935-943.

[107] Rao T. N., Fujishima A.: Recent advances in electrochemistry of diamond. *Diamond and Related Materials* **9** (2000) 384-389.

[108] Kisacik I., Stefanova A., Ernst S., Baltruschat H.: Oxidation of carbon monoxide, hydrogen peroxide and water at a boron doped diamond electrode: The competition for hydroxyl radicals. *Physical Chemistry Chemical Physics* **15** (2013) 4616-4624.

[109] Kapalka A., Foti G., Comninellis C.: The importance of electrode material in environmental electrochemistry Formation and reactivity of free hydroxyl radicals on boron-doped diamond electrodes. *Electrochimica Acta* **54** (2009) 2018-2023.

[110] Hoffmann R., Obloh H., Tokuda N., Yang N., Nebel C. E.: Fractional surface termination of diamond by electrochemical oxidation. *Langmuir* **28** (2012) 47-50.

[111] Enache T. A., Chiorcea-Paquim A. M., Fatibello O., Oliveira-Brett A. M.: Hydroxyl radicals electrochemically generated in situ on a boron-doped diamond electrode. *Electrochemistry Communications* **11** (2009) 1342-1345.

[112] Salazar-Banda G. R., Andrade L. S., Nascente P. A. P., Pizani P. S., Rocha R. C., Avaca L. A.: On the changing electrochemical behaviour of boron-doped diamond surfaces with time after cathodic pre-treatments. *Electrochimica Acta* **51** (2006) 4612-4619.

[113] Hasoň S., Daňhel A., Schwarzová-Pecková K., Fojta M.: Carbon electrodes in electrochemical analysis of biomolecules and bioactive substances: Roles of surface structures and chemical groups. In *Nanotechnology and Biosensors*. Nikolelis D. P. and Nikoleli G. P. (Eds.), (2018) pp. 51-111, Elsevier Science, Oxford, United Kingdom.

[114] Prochazkova K., Baluchova S., Vosahlova J., Schwarzova-Peckova K.: Boron doped diamond electrodes: The effect of surface pretreatment on voltammetric signals of phenolic compounds. In *XXXVI Moderni Elektrochemicke Metody*. Navratil T., Fojta M. and Schwarzova K. (Eds.), (2016) pp. 171-175, Lenka Srsenova-Best Servis, Usti Nad Labem, Czech Republic.

[115] Baluchova S., Barek J., Tome L. I. N., Brett C. M. A., Schwarzova-Peckova K.: Vanillylmandelic and homovanillic acid: Electroanalysis at non-modified and polymer-modified carbon-based electrodes. *Journal of Electroanalytical Chemistry* **821** (2018) 22-32.

[116] Vosahlova J., Barek J., Schwarzova-Peckova K.: Determination of tartrazine and allura red at boron doped diamond electrodes. In *XXXVI Moderni Elektrochemicke Metody*. Navratil T., Fojta M. and Schwarzova K. (Eds.), (2016) pp. 285-288, Lenka Srsenova-Best Servis, Usti Nad Labem, Czech Republic.

[117] Baluchova S., Schwarzova-Peckova K.: Vanillylmandelic and homovanillic acid electroanalysis at carbon-based electrodes. *Czech Chemical Society Symposium Series* **15** (2017) 52-55.

[118] Marken F., Paddon C. A., Asogan D.: Direct cytochrome c electrochemistry at boron-doped diamond electrodes. *Electrochemistry Communications* **4** (2002) 62-66.

[119] Yardim Y., Keskin E., Senturk Z.: Voltammetric determination of mixtures of caffeine and chlorogenic acid in beverage samples using a boron-doped diamond electrode. *Talanta* **116** (2013) 1010-1017.

[120] McEvoy J. P., Foord J. S.: Direct electrochemistry of blue copper proteins at boron-doped diamond electrodes. *Electrochimica Acta* **50** (2005) 2933-2941.

[121] Li Y. R., Li H. J., Li M. J., Li C. P., Sun D. Z., Yang B. H.: Porous boron-doped diamond electrode for detection of dopamine and pyridoxine in human serum. *Electrochimica Acta* **258** (2017) 744-753.

[122] Hrdlicka V., Barek J., Navratil T., Taylor A.: Miniaturized boron doped diamond film electrode for neuroblastoma biomarkers determination. In *Proceedings of the 13th International Students Conference Modern Analytical Chemistry.* Nesmerak K. (ed.), (2017) pp. 273-278, Charles University, Faculty of Science, Prague 2, Czech Republic.

[123] Chylkova J., Tomaskova M., Jehlicka V., Selesovska R., Hlavata P.: Voltammetric determination of plant growth stimulants based on organic acids. *Monatshefte Fur Chemie* **148** (2017) 473-479.

[124] Scheel G. L., de Oliveira F. M., de Oliveira L. L. G., Medeiros R. A., Nascentes C. C., Tarley C. R. T.: Feasibility study of ethylone determination in seized samples using boron-doped diamond electrode associated with solid phase extraction. *Sensors and Actuators B-Chemical* **259** (2018) 1113-1122.

[125] Spataru T., Radu M. M., Spataru N., Fujishima A.: Voltammetric determination of N-hydroxysuccinimide at conductive diamond electrodes. *Analyst* **143** (2018) 2356-2362.

[126] Cinkova K., Kianickova K., Stankovic D. M., Vojs M., Marton M., Sovrc L.: The doping level of boron-doped diamond electrodes affects the voltammetric sensing of uric acid. *Analytical Methods* **10** (2018) 991-996.

[127] da Silva A. R. L., dos Santosa A. J., Martinez-Huitle C. A.: Electrochemical measurements and theoretical studies for understanding the behavior of catechol, resorcinol and hydroquinone on the boron doped diamond surface. *Rsc Advances* **8** (2018) 3483-3492.

[128] Liu Z. L., Li H. J., Li M. J., Li C. P., Qian L. R., Su L., Yang B. H.: Preparation of polycrystalline BDD/Ta electrodes for electrochemical oxidation of organic matter. *Electrochimica Acta* **290** (2018) 109-117.

[129] Brocenschi R. F., Silva T. A., Lourencao B. C., Fatibello O., Rocha R. C.: Use of a boron-doped diamond electrode to assess the electrochemical response of the naphthol isomers and to attain their truly simultaneous electroanalytical determination. *Electrochimica Acta* **243** (2017) 374-381.

[130] Chylkova J., Tomaskova M., Janikova L., Selesovska R., Navratil T., Chudobova P.: Sensitive voltammetric method for the fast analysis of the antioxidant pyrogallol using a boron-doped diamond electrode in biofuels. *Chemical Papers* **71** (2017) 1047-1054.

[131] Abdullah A. A., Yardim Y., Senturk Z.: The performance of cathodically pretreated boron-doped diamond electrode in cationic surfactant media for enhancing

the adsorptive stripping voltammetric determination of catechol-containing flavonoid quercetin in apple juice. *Talanta* **187** (2018) 156-164.

[132] Yardim Y.: Electrochemical determination of resveratrol in dietary supplements at a boron-doped diamond electrode in the presence of hexadecyltrimethylammonium bromide using square-wave adsorptive stripping voltammetry. *Journal of the Serbian Chemical Society* **82** (2017) 175-188.

[133] Gong S., Gao C. Y., Wang J. F., Tong J. H., Bian C., Wu K. B., Xia S. H.: Reusable boron-doped diamond electrodes for the semi-continuous detection of tetrabromobisphenol A. *Ieee Sensors Journal* **18** (2018) 5219-5224.

[134] Eisele A. P. P., Valezi C. F., Sartori E. R.: Exploiting the high oxidation potential of carisoprodol on a boron-doped diamond electrode: An improved method for its simultaneous determination with acetaminophen and caffeine. *Analyst* **142** (2017) 3514-3521.

[135] Samiec P., Svorc L., Stankovic D. M., Vojs M., Marton M., Navratilova Z.: Mercury-free and modification-free electroanalytical approach towards bromazepam and alprazolam sensing: A facile and efficient assay for their quantification in pharmaceuticals using boron-doped diamond electrodes. *Sensors and Actuators B-Chemical* **245** (2017) 963-971.

[136] Moraes J. T., Salamanca-Neto C. A. R., Svorc L., Sartori E. R.: Advanced sensing performance towards simultaneous determination of quaternary mixture of antihypertensives using boron-doped diamond electrode. *Microchemical Journal* **134** (2017) 173-180.

[137] Rebech I., Neto A. R. S., Scremin J., Sartori E. R.: Simultaneous voltammetric determination of amlodipine and atorvastatin on anodically pretreated boron-doped diamond electrode. *Orbital-the Electronic Journal of Chemistry* **9** (2017) 225-233.

[138] Salusova I., Cinkova K., Brtkova B., Vojs M., Marton M., Svorc L.: Electrochemical and analytical performance of boron-doped diamond electrode for determination of ascorbic acid. *Acta Chimica Slovaca* **10** (2017) 21-28.

[139] Scremin J., Sartori E. R.: Simultaneous determination of nifedipine and atenolol in combined dosage forms using a boron-doped diamond electrode with differential pulse voltammetry. *Canadian Journal of Chemistry* **96** (2018) 1-7.

[140] Pysarevska S., Dubenska L., Plotycya S., Svorc L.: A state-of-the-art approach for facile and reliable determination of benzocaine in pharmaceuticals and biological samples based on the use of miniaturized boron-doped diamond electrochemical sensor. *Sensors and Actuators B-Chemical* **270** (2018) 9-17.

[141] Silva W. P., Silva L. A. J., Franca C. H., Sousa R. M. F., Munoz R. A. A., Richter E. M.: Square-wave voltammetric determination of propyphenazone, paracetamol, and caffeine: Comparative study between batch injection analysis and conventional electrochemical systems. *Electroanalysis* **29** (2017) 1860-1866.

[142] Feier B., Gui A., Cristea C., Sandulescu R.: Electrochemical determination of cephalosporins using a bare boron-doped diamond electrode. *Analytica Chimica Acta* **976** (2017) 25-34.

[143] Culkova E., Lukacova-Chomistekova Z., Bellova R., Melichercikova D., Durdiak J., Timko J., Rievaj M., Tomcik P.: Boron-doped diamond film electrode as voltammetric sensor for cetirizine. *International Journal of Electrochemical Science* **13** (2018) 6358-6372.

[144] Radicova M., Behul M., Marton M., Vojs M., Bodor R., Redhammer R., Stanova A. V.: Heavily boron doped diamond electrodes for ultra sensitive determination of ciprofloxacin in human urine. *Electroanalysis* **29** (2017) 1612-1617.

[145] Stankovic D. M., Svorc L., Mariano J., Ortner A., Kalcher K.: Electrochemical determination of natural drug colchicine in pharmaceuticals and human serum sample and its interaction with DNA. *Electroanalysis* **29** (2017) 2276-2281.

[146] Donmez F., Yardim Y., Senturk Z.: Electroanalytical determination of enrofloxacin based on the enhancement effect of the anionic surfactant at anodically pretreated boron-doped diamond electrode. *Diamond and Related Materials* **84** (2018) 95-102.

[147] Nigovic B., Milanovic I.: Green Electroanalytical method for fast measurement of xanthine oxidase inhibitor febuxostat. *Analytical Sciences* **33** (2017) 1219-1223.

[148] Svorc L., Borovska K., Cinkova K., Stankovic D. M., Plankova A.: Advanced electrochemical platform for determination of cytostatic drug flutamide in various matrices using a boron-doped diamond electrode. *Electrochimica Acta* **251** (2017) 621-630.

[149] Mattos G. J., Scremin J., Salamanca-Neto C. A. R., Sartori E. R.: The performance of boron-doped diamond electrode for the determination of ramipril and its association with hydrochlorothiazide. *Electroanalysis* **29** (2017) 1180-1187.

[150] Petkovic B. B., Kuzmanovic D., Dimitrijevic T., Krstic M. P., Stankovic D. M.: Novel strategy for electroanalytical detection of antipsychotic drugs chlorpromazine and thioridazine; Possibilities for simultaneous determination. *International Journal of Electrochemical Science* **12** (2017) 3709-3720.

[151] Svorc L., Strezova I., Kianickova K., Stankovic D. M., Otrisal P., Samphao A.: An advanced approach for electrochemical sensing of ibuprofen in pharmaceuticals and human urine samples using a bare boron-doped diamond electrode. *Journal of Electroanalytical Chemistry* **822** (2018) 144-152.

[152] Cinkova K., Matokarova M., Salusova I., Plankova A., Brtkova B., Borovska K., Marton M., Vojs M., Svorc L.: Voltammetric determination of antidepressant imipramine in pharmaceutical preparations using boron-doped diamond electrode. *Chemicke Listy* **111** (2017) 392-397.

[153] Oliveira S. N., Ribeiro F. W. P., Sousa C. P., Soares J. E. S., Suffredini H. B., Becker H., de Lima-Neto P., Correia A. N.: Imipramine sensing in pharmaceutical

formulations using boron-doped diamond electrode. *Journal of Electroanalytical Chemistry* **788** (2017) 118-124.

[154] Salamanca-Neto C. A. R., Yoshida F. A., Sartori E. R., Moraes J. T.: Boron-doped diamond electrode: A modification-free platform for sensitive square-wave voltammetric determination of indapamide hydrochloride. *Analytical Methods* **10** (2018) 3347-3352.

[155] Ensch M., Maldonado V. Y., Swain G. M., Rechenberg R., Becker M. F., Schuelke T., Rusinek C. A.: Isatin detection using a boron-doped diamond 3-in-1 sensing platform. *Analytical Chemistry* **90** (2018) 1951-1958.

[156] Selesovska R., Krankova B., Stepankova M., Martinkova P., Janikova L., Chylkova J., Vojs M.: Influence of boron content on electrochemical properties of boron-doped diamond electrodes and their utilization for leucovorin determination. *Journal of Electroanalytical Chemistry* **821** (2018) 2-9.

[157] Selesovska R., Krankova B., Stepankova M., Martinkova P., Janikova L., Chylkova J., Navratil T.: Voltammetric determination of leucovorin in pharmaceutical preparations using a boron-doped diamond electrode. *Monatshefte Fur Chemie* **149** (2018) 1701-1708.

[158] Rkik M., Ben Brahirn M., Samet Y.: Electrochemical determination of levofloxacin antibiotic in biological samples using boron doped diamond electrode. *Journal of Electroanalytical Chemistry* **794** (2017) 175-181.

[159] Alpar N., Pinar P. T., Yardim Y., Senturk Z.: Voltammetric method for the simultaneous determination of melatonin and pyridoxine in dietary supplements using a cathodically pretreated boron-doped diamond electrode. *Electroanalysis* **29** (2017) 1691-1699.

[160] Stepankova M., Selesovska R., Janikova L., Chylkova J.: Voltammetric determination of mesalazine in pharmaceutical preparations and biological samples using boron-doped diamond electrode. *Chemical Papers* **71** (2017) 1419-1427.

[161] Chomistekova Z., Culkova E., Bellova R., Melichercikova D., Durdiak J., Timko J., Rievaj M., Tomcik P.: Oxidation and reduction of omeprazole on boron-doped diamond electrode: Mechanistic, kinetic and sensing performance studies. *Sensors and Actuators B-Chemical* **241** (2017) 1194-1202.

[162] Feier B., Ionel I., Cristea C., Ndulescu R. S.: Electrochemical behaviour of several penicillins at high potential. *New Journal of Chemistry* **41** (2017) 12947-12955.

[163] Pereira G. F., Deroco P. B., Silva T. A., Ferreira H. S., Fatibello O., Eguiluz K. I. B., Salazar-Banda G. R.: Study of electrooxidation and enhanced voltammetric determination of beta-blocker pindolol using a boron-doped diamond electrode. *Diamond and Related Materials* **82** (2018) 109-114.

[164] Stradolini F., Kilic T., Taurino I., De Micheli G., Carrara S.: Cleaning strategy for carbon-based electrodes: Long-term propofol monitoring in human serum. *Sensors and Actuators B-Chemical* **269** (2018) 304-313.

[165] Talay Pinar P., Ali H. S., Abdullah A. A., Yardim Y., Senturk Z.: Electroanalytical determination of salbutamol in pharmaceutical formulations using cathodically pretreated boron-doped diamond electrode. *Marmara Pharmaceutical Journal* **22** (2018) 460-468.

[166] Sartori E. R., Clausen D. N., Pires I. M. R., Salamanca-Neto C. A. R.: Sensitive square-wave voltammetric determination of tadalafil (Cialis (R)) in pharmaceutical samples using a cathodically pretreated boron-doped diamond electrode. *Diamond and Related Materials* **77** (2017) 153-158.

[167] Morawska K., Poplawski T., Ciesielski W., Smarzewska S.: Electrochemical and spectroscopic studies of the interaction of antiviral drug tenofovir with single and double stranded DNA. *Bioelectrochemistry* **123** (2018) 227-232.

[168] Ali H. S., Abdullah A. A., Pinar P. T., Yardim Y., Senturk Z.: Simultaneous voltammetric determination of vanillin and caffeine in food products using an anodically pretreated boron-doped diamond electrode: Its comparison with HPLC-DAD. *Talanta* **170** (2017) 384-391.

[169] Alpar N., Yardim Y., Senturk Z.: Selective and simultaneous determination of total chlorogenic acids, vanillin and caffeine in foods and beverages by adsorptive stripping voltammetry using a cathodically pretreated boron-doped diamond electrode. *Sensors and Actuators B-Chemical* **257** (2018) 398-408.

[170] Mehmeti E., Stankovic D. M., Ortner A., Zavasnik J., Kalcher K.: Highly selective electrochemical determination of phlorizin using square wave voltammetry at a boron-doped diamond electrode. *Food Analytical Methods* **10** (2017) 3747-3752.

[171] Svorc L., Hasso M., Sarakhman O., Kianickova K., Stankovic D. M., Otrisal P.: A progressive electrochemical sensor for food quality control: Reliable determination of theobromine in chocolate products using a miniaturized boron-doped diamond electrode. *Microchemical Journal* **142** (2018) 297-304.

[172] Jevtic S., Stefanovic A., Stankovic D. M., Pergal M. V., Ivanovic A. T., Jokic A., Petkovic B. B.: Boron-doped diamond electrode – A prestigious unmodified carbon electrode for simple and fast determination of bentazone in river water samples. *Diamond and Related Materials* **81** (2018) 133-137.

[173] Lima T. D., Simoes F. R., Codognoto L.: Simultaneous voltammetric determination of carbendazim and carbaryl in medicinal plant infusions with a boron-doped diamond electrode. *International Journal of Environmental Analytical Chemistry* **97** (2017) 768-782.

[174] Djurdjic S., Vukojevic V., Jevtic S., Pergal M. V., Petkovic B. B., Stankovic D. M.: Herbicide clomazone detection using electroanalytical approach using boron doped diamond electrode. *International Journal of Electrochemical Science* **13** (2018) 2791-2799.

[175] Duarte E. H., Casarin J., Sartori E. R., Tarley C. R. T.: Highly improved simultaneous herbicides determination in water samples by differential pulse

voltammetry using boron-doped diamond electrode and solid phase extraction on cross-linked poly(vinylimidazole). *Sensors and Actuators B-Chemical* **255** (2018) 166-175.

[176] Franca R. F., Lima T. D. S., Simoes F. R., Codognoto L.: Electroanalytical determination of fenthion in passiflora alata tincture samples. *Orbital-the Electronic Journal of Chemistry* **10** (2018) 92-97.

[177] Ribeiro F. W. P., Sousa C. P., Morais S., de Lima-Neto P., Correia A. N.: Sensing of formetanate pesticide in fruits with a boron-doped diamond electrode. *Microchemical Journal* **142** (2018) 24-29.

[178] Stankovic D. M.: Electroanalytical approach for quantification of pesticide maneb. *Electroanalysis* **29** (2017) 352-357.

[179] Costa D. J. E., Santos J. C. S., Sanches-Brandao F. A. C., Ribeiro W. F., Salazar-Banda G. R., Araujo M. C. U.: Boron-doped diamond electrode acting as a voltammetric sensor for the detection of methomyl pesticide. *Journal of Electroanalytical Chemistry* **789** (2017) 100-107.

[180] Brycht M., Leniart A., Robak J., Burnat B., Kaczmarska K., Sipa K., Skrzypek S.: First electrochemical study of the fungicide oxycarboxin. *International Journal of Environmental Analytical Chemistry* **97** (2017) 1298-1314.

[181] Jevtic S., Vukojevic V., Djurdjic S., Pergal M. V., Manojlovic D. D., Petkovic B. B., Stankovic D. M.: First electrochemistry of herbicide pethoxamid and its quantification using electroanalytical approach from mixed commercial product. *Electrochimica Acta* **277** (2018) 136-142.

[182] Selva T. M. G., de Araujo W. R., Bacil R. P., Paixao T.: Study of electrochemical oxidation and quantification of the pesticide pirimicarb using a boron-doped diamond electrode. *Electrochimica Acta* **246** (2017) 588-596.

[183] Vukojevic V., Djurdjic S., Svorc L., Velickovic T. C., Mutic J., Stankovic D. M.: Analytical approach for detection of ergosterol in mushrooms based on modification free electrochemical sensor in organic solvents. *Food Analytical Methods* **11** (2018) 2590-2596.

[184] Buzid A., Reen F. J., O'Gara F., McGlacken G. P., Glennon J. D., Luong J. H. T.: Simultaneous chemosensing of tryptophan and the bacterial signal molecule indole by boron doped diamond electrode. *Electrochimica Acta* **282** (2018) 845-852.

[185] Souza G. A., Pimentel D. M., Lima A. B., Guedes T. J., Arantes L. C., de Oliveira A. C., Sousa R. M. F., Munoz R. A. A., dos Santos W. T. P.: Electrochemical sensing of NBOMes and other new psychoactive substances in blotting paper by square-wave voltammetry on a boron-doped diamond electrode. *Analytical Methods* **10** (2018) 2411-2418.

[186] Ribeiro W. F., da Costa D. J. E., Lourenco A. S., de Medeiros E. P., Salazar-Banda G. R., do Nascimento V. B., Araujo M. C. U.: Adsorptive stripping

voltammetric determination of trace level ricin in castor seeds using a boron-doped diamond electrode. *Electroanalysis* **29** (2017) 1783-1793.

[187] Cizek K., Barek J., Fischer J., Peckova K., Zima J.: Voltammetric determination of 3-nitrofluoranthene and 3-aminofluoranthene at boron doped diamond thin-film electrode. *Electroanalysis* **19** (2007) 1295-1299.

[188] Vyskocil V., Barek J.: Electroanalysis of nitro and amino derivatives of polycyclic aromatic hydrocarbons. *Current Organic Chemistry* **15** (2011) 3059-3076.

[189] Seo E. T., Nelson R. F., Fritsch J. M., Marcoux L. S., Leedy D. W., Adams R. N.: Anodic oxidation pathways of aromatic amines. Electrochemical and electron paramagnetic resonance studies. *Journal of the American Chemical Society* **88** (1966) 3498-3503.

[190] Barek J., Jandova K., Peckova K., Zima J.: Voltammetric determination of aminobiphenyls at a boron-doped nanocrystalline diamond film electrode. *Talanta* **74** (2007) 421-426.

[191] Zima J., Vaingatova S., Barek J., Brichac J.: HPLC monitoring of biphenyl derivatives with UV and electrochemical detection modes. *Chemia Analityczna* **48** (2003) 805-816.

[192] Zima J., Dejmkova H., Barek J.: HPLC determination of naphthalene amino derivatives using electrochemical detection at carbon paste electrodes. *Electroanalysis* **19** (2007) 185-190.

[193] Bluthgen N., Zucchi S., Fent K.: Effects of the UV filter benzophenone-3 (oxybenzone) at low concentrations in zebrafish (Danio rerio). *Toxicology and Applied Pharmacology* **263** (2012) 184-194.

[194] Kim S., Jung D., Kho Y., Choi K.: Effects of benzophenone-3 exposure on endocrine disruption and reproduction of Japanese medaka (Oryzias latipes) – A two generation exposure study. *Aquatic Toxicology* **155** (2014) 244-252.

[195] Suzuki T., Kitamura S., Khota R., Sugihara K., Fujimoto N., Ohta S.: Estrogenic and antiandrogenic activities of 17 benzophenone derivatives used as UV stabilizers and sunscreens. *Toxicology and Applied Pharmacology* **203** (2005) 9-17.

[196] Kim S., Choi K.: Occurrences, toxicities, and ecological risks of benzophenone-3, a common component of organic sunscreen products: A mini-review. *Environment International* **70** (2014) 143-157.

[197] Laranjeira M. T., de Lima F., de Oliveira S. C., Ferreira V. S., de Oliveira R. T. S.: Analytical determination of benzophenone-3 in sunscreen preparations using boron-doped diamond electrodes. *American Journal of Analytical Chemistry* **2** (2011) 383-391.

[198] Vidal L., Chisvert A., Canals A., Psillakis E., Lapkin A., Acosta F., Edler K. J., Holdaway J. A., Marken F.: Chemically surface-modified carbon nanoparticle carrier

for phenolic pollutants: Extraction and electrochemical determination of benzophenone-3 and triclosan. *Analytica Chimica Acta* **616** (2008) 28-35.

[199] Vyskocil V., Jiranek I., Danhel A., Zima J., Barek J., Wang J., Peckova K.: Polarographic and voltammetric determination of genotoxic nitro derivatives of quinoline using mercury electrodes. *Collection of Czechoslovak Chemical Communications* **76** (2011) 1991-2004.

[200] Jiranek I., Peckova K., Kralova Z., Moreira J. C., Barek J.: The use of silver solid amalgam electrode for voltammetric and amperometric determination of nitroquinolines. *Electrochimica Acta* **54** (2009) 1939-1947.

# *Appendix I*

*Publication 1*

Sensing in Electroanalysis

*Vol. **8** (K. Kalcher, R. Metelka, I. Švancara, K. Vytřas; Eds.), pp. 21–34.*
*2013/2014 University Press Centre, Pardubice, Czech Republic.*
*ISBN 978-80-7395-782-7 (print); ISBN 978-80-7395-783-4 (pdf)*

## Boron Doped Diamond Electrodes in Voltammetry: New Designs and Applications. An Overview

**Jaroslava Zavázalová**, **Jiří Barek**, and **Karolina Pecková***

*Charles University in Prague, Faculty of Science, University Centre of Excellence "Supramolecular Chemistry", Department of Analytical Chemistry, UNESCO Laboratory of Environmental Electrochemistry, Albertov 6, CZ-128 43 Prague 2, Czech Republic.*

**Abstract:** In this overview, the recent progress in the development and applications of bare boron doped diamond electrodes in voltammetry of organic compounds is summarized. Attention is paid to important issues reflected in last five years in electroanalytical studies, *e.g.* fouling and pretreatment of BDD surface, influence of boron concentration on performance of BDD-based sensors, and application of adsorptive stripping voltammetry.

**Keywords:** Boron doped diamond electrode; Organic compounds; Voltammetry; Review

*) Author to whom correspondence should be addressed. E-mail: kpeckova@natur.cuni.cz

### Introduction

Boron doped diamond (BDD) is a versatile electrode material, which has gained deserved popularity in a variety of electrochemical applications since its introduction in 1992 [1-3]. It is substantiated by its excellent mechanical, physical, and electrochemical properties, such as extreme hardness, very low and stable capacitive background current over a wide potential range, microstructural stability at extreme cathodic and anodic potentials, electrochemical stability in both alkaline and acidic media, good responsiveness for many redox analytes without pretreatment, and resistance to electrode fouling. Four main application ways

established during the twenty year history of BDD-related research: (i) Electrochemical oxidation of environmental pollutants at BDD anodes proposed for their quantitative conversion or destruction in wastewaters, (ii) electrochemical disinfection of drinking and bathing water, (iii) use of BDD electrodes in electroanalysis for detection of organic and inorganic species in environmental, biological and pharmaceutical matrices, (iv) developing of BDD-based sensors and biosensors, and (v) electrochemical synthesis, in particular in the production of strong inorganic oxidizing agents, or in electroorganic synthesis [4].

The properties of BDD films are fundamentally influenced by the quantity and kind of the doping agent, morphologic factors and defects in the film, presence of impurities ($sp^2$ carbon), crystallographic orientation, and surface termination (most frequently oxygen or hydrogen). While the former factors are given by the preparation method, the latter can be determined by post-preparation procedures including electrochemical pretreatment.

The preparation of doped diamond films relies on energy-assisted chemical vapor deposition (CVD) methods, when a carbon containing gas, most frequently methane is energetically activated to decompose the molecules into methyl-radicals and atomic hydrogen and deposited on a suitable substrate. The boron doping agent is most frequently added as small amounts of diborane or trimethyl boron in the gas phase. The gas activation is accomplished using microwave plasma (MP CVD) or hot filament (HF CVD) techniques. Typical growth conditions are: 0.3-1.0 % $CH_4$ in $H_2$, pressures of 10-150 torr, substrate temperatures of 700-1000 °C, and microwave powers of 1000-1300 W, or filament temperatures up to ~ 2800 °C, depending on the methods used. The film grows by nucleation at rates in the 0.1-2 μm $h^{-1}$ range. For the substrates to be continuously coated with diamond, the nominal film thickness must be ~ 1 μm. The resulting films differ in morphology – microcrystalline films are characterized by crystallite size < 1-5 μm, nanocrystalline films 10-500 nm [5] – and quality. It is generally accepted, that the quality of MP CVD films, *i.e.* content of $sp^2$ impurities and structure defects is enhanced compared with HF CVD film.

The as-deposited diamond surface is hydrogen-terminated, because the films are grown under hydrogen plasma or in a hydrogen atmosphere. Such hydrogen-terminated diamond surfaces are known to be remarkably stable, but the oxygen-terminated surface can easily be formed by exposing the surface to oxygen plasma, boiling in strong acid or electrochemical exposure to the high anodic potential in the region of water decomposition. The change of the chemical termination affects the electrochemical properties of the diamond electrode. The water decomposition reaction is extremely important for the application fields (i-iii) listed above. At BDD electrode, water decomposes according to the following equation:

$$H_2O(BDD) \rightarrow HO^{\bullet}(BDD) + H^+ + e^- \qquad (1)$$

The $OH^{\bullet}$ radicals are confined to the BDD surface and as powerful oxidizing agents are capable of oxidation of a wide range of compounds, non-oxidizable using other electrode materials. Reaction (1) is enabled by the high oxygen overvoltage at BDD surface.

This overview is based on findings gained by going through the papers devoted to the use of BDD electrodes in voltammetric analysis and personal experience of the authors and their coworkers. Table I summarizes selected examples of organic compounds investigated since 2008 by means of batch voltammetric methods using bare BDD electrodes. The table contains for each analyte electroanalytical method, characterization of used BDD electrode, achieved limit of detection (LOD), eventually matrix, and thus enables an insight in the progress in application of BDD electrodes in last five years.

## Applications of BDD Electrodes in Voltammetry

Organic compounds can be oxidized on BDD electrodes by two basic mechanisms: (i) directly by electron transfer from BDD surface to compound, or (ii) in indirect way by oxidizing entities, *e.g.* hydroxyl radicals, generated on electrode surface by reaction (1). The latter mechanism is unique for BDD electrodes and enables oxidation of organic compounds at far positive potentials, non-achievable at other electrode materials in aqueous or mixed aqueous-organic media. Methods based on reductive determinations are still not that frequent. Nevertheless, they benefit from the low sensitivity of BDD surface to dissolved oxygen that is being recognized in increasing number of publications [6, 7].

In the following paragraphs, the selected factors and approaches influencing the development of batch voltammetric methods by means of planar bare BDD electrodes are briefly analyzed and demonstrated on examples mostly coming from experimental work of the authors and coworkers.

**Table I**: *Selected applications of bare BDD electrodes in voltammetric determination of organic analysis.*

| Analyte | BDD electrode, pretreatment[a] | Method (matrix[B]) | LOD[A] [μmol $L^{-1}$] | Ref. |
|---|---|---|---|---|
| *Phenolic Compounds* | | | | |
| Benzophenon-3 | HFCVD BDD[b], AT at +3.2 V, CT at −2.8 V (30 s) in 0.1 mol $L^{-1}$ $HClO_4$ | SWV[c] | 0.14[d, C] | [23] |
| Bisphenol A | Commercial BDD [28], CT at −250 mA $cm^{-2}$ (180 s) | DPV | 0.21 | [29] |
| *Nitrophenols and Other Nitroaromatics* | | | | |
| 4-Nitrophenol | Commercial BDD [30], oxidation by repeated cycling between –2.5 V and | DPV | [F] 1[e], 0.1[d] | [6] |
| 2,4-Dinitrophenol | +2.5 V in 1 mol $L^{-1}$ $HNO_3$ | (river water) | 0.3[e], 0.6[d] | |
| 2-Nitrophenol | | | 0.1[d] | |
| 5-Nitroimidazole | MPCVD microcrystalline BDD, AT at +2.5 V (15 min), before each scan 100 ms pulses at 0 V and +1.7 V for 30 s | DCV, DPV (river water) | 0.9, 0.7 [d,E] | [16] |
| *Aromatic Hydrocarbons and Their Amino-, Nitro-, and Hydroxy Derivatives* | | | | |
| Benzo[*a*]pyrene | Commercial polished BDD [30], manual polishing by $Al_2O_3$ slurry followed by AT at +1.3 V (30 s) | AdSSWV [f] (tap water) | 0.0102 | [22] |
| 1-, 2-Naphthylamine | MPCVD microcrystalline BDD, AT at +2.4 V (60 s) in 0.1 mol $L^{-1}$ $HNO_3$ | DPV | 0.89, 0.44[E] | [31] |
| 1-Aminopyrene | Commercial polished BDD [30] | DPV | 0.06 | [32] |
| 1-Nitropyrene | | | 0.3 | |
| 1-Hydroxypyrene | | | 0.1 | |
| Aminonitrophenols | Commercial BDD [28], CT at –3.0 (10 s) followed by AT at +3.0 V (10 s) in 1 M $HNO_3$ | DPV | 0.4-0.9[e] 0.2-0.6 [d] | [33] |

| Analyte | BDD electrode, pretreatment [a] | Method (matrix[B]) | LOD[A] [μmol $L^{-1}$] | Ref. |
|---|---|---|---|---|
| *Agrochemicals* | | | | |
| Carbendazime, | Commercial BDD [28], AT at +3.0 (10 min) followed by CT at –3.0 V (10 min) | SWV | 0.12 [C] | [34] |
| Fenamiphos | in 0.5 mol $L^{-1}$ $H_2SO_4$ | | 0.10 | |
| Dichloran | MPCVD microcrystalline BDD, oxidation as in [6] | DPV | 0.5[d,E] | [35] |
| | | LSV | 1.9[d,E] | |
| Methyl parathion | Commercial BDD [28], AT at +3.0 (1 s) followed by CT at –3.0 V (30 s) in 0.5 mol $L^{-1}$ $H_2SO_4$ | Sono-SWV | 0.019[d,C] | [36] |
| *Pharmaceuticals* | | | | |
| Acetylsalicylic acid | HFCVD BDD [b], AT at +1.0 V (60 s) followed by CT at –1.0 V(120 s) in 0.5 mol $L^{-1}$ $H_2SO_4$ | SWV | 2[C] | [37] |
| Bezafibrate | HFCVD BDD (8000 ppm, [28]), AT at $i$ = +0.5 mA $cm^{-2}$ (20 s) followed by CT at $i$ = –0.5 mA $cm^{-2}$ (80 s) in 0.5 mol $L^{-1}$ $H_2SO_4$ | DPV | 0.098 | [38] |
| Brimonidine | Commercial BDD [30], polishing by $Al_2O_3$ slurry AT at +1.2 V (60 s), CT at –1.5 V (60 s) in 0.25 mol $L^{-1}$ $H_2SO_4$ | DPV | 0.64[d,G] | [7] |
| | | SWV | 0.13[d,G] | |
| Caffeine | HFCVD BDD [b], CT in 0.5 mol $L^{-1}$ $H_2SO_4$ at −9 C $cm^{-2}$, AT in 0.5 mol $L^{-1}$ | DPV | 0.16 | [39] |
| Acetylic acid [g] | $H_2SO_4$ at +5 C $cm^{-2}$ | | 0.23 | |
| Caffeine | HFCVD BDD [b], CT in 0.5 mol $L^{-1}$ $H_2SO_4$ 180 s at $i$ = −1.0 A $cm^{-2}$ (180 s) | DPV | 0.49 | [40] |
| Paracetamol [g] | | | 0.035 | |
| Chloramphenicol | MPCVD microcrystalline BDD, oxidation as in [6], stirring between individual scans | DCV | 3[d,H] | [41] |
| | | DPV | 3 | |
| Codeine | Commercial BDD [30], 1000 ppm, AT by CV from −2 V to +2 V (10 min) in 0.1 mol $L^{-1}$ $HNO_3$ | DPV | 0.08[C] | [42] |
| Penicillin V | Commercial BDD [30], no pretreatment | DPV | 0.5-40[C] | [43] |

| Analyte | BDD electrode, pretreatment [a] | Method (matrix[B]) | LOD[A] [μmol $L^{-1}$] | Ref. |
|---|---|---|---|---|
| Penicillin V, | Commercial BDD [30], no pretreatment | SWV | 0.21 | [44] |
| Paracetamol [g] | | | 0.32 | |
| Lornoxicam | Commercial BDD [30], polishing by $Al_2O_3$ slurry before each scan | SWV (plasma) | 0.16 (0.037) | [45] |
| | | DPV | 0.17 [F] | |
| Ofloxacin | MPCVD microcrystalline BDD, oxidation as in [6], stirring between individual scans | DCV | 0.4[H] | [41] |
| | | DPV | 1 | |
| Quinine | MPCVD microcrystalline O-BDD, stirring between individual scans | DPV | 1.3[e] | [46] |
| | | | 43.3[d] | |
| Quinizarin | BDD, manual polishing by $Al_2O_3$ slurry and sonication for 1 min before each scan | CV | 0.2[d,I] | [47, |
| | | | 0.005[h,I] | 48] |
| Sertindole | Commercial BDD [30], manual polishing by $Al_2O_3$ slurry before each scan | SWV (plasma) | 0.22 (0.25)[E] | [49] |
| | | DPV (plasma) | 0.24 (0.25) | |
| Sildenafil | HFCVD BDD [b], CT in 0.5 mol $L^{-1}$ $H_2SO_4$ (240 s) at $i = +1.0$ A $cm^{-2}$ | DPV | 6.4[C] | [50] |
| Sulfamethoxazole | HFCVD BDD [b], CT at $i = -0.5$ mA $cm^{-2}$ (60 s) in 0.5 mol $L^{-1}$ $H_2SO_4$ | DPV | 0.014,0.0135 | [51] |
| Trimethoprim | | DPV [i] | 0.065,0.063[C] | [52] |
| 6-Thioguanine | Commercial BDD [30], pretreatment by CV as in [6] | DCV, DPV | 0.6, 0.6 [F] | [53] |
| Zolmitriptan | Commercial BDD [30], manual polishing by $Al_2O_3$ slurry before each scan | DPV (plasma) | 0.073 (0.294) | [54] |
| | | SWV | 0.263 [E] | |
| *Food Components and Additives* | | | | |
| BHA | Commercial HFCVD BDD [28], CT at −1 A $cm^{-2}$ V (120 s) in 0.5 mol $L^{-1}$ | SWV | 0.14[C] | [55] |
| BHT | $H_2SO_4$ | | 0.25 | |
| Capsaicin | Commercial polished BDD [30], manual polishing by $Al_2O_3$ slurry | AdSSWV [f] | 0.034[C] | [21] |
| Chlorogenic acid | Commercial polished BDD [30], manual polishing by $Al_2O_3$ slurry | AdTSSWV | 0.049[C] | [20] |

| Analyte | BDD electrode, pretreatment [a] | Method (matrix[B]) | LOD[A] [μmol $L^{-1}$] | Ref. |
|---|---|---|---|---|
| *Other Compounds* | | | | |
| Glucose [j] | n-Si (111)/ HF CVD BDD, used as deposited | LSV | 25 | [56] [57] |
| Glycerol | Commercial polished BDD [30] | CV, DPV<br>SWV | 149, 356<br>1100 | [58] |
| Oxalic acid | Commercial polished BDD [30], oxidation by three repetitive cycling between –0.5 V to +1.75 V in 0.1 mol $L^{-1}$ $Na_2SO_4$ | DPV | Not given | [59] |
| Estriol | HFCVD BDD [b], CT in 0.5 mol $L^{-1}$ $H_2SO_4$ for 30 min at −3 V, CT for 30 s in measured solution at −3 V prior to each scan | SWV | 0.17 [J] | [60] |
| Indole-3-acetic acid | Commercial BDD [30], AT in 0.5 mol $L^{-1}$ $H_2SO_4$ for 30 s at +3 V, AT for 30 s in measured solution at +3 V prior to each scan | SWV | 1.22[F] | [61] |

*Legend*: AdSSWV – adsorptive stripping – square wave voltammetry; AdTSSWV – adsorptive transfer stripping – square wave voltammetry; AT –anodic treatment; BHA - butylated hydroxyanisole; BHT - butylated hydroxytoluene; CT – cathodic treatment; CVD – chemical vapor deposition; CV – cyclic voltammetry; DPV – differential pulse voltammetry; LSV – linear sweep voltammetry; SDS – sodium dodecylsulfate; SWV – square wave voltammetry.

[a] if no details are given, as deposited polycrystalline H-terminated electrodes and undefined silica support used; [b] polycrystalline BDD from CSEM, B/C ratio 8000 ppm; [c] in the presence of CTAB; [d] reductive determination; [e] oxidative determination; [f] in the presence of SDS; [g] simultaneous voltammetric determination; [h] quanizarine-mediated oxygen reduction; [i] in stopped flow system with thin-layer cell; [j] in the presence of ascorbic and uric acid.

[A] *LOD* for $S/N = 3$, if not otherwise specified; [B] if no matrix given, listed *LOD*s are for model experiments in solutions prepared with deionized water; [C] $LOD = 3s_b/m$, and [D] $LOQ = 10s_b/m$ where $s_b$ is the standard deviation of the mean of the current at the peak potential for repeated voltammograms of the blank solution, $m$ is slope of the calibration curve; [E] $LOD = 3\sigma/m$, [F] $LOQ = 10\sigma/m$ where σ is the standard deviation of the signal measured for the lowest analyte concentration corresponding to calibration plot, $m$ is slope of the analytical curve; [G] $LOD = 3s_i/m$ where $s_i$ is standard deviation of the intercept and $m$ is slope of the calibration curve; [H] *LOQ* calculated using statistic software ADSTAT version 2.0 (Trilobyte, Czech Republic). This software uses confidence bands ($\alpha = 0.05$) for calculation of the *LOQ*. It corresponds to the lowest signal for which relative standard deviation RSD is equal 0.1; [I] the lowest measured concentration; [J] $LOD = 2s_i/m$, explanation as for [G].

***Fouling of the BDD Surface***

Initially, BDD electrodes have been considered as resistant to fouling due to the paraffin-like, hydrogen terminated surface [8]. Nevertheless, it has been clearly proven that this is not a general rule and a number of studies demonstrated fouling problems. Formation of polymeric film on the electrode surface causes rapid deactivation of electrode by blocking electron transfer and slowing down further oxidation. Choosing appropriate solvents and supporting electrolyte systems and electrochemical pretreatment of the electrode may be an alternative option for the reactivation of the electrode surface. An example of electrode fouling in the presence of 2-aminobiphenyl and remediation of the surface using anodic and cathodic pretreatment is given in Fig. 1 [9]. Beside aromatic amines (*e.g.*, metoclopramide [10]), also phenolic compounds (*e.g.*, ref. [11]) are susceptible of causing BDD passivation, because both compounds produce reactive radicals (phenoxy radicals or amino cation radicals) capable of further dimerization and polymerization at the electrode surface. The strategies to prevent passivation are discussed below.

***Pretreatment of the BDD Surface***

Pretreatment of the electrode surface can be applied for conditioning of the electrode surface, enhancement of the voltammetric signals, preventing the passivation of electrode surface, and ensuring of repeatable and reproducible response of particular analytes. The basic strategy for conditioning of the electrode surface is its electrochemical anodic oxidation (~ θ +2.0 V) for minutes in the region of water decomposition. The formation of OH radicals (Eq. 1) causes oxidation and stabilization of the electrode surface with the prevalence of the ketonic, alcoholic and carboxylic groups [12]. While at the beginnings many studies were presented to be performed at as grown, H-terminated BDD surfaces, this approach is superannuated nova days because the maintenance of H-termination is complicated due to the easy of electrochemical oxidation and even oxidation of BDD surface by air oxygen [13]. The re-hydrogenation of an oxidized BDD surface is achievable only by hydrogen-flame annealing or hydrogen-plasma treatment, which requires adequate equipment. It can be presumed that many of the early studies performed using allegedly H-terminated surfaces were in fact conducted at oxidized BDD surfaces.

Further optimization of electrode pretreatment has to result in experimental protocol ensuring possibly repeatable, maximized, and well evaluable signals. For this purpose, most frequently high positive/negative current densities or potentials (~ θ ±2.0 V) applied for few seconds to minutes are used. As results of this anodic/cathodic pretreatment, oxygen-terminated (O-BDD) or hydrogen-terminated (H-BDD) surfaces are produced. The importance of cathodic pretreatment was called by Suffredini *et al.*, who presented faster electron transfer for $[Fe(CN)_6]^{4-/3-}$ and signal increase and improved repeatability for selected chlorophenols [14]. The cathodic pretreatment has to be applied just before the electrochemical experiments to ensure reliable and reproducible results, especially when the electrode has not been used for a long period of time due to its instability in air [15]. It facilitates the interaction and adsorption of the electrochemical species with the electrode surface and thus clearly leads to a larger electrochemical activity for a number of compounds, as can be traced in Table I.

Anodic pretreatment before each scan is a powerful tool for preventing electrode fouling, as demonstrated at Fig. 1C for 2-aminobiphenyl. The peak height repeatability characterized by relative standard deviation is 2.7 %, and anodic pretreatment is thus favorable compared with cathodic pretreatment, leading to instability of voltammetric responses (Fig. 1B).

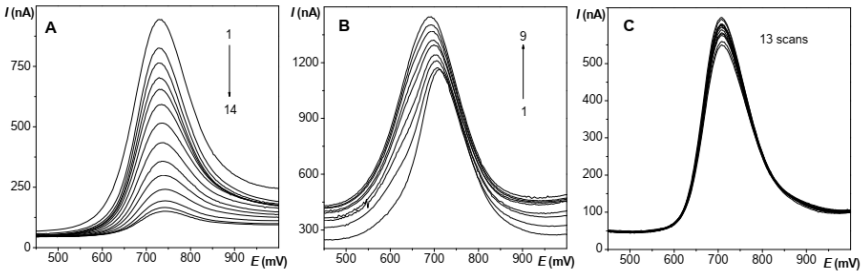


**Fig. 1**: *Influence of the electrode pretreatment on the differential pulse voltammograms of 2-aminobiphenyl ($c = 5 \cdot 10^{-5}$ mol dm$^{-3}$) in BR buffer pH 7.0.* Measured on BDD without pretreatment (A) and with pretreatment consisting of stirring and applying the potential of –2.4 V (B) or +2.4 V (C) for 15 s on working electrode in measured solution between individual measurements. The number of scans is indicated in particular figures.

Other option of electrode activation includes application of cyclic voltammetry, mostly in acidic media, or repeated application of short potential pulses close or in the onset of supporting electrolyte curve. Examples of these approaches include determination of 5-nitroimidazole (basic structural unit of some antibiotics) in model samples of drinking water (see ref. [16] and fig. 2 therein).

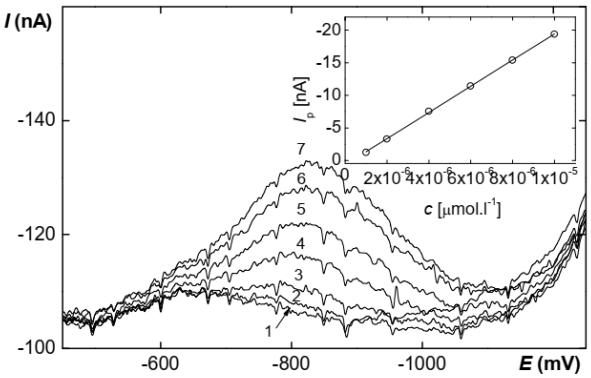


**Fig. 2**: *Differential pulse voltammograms of 5-nitroimidazole in model samples of river water (river water – acetate buffer pH 4.6 (9:1)).* Concentration *c* of 5-nitroimidazole: 0 (1); $1 \cdot 10^{-6}$ (2); $2 \cdot 10^{-6}$ (3); $4 \cdot 10^{-6}$ (4); $6 \cdot 10^{-6}$ (5); $8 \cdot 10^{-6}$ (6) a $10 \cdot 10^{-6}$ (7) mol $l^{-1}$. Measured on BDD with pretreatment consisting of stirring and applying 100 ms lasting potential regeneration pulses $E_{reg.1} = 0$ V, $E_{reg.2} = 1.7$ V for 30 s on working electrode in measured solution between individual measurements. Inset corresponding calibration dependence. Reproduced from [16].

***Boron Concentration***

The concentration of boron influences significantly the electrochemical properties of the BDD films. It is usually given as B/C ratio in the gas phase during the CVD process and films deposited at B/C ratio 100 – 10000 ppm corresponding to final boron concentration in the film [B] $\sim 1.10^{19}$ cm$^{-3}$ $-$ $1.10^{21}$ cm$^{-3}$ were tested in last years. Obviously, increased boron content leads to higher capacitance, slightly narrower solvent windows and can increase the likelihood of undesirable incorporation of $sp^2$ impurities. Depending on the doping level, BDD films present either semiconducting or metallic electronic properties, with boundary

boron content of about 1-3.$10^{20}$ $cm^{-3}$ (ref. [13, 17]). These concentrations are sufficient to achieve fast electron transfer. Despite the fact that increased interest may be traced in last five years on this problematic and the information on boron doping level is frequently present in electroanalytical publications, only few studies address its influence on electroanalytical characteristics including the width of the potential window [13, 17] or on sensitivity for particular analytes including *e.g.* the floroquinolone enrofloxacin [18] or our results for 2-aminobiphenyl [19].

***Adsorptive Stripping Voltammetry***

Bare BDD surfaces have been considered for a long period as relatively inert to the adsorption for organic compounds, nevertheless a few examples on the use anodic adsorptive stripping voltammetry for oxidizable compounds have been reported in last five years. These include utilization of the adsorption of the analyte itself or the absorption of surfactants interacting with organic analytes on the BDD surface. The former approach enabled determination of antioxidant capacity in the coffee samples based on the oxidation peaks of present phenolic compounds – chlorogenic, caffeic, and gallic using adsorptive transfer stripping voltammetry [20]. The interaction of surfactant and an organic compound can change the redox potential, charge transfer coefficient or diffusion coefficient of the electrode processes and thus leads to improved analytical figures of merit as presented for detection of capsaicin [21] or benzo(*a*)pyrene [22] in the presence of sodium dodecylsulfate or benzophenone-3 in the presence of cetyltrimethylammonium bromide (CTAB) [23]. The main disadvantage of this approach is the necessity of manual polishing of the BDD surface after each scan. On the other hand, the interaction of the surfactant or transfer of the adsorbed species from the matrix to pure supporting electrolytes can substantially increase the selectivity of the method.

***BDD-Based Electrodes and Sensors***

Beside the classical planar nanocrystalline and microcrystalline BDD films deposited at silica, eventually tungsten, numerous attempts were made to design BDD-based microelectrodes, BDD microdisc arrays or other variations (summarized in review [24]). Regardless on the miniaturization trend, benefits of increase of active electrode area and roughness of the

surface were demonstrated in detection of dopamine and non-enzymatic amperometric detection of glucose [25] using 3D-structured BDD nanorod forest electrode. Conductive BDD powder and polyester binder were used to fabricate screen-printed electrode on polyimide sheets and exhibited greater durability to fouling by dopamine than carbon screen-printed electrode [26]. Further, many studies exist on modified BDD surfaces and their utilizations in construction of BDD-based sensors (for details, see [2, 27]). Further development in this field can be foreseen thanks to the progress in the deposition technology of the BDD films, their modification and widening insights in the principles of biosensing.

## Conclusions

Obviously, the possibilities of BDD electrodes in voltammetric methods hold an unceasing interest, which can be documented by a number of publications demonstrating practical applicability of the developed methods on analysis of various matrices. The most vivid field is presumably their utilization for detection of pharmaceutical substances. Hopefully, further research will supports their expansion in pharmaceutical, clinical and environmental laboratories, so that their advantageous properties enabling versatile use can be appreciated not only in the academic, but more in commercial sphere.

### Acknowledgements

*This research was carried out within the framework of Specific University Research (SVV260084). The research was financially supported by the Grant Agency of Charles University in Prague (Project GAUK 684213).*

## References

1. G. M. Swain, R. Ramesham: *Anal. Chem.* ***65*** (1993) 345.
2. A. Kapalka, H. Baltruschat, C. Comninellis: *Synthetic Diamond Films - Preparation, Electrochemistry, Characterization and Applications*. Wiley, Hoboken, 2010.
3. A. Fujishima, Y. Einaga, T. N. Rao, D. A. Tryk: *Diamond Electrochemistry*. Elsevier, Amsterdam, 2005.
4. K. Peckova, J. Musilova, J. Barek: *Crit. Rev. Anal. Chem.* ***39*** (2009) 148.

5. P. W. May, W. J. Ludlow, M. Hannaway, P. J. Heard, J. A. Smith, K. N. Rosser: *Diam. Relat. Mat.* ***17*** (2008) 105.
6. J. Musilova, J. Barek, K. Peckova: *Electroanalysis* ***23*** (2011) 1236.
7. V. Radulovic, M. M. Aleksic, D. Agbaba, V. Kapetanovic: *Electroanalysis* ***25*** (2013) 230.
8. J. Barek, J. Fischer, T. Navratil, K. Peckova, B. Yosypchuk, J. Zima: *Electroanalysis* ***19*** (2007) 2003.
9. J. Zavazalova, J. Vosáhlová, I. Šloufová, E. Pawlova, V. Petrák, K. Pecková: *Electrochim. Acta*: article in preparation.
10. H. Dejmkova, C. Dag, J. Barek, J. Zima: *Cent. Eur. J. Chem.* ***10*** (2012) 1310.
11. H. Dejmkova, M. Scampicchio, J. Zima, J. Barek, S. Mannino: *Electroanalysis* ***21*** (2009) 1014.
12. I. Duo, C. Levy-Clement, A. Fujishima, C. Comninellis: *J. Appl. Electrochem.* ***34*** (2004) 935.
13. L. A. Hutton, J. G. Iacobini, E. Bitziou, R. B. Channon, M. E. Newton, J. V. MacPherson: *Anal. Chem.* ***85*** (2013) 7230.
14. H. B. Suffredini, V. A. Pedrosa, L. Codognoto, S. A. S. Machado, R. C. Rocha-Filho, L. A. Avaca: *Electrochim. Acta* ***49*** (2004) 4021.
15. G. R. Salazar-Banda, L. S. Andrade, P. A. P. Nascente, P. S. Pizani, R. C. Rocha, L. A. Avaca: *Electrochim. Acta* ***51*** (2006) 4612.
16. M. Smidkova: *MSc Thesis* (in Czech). Faculty of Science, Charles Univesity in Prague, Prague; 2013.
17. Z. V. Zivcova, O. Frank, V. Petrak, H. Tarabkova, J. Vacik, M. Nesladek, L. Kavan: *Electrochim. Acta* ***87*** (2013) 518.
18. E. Guinea, J. A. Garrido, R. M. Rodriguez, P. L. Cabot, C. Arias, F. Centellas, E. Brillas: *Electrochim. Acta* ***55*** (2010) 2101.
19. J. Vosahlova: *Bc Thesis* (in Czech). Faculty of Science, Charles Univesity in Prague, Prague; 2013.
20. Y. Yardim: *J. Food Sci.* ***77*** (2012) C408.
21. Y. Yardim: *Electroanalysis* ***23*** (2011) 2491.
22. Y. Yardim, A. Levent, E. Keskin, Z. Senturk: *Talanta* ***85*** (2011) 441.
23. M. T. Laranjeira, F. de Lima, S. C. de Oliveira, V. S. Ferreira, R. T. S. de Oliveira: *Amer.J. Anal. Chem.* ***2*** (2011) 383.
24. K. Peckova, J. Barek: *Curr. Org. Chem.* ***15*** (2011) 3014.
25. D. B. Luo, L. Z. Wu, J. F. Zhi: *ACS Nano* ***3*** (2009) 2121.
26. T. Kondo, H. Sakamoto, T. Kato, M. Horitani, I. Shitanda, M. Itagaki, M. Yuasa: *Electrochem. Commun.* ***13*** (2011) 1546.
27. S. Szunerits, R. Boukherroub: *J. Solid State Electrochem.* ***12*** (2008) 1205.
28. http://neocoat.ch; downloaded on March 10, 2014.
29. G. F. Pereira, L. S. Andrade, R. C. Rocha, N. Bocchi, S. R. Biaggio: *Electrochim. Acta* ***82*** (2012) 3.
30. http://windsorscientific..co.uk; downloaded on March 10, 2014.
31. J. Zavazalova, H. Dejmkova, J. Barek, K. Peckova: *Electroanalysis* ***25*** (2013) 253.
32. O. Yosypchuk, J. Barek, V. Vyskocil: *Anal. Lett.* ***45*** (2012) 449.
33. H. Dejmkova, J. Barek, J. Zima: *Int. J. Electrochem. Sci.* ***6*** (2011) 3550.
34. R. F. Franca, H. P. M. de Oliveira, V. A. Pedrosa, L. Codognoto: *Diam. Relat. Mater.* ***27-28*** (2012) 54.

35. L. Jílková: *Bc Thesis* (in Czech). Faculty of Science, Charles Univesity in Prague, Prague; 2008.
36. G. S. Garbellini, G. R. Salazar-Banda, L. A. Avaca: *Food Chem.* ***116*** (2009) 1029.
37. E. R. Sartori, R. A. Medeiros, R. C. Rocha-Filho, O. Fatibello-Filho: *J. Braz. Chem. Soc.* ***20*** (2009) 360.
38. J. A. Ardila, E. R. Sartori, R. C. Rocha-Filho, O. Fatibello-Filho: *Talanta* ***103*** (2013) 201.
39. E. O. Faria, A. C. V. Lopes, D. E. P. Souto, F. R. F. Leite, F. S. Damos, R. D. S. Luz, A. S. dos Santos, D. L. Franco, W. T. P. dos Santos: *Electroanalysis* ***24*** (2012) 1141.
40. B. C. Lourencao, R. A. Medeiros, R. C. Rocha-Filho, L. H. Mazo, O. Fatibello: *Talanta* ***78*** (2009) 748.
41. J. Jecminkova, *MSc Thesis* (in Czech). Faculty of Science, Charles Univesity in Prague, Prague; 2011.
42. L. Svorc, J. Sochr, J. Svitkova, M. Rievaj, D. Bustin: *Electrochim. Acta* ***87*** (2013) 503.
43. L. Svorc, J. Sochr, M. Rievaj, P. Tomcik, D. Bustin: *Bioelectrochemistry* ***88*** (2012) 36.
44. L. Svorc, J. Sochr, P. Tomcik, M. Rievaj, D. Bustin: *Electrochim. Acta* ***68*** (2012) 227.
45. B. Bozal, B. Uslu: *Comb. Chem. High Throughput Screen* ***13*** (2010) 599.
46. V. Brunovska, *Bc Thesis* (in Czech). Faculty of Science, Charles Univesity in Prague, Prague; 2013.
47. I. B. Dimov, C. Batchelor-McAuley, L. Aldous, R. G. Compton: *Phys. Chem. Chem. Phys.* ***14*** (2012) 2375.
48. C. Batchelor-McAuley, I. B. Dimov, L. Aldous, R. G. Compton: *Proc. Natl. Acad. Sci. U. S. A.* ***108*** (2011) 19891.
49. Y. Altun, B. Dogan-Topal, B. Uslu, S. A. Ozkan: *Electrochim. Acta* ***54*** (2009) 1893.
50. E. F. Batista, E. R. Sartori, R. A. Medeiros, R. C. Rocha-Filho, O. Fatibello-Filho: *Anal. Lett.* ***43*** (2010) 1046.
51. L. S. Andrade, R. C. Rocha-Filho, Q. B. Cass, O. Fatibello-Filho: *Electroanalysis* ***21*** (2009) 1475.
52. L. S. Andrade, R. C. Rocha-Filho, Q. B. Cass, O. Fatibello-Filho: *Anal. Methods* ***2*** (2010) 402.
53. J. Humpolikova, *MSc Thesis* (in Czech). Faculty of Science, Charles Univesity in Prague, Prague; 2013.
54. B. Uslu, D. Canbaz: *Pharmazie* ***65*** (2010) 245.
55. R. A. Medeiros, R. C. Rocha-Filho, O. Fatibello-Filho: *Food Chem.* ***123*** (2010) 886.
56. J. W. Zhao, L. Z. Wu, J. F. Zhi: *Analyst* ***134*** (2009) 794.
57. J. W. Zhao, J. L. Wang, J. F. Zhi, Z. M. Zhang: *Sci. China-Chem.* ***53*** (2010) 1378.
58. A. Pop, F. Manea, C. Radovan, D. Dascalu, N. Vaszilcsin, J. Schoonman: *Analyst* ***137*** (2012) 641.
59. A. Pop, E. Ilinoiu, F. Manea, I. Pisoi, G. Burtica: *Environ. Eng. Manag. J.* ***10*** (2011) 75.
60. K. D. Santos, O. C. Braga, I. C. Vieira, A. Spinelli: *Talanta* ***80*** (2010) 1999.
61. Y. Yardim, M. E. Erez: *Electroanalysis* ***23*** (2011) 667.

# *Appendix II*

*Publication 2*

Electrochimica Acta 243 (2017) 170–182

Contents lists available at ScienceDirect

Electrochimica Acta

journal homepage: www.elsevier.com/locate/electacta

## Influence of boron content on the morphological, spectral, and electroanalytical characteristics of anodically oxidized boron-doped diamond electrodes

Karolina Schwarzová-Pecková[a,*], Jana Vosáhlová[a], Jiří Barek[a], Ivana Šloufová[b], Ewa Pavlova[c], Václav Petrák[d], Jaroslava Zavázalová[a]

[a] Charles University, Faculty of Science, Department of Analytical Chemistry, UNESCO Laboratory of Environmental Electrochemistry, Albertov 6, CZ-12843 Prague 2, Czech Republic
[b] Charles University, Faculty of Science, Department of Physical and Macromolecular Chemistry, Albertov 6, CZ-12843 Prague 2, Czech Republic
[c] Institute of Macromolecular Chemistry, Academy of Sciences of the Czech Republic, v.v.i., Heyrovsky Sq. 2, CZ-16206 Prague 6, Czech Republic
[d] Institute of Physics, Academy of Sciences of the Czech Republic, v.v.i., Na Slovance 2, CZ-18221 Prague 8, Czech Republic

ARTICLE INFO

*Article history:*
Received 14 November 2016
Received in revised form 30 April 2017
Accepted 1 May 2017
Available online 2 May 2017

*Keywords:*
2-Aminobiphenyl
Boron content
Boron-doped diamond
Raman spectroscopy
Voltammetry

ABSTRACT

The effect of boron content in nanocrystalline anodically polarized boron doped diamond (BDD) thin films deposited at B/C ratio 500 ppm – 8000 ppm on their morphology, quality, and electrochemical and spectral properties was investigated using scanning electron and atomic force microscopies and Raman spectroscopy, where the shift of maximum Lorentzian component of diamond phonon at ~1332 $cm^{-1}$ was used as the function of boron concentration. Cyclic voltammetry with the outer- and inner sphere redox markers ($[Ru(NH_3)_6]^{3+/2+}$ and $[Fe(CN)_6]^{3-/4-}$) enables to differentiate among the semiconductive films (500 ppm and 1000 ppm) and films with metallic conductivity (2000 ppm – 8000 ppm). Nevertheless, only the inner sphere character of $[Fe(CN)_6]^{3-/4-}$ redox marker enables to visualize the differences between individual boron content for metallic films. Further, reversible behavior with $\Delta E_p$ of 59.8 ± 0.9 mV ($n$ = 5) and $I_{pa}/I_{pc}$ ratio 1.00 at the scan rate of 100 mV $s^{-1}$ was achieved for this redox marker at 2000 ppm film; this film just above the semiconductive/metallic threshold exhibited also favorable spectral (*e.g.*, roughness surface factor) and electrochemical characteristics. The width of the potential window in aqueous media of different pH values and in wide variety of supporting electrolytes decreases with increasing boron content, with independence of anodic potential limit for 2000 ppm – 8000 ppm electrodes and more pronounced dependence of cathodic potential limit on boron content for all tested BDD films. Further, well-defined and highly reproducible anodic DP voltammetric peak of 2-aminobiphenyl with peak current increasing with boron content were obtained at ca +0.7 V (*vs.* Ag/AgCl/3 mol $L^{-1}$ KCl) at all BDD films tested.



### 1. Introduction

Boron doped diamond thin films are since their introduction [1,2] the subject of considerable interest as an electrode material. The boron doping level, structural defects in the diamond film, content of non-diamond ($sp^2$) carbon impurities, size of the diamond crystallites and crystallographic orientation, and surface termination (H, O) are the main factors influencing their quality and properties. Nevertheless, the linkage of the properties of the BDD film to its spectral and electrochemical characteristics is still the subject of continuous interest of scientific community.

The boron content in BDD is one of the factors substantially influencing the film morphology, conductivity, and electrochemical properties [3–10]. Films with boron concentration [B] ~ $1 \times 10^{19}$ $cm^{-3}$–$1 \times 10^{21}$ $cm^{-3}$ were tested in the last years. While films with [B] below $10^{19}$ boron atoms per $cm^{-3}$ exhibit clear valence band, concentration up to $2 \times 10^{20}$ $cm^{-3}$ leads to semiconductivity – this is the theoretical value of semiconducting/metallic transition predicted in 1970 [11]. Practically, the boundary boron concentration of about (1 – 3) × $10^{20}$ $cm^{-3}$ [12,13] or even higher value [B] = $4.5 \times 10^{20}$ $cm^{-3}$ [10] were reported and it seems that this doping level is sufficient to achieve fast electron transfer typical for metallic-type conductivity. Films with [B] > $3 \times 10^{20}$

* Corresponding author.
*E-mail address:* karolina.schwarzova@natur.cuni.cz (K. Schwarzová-Pecková).

http://dx.doi.org/10.1016/j.electacta.2017.05.006
0013-4686/

boron atoms $cm^{-3}$ are sometimes denoted as heavily doped BDD films [8]. Nevertheless, the estimation of boron concentration directly in the film is problematic, achievable only by secondary ion mass spectrometry (SIMS), or boron nuclear reaction analysis [10] (*e.g.*, neutron depth profiling [7]). Several studies were published investigating the location, configuration, and bonding structure of boron in the BDD layers [14–17]. These might be located within grains or grain boundaries of thin films as well as within the core or at the surface of diamond crystallites. It is known that the crystallographic orientation affects boron uptake, with {111} > {110} > {100} [17]. According to the technique of measurement the estimated boron concentration represents a mean value from different growth sectors in each crystallite and for all crystallites of the films, or a total mean concentration including the grains and grain boundaries, where boron segregation may occur [10]. Thus, the boron content is usually given by the B/C ratio, where B and C refer to boron and carbon content in the gaseous phase for chemical vapor deposition procedure. These values usually range from 100 ppm to 15000 ppm and experimental values for semiconducting/metallic transition of conductivity are *ca.* 1000 – 2000 ppm [8].

A wide variety of methods is being used for characterization of BDD thin films. Among them, Raman spectroscopy at visible wavelengths is routinely used for characterization of diamond films due to its sensitivity to the $sp^3$ carbon and to the content of non-diamond $sp^2$ carbon impurities. At the metallic levels of doping the diamond phonon line at 1332 $cm^{-1}$ exhibits asymmetry and a shift to lower wavenumbers, which comes from the Fano interference of this one phonon band induced by quantum mechanical interference between the discrete phonon and electronic continuum. In electrochemistry, several redox probes including $[Fe(CN)_6]^{3-/4-}$, dopamine, $[Ru(NH_3)_6]^{3+/2+}$, or $[IrCl_6]^{2-/3-}$ are being used to evaluate the electrode kinetics. The heterogeneous electron transfer (HET) of the latter two probes proceeds by an outer-sphere electron-transfer pathway with the electrode kinetics being relatively insensitive to the physicochemical properties of diamond [18]. The formal potential of $[Ru(NH_3)_6]^{3+/2+}$ couple ($E^{0'} = -0.16$ V *vs.* SCE) lies in the band gap of the BDD, and thus this probe is capable of showing differences in electrochemical characteristics of the differently doped electrodes. Apparent heterogeneous electron-transfer rate constants, $k^0_{app}$, between 0.01 and 0.2 $cm\,s^{-1}$ are commonly observed for conducting polycrystalline films (both microcrystalline or nanocrystalline) without extensive pretreatment for these outer-sphere redox markers [19,20]. Similarly, the voltammetric response of the $[Fe(CN)_6]^{3-/4-}$ redox couple has been largely studied at BDD electrodes [18,20–23] as the charge transfer proceeds through a more inner-sphere electron transfer pathway, with the electrode kinetics being highly sensitive to the diamond surface termination. Thus, the range of $k^0_{app}$ is several orders of magnitude in dependence on the BDD surface characteristics [20,24,25].

In electroanalysis, most frequently anodized *i.e.*, oxygen-terminated BDD surfaces with prevalence of ether bonds, C—OH, C=O, and (COOH) groups [26] are predominantly used. Nevertheless, cathodically pretreated films with partially hydrogen-terminated surface over performed them in voltammetric response of some organic analytes [21,25,27,28] or in applications in liquid flow techniques [29]. Oxygen atoms become incorporated into the BDD surface mostly via carbon reaction with $HO^{\bullet}$ radicals. These are products of the one electron transfer from water as the first step of oxygen evolution reaction (OER) at high anodic potentials in the region of water instability (eq. (1)) in aqueous media of pH < 9.0 (ref. [30]).

$$H_2O(BDD) \rightarrow HO^{\bullet}(BDD) + H^+ + e^- \quad (1)$$

Quasi-free $HO^{\bullet}$ radicals are confined to the BDD surface and the subsequent reactions include their reactions with each other and/or reactions with intermediates, *e.g.*, $H_2O_2$ and $O_2H^{\bullet}$ radicals including further electron transfers leading to $O_2$ (described in detail in ref. [31,32]). Technically, most frequently highly positive current densities (typically units to tens of mA $cm^{-2}$) or potentials (~ < +2.0 V) applied for few seconds to minutes are used to achieve sufficient O-termination. It was reported that and even tens of seconds may lead to almost complete oxidation when sufficiently high potentials are applied (~ < +3.0 V *vs.* a platinum counter electrode in 1 mol $L^{-1}$ sulfuric acid/0.5 mol $L^{-1}$ nitric acid solution) [33]. The type and distribution of oxygen-containing chemical functionalities on the polycrystalline BDD surface is dependent on the boron doping level [34], grain size, and proportion of different grain orientations [18].

While the investigation of reactions at the anodic potential limit is in the focus of researchers due to the utilization of BDD electrodes for decomposition of organic compounds by quasi-free $HO^{\bullet}$ radicals formed by reaction (1) [30–32,35] or their role in anodic oxidation of BDD surface [26], less attention has been paid to the mechanism of hydrogen evolution reaction (HER) at the cathodic side of potential window [35,36].

HER proceeds in acidic media via Volmer-Heyrovsky mechanism (equations (2) and (3)), where (BDD) represents active site at the BDD surface:

$$BDD + H^+ + e^- \leftrightarrow (BDD)H \quad \text{Volmer reaction} \quad (2)$$

$$(BDD)H + H^+ + e^- \rightarrow BDD + H_2 \quad \text{Heyrovsky reaction} \quad (3)$$

The reaction proceeds via the initial adsorption of the water molecule/proton [35,37]. Afterwards, the weakly adsorbed H presumably catalyzes the hydrogen evolution reaction [36]. In contradiction, both reactions were found to be the rate determining steps: Volmer reaction (Eq. (2)) due to high apparent energy of the $[S\cdots H^+]$ intermediate calculated from Tafel plots [35]. However, lower calculated activation energies for reaction described by eq. (2) than those for eq. (3) indicated the Heyrovsky step as the rate determining one [36]. The adsorption of H is associated with near subsurface substitutional boron defects and thus can be directly associated with boron-doping level [37].

Recently, several papers were published concerning the influence of boron content on the physical and electrochemical characteristics of the BDD films [3–6,38], such as resistivity towards electrochemical corrosion [5], surface resistivity towards fouling [39], effectivity of electrocatalytic anodic oxidation of organic pollutants [40–43], and analytical parameters of determination of selected inorganic ions [38,44]. Despite the fact that increased interest may be traced in last seven years on this topic and that the information on boron doping level (at least as B/C ratio during the deposition procedure) is usually presented in electroanalytical publications, at least as B/C ratio during deposition procedure, only few studies have addressed its influence on electroanalytical characteristics of the BDD films, including the width of the potential window [37,45,46] or voltammetric responses for organic analytes including floroquinolone enrofloxacin [43], dopamine [39], benzophenone-3 [47], 5-nitroquinoline [48], and 4-chloro-3-methylphenol [49].

The aim of this work is to clarify the influence of boron doping level in nanocrystalline, anodically pretreated BDD films on factors important for their applications in organic electroanalysis, including potential window in aqueous media of different pH values and in a wide variety of supporting electrolytes (considering the fact that up to now, almost all studies of the potential limits for different boron doping levels have been performed in acidic [37] or

neutral [9,10] media). Further we studied electrochemical behavior and analytical parameters for the determination of 2-aminobiphenyl. For this purpose, a series of five BDD films with boron contents 500 ppm – 8000 ppm was prepared. The electrodes were characterized by Raman spectroscopy, scanning electron microscopy, and atomic force microscopy (AFM). Changes in the electrochemical responses for the inner $[Fe(CN)_6]^{3-/4-}$ and outer sphere $[Ru(NH_3)_6]^{3+/2+}$ redox markers, widths of potential windows and voltammetric responses to 2-aminobiphenyl, and the shift of maximum Lorentzian component of diamond phonon at ~ 1332 $cm^{-1}$ were assessed as function of boron content.

2-aminobiphenyl was selected as a model analyte, as its amino group on aromatic skeleton is easily oxidisable within the potential window of BDD electrodes. The same functional group is present in many organic compounds of environmental, physiological, or pharmaceutical significance. As all aromatic amines (irrespective of the nature of the medium) the 2-aminobiphenyl undergoes anodic oxidation through the formation of a monocation radical, which, through its resonance structures, is followed by dimerization and/or polymerization [50–52]. In our previous studies, micromolar limits of detection (LOD) were achieved in aqueous media of Britton-Robinson (BR) buffer pH 7.0 [53,54]. Problems with electrode fouling had to be overcome by anodic pretreatment between individual measurements, similarly as for other aromatic amines [50,53,55–60].

Results of this study are discussed to clarify the relationship between boron content, spectral and electrochemical properties of the BDD electrodes and their applicability in organic electroanalysis in aqueous media.

## 2. Experimental

### 2.1. Chemicals

2-Aminobiphenyl (Sigma-Aldrich, ≤95%), $(K_4[Fe(CN)_6]) \times 3H_2O$ (LachNer, Neratovice, Czech Republic, ≤99%), and $[Ru(NH_3)_6]Cl_3$ (Sigma-Aldrich, ≤98%) were used. All other chemicals used as supporting electrolytes were analytical grade from LachNer, Neratovice. All solutions were prepared with high-purity water obtained from a Millipore Milli-Q system with conductivity $< 6 \times 10^{-8}$ S $cm^{-1}$ at 25 °C.

### 2.2. Apparatus and Procedures

DXR Raman microscope (Thermo Scientific, Waltham, MA, USA) interfaced to an Olympus microscope (employing an objective 10x) and the 532 nm (diode pumped solid state laser) excitation line was used. The laser power was 10 mW. High resolution grating, accumulation time 2 s, and number of accumulations 32 were used. The spectra represent average of four measurements. The overlapping bands in spectral regions 150 – 900 $cm^{-1}$ (samples with the highest B/C ratio) and 1030 – 1380 $cm^{-1}$ (all samples) were successfully separated and fitted using the spectral program OMNIC. It was demonstrated that the same results, considering the maximum of the bands, for the 150 – 900 $cm^{-1}$ range were obtained if the Gaussian and Lorentzian profiles and/or the Gaussian/Lorentzian profile were used. In both cases the maximum of the narrow band was the same. For the 1030 – 1380 $cm^{-1}$ range the Gaussian/Lorentzian profile and log-normal profile was used. In all cases, the linear baseline correction was used. AFM measurements were performed using a scanning probe microscope NT-MDT NTEGRA Prima equipped with a Nanosensors silicon cantilever HA-NC (resonant frequency 270 kHz); the tapping mode under ambient conditions was applied.

Morphology of the nanocrystalline films was visualized by means of a high-resolution field-emission gun scanning electron microscopy (FEGSEM; microscope Quanta 200 FEG, FEI Company, Czech Republic). The sample was inserted into the microscope without any coating so that its surface was available for further analyses. Low-vacuum mode (chamber pressure 80 Pa) was used to eliminate charging of the sample. All micrographs are secondary electron (SE) images taken with low-vacuum SE detector at accelerating voltage 30 kV.

Voltammetric measurements were carried out using a computer controlled Eco-Tribo Polarograph with PolarPro software (version 5.1, EcoTrend Plus, Prague, Czech Republic) in a three-electrode arrangement, using a silver chloride reference electrode (Ag|AgCl, 3 mol $L^{-1}$ KCl) (all potentials in further text are given *vs.* this reference electrode), and a platinum wire auxiliary electrode (both Elektrochemické detektory, Turnov, Czech Republic).

The nanocrystalline BDD films were deposited on boron-doped (100) silicon wafers (resistivity 0.005 Ω cm; thickness 300 μm; ON Semiconductor, Rožnov pod Radhoštěm, Czech Republic). Series of five BDD thin films of 1 μm thickness deposited by microwave plasma-assisted chemical vapor deposition (AX5010 Seki ASTeX, San Jose, CA, USA) of mixtures containing 99.0% $H_2$/1.0% $CH_4$ with variable B/C ratio in the gas phase 500 ppm, 1000 ppm, 2000 ppm, 4000 ppm, and 8000 ppm was prepared. The doping was induced by trimethyl boron gas. As usually, the films are denoted by the B/C ratio of the gas mixture used for the deposition; these values given in ppm units are denoted as *boron content* or *boron-doping level*. The symbol [B], *i.e. boron concentration*, is strictly used when referring to the number of B atoms per $cm^{-3}$. The other deposition conditions were: pressure 50 mBar, microwave power 1000 W, temperature 710 °C (measured by pyrometer), run time 240 min. Neutron depth profiling was used for evaluation of total boron concentration in prepared BDD samples. For this purpose the reactor LVR-15, a light water moderated and cooled tank-type nuclear research reactor situated in Nuclear Research Institute Řež (Řež u Prahy, Czech Republic) was used. The beam cross-section 2 × 2 mm and neutron flux $1 \cdot 10^7$ neutron·$cm^{-2}$ $s^{-1}$ were used.

The obtained BDD disks were placed in a laboratory-made BDD disk electrode [55] with active geometric area of 5.72 $mm^2$ (disc diameter 2.7 mm) and used as the working electrode in both voltammetric and amperometric measurements. The newly obtained BDD electrodes were oxidized in 0.1 mol $L^{-1}$ sulfuric acid by applying the potential +2.4 V *vs.* Ag|AgCl, 3 mol $L^{-1}$ KCl for 20 min. Potentiostatic (re)oxidation for 10 min was repeated after each set of experiments involving measurements in the region of hydrogen evolution inevitably causing partial loss of oxygen-containing functionalities (*e.g.*, experiments on the effect of the supporting electrolyte on the potential window (chapter 3.3)). Furthermore, at the beginning of each working day the electrodes were activated in 0.1 mol $L^{-1}$ sulfuric acid by applying the potential of +2.4 V for 180 s. No significant fluctuations of $\Delta E_p$ and $I_p$ values of the redox marker $[Fe(CN)_6]^{3-/4-}$ were observed during the measuring period (ca four months).

During experiments with 2-aminobiphenyl, the electrode was activated directly in the analyte solution by applying the potential +2.4 V for 30 s between individual measurements.

In differential pulse voltammetry, pulse height of +50 mV, pulse width of 100 ms, and scan rate of 20 mV $s^{-1}$ were applied. In linear sweep voltammetry, scan rate of 50 mV $s^{-1}$ and in cyclic voltammetry, scan rate of 100 mV $s^{-1}$ was applied, if not stated otherwise.

Apparent heterogeneous electron-transfer rate constant, $k^{\circ}_{app}$ were calculated according Nicholson [61] for the scan rate of 300 mV $s^{-1}$ assuming $D_{ox} = D_{red}$. The following values of diffusion coefficients were used: $7.6 \times 10^{-6}$ $cm^2$ $s^{-1}$ for $[Fe(CN)_6]^{3-/4-}$ [62] and $5.5 \times 10^{-6}$ $cm^2$ $s^{-1}$ for $[Ru(NH_3)_6]^{3+/2+}$ [63]. The rate constants

are referred to as apparent ones, because no correction for electric double layer effects was made.

Double layer capacities $C$ were calculated from CV data presented in Fig. 5 as $C = I_{av}/vA$, where $I_{av}$ is the average current from the forward and reverse sweep at 0 V, $v$ is the scan rate, and $A$ the geometric electrode area.

All measurements were carried out at laboratory temperature. The pH measurements were carried out by digital pH Meter 3510 (Jenway, UK) with combined glass electrode.

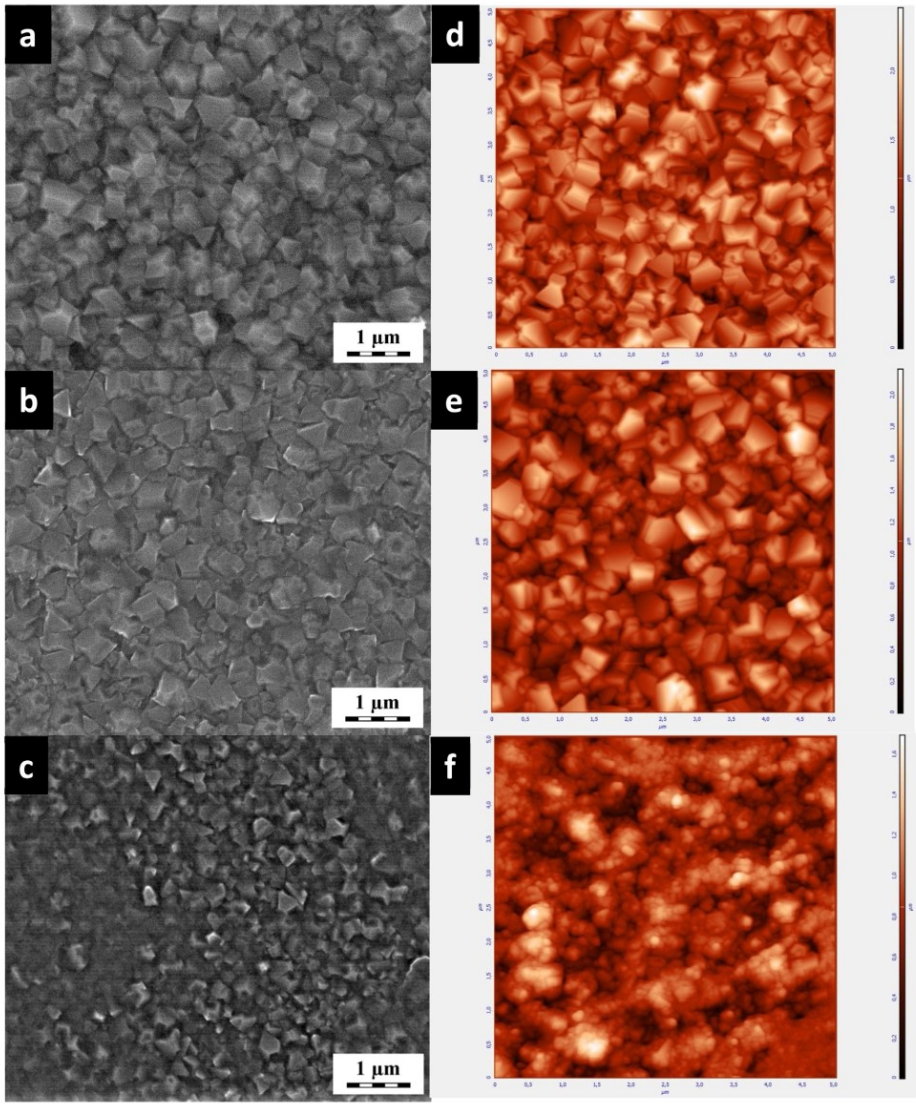


**Fig. 1.** Scanning electron micrographs (a – c) and atomic force micrographs (d – f) of the surface of BDD films with boron content 500 ppm (a + d), 2000 ppm (b + e), and 8000 ppm (c + f). The same magnification.

## 3. Results and discussion

### 3.1. Spectral Characterization – SEM, AFM, and Raman Spectroscopy

The morphology of the BDD films has been investigated by SEM and AFM (Fig. 1). Results obtained using both techniques are in a good mutual agreement and reveal that the boron content obviously influences the morphology of the studied films, which can be divided into three groups: The 500 ppm film is characterized by the best crystal quality with relatively uniform grain size of ~450 nm. The 1000 ppm, 2000 ppm, and 4000 ppm films also show randomly-oriented crystallites of ~450 nm but together with an amorphous phase, and the proportion of the crystallites increases with decreasing boron content. The 8000 ppm film differs significantly from the above ones – the crystallites, if any, are considerably smaller (<100 nm) and the film contains predominantly the amorphous phase. Obviously, the boron-doping level in the range of 500 ppm to 4000 ppm does not influence significantly the grain size, but has a large impact on the ratio of the crystallites to the amorphous phase in the final BDD films. The increase in the proportion of the amorphous phase or in the smaller grain size population with increasing boron content has been reported also for other microcrystalline films [6,64,65], and was ascribed to the formation of B-hydrides, which deprive hydrogen from the gas phase, thus markedly changing the C:H ratio therein [65]. Nevertheless, the overall deterioration of the layer morphology is not accompanied by increased content of $sp^2$ impurities, as proved by Raman spectroscopy. AFM measurements served for the estimation of RMS roughness, average height, maximum range, and the roughness surface factor, *i.e.*, the ratio between the surface area (real area) and the projected area (geometric area). Their dependence on B/C ratio is depicted in Fig. 2. While these values are fluctuating for the semiconductive 500 ppm and 1000 ppm films, for the conductive films there is a clear trend of their continuous decline with the maximum values for the 2000 ppm film, especially for the average height and the roughness surface factor changing from 1.15 (2000 ppm film) to 1.06 (8000 ppm film).

Raman spectra excited at 532 nm for all investigated films are depicted at Fig. 3 and resemble spectra obtained using excitation at 633 nm [7] and other spectra published in other studies for heavily doped BDD films [5,8,12,66,67]. Importantly, there is no obvious Raman response at 1533 $cm^{-1}$ related to the presence of the $sp^2$ carbon, which indicates the high quality of the diamond films. Obviously, the shape of the Raman spectra is significantly influenced by the boron content. None of the films exhibits only the sharp diamond line at 1332 $cm^{-1}$. Nevertheless, Raman spectra of the BDD films with the lowest boron content (500 ppm) are characterized by one band at 1329 $cm^{-1}$ related to the presence of the $sp^3$ diamond, and another sharp peak at 519 $cm^{-1}$ and scattering in the range ~940-980 $cm^{-1}$ corresponding to Si phonon and Si 2nd order phonon present due to transparency of the BDD films. The Fano shape of the former peak (519 $cm^{-1}$) is given by the presence of boron in the silica substrate [68]. These signals associated with silicon are negligible for 2000 ppm films and disappear from the Raman spectrum for higher B/C ratios. This is a consequence of the transition of the semimetallic/metallic conductivity of the BDD films; at the transition the absorption coefficient of diamond increases sharply at the energy of the incident light and as a consequence, the signals associated with silicon disappear from the Raman spectrum [10]. Simultaneously, the relatively symmetric Lorentzian band of the diamond phonon at 1332 $cm^{-1}$ changes towards an asymmetric Fano-like lineshape and downshifts to 1290 $cm^{-1}$ with increasing boron concentration. This feature is typical for nanocrystalline $sp^3$- hybridized carbon Raman peaks due to a Fano-type interference between the discrete zone center optical phonon and a continuum of electronic excitations induced by the presence of the dopant, as described in many studies at [B] concentration < $10^{20}$ boron atoms $cm^{-3}$ (*i.e.*, at the threshold of metallic conductivity [8]). The increase of boron content is also associated with the appearance of a signal around ~1000 $cm^{-1}$ with constant positioning and an increase and shift to lower wavenumbers of wide bands centered at ~500 $cm^{-1}$ and ~1225 $cm^{-1}$. The full understanding of the physical origin and/or of the evolution with the heavy boron incorporation of all these structures still remains unclear. While the former band (~500 $cm^{-1}$) has been associated with local vibrational modes of increased concentration of boron pairs [8,64], the latter band (~1225 $cm^{-1}$) has been ascribed to phonon excitation around the maximum of the one phonon density of state of diamond near its maximum value of approximately 1225 $cm^{-1}$ after a partial removal of the selection rules induced by the heavy boron doping [8,66], or alternatively, for nanocrystalline diamond films to amorphous $sp^3$ bonded carbon [69]. The shift of these bands towards lower wavenumbers with increasing [B] was previously reported for the heavily doped films for the 632.8 nm Raman peak

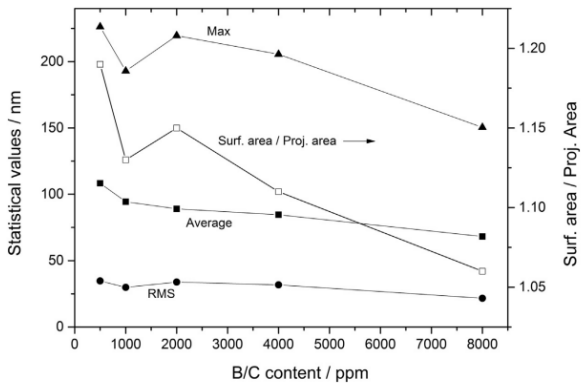


**Fig. 2.** Morphologic parameters of BDD films with boron content 500 ppm–8000 ppm estimated from AFM measurements. Depicted statistical values: Max (maximal roughness), Average (average roughness), RMS (root mean square roughness) and the ratio surface to projected area (right axis).

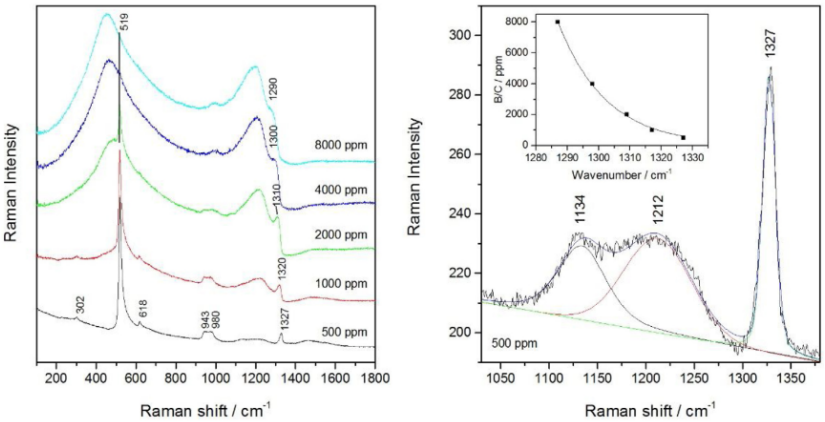


**Fig. 3.** (A) Raman spectra for the different boron doped nanocrystalline films (500 ppm ≤ B/C ≤ 8000 ppm) using 532 nm excitation wave length. The spectra have been offset vertically from each other for clarity. (B) Deconvolution of Raman bands in 1020 $cm^{-1}$–1370 $cm^{-1}$ region (500 ppm). B/C ratio in the gas phase vs. position of deconvoluted diamond phonon band for all B/C ratios is in inset.

[7,66] but not for the 325 nm one [66], where the position of the 500 $cm^{-1}$ band remained unchanged. Nevertheless, the band at ~500 $cm^{-1}$ can be used for calculation of boron concentration according to the empirical logarithmic law (eq. (4)):

$$[B]\ (cm^{-3}) = 8.44 \times 10^{30} \times \exp(-0.048 \times \omega_{500}), \quad (4)$$

where $\omega_{500}$ is the maximum of the Lorentzian component in $cm^{-1}$ (ref. [12,15]). The calculated values are given in Table 1 in comparison with the values obtained using neutron depth profiling for estimation of [B] directly in BDD film. Obviously, the calculation method gives lower boron concentration (by a factor of 1-2) for the 8000, 4000 ppm, and 2000 ppm films and is not suitable for lower boron concentrations due to the interfering Si signal at 519 $cm^{-1}$. Nevertheless, it can be used as a method for rough estimation of [B]. The results are in a better agreement with those obtained by the neutron depth profiling than those obtained for nanocrystalline BDD films using 632.8 nm excitation wavelength [15], where the Lorentzian fit of the 500 $cm^{-1}$ peak resulted in underestimation of the values obtained by SIMS by the factor 3 – 10, which was ascribed to the fact that not all boron atoms are active in the Raman response, while SIMS counts all present atoms.

Interestingly, our results indicate that it is possible to relate the shift of maximum Lorentzian component $\omega_{1332}$ of the diamond phonon at $\omega < 1332\ cm^{-1}$ with B/C ratio using empirical logarithmic function (Fig. 3B) and thus the boron concentration [B] with very high correlation coefficient (eq. (5)):

$$[B]\ (cm^{-3}) = 2.0 \times 10^{59} \times \exp(-0.067 \times \omega_{1332}) \text{ (adjusted } R^2\ 0.9969) \quad (5)$$

Calculation of [B] from measured shift of the Fano-like lineshape at ca 1332 $cm^{-1}$ ($\omega_{1332}$) using eq. (5) gives values relatively close to the values calculated from the shift of the 500 $cm^{-1}$ Raman band (eq. (4)) indicating that both these shifts can be used for rough non-destructive estimation of B concentration in heavily doped BDD films. Previous studies report downshift of the optical-phonon band of diamond at 1332 $cm^{-1}$ for BDD deposited at silica supports when using 632 nm excitation wavelength [7,12] or for BDD deposited at silicon [70,71] or molybdenum supports [72] when using 514 nm argon laser. On the other hand, the band shift to higher wave number with increasing boron doping level was observed for BDD films deposited at titanium substrate using 532 nm excitation wavelength [6]. No attempts to use these shifts for quantitation of boron in the BDD films can be traced in the mentioned studies, despite the fact that they are inevitably caused by the increasing content of boron in the films. The shifts can in principle be used to assess the internal stress in the films, as the optical-phonon band at 1332 $cm^{-1}$ is very sensitive to it with Raman shifts around 3 $cm^{-1}$ caused by a stress of 1 GPa [71]. Defects such as vacancies, dislocation, or grain boundaries produce the tensile stress; compressive intrinsic stress in the films is attributed to impurities in the grain boundaries. While the increase of the tensile stress leads to downshift of the 1332 $cm^{-1}$ band and may lead to the splitting of the film, the

**Table 1**
Boron concentration [B] corresponding to the nominal content of B/C ratio in the gas phase, estimated from neutron depth profiling and calculated from the maximum $\omega < 500\ cm^{-1}$ and $\omega < 1332\ cm^{-1}$ of the Lorentzian component of the Raman signal using 532 nm excitation wave length.

| B/C in the gas phase (ppm) | [B] ($cm^{-3}$) from neutron depths profiling | Peak position $\omega_{500}$ (Lorentzian component) ($cm^{-1}$) | [B] in the solid phase ($cm^{-3}$) | Peak position $\omega_{1332}$ (Lorentzian component) ($cm^{-1}$) | [B] in the solid phase ($cm^{-3}$) |
|---|---|---|---|---|---|
| 500 | $4.0 \times 10^{20}$ | –[a] | – | 1327 | $4.9 \times 10^{20}$ |
| 1000 | $8.5 \times 10^{20}$ | –[a] | – | 1317 | $9.5 \times 10^{20}$ |
| 2000 | $1.3 \times 10^{21}$ | 489 | $5.40 \times 10^{20}$ | 1309 | $1.6 \times 10^{21}$ |
| 4000 | $3.1 \times 10^{21}$ | 463 | $1.88 \times 10^{21}$ | 1298 | $3.4 \times 10^{21}$ |
| 8000 | $5.8 \times 10^{21}$ | 449 | $3.69 \times 10^{21}$ | 1287 | $7.1 \times 10^{21}$ |

[a] Raman signal not present at the spectra.

compressive stress leads to the increase of wavenumber and may cause peeling off the films from the substrate [71]. Incorporation of substantial quantities of boron in the films results in a lattice expansion of diamond or, at higher boron doping levels, to its precipitation at the grain boundaries and is the origin of tensile intrinsic stress. On titanium substrate [6] the shift of the 1332 $cm^{-1}$ diamond peak to higher wavenumber was partially attributed to the thermal stress due to difference in thermal expansion coefficient of the two materials. Measurements of other types of BDD films at various supports at different excitation wavelength with experimentally obtained [B] values are needed to generally confirm the validity of the relationship between maximum Lorentzian component of the diamond phonon at $\omega < 1332\ cm^{-1}$ and [B] in the BDD films.

### 3.2. Electrochemical Characterization

To assess the electrochemical performance of tested BDD films, CVs of inner-sphere $[Fe(CN)_6]^{3-/4-}$ and outer-sphere $[Ru(NH_3)_6]^{3+/2+}$ redox markers showing peaks in either anodic or cathodic potential regions, respectively, were investigated. Table 2 summarizes parameters of the linear dependences of the peak heights $I_p$ of these markers *vs.* square root of the scan rate $v^{1/2}$, calculated values of apparent heterogeneous electron-transfer rate constant, $k^{\circ}_{app}$, and $I_{pa}/I_{pc}$ ratio. Fig. 4 depicts dependence of the peak potential difference between cathodic and anodic peak $\Delta E_p$ on $v^{1/2}$ for all tested films. Corresponding cyclic voltammograms for the selected scan rate $v = 300\ mV\ s^{-1}$ for both redox markers are depicted in Fig. SI1 in the Supporting information. The quasi-reversible character of the redox processes is reflected in relatively low $\Delta E_p$ values and $I_{pa}/I_{pc}$ ratios mostly close to one.

For both redox markers the results indicate that the 500 ppm and 1000 ppm films exhibit significantly slower reaction kinetics than the 2000 ppm–8000 ppm films. This effect is more distinct for $[Fe(CN)_6]^{3-/4-}$ in agreement with its inner sphere character.

For the outer sphere marker $[Ru(NH_3)_6]^{3+/2+}$ the slopes of the $I_p$ *vs.* $v^{1/2}$ dependence (summarized in Table 2) and the peak separation $\Delta E_p$ exhibit for 2000 ppm, 4000 ppm, and 8000 ppm films only small differences up to the scan rate of 100 $mV\ s^{-1}$, with maximum $\Delta E_p$ of 65 mV (Fig. 4A). The 500 ppm and 1000 ppm films exhibit more sluggish kinetics, as $\Delta E_p$ increases significantly with the increasing scan rate, reaching the values of 65 mV – 128 mV up to the scan rate of 100 $mV\ s^{-1}$ with further increase up to 163 mV at higher scan rates. Simultaneously the $I_p$ *vs.* $v^{1/2}$ slope decreases for the latter films in comparison with the more doped ones. Values of $k^{\circ}_{app}$ calculated at the scan rate of 300 $mV\ s^{-1}$ (corresponding CVs depicted in Fig. SI1) for qualitative estimation of charge transfer rate reach the values ranging from $8.96 \times 10^{-3}$ $cm\ s^{-1}$ to $6.76 \times 10^{-4}\ cm\ s^{-1}$ (Table 2) for all electrodes. On the other hand, for lower scan rates the calculated $k^{\circ}_{app}$ are ca 0.1-0.06 $cm\ s^{-1}$, as the potential difference $\Delta E_p$ is only ca 55–61 mV for 2000 ppm – 8000 ppm electrodes. These values are consistent with values for $[Ru(NH_3)_6]^{3+/2+}$ previously reported in ref. [20], where the average values of $k^{\circ}_{app}$ in the range of $0.1–7 \times 10^{-4}\ cm\ s^{-1}$ were reported for different commercially available BDD films, or with the value of 0.015 $cm\ s^{-1}$ given in [73], where this lower $k^{\circ}_{app}$ value compared to metal electrodes was ascribed to lower density of states for the BDD. Our results for $[Ru(NH_3)_6]^{3+/2+}$ indicate that the 2000–8000 ppm films are doped sufficiently to exhibit metallic conductivity, because even at the negative potentials, where charge depletion effects dominate for the semiconducting electrodes, there is a sufficient number of charge carriers available to maintain nearly reversible electron transfer. Thus, the threshold value of [B] for semiconductivity/metallic conductivity for this batch of electrodes is lower than 2000 ppm, *i.e.,* $8.5 \times 10^{20}\ cm^{-3} < [B] < 1.3 \times 10^{21}\ cm^{-3}$ when considering neutron depths values shown in Table 1. This is higher concentration than the theoretical value of $[B] \sim 2 \times 10^{20}\ cm^{-3}$, or than the value obtained experimentally for oxidized microcrystalline electrodes, where for metallic conductivity the lowest $[B] = 1.9 \times 10^{20}\ cm^{-3}$ was reported [8].

For $[Fe(CN)_6]^{3-/4-}$ the $I_p$ *vs.* $v^{1/2}$ dependences exhibit similar trends as described above for $[Ru(NH_3)_6]^{3+/2+}$ *i.e.,* lower slopes for the semiconductive 500 ppm and 1000 ppm films, and higher and mutually comparable values for the 2000 ppm to 8000 ppm films (for both anodic and cathodic peaks; Table 2). Nevertheless, substantial difference arises in the $I_{pa}/I_{pc}$ ratio, where for semiconductive film values significantly differing from one were obtained, and in the peak potential differences. The $\Delta E_p$ values obtained with $[Fe(CN)_6]^{3-/4-}$ are mostly higher than observed with $[Ru(NH_3)_6]^{3+/2+}$, especially at higher scan rates. This applies to all studied films, but particularly it is apparent for the semiconductive 500 ppm and 1000 ppm films (Fig. 4B). The $k^{\circ}_{app}$ values for $[Fe(CN)_6]^{3-/4-}$ span over three orders of magnitude (from $2.07 \times 10^{-2}$ $cm\ s^{-1}$ to $3.75 \times 10^{-5}\ cm\ s^{-1}$; compare with values obtained for $[Ru(NH_3)_6]^{3+/2+}$, where the range of $k^{\circ}_{app}$ is remarkably narrower, Table 2) in agreement with the inner sphere, surface-sensitive character of this marker. For the 2000–8000 ppm films the value of $\Delta E_p$ of $[Fe(CN)_6]^{3-/4-}$ is 59.0–87.0 mV up to scan rate of 100 mV $s^{-1}$. Reversible or nearly reversible behavior with $\Delta E_p$ of 58–64 mV (*e.g.,* $\Delta E_p$ of $59.8 \pm 0.9$ mV ($n = 5$) and $I_{pa}/I_{pc}$ ratio 1.00 at the scan rate of 100 $mV\ s^{-1}$) was achieved for 2000 ppm film. Prior to this

**Table 2**
Parameters of the linear dependence of the peak height *vs.* square root of the scan rate $v^{1/2}$ and apparent heterogeneous electron-transfer rate constant, $k^{\circ}_{app}$ for $[Ru(NH_3)_6]^{3+/2+}$ and $[Fe(CN)_6]^{3-/4-}$.

| BDD film | Slope (anodic peak) ($\mu A\ s^{1/2}\ V^{-1/2}$) | Slope (cathodic peak) ($\mu A\ s^{1/2}\ V^{-1/2}$) | $k^{\circ}_{app}$[a] ($cm\ s^{-1}$) | $I_{pa}/I_{pc}$[a] |
|---|---|---|---|---|
| $[Ru(NH_3)_6]^{3+/2+}$ | | | | |
| 500 ppm | 417.81 | −390.36 | $6.76 \times 10^{-4}$ | 0.991 |
| 1000 ppm | 463.12 | −445.78 | $2.12 \times 10^{-3}$ | 0.993 |
| 2000 ppm | 825.13 | −714.34 | $6.32 \times 10^{-3}$ | 0.974 |
| 4000 ppm | 821.33 | −830.40 | $8.96 \times 10^{-3}$ | 0.985 |
| 8000 ppm | 794.48 | −730.39 | $8.96 \times 10^{-3}$ | 0.959 |
| $[Fe(CN)_6]^{3-/4-}$ | | | | |
| 500 ppm | 636.2 | −178.4 | $3.45 \times 10^{-5}$ | 1.935 |
| 1000 ppm | 628.1 | −561.7 | $4.15 \times 10^{-4}$ | 1.081 |
| 2000 ppm | 965.0 | −978.1 | $1.04 \times 10^{-3}$ | 0.970 |
| 4000 ppm | 866.1 | −894.2 | $2.42 \times 10^{-3}$ | 0.996 |
| 8000 ppm | 923.1 | −944.2 | $2.07 \times 10^{-2}$ | 0.992 |

[a] at the scan rate of 300 $mV\ s^{-1}$.

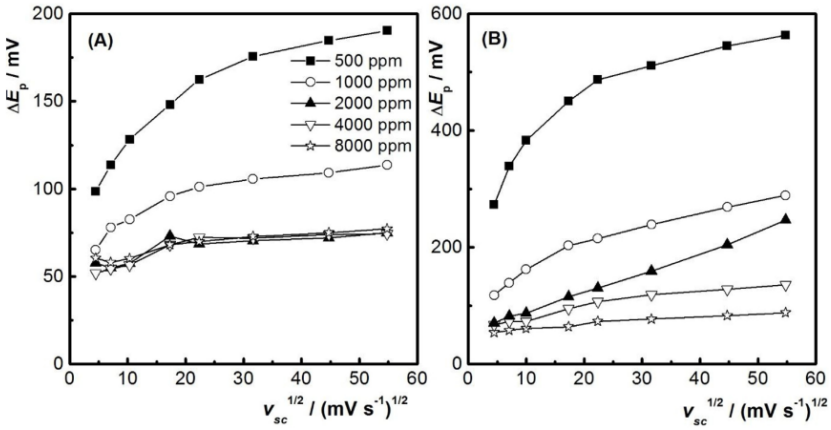


**Fig. 4.** Dependence of potential difference $\Delta E_p$ of cathodic and anodic peak of $[Ru(NH_3)_6]^{3+/2+}$ (A) and $[Fe(CN)_6]^{3-/4-}$ (B) (for both $c = 1$ mmol $L^{-1}$) in 1 mol $L^{-1}$ KCl on the square root of the scan rate $v_{sc}^{1/2}$.

present report on the reversible behavior of $[Fe(CN)_6]^{3-/4-}$ at anodically pretreated BDD, nearly reversible behavior with 60 mV potential difference was reported [5] for mildly oxidized heavily doped BDD films with $[B] > 2 \times 10^{21}$ $cm^{-3}$. Nevertheless, in that case [5] the content of $sp^2$ carbon impurities could have impact on the results. The potential difference of 65 mV was also reported [8] for $[Fe(CN)_6]^{3-/4-}$ at alumina polished microcrystalline BDD with $[B] > 1.9 \times 10^{20}$ $cm^{-3}$, when omitting reports on the reversibility for the cathodically pretreated *i.e.*, predominantly H-terminated BDD films [25,37,74]. In general, the literature data on the kinetics of charge transfer with $[Fe(CN)_6]^{3-/4-}$ couple at H- and O-terminated surfaces are sometimes contradictory. Larger peak separation for $[Fe(CN)_6]^{3-/4-}$ at oxygenated surfaces, compared to values obtained at the hydrogenated ones, was reported for highly doped BDD films *e.g.*, by Duo et al. [22] for BDD films with $[B] = 10^{20}$–$10^{21}$ $cm^{-3}$ or for heavily doped BDD films after oxygen plasma treatment [24]. It was assumed that for highly doped BDD films the peak separation for $[Fe(CN)_6]^{3-/4-}$ at oxygenated surfaces is larger than that of hydrogenated ones, presumably because the reaction proceeds through a specific surface sites, which are in the former case blocked by oxygen [75,76]. On the other hand, improvement of electron transfer and lowering of $\Delta E_p$ was reported for $[Fe(CN)_6]^{3-/4-}$ after anodic pretreatment of the heavily doped BDD films in acidic media [23,77,78]. This short overview indicates that surface termination and the way of its achievement, as well as the boron content, influence the charge transfer rate at BDD films. In this context the effect of non-diamond impurities in grain boundaries should also be considered, as it is known that their content increases with increasing boron doping level, and that their incidence supports further the charge transport mechanisms. As a whole, boron doping results in formation of many distinct conducting regions and different conducting pathways possibly associated with different mechanisms for various redox-active species [14,16]. Our results indicate that both types of redox markers are capable of differentiating between semiconductive and metallic character of the anodically pretreated BDD films based on the differences in the slope of $I_p$ *vs.* $v^{1/2}$ dependence and on the $\Delta E_p$ (or $k^{\circ}_{app}$) values at scan rates > 100 cm $s^{-1}$. But only the surface-sensitive $[Fe(CN)_6]^{3-/4-}$ enables to visualize the differences among metallic films with boron content varying between 2000–8000 ppm, contrary to the outer sphere $[Ru(NH_3)_6]^{3+/2+}$, for which similar characteristics of the latter films, regardless of the boron content in the range of 2000 –8000 ppm, were obtained. Further, even oxidized BDD metallic films exhibited reversible or nearly reversible kinetics for $[Fe(CN)_6]^{3-/4-}$ when sufficiently doped with boron. Further work is needed to better understand the structure-function relationships for $[Fe(CN)_6]^{3-/4-}$ as the results for the heterogeneous electron transfer are different in various literature sources.

### 3.3. Influence of boron content on potential window

The remarkably wide potential window of BDD electrodes in aqueous media is due to adsorption processes required for initiation of the water decomposition reactions [35,37]. The window width was inversely dependent on the boron doping level at the as-received, H-terminated BDD films in acidic media. Both OER and HER at anodic and cathodic side, respectively, contribute to this trend as the boron-rich sites are directly involved in the adsorption steps needed for the gas evolution reactions [37].

In this study the potential window was investigated in aqueous solutions of several supporting electrolytes commonly used in electroanalysis and representing a wide range of pH values: 1 mmol $L^{-1}$ $Na_2SO_4$, 1 mol $L^{-1}$ KCl, 0.1 mol $L^{-1}$ $HClO_4$, 0.1 mol $L^{-1}$ acetate buffer pH 4.0, 0.1 mol $L^{-1}$ phosphate buffer pH 7.0, and 0.05 mol $L^{-1}$ borate buffer pH 9.0. The anodic and cathodic potential limit was defined as the potential, where the anodic/cathodic current passed the current ± 5 μA at cyclic voltammograms recorded at the scan rate of 100 mV $s^{-1}$. These are depicted for all tested electrolytes at Fig. 5C–G, together with estimated potential limits in Fig. 5A and overall width of the potential window in Fig. 5B.

It is obvious from all these figures that, in general, the width of the potential window decreases with the increasing boron doping level, more remarkably at the cathodic side. The voltammograms are mostly featureless in the region of water stability or exhibit few very small shoulders appearing always in the cathodic region for the electrodes with the highest boron content (namely in 1 mmol $L^{-1}$ $Na_2SO_4$, 0.1 mol $L^{-1}$ $HClO_4$, and 0.1 mol $L^{-1}$ acetate buffer pH 4.0).

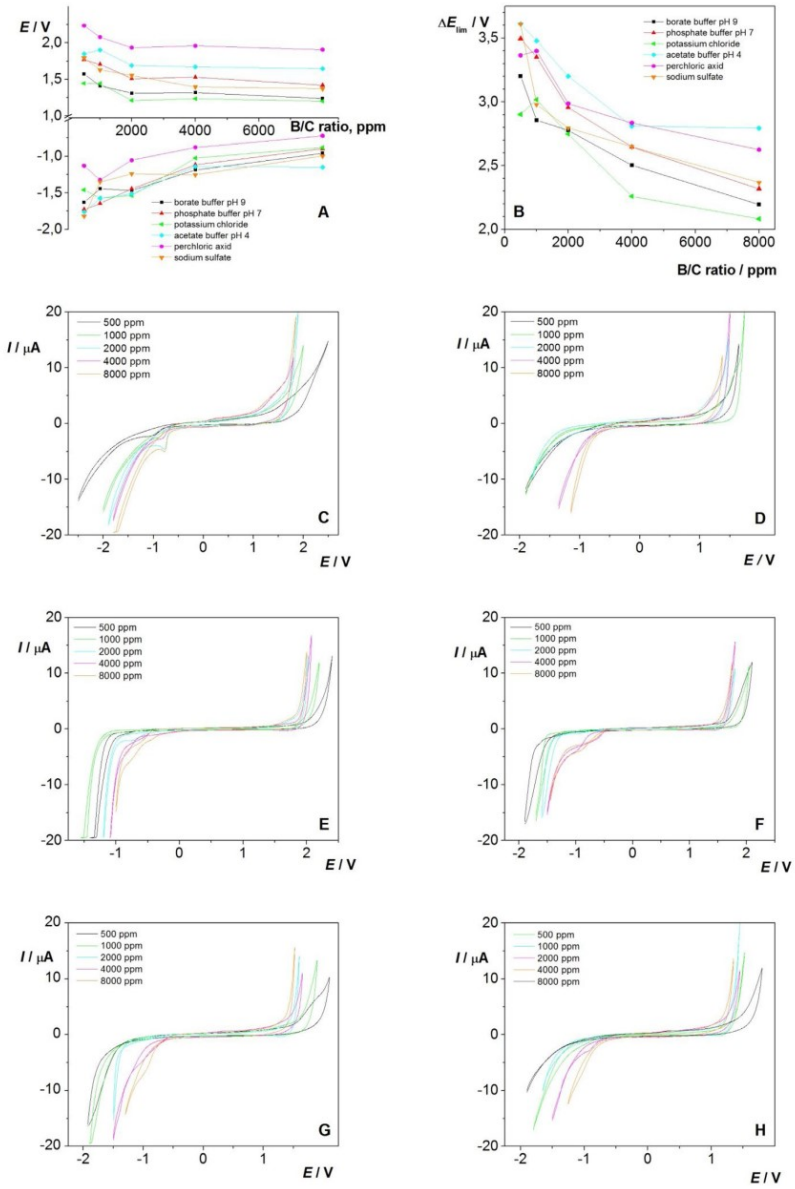


**Fig. 5.** Dependence of the anodic and cathodic potential limit ($E_{lim,C}$ and $E_{lim,A}$) for the current ± 5 μA (A) and the dependence of the width of the potential window $\Delta E_{lim}$ on B/C ratio (B) and cyclic voltammograms of (C) 1 mmol $L^{-1}$ $Na_2SO_4$, (D) 1 mol $L^{-1}$ KCl, (E) 0.1 mol $L^{-1}$ $HClO_4$, (F) 0.1 mol $L^{-1}$ acetate buffer pH 4.0, (G) 0.1 mol $L^{-1}$ phosphate buffer pH 7.0, and (H) 0.05 mol $L^{-1}$ borate buffer pH 9.0. Scan rate 100 mV $s^{-1}$. CVs are vertically offset for clarity, CVs for the third cycle are presented from which all values were calculated.

The following trends and characteristics may be traced:

a.) The overall width of the potential window $\Delta E_{lim}$ decreases with increasing B/C ratio. This decline is more significant for the 500 ppm – 2000 ppm electrodes. Moreover, the 500 ppm electrode exhibits slower response to both hydrogen and oxygen evolution reactions. The widest potential window can be observed for all doping levels with B/C ratio ≥ 1000 ppm in acidic solutions, *i.e.*, in perchloric acid or acetate buffer, the latter with the maximum of ~3600 mV for the 500 ppm electrode (Fig. 5A).

b.) The narrowing of potential window is more remarkable at the cathodic side, where the differences in the cathodic potential limits $E_{lim,C}$ between 500 ppm and 8000 ppm electrodes are in the range from 830 mV (phosphate buffer pH 7.0) to 580 mV (1 mol $L^{-1}$ KCl). The decline is continuous with higher differences of $E_{lim,C}$ for 500 ppm to 4000 ppm electrodes (Fig. 5B).

c.) At the anodic side the difference of the anodic potential limits $E_{lim,A}$ between 500 ppm and 8000 ppm electrode is significantly lower than that for the cathodic side, from 200 mV (acetate buffer pH 4.0) to 420 mV (1 mmol $L^{-1}$ $Na_2SO_4$). This difference is mainly due to the decline of $E_{lim,A}$ for 500 ppm to 2000 ppm electrodes, as 2000 ppm to 8000 ppm electrodes have comparable values of $E_{lim,A}$ for all tested electrolytes (Fig. 5B).

d.) The potential limit at the anodic side $E_{lim,A}$ is increasing with decreasing pH of the solution for all the electrodes, *i.e.*, the highest anodic limit was achieved in 0.1 mol $L^{-1}$ $HClO_4$, the lowest in 0.05 mol $L^{-1}$ borate buffer pH 9.0 (Fig. 5B).

These trends have to be evaluated in the view of presumed mechanism of OER and HER at BDD. Both reactions require an initial adsorption step, obviously associated with boron-rich places, needed for the hydrogen/oxygen evolution reactions. HER is more remarkably influenced by the boron content than OER (independently on pH of the media), as follows from the lower difference of the anodic potential limits $E_{lim,A}$ compared to cathodic limits $E_{lim,C}$ between 500 ppm and 8000 ppm electrode (see *b)* and *c)* above) and the fact that $E_{lim,C}$ is dependent on the boron content in its whole range in contrast to $E_{lim,A}$, where it imparts only the semiconductive electrodes.

For OER there is practically no shift of $E_{lim,A}$ for metallic-type 2000–8000 ppm electrodes. Thus, after water adsorption, its oxidation to $HO^{\bullet}$ radicals (eq. (1)), presumably the rate determining step of OER [31], is independent on the boron content and the activity of these conductive electrodes towards oxygen evolution is controlled by other factors such as pH of the solution and presence of other ions in the solution. Their electrooxidation can start in the vicinity of the oxygen evolution reaction, resulting in the shift of $E_{lim,A}$. An exemplary case for the difference of $E_{lim,A}$ for different anions is the KCl and $Na_2SO_4$ electrolyte: While in the latter case $HO^{\bullet}$ radicals are known to be the main oxidants in the system [41], for KCl the presence of $Cl^-$ and electrogenerated reactive chlorine species ($Cl_2$, HClO) cause anodic shift of the oxygen evolution [79].

For HER, both the formation of $[S\text{-}H]^+$ pair and its reduction (eq. (2)), and the formation of $[SH\text{-}H]^+$ pairs for successful electron transfer in the Heyrovsky step of HER (eq. (3)) are associated with boron-rich sites at the BDD film. Consequently, semiconductive films (with low boron content) are less prone to hydrogen evolution than films with metallic conductivity and thus exhibit more negative cathodic potential limits. Further, the HER proceeds at less negative potentials in strongly acidic media (perchloric acid) due to high concentrations of protons in the solution facilitating their adsorption needed to accomplish the HER described in eq. (2) and (3) and due to the negative charge at the BDD surface as consequence of the negative potential applied and presence of oxygen-containing groups at the surface. These positive effect of both factors on proton adsorption at the surface of all BDD films (irrespective of the boron content) accords with the fact that in the acidic media (perchloric acid, acetate buffer), the difference of $E_{lim,C}$ between 500 ppm and 8000 ppm electrodes is lower than in neutral/base media.

Double layer capacities *C* were calculated for 500 ppm – 8000 ppm electrodes in all tested media from CVs in Fig. 5. For neutral and alkaline solutions values ranging between 0.3 and 6 μF $cm^{-2}$ were obtained, independently on the boron-doping level. In acidic media, especially in 0.1 mol $L^{-1}$ $HClO_4$, the *C* values are higher and increasing from 10 to 33 μF $cm^{-2}$ with increasing boron content from 500 to 8000 ppm. The mentioned lower capacitance values are similar to the values reported previously for O-terminated BDD electrodes [7,80] and presumably originate from a low local density of states witnessing low contents of non-diamond impurities for all doping levels as confirmed by Raman spectra (see above). The increase of *C* in acidic media is probably associated with interactions of the oxygen-terminated surface with $H^+$ ions.

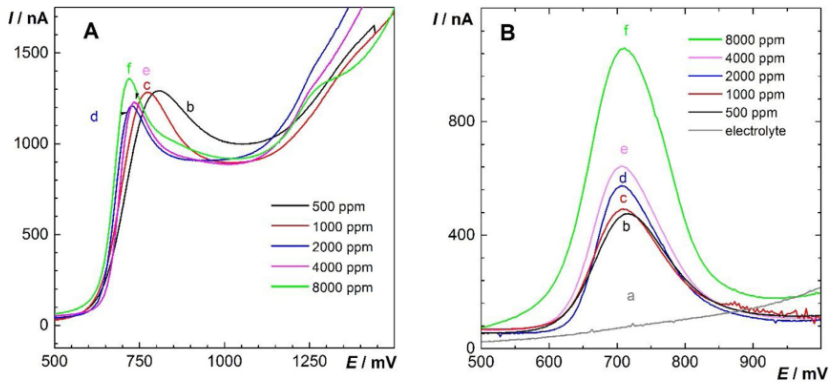


**Fig. 6.** Linear sweep (A) and DP voltammograms (B) of 2-AB ($c = 5 \times 10^{-5}$ mol $L^{-1}$) in BR buffer pH 7.0 (curve a) measured at BDD electrodes with boron doping level: (b) 500 ppm, (c) 1000 ppm, (d) 2000 ppm, (e) 4000 ppm, and (f) 8000 ppm.

### 3.4. Voltammetry of 2-aminobiphenyl

Fig. 6 compares linear sweep and DP voltammograms of 2-aminobiphenyl using 500 ppm – 8000 ppm BDD electrodes in BR buffer pH 7.0 (medium optimized for measurements of aromatic amines in our previous studies [53,54]). In linear sweep voltammetry, the boron doping level influences the peak shape rather than peak current, contrary to DPV, where the height of symmetric peaks increases with increasing boron content. This trend is also obvious from Table 3 summarizing peak potentials and currents and their repeatability, and Table 4 summarizing parameters of calibration dependences for all tested electrodes measured by DPV in the concentration range of 2-minobiphenyl of 0.25 μmol $L^{-1}$–50 μmol $L^{-1}$. An example representing DP voltammograms obtained at 8000 ppm BDD film is given in Fig. SI2. The sensitivity (*i.e.*, slope of the calibration straight line) is *ca* 2.5 times higher for the 8000 ppm electrode than for the 500 ppm electrode; the limits of detection are in the $10^{-7}$ mol $L^{-1}$ concentration range for all tested electrodes. This is given by the satisfactory repeatability (Table 3) of the peak height for the lowest measurable concentration that was 1.6% – 6.0% for all tested electrodes.

Obviously, the boron content influences significantly the kinetics of electron transfer. For 2-aminobiphenyl, the electrochemical oxidation consists in the first step in the formation of a nitrene monocation radical from unprotonized amino group ($pK_a$ value of cationic form of 2-AB is 3.83 [53]). Our results suggests the same mechanism to take place at all electrodes tested, which is supported by the fact that in linear sweep voltammetry, the areas under the curves are for all electrodes comparable (within ± 10%) regardless of the peak shape, the changes of which nevertheless indicate changes in the electron transfer rate. Besides the increasing peak height in DPV, the faster kinetics can be also traced from a slight continuous shift of peak potentials with increasing boron content to less positive values (indicating more facile electrooxidation of the analyte), obvious from Fig. 6 and Table 4. When focusing on the differences between semiconductive and conductive electrodes, only small difference in peak heights can be observed for semiconductive 500 and 1000 ppm electrodes. However, significant differences between these and all electrodes with metallic conductivity were observed. In contrast to results obtained with the 2-aminobiphenyl, significant differences between semiconductive electrodes 500 ppm and 1000 ppm were found with the redox markers $[Ru(NH_3)_6]^{3+/2+}$ and $[Fe(CN)_6]^{3-/4-}$. However, the conductive electrodes 2000–8000 ppm exhibit relatively large differences in electron transfer kinetics, similarly as observed for $[Fe(CN)_6]^{3-/4-}$.

Isolated studies on the influence on boron content on voltammetric signals of organic compounds reveal similar trend: The well-shaped oxidative signal of 4-chloro-3-methylphenol was obtained for the same set of BDD electrodes. The signal obtained using the semiconductive electrodes was placed at slightly more positive potentials and simultaneously, corresponding peak height was lower, especially using DPV confirming a slower kinetics of the electron transfer [49]. In our study on oxidation of benzophenone-3 the DPV peaks were not fully developed for the semiconductive 500 ppm and 1000 ppm films, but were symmetric, well-shaped and of increasing height for 2000 ppm – 8000 ppm films [47]. Furthermore, the peak potential of benzophenone-3 was moving toward less positive values with increasing content of boron in the BDD films. Similarly, in the reduction of 5-nitroquinoline BDD films with metallic type of conductivity exhibited faster electron transfer at lower potential for nitro group reduction than semiconductive films 500 and 1000 ppm, where the voltammetric peaks were not well developed [48]. The floroquinoline antibiotic enrofloxacin showed sigmoidal signal in linear sweep voltammograms at ca. +1300 mV *vs.* Ag/AgCl due to its direct anodic oxidation, but it appeared only for 2500 ppm BDD, not for 1300 ppm, 200 ppm, and 100 ppm presumably semiconductive electrodes (type of conductivity and real boron concentration [B] are not given in the study [43]). In contrast, not such sharp changes were obtained between 100 ppm – 8000 ppm BDD electrodes in the case of indirect complete oxidation of enrofloxacin to carbon dioxide by hydroxyl radicals electrogenerated at high anodic potential, where the mineralization is enhanced as the diamond becomes richer in boron. This suggests that direct transfer of electrons for oxidation/reduction of the mentioned organic compounds is favored at BDD films with metallic type of conductivity, presumably due to the increased presence of adsorption sites thus enhancing the electrocatalytic activity of the surface towards adsorption. On the other hand, semiconductive BDD films exhibit lower or even insufficient sensitivity to oxidation of organic species studied so far and thus are not recommendable for electroanalytical purposes. Indirect way of oxidation mediated by hydroxyl radicals is not that sensitive to boron content, as these radicals are produced in the region of water decomposition independently on the boron content.

**Table 3**
Peak parameters of current response of 2-aminobiphenyl ($c = 5 \times 10^{-5}$ mol $L^{-1}$) in BR buffer pH 7.0 evaluated from ten consecutive scans using linear sweep and DP voltammetry at BDD electrodes with boron doping level 500 ppm – 8000 ppm.

| B/C ratio (ppm) | Linear sweep voltammetry | | | Differential pulse voltammetry | | |
|---|---|---|---|---|---|---|
| | $E_p$ (mV) | $I_p$ (μA) | RSD (%) | $E_p$ (mV) | $I_p$ (μA) | RSD (%) |
| 500 | 806 ± 2 | 1.23 | 0.99 | 720 ± 1 | 0.35 | 3.7 |
| 1000 | 777 ± 3 | 1.23 | 2.3 | 710 ± 2 | 0.36 | 2.7 |
| 2000 | 727 ± 2 | 1.15 | 1.34 | 707 ± 2 | 0.58 | 3.0 |
| 4000 | 733 ± 1 | 1.17 | 2.70 | 709 ± 1 | 0.68 | 1.4 |
| 8000 | 724 ± 1 | 1.28 | 2.50 | 710 ± 1 | 0.90 | 0.9 |

**Table 4**
Parameters of calibration dependences (linear dynamic range 0.25 – 50 μmol $L^{-1}$) and limits of detection of 2-AB in BR buffer pH 7.0 by DPV at BDD electrodes with boron doping level 500 ppm – 8000 ppm.

| B/C ratio (ppm) | Slope (mA L $mol^{-1}$) | Intercept (nA) | R | $L_D$ (μmol $L^{-1}$) |
|---|---|---|---|---|
| 500 | 7.67 ± 0.27 | 20.3 ± 5.9 | 0.992 | 0.72 |
| 1000 | 7.50 ± 0.45 | 12.5 ± 9.9 | 0.978 | 0.48 |
| 2000 | 11.1 ± 0.21 | 13.0 ± 6.1 | 0.998 | 0.80 |
| 4000 | 14.9 ± 1.75 | 40.8 ± 41.0 | 0.959 | 0.48 |
| 8000 | 18.0± 0.88 | 8.6 ± 1.8 | 0.999 | 0.21 |

## 4. Conclusions

The experiments presented in this study for a set a of anodically pretreated BDD films deposited at B/C ratio 500 ppm – 8000 ppm represent a consistent study of the effect of boron content on their selected morphologic, spectral, and electrochemical characteristics. The semiconductive/metallic threshold of conductivity has been evaluated based on Raman spectra and on cyclic voltammograms with selected redox markers. The results from Raman spectroscopy indicate that the shift of maximum Lorentzian component of diamond phonon at ~ 1332 $cm^{-1}$ can be assessed as the function of boron concentration [B]. The slope of $I_p$ *vs.* $v^{1/2}$ dependence and the course of $\Delta E_p$ *vs.* $v^{1/2}$ dependence obtained from cyclic voltammograms at scan rates > 100 mV $s^{-1}$ with the outer- and inner sphere redox markers ($[Ru(NH_3)_6]^{3+/2+}$ and $[Fe(CN)_6]^{3-/4-}$, respectively) enables to differentiate between the semiconductive films (500 ppm and 1000 ppm) and films exhibiting metallic conductivity (2000 ppm – 8000 ppm). Nevertheless, only the inner sphere character of $[Fe(CN)_6]^{3-/4-}$ redox marker

enables to visualize differences between various boron contents for the metallic films. Further, reversible behavior with $\Delta E_p$ of $59.8 \pm 0.9$ mV ($n = 5$) and $I_{pa}/I_{pc}$ ratio 1.00 at the scan rate of 100 mV $s^{-1}$ was achieved for this redox marker at the 2000 ppm film. Such doping level just above the semiconductive/metallic threshold conferred favorable characteristics for the reduction of 5-nitroquinoline [48] and oxidation of phenolic compounds [47,49]. Further, it exhibits also favorable spectral characteristics among the metallic BDD films, *e.g.*, the highest roughness surface factor. Thus it seems that the doping level just above the conductivity threshold seems to be favorable in terms of charge transfer and electroanalytical performance due to minimized frequency of incorporation of $sp^2$ impurities and other risks connected with high boron content during the CVD procedure.

The width of the potential window decreases with increasing boron doping level, more markedly at the cathodic side. The practical independency of anodic potential limit on boron content for electrodes with metallic type of conductivity 2000–8000 ppm suggests that the hydroxyl radical formation relies on surface conductivity rather than on the number of boron-active sites and other factors such as pH and presence of other possible reactive species in the solution. On the other hand, the hydrogen evolution on the cathodic side is dependent on boron content in the whole range investigated, assuming the $H^+/H_2O$ adsorption and subsequent hydrogen evolution is associated with boron-rich sites. The sluggish kinetics of hydrogen evolution for semiconductive films is in concordance with the slow charge transfer for the initial step of oxidation of 2-aminobiphenyl and other investigated organic compounds [47–49] at this set of electrodes indicating their limitations in electroanalysis of organic compounds.

Obviously the boron-doping level in BDD thin films has an impact on their morphology and microstructure, quality, electrochemical properties, corrosion resistance, and other characteristics, which, in the end influence parameters important for applications in electroanalysis. Notably, there is a multitude of recent papers devoted to analytical applications of not only different BDD films, but films deposited under the same conditions but subsequently subjected to various pre-treatments using different electrochemical procedures and other conditions. Therefore, one should be careful when comparing results of different studies. Further studies involving capacitance-voltage dependence and X-ray photoelectron spectroscopy (XPS) are needed to understand the interplay among the boron-doping level, oxygen content and electrochemical properties of studied films.

## Acknowledgement

This research was carried out within the framework of Specific University Research (SVV 260440). The research was financially supported by the Czech Science Foundation (project P206/12/G151). Electron microscopy at the Institute of Macromolecular Chemistry was supported by project TE01020118 (Technology Agency of the CR).

## Appendix A. Supplementary data

Supplementary data associated with this article can be found, in the online version, at http://dx.doi.org/10.1016/j.electacta.2017.05.006.

## References

[1] K. Patel, K. Hashimoto, A. Fujishima, Application of boron-doped CVD-diamond film to photoelectrode, Denki Kagaku 60 (1992) 659.
[2] N. Fujimori, T. Imai, A. Doi, Characterization of conducting diamond films, Vacuum 36 (1986) 99.
[3] K.B. Holt, A.J. Bard, Y. Show, G.M. Swain, Scanning electrochemical microscopy and conductive probe atomic force microscopy studies of hydrogen-terminated boron-doped diamond electrodes with different doping levels, J. Phys. Chem. B 108 (2004) 15117.
[4] D. Becker, K. Juttner, The mpedance of fast charge transfer reactions on boron doped diamond electrodes, Electrochim. Acta 49 (2003) 29.
[5] T. Watanabe, T.K. Shimizu, Y. Tateyama, Y. Kim, M. Kawai, Y. Einaga, Giant electric double-layer capacitance of heavily boron-doped diamond electrode, Diam. Relat. Mat. 19 (2010) 772.
[6] J.J. Wei, C.M. Li, X.H. Gao, L.F. Hei, F.X. Lvun, The influence of boron doping level on quality and stability of diamond film on Ti substrate, Appl. Surf. Sci. 258 (2012) 6909.
[7] Z.V. Zivcova, O. Frank, V. Petrak, H. Tarabkova, J. Vacik, M. Nesladek, L. Kavan, Electrochemistry and in situ Raman spectroelectrochemistry of low and high quality boron doped diamond layers in aqueous electrolyte solution, Electrochim. Acta 87 (2013) 518.
[8] M. Bernard, C. Baron, A. Deneuville, About the origin of the low wave number structures of the Raman spectra of heavily boron doped diamond films, Diam. Relat. Mat. 13 (2004) 896.
[9] C. Levy-Clement, F. Zenia, N.A. Ndao, A. Deneuville, Influence of boron content on the electrochemical properties of diamond electrodes, New Diam. Front. Carbon Technol. 9 (1999) 189.
[10] C. Levy-Clement, Semiconducting and metallic boron-doped diamond electrodes, in: A. Fujishima, Y. Einaga, T.N. Rao, D.A. Tryk (Eds.), Diamond Electrochemistry, Elsevier, Amsterdam, 2005 pp. 80.
[11] A.W. Williams, E.C. Lightowl, A.T. Collins, Impurity conduction in synthetic semiconducting diamond, J. Phys. C: Solid State Phys. 3 (1970) 1727.
[12] M. Bernard, A. Deneuville, P. Muret, Non-destructive determination of the boron concentration of heavily doped metallic diamond thin films from Raman spectroscopy, Diam. Relat. Mat. 13 (2004) 282.
[13] F. Pruvost, E. Bustarret, A. Deneuville, Characteristics of homoepitaxial heavily boron-doped diamond films from their Raman spectra, Diam. Relat. Mat. 9 (2000) 295.
[14] P. Ashcheulov, J. Sebera, A. Kovalenko, V. Petrak, F. Fendrych, M. Nesladek, A. Taylor, Z.V. Zivcova, O. Frank, L. Kavan, M. Dracinsky, P. Hubik, J. Vacik, I. Kraus, I. Kratochvilova, Conductivity of boron-doped polycrystalline diamond films: influence of specific boron defects, Eur. Phys. J. B 86 (2013) 443.
[15] P.W. May, W.J. Ludlow, M. Hannaway, P.J. Heard, J.A. Smith, K.N. Rosser, Raman and conductivity studies of boron-doped micro crystalline diamond, facetted nanocrystalline diamond and cauliflower diamond films, Diam. Relat. Mat. 17 (2008) 105.
[16] A.S. Barnard, M. Sternberg, Substitutional boron in nanodiamond, bucky-diamond, and nanocrystalline diamond grain boundaries, J. Phys. Chem. B 110 (2006) 19307.
[17] G. Janssen, W.J.P. van Enckevort, W. Vollenberg, L.J. Giling, Characterization of single-crystal diamond grown by chemical vapor-deposition processes, Diam. Relat. Mat. 1 (1992) 789.
[18] J.V. Macpherson, A practical guide to using boron doped diamond in electrochemical research, Phys. Chem. Chem. Phys. 17 (2015) 2935.
[19] G.M. Swain, Electrically conducting diamond thin films: Advanced electrode materials for electrochemical technologies, in: A.J. Bard, I. Rubinstein (Eds.), Electroanalytical Chemistry: A Series of Advances, Marcel Dekker, New York, 2005, pp. 182.
[20] A.E. Fischer, Y. Show, G.M. Swain, Electrochemical performance of diamond thin-film electrodes from different commercial sources, Anal. Chem. 76 (2004) 2553.
[21] H.B. Suffredini, V.A. Pedrosa, L. Codognoto, S.A.S. Machado, R.C. Rocha-Filho, L. A. Avaca, Enhanced electrochemical response of boron-doped diamond electrodes brought on by a cathodic surface pre-treatment, Electrochim. Acta 49 (2004) 4021.
[22] I. Duo, C. Levy-Clement, A. Fujishima, C. Comninellis, Electron transfer kinetics on boron-doped diamond Part I: Influence of anodic treatment, J. Appl. Electrochem. 34 (2004) 935.
[23] J.P. McEvoy, J.S. Foord, Direct electrochemistry of blue copper proteins at boron-doped diamond electrodes, Electrochim. Acta 50 (2005) 2933.
[24] I. Yagi, H. Notsu, T. Kondo, D.A. Tryk, A. Fujishima, Electrochemical selectivity for redox systems at oxygen-terminated diamond electrodes, J. Electroanal. Chem. 473 (1999) 173.
[25] R.F. Brocenschi, P. Hammer, C. Deslouis, R.C. Rocha-Filho, Assessments of the effect of increasingly severe cathodic pretreatments on the electrochemical activity of polycrystalline boron-doped diamond electrodes, Anal. Chem. 88 (2016) 5363.
[26] B.P. Chaplin, D.K. Hubler, J. Farrell, Understanding anodic wear at boron doped diamond film electrodes, Electrochim. Acta 89 (2013) 122.
[27] B.C. Lourencao, M. Baccarin, R.A. Medeiros, R.C. Rocha-Filho, O. Fatibello-Filho, Differential pulse voltammetric determination of albendazole in pharmaceutical tablets using a cathodically pretreated boron-doped diamond electrode, J. Electroanal. Chem. 707 (2013) 15.
[28] R.A. Medeiros, M. Baccarin, O. Fatibello-Filho, R.C. Rocha-Filho, C. Deslouis, C. Debiemme-Chouvy, Comparative study of basal-plane pyrolytic graphite, boron-doped diamond, and amorphous carbon nitride electrodes for the voltammetric determination of furosemide in pharmaceutical and urine samples, Electrochim. Acta 197 (2016) 179.
[29] R.A. Medeiros, B.C. Lourencao, R.C. Rocha-Filho, O. Fatibello-Filho, Simple flow injection analysis system for simultaneous determination of phenolic

antioxidants with multiple pulse amperometric detection at a boron-doped diamond electrode, Anal. Chem. 82 (2010) 8658.

[30] T.A. Enache, A.M. Chiorcea-Paquim, O. Fatibello-Filho, A.M. Oliveira-Brett, Hydroxyl radicals electrochemically generated in situ on a boron-doped diamond electrode, Electrochem. Commun. 11 (2009) 1342.

[31] I. Kisacik, A. Stefanova, S. Ernst, H. Baltruschat, Oxidation of carbon monoxide, hydrogen peroxide and water at a boron doped diamond electrode: The competition for hydroxyl radicals, Phys. Chem. Chem. Phys. 15 (2013) 4616.

[32] A. Kapalka, G. Foti, C. Comninellis, The importance of electrode material in environmental electrochemistry: Formation and reactivity of free hydroxyl radicals on boron-doped diamond electrodes, Electrochim. Acta 54 (2009) 2018.

[33] R. Hoffmann, H. Obloh, N. Tokuda, N. Yang, C.E. Nebel, Fractional surface termination of diamond by electrochemical oxidation, Langmuir 28 (2012) 47.

[34] G.R. Salazar-Banda, L.S. Andrade, P.A.P. Nascente, P.S. Pizani, R.C. Rocha-Filho, L. A. Avaca, On the changing electrochemical behaviour of boron-doped diamond surfaces with time after cathodic pre-treatments, Electrochim. Acta 51 (2006) 4612.

[35] H.B. Suffredini, S.A.S. Machado, L.A. Avaca, The water decomposition reactions on boron-doped diamond electrodes, J. Braz. Chem. Soc. 15 (2004) 16.

[36] Y. Cai, A.B. Anderson, J.C. Angus, L.N. Kostadinov, Hydrogen evolution on diamond electrodes by the Volmer-Heyrovsky mechanism, J. Electrochem. Soc. 154 (2007) F36.

[37] G.R. Salazar-Banda, A.E. de Carvalho, L.S. Andrade, R.C. Rocha-Filho, L.A. Avaca, On the activation and physical degradation of boron-doped diamond surfaces brought on by cathodic pretreatments, J. Appl. Electrochem. 40 (2010) 1817.

[38] Y.Y. Jiang, D. Liu, Z.C. Jiang, B.J. Mao, X. Ma, Q.B. Li, Investigation on electrochemically cathodic polarization of boron-doped diamond electrodes and its influence on lead ions analysis, J. Electrochem. Soc. 161 (2014) H410.

[39] R. Trouillon, D. O'Hare, Y. Einaga, Effect of the doping level on the biological stability of hydrogenated boron doped diamond electrodes, Phys. Chem. Chem. Phys. 13 (2011) 5422.

[40] Y.J. Feng, J.W. Lv, J.F. Liu, N. Gao, H.Y. Peng, Y.Q. Chen, Influence of boron concentration on growth characteristic and electro-catalytic performance of boron-doped diamond electrodes prepared by direct current plasma chemical vapor deposition, Appl. Surf. Sci. 257 (2011) 3433.

[41] R. Bogdanowicz, A. Fabianska, L. Golunski, M. Sobaszek, M. Gnyba, J. Ryl, K. Darowicki, T. Ossowski, S.D. Janssens, K. Haenen, E.M. Siedlecka, Influence of the boron doping level on the electrochemical oxidation of the azo dyes at Si/BDD thin film electrodes, Diamond Relat. Mater. 39 (2013) 82.

[42] A. Fabianska, R. Bogdanowicz, P. Zieba, T. Ossowski, M. Gnyba, J. Ryl, A. Zielinski, S.D. Janssens, K. Haenen, E.M. Siedlecka, Electrochemical oxidation of sulphamerazine at boron-doped diamond electrodes: Influence of boron concentration, Phys. Status Solidi A 210 (2013) 2040.

[43] E. Guinea, F. Centellas, E. Brillas, P. Canizares, C. Saez, M.A. Rodrigo, Electrocatalytic properties of diamond in the oxidation of a persistant pollutant, Appl. Catal. B Environ. 89 (2009) 645.

[44] J.T. Matsushima, W.M. Silva, A.F. Azevedo, M.R. Baldan, N.G. Ferreira, The influence of boron content on electroanalytical detection of nitrate using BDD electrodes, Appl. Surf. Sci. 256 (2009) 757.

[45] J. Muff, L.R. Bennedsen, E.G. Sogaard, Study of electrochemical bleaching of p-nitrosodimethylaniline and its role as hydroxyl radical probe compound, J. Appl. Electrochem. 41 (2011) 599.

[46] R.M. Dornellas, R.A.A. Franchini, A.R. da Silva, R.C. Matos, R.Q. Aucelio, Determination of the fungicide kresoxim-methyl in grape juices using square-wave voltammetry and a boron-doped diamond electrode, J. Electroanal. Chem. 708 (2013) 46.

[47] J. Zavazalova, K. Prochazkova, K. Schwarzova-Peckova, Boron-doped diamond electrodes for voltammetric determination of benzophenone-3, Anal. Lett. 49 (2016) 80.

[48] J. Vosahlova, J. Zavazalova, V. Petrak, K. Schwarzova-Peckova, Factors influencing voltammetric reduction of 5-nitroquinoline at boron-doped diamond electrodes, Monatsh. Chem 147 (2016) 21.

[49] M. Brycht, P. Lochynski, J. Barek, S. Skrzypek, K. Kuczewski, K. Schwarzova-Peckova, Electrochemical study of 4-chloro-3-methylphenol on anodically pretreated boron-doped diamond electrode in the absence and presence of a cationic surfactant, J. Electroanal. Chem. 771 (2016) 1.

[50] V. Vyskocil, J. Barek, Electroanalysis of nitro and amino derivatives of polycyclic aromatic hydrocarbons, Curr. Org. Chem. 15 (2011) 3059.

[51] E.T. Seo, R.F. Nelson, J.M. Fritsch, L.S. Marcoux, D.W. Leedy, R.N. Adams, Anodic oxidation pathways of aromatic amines. Electrochemical and electron paramagnetic resonance studies, J. Am. Chem. Soc. 88 (1966) 3498.

[52] K. Peckova, J. Musilova, J. Barek, Boron-doped diamond film electrodes – new tool for voltammetric determination of organic substances, Crit. Rev. Anal. Chem. 39 (2009) 148.

[53] J. Zavazalova, H. Dejmkova, J. Barek, K. Peckova, Voltammetric and amperometric determination of mixtures of aminobiphenyls and aminonaphthalenes using boron doped diamond electrode, Electroanalysis 25 (2013) 253.

[54] J. Barek, K. Jandova, K. Peckova, J. Zima, Voltammetric determination of aminobiphenyls at a boron-doped nanocrystalline diamond film electrode, Talanta 74 (2007) 421.

[55] K. Cizek, J. Barek, J. Fischer, K. Peckova, J. Zima, Voltammetric determination of 3-nitrofluoranthene and 3-aminofluoranthene at boron doped diamond thin-film electrode, Electroanalysis 19 (2007) 1295.

[56] L.J. Felice, R.E. Schirmer, D.L. Springer, C.V. Veverka, Determination of polycyclic aromatic-amines in skin by liquid-chromatography with electrochemical detection, J. Chromatogr. 354 (1986) 442.

[57] L. Maixnerova, J. Barek, K. Peckova, Thin-layer and wall-jet arrangement of amperometric detector with boron-doped diamond electrode: Comparison of amperometric determination of aminobiphenyls in HPLC-ED, Electroanalysis 24 (2012) 649.

[58] D.C. Shin, D.A. Tryk, A. Fujishima, A. Muck, G. Chen, J. Wang, Microchip capillary electrophoresis with a boron-doped diamond electrochemical detector for analysis of aromatic amines, Electrophoresis 25 (2004) 3017.

[59] K. Peckova, V. Mocko, F. Opekar, G.M. Swain, J. Zima, J. Barek, Miniaturized amperometric detectors for HPLC and capillary zone electrophoresis, Chem. Listy 100 (2006) 124.

[60] J. Zavazalova, M.E. Ghica, K. Schwarzova-Peckova, J. Barek, C.M.A. Brett, Carbon-based electrodes for sensitive electroanalytical determination of aminonaphthalenes, Electroanalysis 27 (2015) 1556.

[61] R.S. Nicholson, Theory and application of cyclic voltammetry for measurement of electrode reaction kinetics, Anal. Chem. 37 (1965) 1351.

[62] A.J. Bard, L.R. Faulkner, Electrochemical Methods: Fundamentals and Applications, 2nd ed., John Wiley and Sons, New York, 2001, pp. 814.

[63] Y.J. Wang, J.G. Limon-Petersen, R.G. Compton, Measurement of the diffusion coefficients of $[Ru(NH_3)_6]^{3+}$ and $[Ru(NH_3)_6]^{2+}$ in aqueous solution using microelectrode double potential step chronoamperometry, J. Electroanal. Chem. 652 (2011) 13.

[64] A.F. Azevedo, M.R. Baldan, N.G. Ferreira, Doping level influence on chemical surface of diamond electrodes, J. Phys. Chem. Solids 74 (2013) 599.

[65] I. Gerger, R. Haubner, The behaviour of Ti-substrates during deposition of boron doped diamond, Int. J. Refract. Met. Hard Mat. 26 (2008) 438.

[66] S. Ghodbane, A. Deneuville, Specific features of 325 nm Raman excitation of heavily boron doped polycrystalline diamond films, Diam. Relat. Mat. 15 (2006) 589.

[67] K. Ushizawa, K. Watanabe, T. Ando, I. Sakaguchi, M. Nishitani-Gamo, Y. Sato, H. Kanda, Boron concentration dependence of Raman spectra on {100} and {111} facets of B-doped CVD diamond, Diam. Relat. Mat. 7 (1998) 1719.

[68] B.G. Burke, J. Chan, K.A. Williams, Z.L. Wu, A.A. Puretzky, D.B. Geohegan, Raman study of Fano interference in p-type doped silicon, J. Raman Spectrosc 41 (2010) 1759.

[69] S. Prawer, K.W. Nugent, D.N. Jamieson, J.O. Orwa, L.A. Bursill, J.L. Peng, The Raman spectrum of nanocrystalline diamond, Chem. Phys. Lett. 332 (2000) 93.

[70] N.G. Ferreira, E. Abramof, E.J. Corat, N.F. Leite, V.J. Trava-Airoldi, Stress study of HFCVD boron-doped diamond films by X-ray diffraction measurements, Diam. Relat. Mat. 10 (2001) 750.

[71] W.L. Wang, M.C. Polo, G. Sanchez, J. Cifre, J. Esteve, Internal stress and strain in heavily boron-doped diamond films grown by microwave plasma and hot filament chemical vapor deposition, J. Appl. Phys. 80 (1996) 1846.

[72] A.F. Azevedo, R.C.M. De Barros, S.H.P. Serrano, N.G. Ferreira, SEM and Raman analysis of boron-doped diamond coating on spherical textured substrates, Surf. Coat. Technol. 200 (2006) 5973.

[73] K. Bano, J. Zhang, A.M. Bond, P.R. Unwin, J.V. Macpherson, Diminished Electron Transfer Kinetics for $[Ru(NH_3)]_6^{3+/2+}$, $[\alpha\text{-}SiW_{12}O_{40}]^{4-/5-}$, and $[\alpha\text{-}SiW_{12}O_{40}]^{5-/6-}$ processes at boron-doped diamond electrodes, J. Phys. Chem. C 119 (2015) 12464.

[74] S.C.B. Oliveira, A.M. Oliveira-Brett, Voltammetric and electrochemical impedance spectroscopy characterization of a cathodic and anodic pre-treated boron doped diamond electrode, Electrochim. Acta 55 (2010) 4599.

[75] P. Actis, A. Denoyelle, R. Boukherroub, S. Szunerits, Influence of the surface termination on the electrochemical properties of boron-doped diamond (BDD) interfaces, Electrochem. Commun. 10 (2008) 402.

[76] M.C. Granger, G.M. Swain, The influence of surface interactions on the reversibility of ferri/ferrocyanide at boron-doped diamond thin-film electrodes, J. Electrochem. Soc. 146 (1999) 4551.

[77] C.H. Goeting, F. Marken, A. Gutierrez-Sosa, R.G. Compton, J.S. Foord, Boron-doped diamond electrodes: Growth, surface characterisation and sono-electrochemical applications, New Diam. Front. Carbon Technol. 9 (1999) 207.

[78] M.N. Latto, G. Pastor-Moreno, D.J. Riley, The influence of doping levels and surface termination on the electrochemistry of polycrystalline diamond, Electroanalysis 16 (2004) 434.

[79] O. Scialdone, S. Randazzo, A. Galia, G. Silvestri, Electrochemical oxidation of organics in water: Role of operative parameters in the absence and in the presence of NaCl, Water Research 43 (2009) 2260.

[80] L.A. Hutton, J.G. Iacobini, E. Bitziou, R.B. Channon, M.E. Newton, J.V. Macpherson, Examination of the factors affecting the electrochemical performance of oxygen-terminated polycrystalline boron-doped diamond electrodes, Anal. Chem. 85 (2013) 7230.

# Appendix III

## Publication 3

Chem. Listy *108*, s270–s273 (2014) Cena Merck 2014

# BOREM DOPOVANÉ DIAMANTOVÉ ELEKTRODY: VLIV KONCENTRACE BORU NA STANOVENÍ 2-AMINOBIFENYLU

**JANA VOSÁHLOVÁ, JAROSLAVA ZAVÁZALOVÁ a KAROLINA SCHWARZOVÁ-PECKOVÁ**

*Univerzita Karlova v Praze, Přírodovědecká fakulta, Univerzitní výzkumné centrum UNCE „Supramolekulární chemie“, Katedra analytické chemie, UNESCO laboratoř elektrochemie životního prostředí, Albertov 6, 128 43 Praha 2*
*kpeckova@natur.cuni.cz*

## Úvod

Borem dopované diamantové (BDD) elektrody patří od devadesátých let k populárním elektrodovým materiálům na bázi uhlíku. Mají široké využití především v environmentálních analýzách díky své malé náchylnosti k pasivaci elektrodového povrchu a širokému potenciálovému oknu, obzvláště v anodické oblasti[1,2]. BDD filmy se obvykle připravují v komerčních reaktorech metodou chemické depozice par (CVD – „chemical vapor deposition“) při použití žhavených vláken („hot filament“ – HF CVD) nebo mikrovlnného ohřevu („microwave plasma“ – MP CVD) jako zdroje energie. K depozici diamantového filmu je nejčastěji používána směs methanu (zdroj uhlíku) a vodíku. Dopace borem se provádí přidáním diboranu či trimethylboru do směsi par pro depozici diamantu. Jeho obsah se udává jako poměr B/C v plynné fázi. Používají se koncentrace 500 ppm až 15 000 ppm, které vedou ke konečné koncentraci boru ve filmu $1\cdot10^{18}$ $cm^{-3}$ až $1\cdot10^{21}$ $cm^{-3}$, přičemž koncentrace $1\cdot10^{20}$ $cm^{-3}$ odpovídá jednomu atomu boru na tisíc atomů uhlíku[3]. Přibližně při této koncentraci dochází ke změně vodivosti BDD filmů, která vykazuje při nižších koncentracích polovodičový a při vyšších koncentracích kovový charakter[4]. V poslední době se objevilo několik prací studujících vliv koncentrace boru na fyzikální a elektrochemické charakteristiky BDD filmů[5–8], odolnost vůči elektrochemické korozi[7], odolnost povrchu vůči pasivaci[9], účinnost elektrokatalytické anodické oxidace organických polutantů[10] a analytické parametry stanovení vybraných anorganických iontů[11]. Pro tyto účely byly připraveny BDD filmy s koncentrací boru v rozmezí cca $10^{17}$ $cm^{-3}$ až $10^{22}$ $cm^{-3}$.

Cílem této práce byla charakteristika BDD filmů s koncentrací boru 500–8000 ppm vybranými spektrálními a elektrochemickými metodami a určení vlivu koncentrace boru na velikost potenciálového okna vybraných vodných roztoků základních elektrolytů a na voltametrické stanovení 2-aminobifenylu.

## Experimentální část

Bylo použito pět borem dopovaných diamantových filmových elektrod s B/C poměrem 500 ppm, 1000 ppm, 2000 ppm, 4000 ppm a 8000 ppm. Tyto elektrody byly připraveny na Fyzikálním ústavu Akademie věd České republiky v Oddělení funkčních materiálů. Jako substrát pro chemickou depozici par s pomocí mikrovlnného ohřevu (System Seki ASTeX 5010, Woburn, MA, USA) byl použit p-křemík (ON Semiconductor, Rožnov pod Radhoštěm, ČR) s rezistivitou 0,005 Ω $cm^{-1}$ a tloušťkou 300 μm. Takto připravené BDD destičky byly umístěny do teflonového elektrodového těla s velikostí otvoru ve šroubovacím nástavci 7,1 $mm^2$. Pro elektrochemická měření byl použit přístroj Eco-Tribo Polarograph se softwarem PolarPro (verze 5.1, Polaro-Sensors, Praha, ČR) a tříelektrodové zapojení s referentní argentchloridovou elektrodou (3 mol $l^{-1}$ KCl) a pomocnou platinovou elektrodou (obě Elektrochemické detektory, Turnov, ČR). Pro diferenční pulsní voltametrii (DPV) byla použita výška pulsu +50 mV, šířka pulsu 100 ms a rychlost 20 mV $s^{-1}$. Před každou sérií měření byly elektrody aktivovány v 0,5 mol $l^{-1}$ kyselině sírové s vloženým potenciálem +2,4 V po dobu 5 min.

Pro spektrální charakterizaci povrchu diamantového filmu byla použita Ramanova spektroskopie (DXR Raman microscope (Thermo Scientific, Waltham, MA, USA) s mikroskopem Olympus, excitační vlnová délka 532 nm), mikroskopie atomárních sil (NT-MDT NTEGRA Prima AFM s křemíkovým ohebným nosníkem HA-NC, resonanční frekvence 270 kHz) a skenovací elektronová mikroskopie (FEGSEM; mikroskop Quanta 200 FEG, FEI, ČR). Hodnoty pH byly měřeny digitálním pH metrem (pH Meter 3510, Jenway, UK) se skleněnou kombinovanou elektrodou.

Všechny použité chemikálie pro přípravu základních elektrolytů byly čistoty p.a. (Lach-Ner, Neratovice, ČR). Dále byl použit 2-aminobifenyl (čistota ≤ 95%, Sigma-Aldrich, USA), $K_4[Fe(CN)_6] \cdot 3\ H_2O$ (čistota ≤ 99%, Lach-Ner, Neratovice, ČR) a $[Ru(NH_3)_6]Cl_3$ (čistota ≤ 98%, Sigma-Aldrich, USA).

## Výsledky a diskuse

Nejprve byla provedena spektrální charakterizace studovaných filmů pomocí Ramanovy spektroskopie, spektroskopie atomárních sil (AFM) a skenovací elektronové spektroskopie (SEM). Obě zobrazovací metody prokázaly nanokrystalickou strukturu filmů s velikostí krystalů 100–300 nm pro filmy s obsahem boru 500–4000 ppm. Pro film s obsahem boru 8000 ppm byla zaznamenána větší nejednotnost velikosti a současně menší krystaly.

Chem. Listy *108*, s270–s273 (2014) Cena Merck 2014

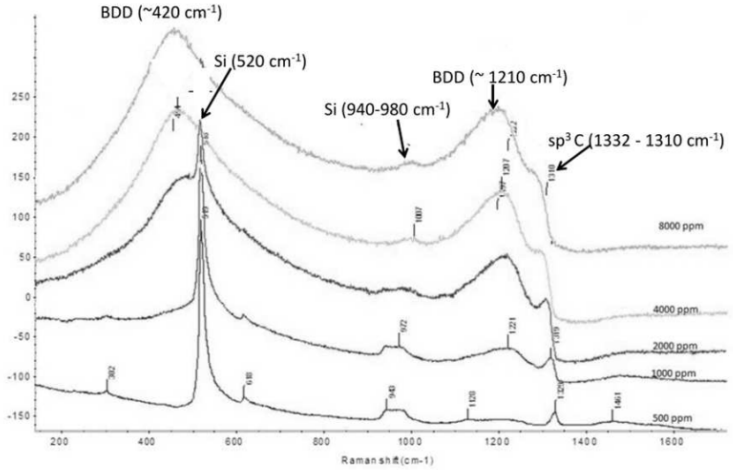


Obr. 1. **Ramanova spektra BDD filmů s koncentrací boru 500–8000 ppm, excitační vlnová délka 532 nm**

Tloušťka filmu je 1 μm (určeno pomocí AFM). Ramanova spektra (obr. 1) vykazují nepřítomnost $sp^2$ nečistot při 1533 $cm^{-1}$ a naopak s rostoucí koncentrací boru nárůst signálu při ~1332 $cm^{-1}$ odpovídající $sp^3$ uhlíku s typickým tvarem pro Fanovy resonance poukazující na přítomnost delokalizovaných stavů pocházejících z B-C vazeb. Dále jsou zřejmé typické signály křemíku (520 $cm^{-1}$ a ~940 až 980 $cm^{-1}$), které odpovídají fononové linii křemíku prvního a druhého řádu a pocházejí ze substrátu. Původ širokých pásů u ~420 $cm^{-1}$ and ~1220 $cm^{-1}$ je nejasný[3].

Elektrochemická charakterizace byla provedena pomocí redoxních markerů $[Fe(CN)_6]^{4-/3-}$ a $[Ru(NH_3)_6]^{4+/3+}$ a pro oba bylo zjištěno quasi-reversibilní chování: při aplikaci anodické aktivace BDD filmů při potenciálu +2,4 V v 0,5 mol $l^{-1}$ kyselině sírové se zvětšila proudová odezva katodického ($I_K$) a anodického píku ($I_A$), zmenšil se rozdíl potenciálů píků ($\Delta E_P$) na hodnoty 69 mV až 150 mV a poměr velikosti píků $I_A/I_K$ se přiblížil hodnotě 1,0. Obsah boru v diamantovém filmu nemá významný vliv na velikost jejich proudové odezvy a $\Delta E_P$.

Cyklická voltametrie byla dále použita pro zjištění vlivu koncentrace boru v BDD elektrodách na velikost potenciálového okna pro několik běžných základních elektrolytů: 1 mol $l^{-1}$ KCl, borátový pufr pH 9,0; fosfátový pufr pH 7,0; octanový pufr pH 4,0; 0,1 mol $l^{-1}$ $HClO_4$ a $1 \cdot 10^{-3}$ mol $l^{-1}$ $Na_2SO_4$. U všech vybraných základních elektrolytů bylo pozorováno celkové zúžení potenciálového okna o cca 800 mV s rostoucí koncentrací boru. Výrazněji se okno zužuje z katodické strany. Na anodické straně není zúžení potenciálového okna tak průkazné, nicméně rozdíl krajního anodického potenciálu pro elektrodu s nejvyšší a nejnižší koncentrací byl zaznamenán na všech studovaných BDD filmech v rozmezí přibližně 150 mV až 250 mV. Na obr. 2 jsou tyto trendy zřejmé z cyklických voltamogramů 0,1 mol $l^{-1}$ kyseliny chloristé.

Dále byl metodou diferenční pulzní voltametrie sledován vliv koncentrace boru na stanovení 2-aminobifenylu v Brittonově-Robinsonově pufru o pH 7,0. Jelikož oxidač-

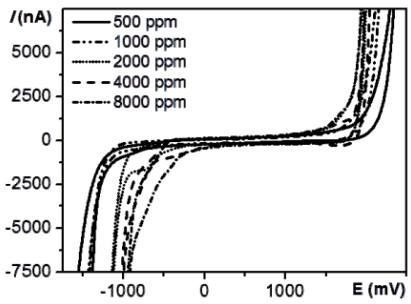


Obr. 2. **Cyklické voltamogramy 0,1 mol $l^{-1}$ kyseliny chloristé pro všechny studované diamantové filmy s různým obsahem boru.** Rychlost polarizace 100 mV $s^{-1}$

Chem. Listy *108*, s270–s273 (2014) Cena Merck 2014

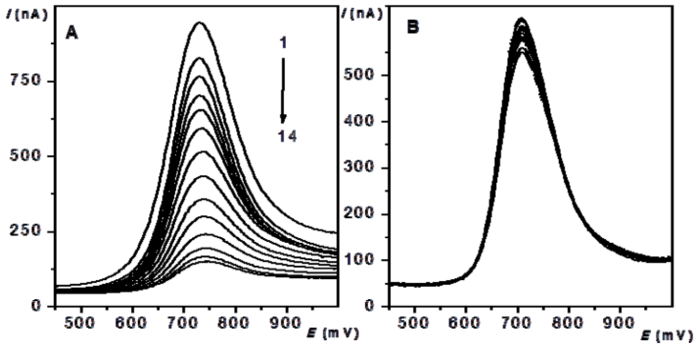


Obr. 3. **DP voltamogramy 2-aminobifenylu ($c$ = 5·10$^{-5}$ mol l$^{-1}$) v prostředí Brittonova-Robinsonova pufru o pH 7,0 (A) bez čištění elektrodového povrchu mezi 14 jednotlivými skeny a (B) s čištěním při potenciálu +2,4 V a mícháním roztoku po dobu 30 s**

Tabulka I
Parametry kalibrační závislosti pro stanovení 2-aminobifenylu metodou DPV na BDD elektrodách v rozmezí 5·10$^{-5}$ mol l$^{-1}$ až 1·10$^{-7}$ mol l$^{-1}$

| Poměr B/C [ppm] | Směrnice [mA l mol$^{-1}$] | Úsek [nA] | Korelační koeficient | Limit detekce [mmol l$^{-1}$] |
|---|---|---|---|---|
| 500 | 7,7 ± 0,3 | 20,3 ± 5,9 | 0,992 | 0,716 |
| 1000 | 7,5 ± 0,5 | 12,5 ± 9,9 | 0,978 | 0,475 |
| 2000 | 11,1 ± 0,2 | 13,0 ± 6,1 | 0,998 | 0,799 |
| 4000 | 14,9 ± 1,8 | 40,8 ± 41 | 0,959 | 0,477 |
| 8000 | 18,0 ± 0,1 | 8,5 ± 1,8 | 0,999 | 0,208 |

ní produkty 2-aminobifenylu výrazně pasivují elektrodový povrch (obr. 3A), byl optimalizován postup čištění elektrodového povrchu. Jako optimální byla vybrána kombinace elektrochemického a mechanického čištění: na obr. 3B jsou vyobrazeny DP voltamogramy pro čištění elektrodového povrchu pomocí vloženého kladného potenciálu +2,4 V a míchání roztoku po dobu 30 s přímo v měřeném roztoku. S takto zvoleným čištěním se proudová odezva 2-aminobifenylu výrazně neměnila, směrodatná odchylka výšky píku pro všechny studované BDD filmy byla menší než 4 %.

S tímto aktivačním programem byla změřena kalibrační závislost 2-aminobifenylu v rozsahu koncentrací 5·10$^{-5}$ až 1·10$^{-7}$ mol l$^{-1}$ pro všechny studované BDD filmy. Parametry a detekční limity jsou uvedeny v tab. I. Je zřejmé, že s rostoucí koncentrací boru v BDD filmu se zvyšuje směrnice kalibrační závislosti, tj. proudová odezva 2-aminobifenylu, a snižuje se mez detekce a dále se zlepšuje opakovatelnost výšky píku 2-AB.

## Závěr

Byla provedena základní spektrální a elektrochemická charakterizace BDD filmů s obsahem boru 500–8000 ppm. Z analytického hlediska se jeví významná závislost šířky potenciálového okna na koncentraci boru a její vliv na velikost píku 2-aminobifenylu při DP voltametrii, kdy mez detekce ($L_D$) leží pro všechny filmy v koncentračním řádu 10$^{-7}$ mol l$^{-1}$ a s rostoucí koncentrací boru v BDD filmu klesá, rozdíl mezi elektrodou s obsahem boru 500 ppm ($L_D$ = 7,2·10$^{-7}$ mol l$^{-1}$) a 8000 ppm ($L_D$ = 2,1·10$^{-7}$ mol l$^{-1}$) je zhruba trojnásobný. Se zvyšující se koncentrací boru v BDD filmu se zlepšuje opakovatelnost výšky píku 2-AB. Koncentrace boru v BDD filmech se tudíž jeví jako důležitý parametr při voltametrických stanoveních organických sloučenin s ohledem na jejich reakční mechanismus, oxidační či redukční potenciál a typ elektroanalytické metody.

*Tato práce byla finančně podporována Grantovou agenturou Univerzity Karlovy v Praze (projekt GAUK 684213) a Grantovou agenturou České republiky (projekt P206/12/G151). JZ děkuje za podporu PřF UK v Praze v rámci projektů STARS a SVV. Děkujeme Ing. Václavu Petrákovi z FZÚ AVČR za přípravu BDD elektrod a RNDr. Ivaně Šloufové, Ph.D. za pomoc s jejich spektrální charakterizací.*

LITERATURA

1. Fujishima A., Einaga Y., Rao T. N., Tryk D. A.: *Diamond Electrochemistry.* Elsevier, Amsterdam 2005.
2. Peckova K., Musilova J., Barek J.: Crit. Rev. Anal. Chem. *39*, 148 (2009).
3. Zivcova Z. V., Frank O., Petrak V., Tarabkova H., Vacik J., Nesladek M., Kavan L.: Electrochim. Acta *87*, 518 (2013).
4. Holt K. B., Bard A. J., Show Y., Swain G. M.: J. Phys. Chem. B *108*, 15117 (2004).
5. Becker D., Juttner K.: Electrochim. Acta *49*, 29 (2003).
6. Watanabe T., Shimizu T. K., Tateyama Y., Kim Y., Kawai M., Einaga Y.: Diam. Relat. Mat. *19*, 772 (2010).
7. Wei J. J., Li C. M., Gao X. H., Hei L. F., Lvun F. X.: Appl. Surf. Sci. *258*, 6909 (2012).
8. Trouillon R., O'Hare D., Einaga Y.: Phys. Chem. Chem. Phys. *13*, 5422 (2011).
9. Feng Y. J., Lv J. W., Liu J. F., Gao N., Peng H. Y., Chen Y. Q.: Appl. Surf. Sci. *257*, 3433 (2011).
10. Matsushima J. T., Silva W. M., Azevedo A. F., Baldan M. R., Ferreira N. G.: Appl. Surf. Sci. *256*, 757 (2009).
11. May P. W., Ludlow W. J., Hannaway M., Heard P. J., Smith J. A., Rosser K. N.: Diam. Relat. Mat. *17*, 105 (2008).

# Appendix IV

*Publication 4*





# Voltammetric and Amperometric Determination of Mixtures of Aminobiphenyls and Aminonaphthalenes Using Boron Doped Diamond Electrode

*Jaroslava Zavázalová, Hana Dejmková, Jiří Barek, Karolina Pecková**

Charles University in Prague, Faculty of Science, Department of Analytical Chemistry, UNESCO Laboratory of Environmental Electrochemistry, Albertov 6, CZ-12843 Prague 2, Czech Republic
*e-mail: kpeckova@natur.cuni.cz

Received: August 3, 2012
Accepted: September 19, 2012
Published online: November 13, 2012

**Abstract**
An anodically pretreated boron-doped diamond (BDD) electrode was used for the voltammetric and amperometric determination of the genotoxic pollutants 2-aminobiphenyl, 4-aminobiphenyl, 1-aminonaphthalene, and 2-aminonaphthalene. Their simultaneous voltammetric determination is only possible when the difference of the peak potentials of the particular analytes is higher than ca. 140 mV. Their complete separation using high performance liquid chromatography (HPLC) with amperometric detection at a BDD film electrode in wall-jet arrangement results in limits of detection in the $10^{-8}$ mol L$^{-1}$ concentration range and can be lowered to nanomolar concentrations, as demonstrated by their determination in azo dye sunset yellow using solid-phase extraction at Lichrolut EN cartridges.

**Keywords:** Amino aromatics, Amperometry, Boron-doped diamond film electrode, Dyes/Pigments, Voltammetry

DOI: 10.1002/elan.201200424

Supporting Information for this article is available on the WWW under http://dx.doi.org/10.1002/elan.201200424.

## 1 Introduction

Boron-doped diamond (BDD) has become a popular electrode material for electroanalysis since the first report on its analytical application in 1993 [1] thanks to its commercial availability and advantageous electrochemical and mechanical properties [2,3]. For voltammetric techniques a low and stable background current, a wide potential range in aqueous media, and fouling resistance are the most important ones. The mechanical durability and low double layer capacitance compared with metallic and most of carbon-based electrode materials minimizing the time to stabilize the background current prior and the current drift during amperometric detection substantiate the popularity of BDD electrodes in liquid flow methods including high performance liquid chromatography (HPLC) and flow injection analysis with electrochemical detection. The possibility of miniaturization of BDD electrodes and modification of the BDD surface opened research fields for detection in capillary electrophoresis (CE) [4], in vitro/in vivo detection [5], and functionalization of the BDD surface for designing of electrochemical sensors [6].

A wide spectrum of oxidizable organic compounds has been studied by means of BDD electrodes during preliminary voltammetric experiments followed by their applications either for anodic decomposition of organic compounds or for electroanalytical purposes [2,3]. Among them, attention was paid also to aromatic amines [7–14], widely applied in many industrial processes, including production of dyes and other chemicals [15,16], and occurring in environmental matrices including waste and surface water [17]. Further, they may be formed as results of anaerobic azo bond reduction of dyes [15] and also used as biomarkers of exposure to parent nitro derivatives of polycyclic aromatic hydrocarbons [18]. Due to their resistance to microbial degradation and adverse toxic effects including potential or proven mutagenicity and/or carcinogenity to living organisms including humans [18], the demands on their selective and sensitive monitoring in working and living environment are increasing [7]. 4-Aminobiphenyl (4-AB) and 2-aminonaphthalene (2-AN) were together with benzidine among the first chemicals classified as human carcinogens. There is an ongoing interest in these compounds which can be documented by an extensive monograph of International Agency for Research on Cancer (IARC) summarizing their occurrence and use, metabolism of carcinogenesis and methods of analysis [18]. The general population can be exposed to 2-AN and 4-AB through environmental exposure, via tobacco smoke, via other fumes containing these compounds (e.g., emissions from cooking oils), or when in contact with dyes and hair dyes contaminated with 2-AN and 4-AB ([18] and references therein).

  

Method developments have enabled the detection of amino derivatives of naphthalene and biphenyl at extremely low concentrations, down to the picogram level (reviewed in [18]). Gas chromatography/mass spectrometry (GC/MS) of derivatized samples and liquid chromatography/mass spectrometry (LC/MS) of nonderivatized samples are the most often used. Electrochemical methods represent an independent alternative to these more expensive MS/chromatographic methods. They rely on the oxidation of the amino group at the aromatic skeleton as demonstrated on the determination of amimobiphenyls by differential pulse voltammetry (DPV) at carbon paste or glassy carbon electrodes [19]. Nanomolar concentration of 2-AB was determined after its accumulation using $\beta$-cyclodextrin modified screen printed electrode [20]. Further, electrochemical detection (ED) has been successfully used in connection with liquid flow techniques including CE [21], flow injection analysis (FIA) [22,23], HPLC [24–26], or reversed-phase μ-HPLC [27]. It has the advantage of easier removal of the possibly passivating intermediates and end-products of the electrode reaction from the vicinity of the electrode surface by the stream of the mobile phase. These passivating films are formed as result of dimerization and further polymerization of nitrene cation radicals – products of initial one-electron oxidation of the amino group [7,28]. On the other side, experimentally controlled electropolymerization leads to formation of conducting electroactive polymers suitable for the modification of metallic or carbon-based electrodes and offering attractive possibilities for sensors designing and electrocatalysis as widely presented for polyaniline [29,30] and recently also for poly(1-naphthylamine) [31–33] and poly(2-aminobiphenyl) films [34].

This work is connected with our previous ones, devoted to voltammetric and amperometric determination of aminobiphenyls [8,10,11,14] using nanocrystalline and microcrystalline anodically pretreated BDD and its objective is to study the possibilities of simultaneous detection of 2-aminobiphenyl (2-AB), 3-aminobiphenyl (3-AB), 4-aminobiphenyl (4-AB), 1-aminonaphthalene (1-AN), and 2-aminonaphthalene (2-AN) by means of BDD electrodes. For this purpose, batch voltammetry and amperometric detection coupled to HPLC were used and after optimization of separation and detection conditions the model samples of the food colorant dye sunset yellow (E-110) were analyzed. In this case, solid phase extraction (SPE) was used for the preliminary preconcentration and separation of tested analytes to decrease limit of detection ($L_D$).

## 2 Experimental

### 2.1 Reagents

The $1\times10^{-4}$ mol L$^{-1}$ stock solutions of 1-AN (Sigma-Aldrich, 98%), 2-AN (Sigma-Aldrich, 95%), 3-AB (synthesized at the Department of Organic Chemistry, Charles University in Prague), 2-AB, and 4-AB (both Sigma-Aldrich, 97%) were prepared by dissolving of exact weight of each compound in deionized water (Millipore Q-plus System, Millipore, USA) and kept in the dark at laboratory temperature. Britton–Robinson (BR) buffers were prepared by mixing a solution of phosphoric, acetic and boric acid (concentration of each 0.04 mol L$^{-1}$) with an appropriate amount of 0.2 mol L$^{-1}$ sodium hydroxide solution (all p.a., Lach-Ner, Czech Republic). Acetonitrile (HPLC grade, Merck, Prague, Czech Republic) was used as the organic part of the mobile phase. The aqueous part of the mobile phase was phosphate buffer consisting of 0.01 mol L$^{-1}$ sodium dihydrogen phosphate (p.a., Lachema, Czech Republic), its pH was adjusted by the addition of concentrated phosphoric acid (p.a., Lach-Ner, Neratovice, Czech Republic). Sunset yellow (E 110) (Sigma-Aldrich, Prague, CZ) with dye content $\geq$90% was used. All the solutions were stored in the dark. Other used chemicals were: methanol (HPLC grade, Merck, Prague, Czech Republic), ethyl acetate, sodium hydroxide, and concentrated nitric acid (all p.a., Lach-Ner, Neratovice, Czech Republic).

### 2.2 Apparatus

Voltammetric measurements were carried out using a computer controlled Eco-Tribo Polarograph with PolarPro software (version 5.1, Polaro-Sensors, Czech Republic). In differential pulse voltammetry, a pulse height of +50 mV, pulse width of 100 ms and scan rate of 20 mV s$^{-1}$ were applied.

For HPLC, degasser DG 3014 on-line, gradient pump BETA 10, SAPPHIRE UV-vis detector (all ECOM, Czech Republic) were used. For amperometric detection, the potentiostat ADLC 2 (Laboratorní přístroje, Czech Republic), the precolumn LiChroCART 4–4, Purospher, RP-18 (5 μm), the column LichroCART 125–4 PurospherSTAR RP-18e (5 μm) (all Merck, Germany), mobile phase consisting of acetonitrile and 0.01 mol L$^{-1}$ phosphate buffer pH 3.0 (40:60, v/v), and detection potential +1.0 V were used. Spectrophotometric detector (detection wavelength $\lambda$ of 290 nm) and amperometric detector were connected in series. The HPLC system was controlled by software Clarity Chromatography Station (DataApex, Prague, Czech Republic) working under Windows 7 (Microsoft, USA). The injected volume was 20 μL and the flow rate $Q$ was 1 mL min$^{-1}$.

All electrochemical measurements were performed in a three-electrode arrangement, using a silver chloride reference electrode (Ag|AgCl, 3 mol L$^{-1}$ KCl) and a platinum wire auxiliary electrode (both Monokrystaly Turnov, Czech Republic). The microcrystalline BDD film electrode deposited on silica wafers was prepared and characterized by procedures described previously [35] at Michigan State University, East Lansing, USA. Concretely, microcrystalline BDD was deposited at 1000 W, using a $CH_4/H_2/B_2H_6$ source gas mixture consisting of 0.5% $CH_4/H_2$ with 10 ppm $B_2H_6$ added for boron doping. The system pressure was 45 Torr, the substrate temperature

  

was 800 °C (estimated via an optical pyrometer), and the growth time was 10 hours.

It was placed in a laboratory-made BDD disk electrode [36] with active geometric area of 12.6 $mm^2$ and used as the working electrode in both voltammetric and amperometric measurements. The electrode surface–capillary outlet distance for the amperometric detector in the wall-jet arrangement was kept at 0.5 mm; the jet diameter was 0.15 mm. All measurements were carried out at laboratory temperature. The pH measurements were carried out by digital pH Meter 3510 (Jenway, UK) with combined glass electrode.

For solid phase extraction (SPE), LiChrolut RP-18 E 200 mg/3 mL and LiChrolut EN 200 mg/3 mL polypropylene columns (both Merck, Prague, Czech Republic) and vacuum manifold (Burdick & Jackson, USA) were used.

### 2.3 Procedures

The indicator electrode was activated at the beginning of each working day in 0.1 mol $L^{-1}$ nitric acid by applying a potential of +2.4 V for 60 s. Between individual measurements, an activation program consisting of stirring and applying the potential of +2.4 V for 15 s on working electrode in measured solution was applied. This procedure was followed in the case of voltammetric experiments with aminonaphthalenes and all HPLC-ED experiments. For the simultaneous voltammetric determination of aminobiphenyls, the measured solution was always bubbled with nitrogen for 15 s between individual measurements.

The solutions for voltammetric measurements were prepared by measuring the proper volume of the aqueous stock solution of the test substance and filling by BR buffer of the required pH to 10 mL. The peak heights ($I_p$) were measured from the tangent of voltammetric curve before and after the peak. All calibration curves were measured in triplicate. The calibration dependences were processed using linear regression method. For voltammetric measurements, limits of detection ($L_D$) and determination ($L_Q$) were calculated as the concentration of the analyte, which gave the signal equal to ten times and three times, respectively, the standard deviation of peak heights estimated from ten consecutive measurements of the lowest measurable concentration. For HPLC measurements, the limits of detection and determination were calculated as the concentration of the analytes corresponding to the signal height ten times and three times, respectively, higher than the background noise.

The model samples of 2-AB, 4-AB, 1-AN, and 2-AN in the dye sunset yellow were prepared by spiking of sunset yellow solution, prepared by dilution of 1.0 g sunset yellow in 10 mL of 0.05 mol $L^{-1}$ phosphate buffer pH 7.0 (final concentration of sunset yellow was 0.1 g $mL^{-1}$).

For SPE, two different extraction columns were tested (both Merck, Prague, CZ). Using LiChrolut RP-18 E 200 mg/3 mL columns the solid phase was conditioned on a vacuum manifold with 3 mL of methanol followed by 4 mL of deionized water and 4 mL of 0.05 mol $L^{-1}$ phosphate buffer (pH 7.0), which was allowed to pass through the cartridge without the use of vacuum. Thereafter, 10 mL of spiked sample of the dye sunset yellow containing appropriate amounts of added analytes were loaded on the column without the use of vacuum. Following the sample application, the cartridges were washed with 2 mL of 0.05 mol $L^{-1}$ phosphate buffer (pH 7.0) and dried under the vacuum for 2 min. Elution of adsorbed aminobiphenyls and aminonaphthalenes was carried out with consecutive fractions of 1 mL of methanol, which was allowed to pass through the column without the use of vacuum. Finally, the vacuum was applied for 30 s to remove the residual methanol from the cartridge. 20 µL of the solution after the extraction was injected into the HPLC system for the analysis.

Using LiChrolut EN 200 mg/3 mL cartridges, solid phase extraction was performed as follows: the solid phase was conditioned on a vacuum manifold with 3 mL of ethyl acetate followed by 3 mL of methanol, 1 mL of deionized water, and 3 mL of 0.05 mol $L^{-1}$ phosphate buffer (pH 7.0), which was allowed to pass through the cartridge without the use of vacuum. Thereafter, 10 mL of spiked sample of the dye sunset yellow containing appropriate amounts of added analytes were loaded on the column without the use of vacuum. Following the sample application, the cartridges were washed with 3 mL of 0.05 mol $L^{-1}$ phosphate buffer (pH 7.0) and dried under the vacuum for 2 min. Elution of adsorbed aminobiphenyls and aminonaphthalenes was carried out with consecutive fractions of 1 mL of acetonitrile, which was allowed to pass through the column without the use of vacuum. Finally, the vacuum was applied for 30 s to remove the residual acetonitrile from the cartridge. 20 µL of the solution after the extraction was injected into the HPLC system for the analysis.

Extraction recovery was calculated from the ratio $I_p/I_p^\circ$, where $I_p$ is the height of the chromatographic peak of 2-AB, 4-AB, 2-AN, or 1-AN recorded by HPLC-ED after SPE and $I_p^\circ$ is the height of the peak of the analyte in a reference solution prepared by the addition of standard solution of the analyte to the blank solution so that its final concentration is equal to the product of the concentration of the analyte in the sample and the preconcentration factor.

## 3 Results and Discussion

### 3.1 Differential Pulse Voltammetry

Firstly, differential pulse voltammetry was used for the investigation of fouling of the electrode surface in the presence of 1-AN and 2-AN in measured solution, because aromatic amines are suspected of formation of dimers and polyamine films covering the electrode surface [7,28] as mentioned above. Fouling of the electrode surface was observed also in our previous study on voltammetry of 2-AB, 3-AB, and 4-AB at a nanocrystalline BDD electrode, where decrease of sensitivity of the calibration de-

  

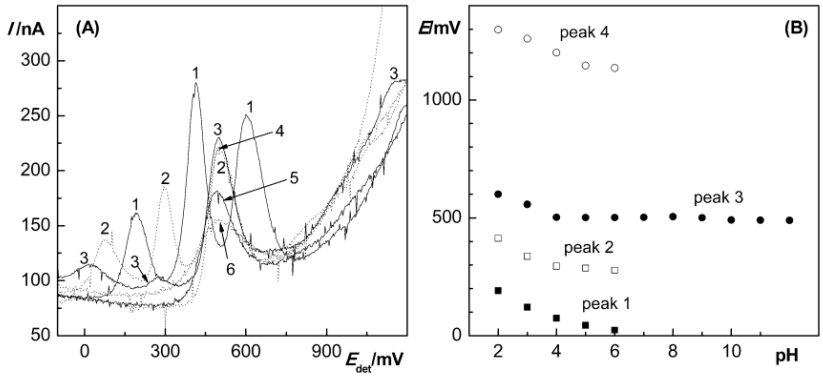


Fig. 1. (A) Selected DP voltammograms of 1-AN ($c = 1 \times 10^{-5}$ mol L$^{-1}$) at the BDD electrode in Britton–Robinson buffer pH 2.0 (1); 4.0 (2); 6.0 (3); 8.0 (4); 10.0 (5) a 12.0 (6). (B) Dependence of the peak potential of 1-AN ($c = 1 \times 10^{-5}$ mol L$^{-1}$) on pH. Measured at the BDD electrode in BR buffer.

pendence with increasing concentration of aminobiphenyls was ascribed to the formation of polyamine films at the surface of the working electrode [14]. In this case its simple immersion in methanol and bubbling with nitrogen for 15 s eliminated most problems with electrode passivation [14]. In the present study the problem with passivation in the presence of aminonaphthalenes was visualized by the decrease of their peak heights at repetitive DP voltammograms of about 80% and potential shift of ca 35 mV to more positive value during consecutive 10 scans (Figure SI1 in Supporting information). As the attempts to recover the electrode surface by stirring in organic solvents (methanol, propan-2-ol, acetonitrile) failed, an electrochemical activation program consisting of stirring and applying the potential of +2.4 V for 15 s on the BDD working electrode in measured solution was successfully applied. As result reproducible peak heights with relative standard deviation 2.0% were obtained for ten repetitive DP voltammograms of 1-AN ($c = 1 \times 10^{-5}$ mol L$^{-1}$ in BR buffer pH 5.0). This procedure succeeded in BR buffer regardless of its pH value. At this high anodic activation potential in the potential region of water discharge, the highly reactive hydroxyl radicals ($^{\bullet}$OH) weakly adsorbed at the BDD surface are formed from water oxidation according to Equation 1:

$$BDD + H_2O \rightarrow BDD(^{\bullet}OH) + H^+ + e^- \quad (1)$$

These hydroxyl radicals are capable of promoting unselectively the oxidation/mineralization of different organic compounds, including polymers in the region close to the electrode surface [37], as proved for the polyaniline film formed by electrooxidation of aniline at the BDD electrode. The reluctance of the polymeric film formed of tested aminonaphthalenes to be removed by organic solvents during stirring proves their more complex polymeric structure. While, in the case of 4-AB, the conventional C–N head-to-tail coupling is presumed at a platinum electrode [38] leading to linear polymers in which biphenyl groups are incorporated in the main macromolecular chain, the electropolymerization of aminonaphthalenes presumably leads to a more crosslinked adhesive polymeric structure resistant to simple dissolution. Different structures of dimers formed during anodic oxidation of 1-aminonaphthalene at platinum and vitreous carbon electrode in dichloromethane, i.e. 1,1′-naphthidine (1,1′-binaphthalene-4,4′-diamine) and 4-amino-1,1′-dinaphthylamine [39] supports this idea. Nevertheless, in the viewpoint of these suggestions it should be noted that the literature aiming at the structure of polymeric films formed by electrooxidation of aromatic amines is scarce.

The influence of pH on signals of aminonaphthalenes ($c = 1 \times 10^{-5}$ mol L$^{-1}$) was investigated in BR buffer in the range of pH 2.0–12.0. Selected DP voltammograms of 1-AN are shown in Figure 1A. 1-AN gives four peaks in the range of pH 2.0–6.0 and one peak at pH 7.0–12.0. The peak potential vs. pH dependence for 1-AN is well recognizable from Figure 1B. 2-AB offers four peaks in the region of pH 2.0 and 3.0, three peaks at pH 4.0, and only one peak at pH 5.0–12.0. The pH dependence has analogous trend as for 1-AN. The gradual shift of the original oxidation peak (peak 3 in Figure 1B) with peak potential of +602 mV and +672 mV for 1-AN and 2-AN, respectively at pH 2.0 toward negative values with increasing pH can be observed, nevertheless, only up to pH 4.0. At higher pH values up to pH 12.0 the peak potentials are constant (ca +504 mV and +580 mV for 1-AN and 2-AN, respectively). These peaks correspond to the first, one–electron stage of oxidation of the amino group to nitrene cation radical and negative shift of peak potential up to pH 4.0 can be explained by protonation of nitrogen atom causing the decrease in electron density which results in

  

Table 1. Parameters of calibration dependences for the DP voltammetric determination of 2-AN, 1-AN, 4-AB, and 2-AB by DPV at the BDD electrode in BR buffer.

| Analyte | pH of BR buffer | Linear dynamic range ($\mu mol\,L^{-1}$) | Slope ($nA\,\mu mol^{-1}\,L$) | Intercept (nA) | Correlation coefficient | $L_O$ ($\mu mol\,L^{-1}$) |
|---|---|---|---|---|---|---|
| 2-AN | 7.0 | 1–66 | 19.6 | −12.8 | 0.9990 | 1.48 |
| 1-AN | 7.0 | 1–100 | 15.1 | −6.1 | 0.9958 | 2.96 |
| 4-AB[a] | 9.0 | 2–10 | 32.4 | 26.0 | 0.9968 | 0.25 |
| | | 0.1–1 | 43.3 | 3.9 | 0.9976 | |
| 2-AB[a] | 7.0 | 2–10 | 41.9 | 54.5 | 0.9988 | 0.12 |
| | | 0.1–1 | 63.3 | 0.9 | 0.9988 | |

[a] Results from our previous study [14]

more difficult oxidation. The change in the slope at pH 4.0 is obviously connected to the $pK_a$ values of nitrene cations of 1-AN (3.92) and 2-AN (4.16). Similar drop of the peak potentials was reported for 3-AB, and 4-AB in our previous study and drop up the pH 5.0 for aniline having the $pK_a$ value of the anilium cation equal to 4.6 [40]. For 2-AB, continuous drop of the peak potential with increasing pH was observed for the whole pH range mentioned above in our study [14]. While the high number of oxidation peaks in acidic media is presumably connected with the formation of dimers and polymeric films confined at the electrode surface as described above, the presence of only one peak at DP voltammograms in more alkaline media and improved repeatability of peak heights even without the application of the activation program between the consecutive scans indicates that at higher pH values the reaction polymeric product are less stable resulting in lower passivation of the BDD surface. This is in agreement with the findings for aniline oxidation at BDD [40], where it was ascribed to the possible water-degradability of insulating polyaniline films [29].

For electroanalytical purposes, the optimum pH 7.0 was chosen for both aminonaphthalenes on the basis of the presence of one symmetric peak, similarly as for 2-AB in our previous study.

Calibration dependences of aminonaphthalenes were measured under these optimized conditions in the concentration range from 1 to 100 $\mu mol\,L^{-1}$. For 1-AN, calibration dependence is linear in the whole concentration range, for 2-AN it is linear in the range from 1 to 66 $\mu mol\,L^{-1}$. Selected parameters of the dependences are summarized in the Table 1. Limits of determination were obtained in the range from 0.25 $\mu mol\,L^{-1}$ for 4-AB to 2.96 $\mu mol\,L^{-1}$ for 1-AN using these optimum conditions.

Further, an attempt was made to use DPV for simultaneous determination of the studied analytes, including 3-AB. It succeeded only thanks to the lower oxidation potential of 4-AB and in the case that the difference of peak potentials of particular analytes was higher than ca 140 mV, i.e. for the pair of 2-AB ($E_p$=620 mV) or 3-AB ($E_p$=610 mV) and 4-AB ($E_p$=470 mV) using BR buffer pH 12.0 as supporting electrolyte (for the mixture 2-AB and 4-AB see Figure 2A). For pH 7.0 and pH 9.0, the optimum pH values for the individual determination of 2-AB and 4-AB, the differences of peak potentials are insufficient, i.e. $\Delta E_p$=111 mV and $\Delta E_p$=78 mV.

The easier oxidation of 4-AB in comparison with the other two ABs was observed also in our previous voltammetric and amperometric studies at BDD electrodes [11], and in HPLC-ED with platinum tubular detector in acidic media [26,41] and was ascribed to the easier accessibility of the tail-placed amino group of 4-AB for the initial oxidation reaction – the loss of one electron forming a radical cation at the nitrogen atom. 1-AN and 2-AN could not be incorporated in the mixtures, because the difference of the oxidation potential is low with respect to each other and all tested aminobiphenyls. Parameters of calibration dependences were evaluated from peak heights of 2-AB (3-AB) and 4-AB for constant concentration of 2-AB (3-AB) and changing concentration of 4-AB (corresponding voltammograms depicted in Figure 2B) and vice versa and micromolar detection limits were obtained (see Table 2). The accuracy assayed with related calibration curves and precision of the proposed methods determined as the *RSD* values of peak heights was evaluated by repeating five experiments on the same day in the same solutions (repeatability) for the mixture of 2-AN/4-AB and 3-AB/4-AB, concentration $1\times10^{-5}\,mol\,L^{-1}$ of each analyte and the results (*RSD* 3.8% and 4.4%) demonstrate satisfactory precision and accuracy. Nevertheless, for the analysis of model samples of tartrazine containing mixture of aminobiphenyls and aminonaphthalenes a HPLC-ED method was developed offering better selectivity and sensitivity as described in the following chapter.

### 3.2 High Performance Liquid Chromatography with Electrochemical Detection

#### *3.2.1 Optimization of Separation and Detection Conditions*

The separation of 2-AB, 4-AB, 1-AN, and 2-AN on reversed phase is strongly affected by the polarity and the pH of the mobile phase in the region of $pK_a$ values of their cationic forms, being $pK_a$=4.16 for 2-AN; $pK_a$=3.92 for 1-AN; $pK_a$=4.35 for 4-AB, and $pK_a$=3.83 for

  

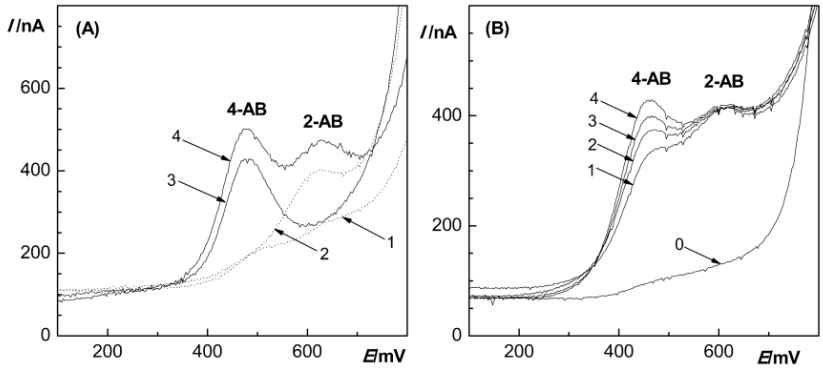


Fig. 2. (A) DP voltammograms of 2-AB (2), 4-AB (3) and a mixture of 2-AB and 4-AB (4) (concentration $1\times10^{-5}$ mol L$^{-1}$ of each) at the BDDE in BR buffer pH 12.0 (1). (B) DP voltammograms of mixtures of 2-AB and 4-AB in the concentration range from 4.0 to 10.0 μmol L$^{-1}$ with a constant concentration of 2-AB (10 μmol L$^{-1}$) and changing concentration of 4-AB. Measured by DPV at the BDD electrode in BR buffer pH 12.0. Concentrations of 4-AB: 0 (0), 4.0 (1), 6.0 (2), 8.0 (3), and 10.0 (4) μmol L$^{-1}$.

Table 2. Limits of detection for the DP voltammetric determination of 2-AB and 3-AB in the mixture with 4-AB. Estimated for changing concentration of 2-AB or 3-AB in the concentration range from 4 to 10 μmol L$^{-1}$ and constant concentration of 4-AB and vice versa. Measured at the BDD electrode in BR buffer pH 12.0, evaluated from peak heights.

| Concentration of 2-AB (μmol L$^{-1}$) | Concentration of 4-AB (μmol L$^{-1}$) | $L_D$ (μmol L$^{-1}$) | Concentration of 4-AB (μmol L$^{-1}$) | Concentration of 2-AB (μmol L$^{-1}$) | $L_D$ (μmol L$^{-1}$) |
|---|---|---|---|---|---|
| 4.0–10.0 | 10.0 | 2.3 | 4.0–10.0 | 10.0 | 0.19 |
| | 8.0 | 1.8 | | 8.0 | 0.22 |
| | 6.0 | 2.8 | | 6.0 | 0.17 |
| | 4.0 | 2.9 | | 4.0 | 0.25 |
| Concentration of 3-AB (μmol L$^{-1}$) | Concentration of 4-AB (μmol L$^{-1}$) | $L_D$ (μmol L$^{-1}$) | Concentration of 4-AB (μmol L$^{-1}$) | Concentration of 3-AB (μmol L$^{-1}$) | $L_D$ (μmol L$^{-1}$) |
| 4.0–10.0 | 10.0 | 1.9 | 4.0–10.0 | 10.0 | 0.39 |
| | 8.0 | 1.5 | | 8.0 | 0.42 |
| | 6.0 | 1.5 | | 6.0 | 0.41 |
| | 4.0 | 1.7 | | 4.0 | 0.33 |

2-AB, respectively. In previous studies, the separation of studied aminobiphenyls at classical $C_{18}$ reversed phases succeeded in 10 min in acetonitrile-phosphate buffer (pH 2.0; 1:1) [26]; studied aminonaphthalenes together with selected diaminonaphthalenes were separated in 0.01 mol L$^{-1}$ phosphate buffer pH 3.0:methanol (40:60, v/v) mobile phase within 8 minutes [42]. Based on these studies optimization of the mobile phase consisting of acetonitrile as organic modificator and 0.01 mol L$^{-1}$ phosphate buffer was carried out. While the content of acetonitrile was 30%, 35% or 40%, the pH of the buffer was changed in the range from pH 2.0 to pH 5.0. Under all tested separation conditions the analytes were eluted in the order 2-AN, 1-AN, 4-AB, 2-AB. The problems in the separation were given on one side [18] by low or absent resolution of 2-AN, 1-AN, and 4-AB, which are eluting in a fast sequence, and on the other side by long elution time of 2-AB. At higher pH values than 5.0 low separation or coelution of aminonaphthalenes was observed irrespective of the content of the organic modificator in the mobile phase. Using pH 4.0, sufficient resolution of these analytes was obtained only in mobile phase with 35% of acetonitrile, nevertheless the retention time of 2-AB (22 min) was too long.

Higher resolution than 1.5 was for all analytes obtained at pH 3.0 independently on the content of acetonitrile in the mobile phase. Corresponding dependence of the reduced retence times of tested compounds on the content of acetonitrile at pH 3.0 at Figure 3A presents elution time of 9.8 min of the lastly eluted 2-AB for 40% of acetonitrile in the mobile phase. Because at low pH values the problems with coelution of aminonaphthalenes and even 4-AB arised again as obvious from Figure 3B, optimum mobile phase consisting of acetonitrile and

  

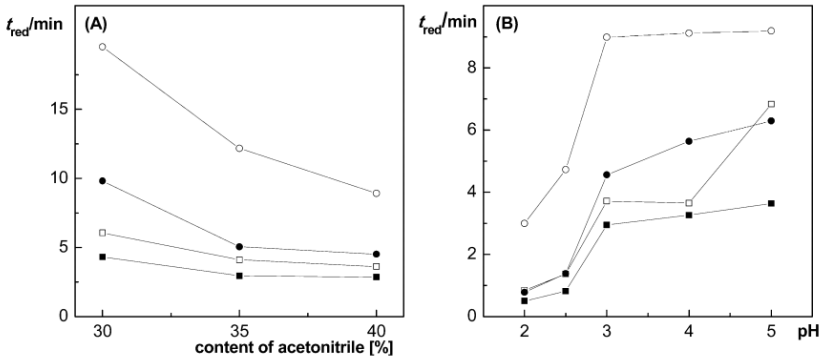


Fig. 3. Dependence of the reduced retention times $t_{red}$ of 2-AN (■), 1-AN (□), 4-AB (●), and 2-AB (○) on: (A) acetonitrile content in the mobile phase (acetonitrile and 0.01 mol L$^{-1}$ phosphate buffer (pH 3)); (B) pH of 0.01 mol L$^{-1}$ phosphate buffer (mobile phase acetonitrile and 0.01 mol L$^{-1}$ phosphate buffer (40:60, v/v)). Measured by HPLC-UV, column LichroCART 125-4 PurospherSTAR RP-18e (5 µm), injection volume 20 µL, $Q$ = 1.0 mL min$^{-1}$, $\lambda_{det}$ = 290 nm.

0.01 mol L$^{-1}$ phosphate buffer pH 3.0 (40:60, v/v) and flow rate of 1 mL min$^{-1}$ was used for further studies. The attempts to decrease the elution time by increase of the flow rate failed as the resolution of 2-AN, 1-AN, and 4-AB was not sufficient at higher flow rates. Chromatograms obtained under the optimum conditions are depicted at Figure 4.

Further, the optimization of the detection potential $E_{det}$ imposed on the working electrode was carried out under the optimum separation conditions. Its potential was increased from +500 mV to +1500 mV in steps of 100 mV and the peak heights of tested analytes and absolute value of the background current were recorded (Figure 5). The detection potentials $E_{det}$ higher than +900 mV provided similar peak heights, nevertheless, destabilization of the baseline occurred at $E_{det}$ higher than +1000 mV, complicating the evaluation. Further, a slight increase of the peak-to-peak noise was observed at potentials higher than +1100 mV, in concordance with our previous study utillizing wall-jet arrangement of amperomet-

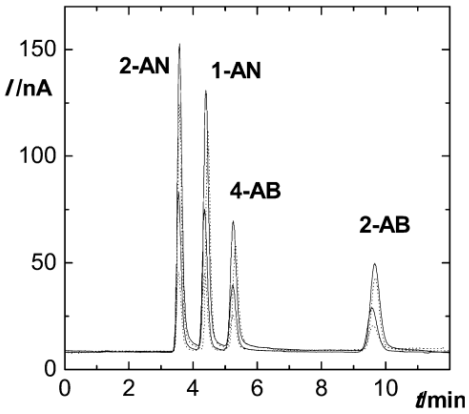


Fig. 4. Chromatograms of the mixture of 2-AN, 1-AN, 4-AB, and 2-AB using HPLC with amperometric detection at the BDD electrode, concentration range 2–8 µmol L$^{-1}$. Measured by HPLC-ED, column LichroCART 125-4 PurospherSTAR RP-18e (5 µm), mobile phase acetonitrile and 0.01 mol L$^{-1}$ phosphate buffer pH 3.0 (40:60, v/v), injection volume 20 µL, $Q$ = 1.0 mL min$^{-1}$, $E_{det}$ = +1.0 V.

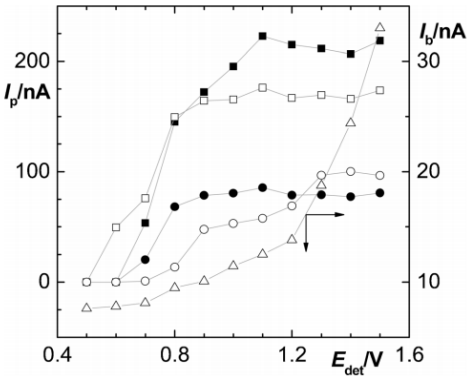


Fig. 5. Hydrodynamic voltammograms of 2-AN (■), 1-AN (□), 4-AB (●), and 2-AB (○) ($c$ = 1 × 10$^{-5}$ mol L$^{-1}$ of each) and dependence of the background current $I_b$ (△) on the applied detection potential ($E_{det}$) at the BDD electrode measured by HPLC with a wall-jet detection cell. For chromatographic conditions see Figure 4.

  

Table 3. Parameters of calibrations dependences for the determination of 2-AN, 1-AN, 4-AB, and 2-AB using HPLC-ED with amperometric detection cell with indicator BDD electrode in wall-jet arrangement ($E_{det} = +1.0$ V). Evaluated from peak heights, chromatographic conditions as in Figure 4.

| Analyte | Linear dynamic range (μmol L$^{-1}$) | Slope (nA μmol$^{-1}$ L) | Intercept (nA) | Correlation coefficient | $L_Q$ (μmol L$^{-1}$) |
|---|---|---|---|---|---|
| 2-AN | 0.02–10 | 19.1 | −0.55 | 0.9996 | 0.06 |
| 1-AN | 0.02–10 | 16.2 | 0.52 | 0.9994 | 0.07 |
| 4-AB | 0.09–10 | 7.99 | 0.21 | 0.9995 | 0.13 |
| 2-AB | 0.16–10 | 5.40 | 0.14 | 0.9995 | 0.20 |

ric detection cell with BDD as an indicator electrode [11]. Therefore, detection potential +1000 mV was selected as optimum based on stable background current and satisfactory peak heights. Under these conditions, ten consecutive injections were made to test the stability of the response; peak heights of 2-AN, 1-AN, 4-AB, and 2-AB are stable with *RSD* 3.3–4.5%, respectively.

It should be mentioned at this point that between the particular HPLC measurements on-line electrochemical activation had to be carried out due to passivation of the electrode surface. We had not any problems of that kind in our previous studies dealing with HPLC-ED of aminobiphenyls [8,11] and our experimental tests revealed that the fouling is caused by aminonaphthalenes. For seven consecutive injections, a drop of about 23% was observed for their peak heights. Surprisingly, fouling has not been reported for detection of 1-AN at a BDD electrode employed in HPLC-ED [4] probably due to higher pH value of the aqueous phase in the mobile phase leading to less adhesive endproducts.

Thus, despite the assumption that the passivation in liquid flow methods is prevented by the stream of the carrier solution removing possible fouling intermediates and endproduct from the vicinity of the electrode surface, the passivation occurs similarly as in the case of total phenols [43].

Nevertheless, the fast in-situ electrochemical activation of the electrode surface does not represent any significant drawback in the analytical procedure, as it would be in the case of mechanical cleaning common for other solid electrode materials.

The adequate activation procedure was reflected in highly linear concentration dependences (correlation coefficients > 0.999) with well defined peaks as presented at chromatograms in Figure 4. The calibration dependences were measured in the concentration range from 0.02 to 10 μmol L$^{-1}$ and their parameters are summarized in Table 3. Limits of determination reached values between 0.06 μmol L$^{-1}$ for 2-AN and 0.20 μmol L$^{-1}$ for 2-AB. Other amperometric methods offer similar quantitation and detection limit in the $10^{-7}$ mol L$^{-1}$ to $10^{-8}$ mol L$^{-1}$ concentration ranges: Amperometric detection of 2-AB and 4-AB with platinum tubular detector [26] or with BDD as an indicator electrode in thin-layer [8] or wall-jet arrangement [11] or detection of 1-AN and 2-AN at carbon paste electrode [42], platinum microcylindrical electrode [44], or thin-layer arrangement using glassy carbon electrode and BDD for the determination of 1-AN and 2-AB [45].

### 3.2.2 *Determination of Studied Analytes in Model Solutions of Sunset Yellow*

The developed HPLC-ED method was further used for the determination of mixtures of aminobiphenyls and aminonaphthalenes in the synthetic colorant sunset yellow (E 110). The dye itself is electrochemically reducible [46,47] due to the presence of the azo group, nevertheless a giant system peak appears at the chromatograms after its direct injection disabling the evaluation of the firstly eluting aminonaphthalenes. Solid-phase extraction enables the washout of the dye matrix and preconcentration of the tested analytes. For this purpose, two different cartridges and procedures were applied (details in Section 2.3). Using extraction columns LiChrolut RP-18 E and 1 mL of the eluent extraction recoveries were satisfactory for aminobiphenyls (i.e., 86% for 4-AB and 88% for 2-AB), but for aminonaphthalenes low recoveries of 31% (2-AN) and 28% (1-AN) were obtained. It was verified by analysis of the filtrate after sample loading that aminonaphthalenes are not quantitatively retained at the solid phase because of about 50% of loaded aminonaphthalenes were detected. Therefore, next determination was carried out using LiChrolut EN cartridges with co-polymeric (poly[styrene-divinylbenzene]) solid phase. High recoveries (more than 96%, listed in Table 4) were obtained for all studied analytes with relative standard deviation up to 4.3% ($n = 5$) using 2 mL of acetonitrile for elution.

The parameters of calibration dependences evaluated from peak heights and corresponding chromatograms are shown in Table 4 and Figure 6. Obviously electrochemical detection has the advantage of relatively narrow and defined system peaks not influencing the firstly eluting compounds contrary to spectrometric detection, where lower concentrations than $1.0 \times 10^{-7}$ mol L$^{-1}$ could not be detected. The calibration dependences are linear in the measured concentration range from $7.5 \times 10^{-9}$ mol L$^{-1}$ to $1 \times 10^{-6}$ mol L$^{-1}$ and nanomolar or slightly higher detection limits were obtained for electrochemical detection of tested compounds.

  

Table 4. Parameters of calibrations dependences and recovery of extraction and its reproducibility (relative standard deviations *RSD*, $n=5$) evaluated from peak heights for solid phase extraction of 2-AN, 1-AN, 4-AB, and 2-AB ($c=1\times10^{-6}$ mol L$^{-1}$) from 10 mL of sunset yellow solution ($c=0.1$ g mL$^{-1}$). Evaluated for HPLC with amperometric detection cell with indicator BDD electrode in wall-jet arrangement ($E_{det}=+1.0$ V). For chromatographic conditions see Figure 4.

| Analyte | Linear dynamic range (μmol L$^{-1}$) | Slope (nA μmol$^{-1}$ L) | Intercept (nA) | Correlation coefficient | Recovery/*RSD* (%) | $L_D$ (nmol L$^{-1}$) |
|---|---|---|---|---|---|---|
| 2-AN | 0.0075–1 | 52.05 | −0.90 | 0.9973 | 101.5/3.2 | 4.62 |
| 1-AN | | 48.27 | −0.20 | 0.9996 | 105.9/2.6 | 4.98 |
| 4-AB | | 21.27 | 0.04 | 0.9978 | 96.5/2.9 | 11.3 |
| 2-AB | | 17.08 | 0.09 | 0.9988 | 103.4/4.3 | 14.1 |

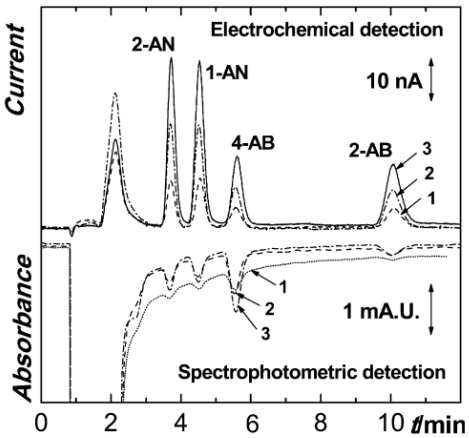


Fig. 6. Chromatograms of the mixture 2-AN, 1-AN, 4-AB, and 2-AB after solid phase extraction from 10 mL of sunset yellow solution (0.1 g mL$^{-1}$) recorded using electrochemical detection at the BDD electrode in wall-jet arrangement ($E_{det}=+1.0$ V) and UV detection ($\lambda_{det}=290$ nm). Concentrations of the analytes $c$: $2.5\times10^{-7}$ (1), $5.0\times10^{-7}$ (2), and $7.5\times10^{-7}$ (3) mol L$^{-1}$; eluent acetonitrile 2 mL. For chromatographic conditions see Figure 4.

## 4 Conclusions

According to the presented results the anodically pretreated BDD disk electrode is a suitable electrochemical sensor for voltammetric and amperometric determination of 1-AN, 2-AN, 2-AB, and 4-AB. Despite the fact, that the resistivity of the BDD electrode towards the passivation declared for a number of compounds causing problems with passivation of common solid electrode materials was not verified in this study and aminonaphthalenes caused passivation using both, batch voltammetric and amperometric detection modes, simple in situ electrochemical activation lasting only 15 s ensured the stable responses. Therefore, the BDD disk electrode could be used without dismantling and no other special electrode cleaning had to be applied.

For DPV determination, limits of quantitation were obtained in the range from 0.25 μmol L$^{-1}$ for 4-AB to 2.96 μmol L$^{-1}$ for 1-AN under optimized conditions. Further, it was verified that DPV determination of the mixture of the studied analytes is possible only in the case that the difference of peak potentials of each compound is higher than ca 140 mV, e.g. for the pair of 2-AB, 4-AB, and 3-AB, 4-AB. However, other mixtures cannot be quantified by this approach due to overlapping peaks, since the analytes have similar peak potentials irrespective of the pH value of the supporting electrolyte.

The developed HPLC-ED method utilizing a BDD electrode in wall-jet arrangement enables in fourteen minutes separation and simultaneous detection of 1-AN, 2-AN, 2-AB, and 4-AB, position isomers with different genotoxic and carcinogenic potential and probability of simultaneous occurrence in industrial products, environment and biological fluids. It offers excellent repeatability and quantitation limits in $10^{-7}$ mol L$^{-1}$ to $10^{-8}$ mol L$^{-1}$ concentration ranges, similar as other solid electrode materials [7,8,11,19,26,42,44,45]. Nevertheless, these often require regular mechanical or electrochemical maintenance to assure reproducible results and thus, the BDD electrode represents the more user-friendly alternative.

The applicability of the developed HPLC-ED method was successfully tested on the determination of the studied analytes in model solutions of azo dye sunset yellow with recoveries of about 100% and nanomolar detection limits.

Thus, it can be concluded that this work presents a valuable contribution to the electroanalysis of amino derivatives of naphthalene and biphenyl having genotoxic and carcinogenic potential. Despite the fact that the limits of detection do not reach the values of highly advanced methods such as HPLC with fluorescence detection, the electrochemical methods represent inexpensive, fast, and relatively selective independent alternative.

## Acknowledgements

The research was supported by the *Ministry of Education, Youth and Sports of the Czech Republic* (Project MSM 0021620857 and *KONTAKT* (*AMVIS*) Project YME10004), *Charles University in Prague* (Project SVV 2012-265201, and *Grant Agency of the Czech Republic* (Project P206/12/G151). JZ thanks to the *Faculty of Sci-*

  

*ence, Charles University in Prague* (Project STARS) for financial support.

## References

[1] G. M. Swain, R. Ramesham, *Anal. Chem.* **1993**, *65*, 345.
[2] A. Fujishima, Y. Einaga, T. N. Rao, D. A. Tryk, *Diamond Electrochemistry*, Elsevier, Amsterdam **2005**.
[3] K. Peckova, J. Musilova, J. Barek, *Crit. Rev. Anal. Chem.* **2009**, *39*, 148.
[4] J. Cvacka, V. Quaiserova, J. Park, Y. Show, A. Muck, G. M. Swain, *Anal. Chem.* **2003**, *75*, 2678.
[5] K. Peckova, J. Barek, *Curr. Org. Chem.* **2011**, *15*, 3014.
[6] S. Szunerits, R. Boukherroub, *J. Solid State Electrochem.* **2008**, *12*, 1205.
[7] V. Vyskocil, J. Barek, *Curr. Org. Chem.* **2011**, *15*, 3059.
[8] K. Peckova, K. Jandova, L. Maixnerova, G. M. Swain, J. Barek, *Electroanalysis* **2009**, *21*, 316.
[9] M. J. Pacheco, V. Santos, L. Ciriaco, A. Lopes, *J. Hazard. Mater.* **2011**, *186*, 1033.
[10] L. Maixnerova, K. Peckova, J. Barek, H. Klimova, *Chem. Listy* **2010**, *104*, 191.
[11] L. Maixnerova, J. Barek, K. Peckova, *Electroanalysis* **2012**, *24*, 649.
[12] K. Cizek, J. Barek, J. Fischer, K. Peckova, J. Zima, *Electroanalysis* **2007**, *19*, 1295.
[13] O. Yosypchuk, J. Barek, V. Vyskocil, *Anal. Bioanal. Chem.* **2012**, *404*, 693.
[14] J. Barek, K. Jandova, K. Peckova, J. Zima, *Talanta* **2007**, *74*, 421.
[15] A. Pandey, P. Singh, L. Iyengar, *Int. Biodeterior. Biodegrad.* **2007**, *59*, 73.
[16] P. G. Rieger, H. M. Meier, M. Gerle, U. Vogt, T. Groth, H. J. Knackmuss, *J. Biotechnol.* **2002**, *94,* 101.
[17] H. M. Pinheiro, E. Touraud, O. Thomas, *Dyes Pigm.* **2004**, *61*, 121.
[18] IARC Working Group on the Evaluation of Carcinogenic Risks to Humans, *Some Aromatic Amines, Organic Dyes, and Related Exposures, IARC monographs on the evaluation of carcinogenic risks to humans*, International Agency for Research on Cancer, Lyon **2010**.
[19] J. Barek, J. Cvacka, A. Muck, V. Quaiserova, J. Zima, *Electroanalysis* **2001**, *13*, 799.
[20] A. Ferancova, E. Korgova, J. Labuda, J. Zima, J. Barek, *Electroanalysis* **2002**, *14*, 1668.
[21] D. C. Shin, D. A. Tryk, A. Fujishima, A. Muck, G. Chen, J. Wang, *Electrophoresis* **2004**, *25*, 3017.
[22] A. G. Fogg, N. K. Bsebsu, M. A. Abdulla, *Analyst* **1982**, *107*, 1462.
[23] A. G. Fogg, M. S. Ali, M. A. Abdulla, *Analyst* **1983**, *108*, 840.
[24] V. Concialini, G. Chiavari, P. Vitali, *J. Chromatogr.* **1983**, *258*, 244.
[25] M. S. Varney, M. R. Preston, *J. Chromatogr.* **1985**, *348*, 265.
[26] J. Zima, S. Vaingatova, J. Barek, J. Brichac, *Chem. Anal. (Warsaw, Pol.)* **2003**, *48*, 805.
[27] M. Shelke, S. K. Sanghi, A. Asthana, S. Lamba, M. Sharma, *J. Chromatogr. A* **2005**, *1089*, 52.
[28] E. T. Seo, R. F. Nelson, J. M. Fritsch, L. S. Marcoux, D. W. Leedy, R. N. Adams, *J. Am. Chem. Soc.* **1966**, *88*, 3498.
[29] B. C. Wang, J. S. Tang, F. S. Wang, *Synth. Met.* **1987**, *18*, 323.
[30] S. Ameen, M. S. Akhtar, M. Husain, *Sci. Adv. Mater.* **2010**, *2*, 441.
[31] A. H. Arevalo, H. Fernandez, J. J. Silber, L. Sereno, *Electrochim. Acta* **1990**, *35*, 741.
[32] X. Li, C. Sun, Z. B. Wei, *Synth. Met.* **2005**, *155*, 45.
[33] F. D'Eramo, L. E. Sereno, A. H. Arevalo, *Electroanalysis* **2007**, *19*, 96.
[34] W. A. Badawy, K. M. Ismail, Z. M. Khalifa, S. S. Medany, *J. Appl. Polym. Sci.* **2012**, *125*, 3410.
[35] A. E. Fischer, Y. Show, G. M. Swain, *Anal. Chem.* **2004**, *76*, 2553.
[36] A. Danhel, K. Peckova, K. Cizek, J. Barek, J. Zima, B. Yosypchuk, T. Navratil, *Chem. Listy* **2007**, *101*, 144.
[37] M. Panizza, E. Brillas, C. Comninellis, *J. Environ. Eng. Manag.* **2008**, *18*, 139.
[38] J. Guay, L. H. Dao, *J. Electroanal. Chem.* **1989**, *274*, 135.
[39] J. M. Marioli, J. J. Silber, L. Sereno, *Electrochim. Acta* **1989**, *34*, 127.
[40] M. Mitadera, N. Spataru, A. Fujishima, *J. Appl. Electrochem.* **2004**, *34*, 249.
[41] J. Zavazalova, H. Dejmkova, S. Ramesova, J. Barek, K. Peckova, in *Sensing in Electroanalysis*, Vol. 5 (Eds: K. Vytřas, K. Kalcher), University of Pardubice, Pardubice **2010**, pp. 163.
[42] J. Zima, H. Dejmkova, J. Barek, *Electroanalysis* **2007**, *19*, 185.
[43] H. Dejmkova, M. Scampicchio, J. Zima, J. Barek, S. Mannino, *Electroanalysis* **2009**, *21*, 1014.
[44] K. Peckova, V. Mocko, F. Opekar, G. M. Swain, J. Zima, J. Barek, *Chem. Listy* **2006**, *100*, 124.
[45] J. Cvačka, G. M. Swain, J. Barek, J. Zima, *Chem. Listy* **2002**, *96*, 33.
[46] P. L. Lopez-de-Alba, L. Lopez-Martinez, L. M. De-Leon-Rodriguez, *Electroanalysis* **2002**, *14*, 197.
[47] M. L. S. Silva, M. B. Q. Garcia, J. Lima, E. Barrado, *Talanta* **2007**, *72*, 282.

  

**Full Paper** Wiley Online Library ELECTROANALYSIS

DOI: 10.1002/elan.201400719

# Carbon-Based Electrodes for Sensitive Electroanalytical Determination of Aminonaphthalenes

Jaroslava Zavazalova,[a] Mariana Emilia Ghica,[b] Karolina Schwarzova-Peckova,[a] Jiri Barek,[a] and Christopher M. A. Brett*[b]

**Abstract**: The electroanalytical performance of bare glassy carbon electrodes (GCE) for the determination of 1-aminonaphthalene (1-AN) and 2-aminonaphthalene (2-AN) was compared with GCE modified by a Nafion permselective membrane or multiwalled carbon nanotubes and with other types of carbon-based materials, carbon film and boron doped diamond. Nafion-modified GCE gave the highest sensitivity and lowest detection limit (0.4 μmol L$^{-1}$) for differential pulse voltammetric determination of 1-AN. Electrochemical impedance spectroscopy gave information about the processes at the electrode surface. Simultaneous determination of 1-AN and 2-AN in a mixture at GCE and their determination in model samples of river water is presented.

**Keywords:** Aminonaphthalenes · Carbon electrode materials · Nafion · Multiwalled carbon nanotubes · Differential pulse voltammetry · Electrochemical impedance spectroscopy

## 1 Introduction

Aminonaphthalenes are aminoderivatives of polycyclic aromatic hydrocarbons (APAHs), significant pollutants of working and living environments, and with carcinogenic, mutagenic, and teratogenic effects. 2-aminonaphthalene (2-AN) is a proven human carcinogen [1], and for 1-aminonaphthalene (1-AN) mutagenic effects have been verified [2]. The first reports on the analytical determination of 2-AN were in the 1960s [3]. Historically, water, urine, and textile samples have been analysed for 2-AN content by gas chromatography (GC) and liquid chromatography-mass spectrometry (LC-MS). These methods permit detection at concentrations down to the pmol L$^{-1}$ level. Recent studies involve the use of GC-MS to determine the concentrations of 2-AN (in derivative form) in cigarette smoke and in the urine of smokers. This method, together with HPLC-MS, is the most often used for various matrices (reviewed in [1]). Modern electrochemical methods represent an independent option to these more expensive chromatographic-MS hyphenated methods. Because amino groups on the aromatic skeleton can easily undergo electrochemical oxidation, voltammetry is an appropriate tool for the monitoring of APAHs in various environmental and biological matrices. Some recently used electrochemical methods for 1-AN and/or 2-AN include the use of boron doped diamond electrodes (BDDE) in Britton-Robinson (BR) buffer pH 7.0 [4], where micromolar limits of detection (*LOD*) were achieved. In other studies of aromatic amines at BDDE, e.g. aminobiphenyls [5] and 3-aminofluoranthene [6], fouling of the electrode surface by passivating intermediates and end products of the electrode reaction was observed. The passivating films covering the electrode surface are created by dimerization and by further polymerization of nitrene cation radical formed in first one-electron step of oxidation of the amino group [7–9]. Further, a nanocomposite-modified glassy carbon electrode (GCE) [10] was used and both analytes were determined after their accumulation using a $\alpha$-, $\beta$-, or $\gamma$-cyclodextrin modified carbon paste electrode or a $\beta$-cyclodextrin modified screen printed electrode [11]. Electrochemical detection has been also successfully used in connection with liquid flow techniques including HPLC [4,12,3], and capillary electrophoresis [4,5].

Glassy carbon is frequently used as an inexpensive sensor electrode material with excellent electrical and mechanical properties, wide potential range, extreme chemical inertness, high resistance to acid attack, impermeability to gases and relatively reproducible performance [6]. Carbon nanotubes (CNT) have been recently used for a wide range of applications, because they represent an important group of nanoscale materials with interesting properties such as high surface area per volume, high electrical conductivity, and interesting electronic properties [17–20]. Their electroactivity is attributed to the presence of reactive groups on the surface, the electrocatalytic effects being associated with structural defects [1,22]. Generally, higher peak currents, and a lower overpotential are observed at CNT modified electrodes [23–25]. Due to these characteristics, CNT have received

[a] J. Zavazalova, K. Schwarzova-Peckova, J. Barek
Charles University in Prague, Faculty of Science, University Research Centre UNCE "Supramolecular Chemistry", Department of Analytical Chemistry, UNESCO Laboratory of Environmental Electrochemistry
Albertov 6, CZ-12843, Prague 2, Czech Republic

[b] M. E. Ghica, C. M. A. Brett
University of Coimbra, Faculty of Science and Technology, Department of Chemistry
Rua Larga, 3004-535 Coimbra, Portugal
*e-mail: cbrett@ci.uc.pt

  

enormous attention for the preparation of electrochemical sensors [20,26–28]. Nafion, a synthetic polymer, is a perfluorosulfonate membrane with high permselectivity of cations vs. anions [29]. It is often used to protect the electrode surface from organic substances present in natural samples that adsorb at the electrode surface, in this way diminishing the response to analyte [30–32].

The present work reports a comparison of bare carbon-based electrodes (glassy carbon (GCE), carbon film (CFE) and boron doped diamond (BDDE)) with GCE surface modified by Nafion permselective membrane or multiwalled carbon nanotubes (MWCNT) for the determination of 1-AN and 2-AN. Electrochemical impedance spectroscopy was employed for the investigation of the electrode interface processes. Simultaneous determination of the two compounds, 1-AN and 2-AN, as well as their determination in model river water samples, is also described.

## 2 Experimental

### 2.1 Reagents

The $1\times10^{-2}$ mol L$^{-1}$ stock solutions of 1-AN (Sigma-Aldrich, 98%), and 2-AN (Sigma-Aldrich, 95%) were prepared by dissolving each compound in deionized water (Millipore Q-plus System, Millipore, USA). More diluted solutions of 1-AN and 2-AN were prepared by appropriate dilution of stock solutions with Britton–Robinson (BR) buffer. BR buffers were prepared by mixing a solution of 0.04 mol L$^{-1}$ phosphoric, acetic (both p.a., Riedel-de Haën, Laborchemikalien, Germany) and boric acid (May&Baker, England), with an appropriate amount of 0.2 mol L$^{-1}$ sodium hydroxide solution (p.a., Riedel-de Haën, Laborchemikalien, Germany). For modification of electrode surfaces, 1% (v/v) Nafion (5% v/v, Aldrich) prepared in pure ethanol (p.a., Merck, Germany) and 1% (m/v) MWCNT (~95% purity, 30±10 nm diameter, 1–5 μm length, NanoLab, USA) dispersed in *N,N*-dimethylformamide (DMF, analytical grade, Fluka, Switzerland) were used.

### 2.2 Apparatus

Voltammetric measurements were carried out using a computer controlled IviumStat electrochemical analyser with IviumSoft software (version 2.024, Ivium Technologies, The Netherlands). In differential pulse voltammetry (DPV), a pulse amplitude of 50 mV, pulse width 50 ms, potential step 2 mV and scan rate 5 mV s$^{-1}$ were used, unless otherwise indicated.

All electrochemical measurements were performed in a three-electrode arrangement, using a silver chloride reference electrode (Ag|AgCl, 3 mol L$^{-1}$ KCl) and a platinum wire auxiliary electrode. The following electrodes were used as working electrodes: 1) a laboratory-made disc GCE with active geometric area of 23.7 mm$^2$; 2) a carbon film electrode (CFE) with active geometric area of 20.0 mm$^2$ (the preparation and characterization of this electrode has been presented elsewhere [33,34]); 3) a laboratory-made boron-doped diamond electrode (BDDE) with active geometric area of 12.6 mm$^2$ [35] made from a microcrystalline boron-doped diamond film deposited on silica wafers, the BDD film having been prepared and characterized by procedures described previously [36].

Electrochemical impedance spectroscopy (EIS) measurements were performed using a Solartron 1250 Frequency Response Analyser, coupled to a Solartron 1286 Electrochemical Interface controlled by ZPlot software. The frequency range used was 65 kHz to 0.1 Hz with 10 frequencies per decade and integration time 60 s, with an rms perturbation voltage of 10 mV. Fitting to electrical equivalent circuits was performed with ZView 3.1 software.

All measurements were carried out at laboratory temperature, approx. 25±1 °C. The pH measurements were carried out by digital pH meter micropH 2001 (Crison, UK) with a combined glass electrode.

### 2.3 Procedures

During the experiments, the blocking of the GCE surface, probably by aminonaphthalene oxidation products, was observed already after the first scan. Because electrochemical pre-treatment of GCE was found not to be efficient, mechanical cleaning of the electrode surface using filter paper and diamond spray (1 μm, Kemet International Ltd., UK) with subsequent rinsing by deionized water was done after each scan. The BDDE was cleaned by electrochemical pre-treatment: between individual measurements, an activation procedure was carried out consisting of stirring and applying a potential of +2.4 V for 15 s to the BDDE in the analyte-containing solution [4]. For CFE no treatment was applied.

Coating of GCE was performed either with 10 μL of 1% Nafion or 2×10 μL of 1% MWCNT solutions in *N,N*-dimethylformamide (DMF) with a micropipette and allowing the coating to dry at room temperature. The carbon nanotubes were prepared as follows: they were first functionalized [26] in 5 mol L$^{-1}$ $HNO_3$ in order to introduce active groups at the end and sidewall defects, then 1 mg of functionalized MWCNT were dispersed in 100 μL of DMF and then sonicated during 4 h to ensure a homogeneous mixture [37].

The solutions for voltammetric measurements were prepared by measuring the appropriate volume of stock solution of the substance to be tested and adding BR buffer of the required pH to give a volume of 10 mL. Values of current density ($j$) used in plots were calculated as $I/A$, where $I$ is the measured current and $A$ is the geometric area of the electrode. The height of the DPV peak was measured from the straight line connecting the baseline on both sides of the peak. All calibration curves were measured in triplicate and their statistical parameters (e.g., slope, intercept, correlation coefficient, standard deviation) and other mathematical and statistical quantities

  

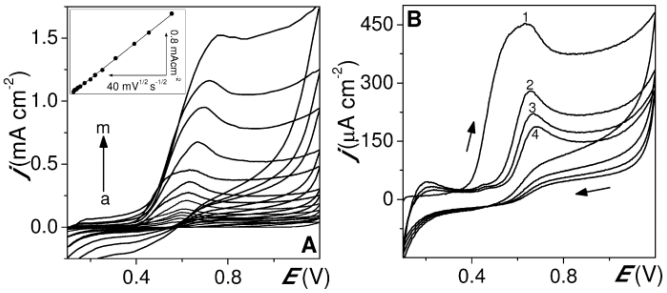


Fig. 1. (A) Cyclic voltammograms of $5\times10^{-4}$ mol L$^{-1}$ 1-AN at GCE in BR buffer pH 4.0 at scan rates 5 (a), 10 (b), 20 (c), 30 (d), 50 (e), 100 (f), 200 (g), 300 (h), 500 (i), 1000 (j), 2000 (k), 3000 (l), and 5000 (m) mV s$^{-1}$. Inset: Dependence of peak current density of 1-AN on the square root of scan rate. (B) Four consecutive cyclic voltammograms of $5\times10^{-4}$ mol L$^{-1}$ 1-AN at GCE in BR buffer pH 4.0 at scan rate 500 mV s$^{-1}$.

were calculated (all for the significance level $\alpha=0.05$) [38]. Limits of detection were calculated as $LOD=(3SD)/b$, where $SD$ is standard deviation of intercept and $b$ is slope of the calibration curve.

A sample of river water taken from Mondego river, Parque Verde, Coimbra, Portugal, was used for electroanalysis. The river water was filtered by filter paper, kept in a refrigerator at 4 °C, and analysed within 3 days after sampling. The solutions for analysis were prepared from 9 mL of filtered river water plus 1 mL of BR buffer pH 2.0, total volume 10 mL, and then spiked with 50 μL or 100 μL of the 0.010 M stock solution of analyte (i.e. concentration of analyte in tested solution was 50 or 100 μmol L$^{-1}$) and directly tested. The concentration in the sample was estimated using the calibration curve.

## 3 Results and Discussion

### 3.1 Electrochemical Oxidation of Aminonaphthalenes at GCE

The electrochemical oxidation of 1-AN and 2-AN was investigated by cyclic voltammetry (CV) and differential pulse voltammetry (DPV). A study of the scan rate dependence by CV and the pH dependence by DPV was carried out. The mechanism of oxidation was assessed by both techniques.

#### *3.1.1 Cyclic Voltammetry*

The electrochemical behavior of 1-AN and 2-AN at GCE was investigated by CV in the potential range from +0.1 to +1.2 V. Cyclic voltammograms obtained at GCE in a $5\times10^{-4}$ mol L$^{-1}$ solution of 1-AN in BR buffer pH 4.0 at different scan rates are depicted in Figure 1A. The linear dependence of current density on square root of scan rate (inset in Figure 1A) indicates that the electrochemical process is diffusion-controlled. A similar behavior was observed for 2-AN (not shown).

A decrease of the oxidation peak currents was observed after successive cycling without cleaning the electrode surface between individual scans, (Figure 1B), a feature common for aromatic amines [7,8]. Their electrooxidation is initiated by the loss of one electron forming a radical cation at the nitrogen atom, which gives rise to dimeric products and polymeric films by rapid follow-up reactions blocking the electrode surface. The electrooxidation of aminonaphthalenes presumably leads to the corresponding radical cations describable by mesomeric forms with the positive charge settled at aromatic rings. These cations undergo further coupling forming simple dimers or polymers. The extension of the positive charge over both aromatic rings is expected to lead to a higher number of coupling modes and therefore, a higher number of anodic voltammetric signals as we described previously for aminonaphthalenes and aminobiphenyls [4,5]. Detailed investigation of the structure of the polymeric films is out of the scope of this study.

#### *3.1.2 Differential Pulse Voltammetry*

The effect of pH on the current and peak potential of aminonaphthalenes was measured at GCE in BR buffer with pH values ranging from 2.0 to 11.0. The DP voltammograms of 1-AN are shown in Figure 2A and the dependence of peak potential of 1-AN and 2-AN ($c=5\times10^{-4}$ mol L$^{-1}$) on pH is shown in Figure 2B. Both, 1-AN and 2-AN, exhibit one peak at pH 2.0 and two peaks in the range of pH 3.0–11.0. With decreasing pH, a gradual shift of the oxidation peak toward more positive potentials was observed, which can be explained by protonation of the nitrogen atom causing a decrease in electron density, resulting in more difficult oxidation. The slopes for peak potential versus pH in the pH range 2.0–4.0 were 50 mV for 1-AN and 49 mV for 2-AN per pH unit, which is close to the theoretical value of 59 mV for an equivalent number of protons and electrons involved in the oxidation prior to the rate determining step. We

  

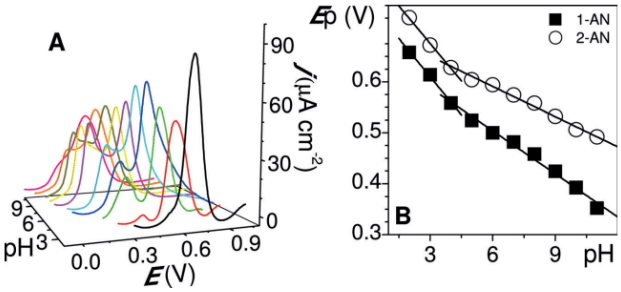


Fig. 2. (A) DP voltammograms of 1-AN measured at GCE in BR buffer pH 2.0–11.0 and (B) pH dependence of peak potential of 1-AN and 2-AN ($c = 5 \times 10^{-4}$ mol L$^{-1}$ of each).

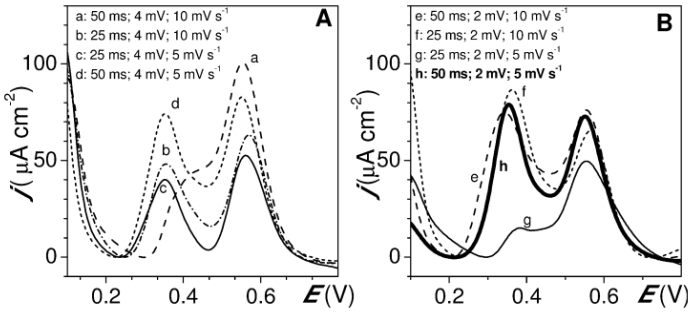


Fig. 3. DP voltammograms of $5 \times 10^{-4}$ mol L$^{-1}$1-AN at GCE in BR buffer pH 4.0 with different DP parameters: constant pulse amplitude 50 mV, constant potential step 4 mV (A) and constant potential step 2 mV (B); the optimum values depicted in bold.

assume that this oxidation step corresponds to the one electron oxidation with loss of one proton of the protonated amino group to give the corresponding aminocation radical Ar-NH$^{2+\bullet}$ [5,7,39,40].

The change in the slope at pH 4.0 is evidently connected to the p$K_a$ values of 1-AN (p$K_a$=3.92) and 2-AN (p$K_a$=4.16). At pH values higher than 4.0, the slopes change to 28 mV for 1-AN and 20 mV for 2-AN per pH unit, thus suggesting the loss of two protons per one electron. Presumably, the initial product of the oxidation of nonprotonated aminonaphthalene is Ar–N$^{+\bullet}$ stabilized by its mesomeric forms extending the radical cation over both aromatic rings. For both tested aminonaphthalenes, substantially higher peak currents and symmetric peak shape was observed at pH 2.0; thus BR buffer pH 2.0 was used for further electroanalytical determinations.

The influence of DPV scan parameters on the response of 1-AN at GCE was also investigated. The experiments were carried out for 1-AN ($c = 5 \cdot 10^{-4}$ mol L$^{-1}$) in BR buffer pH 4.0, where 1-AN gives two peaks, in order to see how the change of parameters influences the shape and the height of both peaks. The parameters were: pulse amplitude (50 mV), pulse time (25 and 50 ms), potential step (2 and 4 mV) and scan rate (5 and 10 mV s$^{-1}$). As an example, DP voltammograms for potential steps of 4 mV and 2 mV are shown in Figure 3. The optimum values of pulse amplitude 50 mV, pulse time 50 ms, potential step 2 mV and scan rate 5 mV s$^{-1}$ were chosen on the basis of the highest and best shaped peak.

### 3.2 Voltammetric Determination of Aminonaphthalenes at Bare Carbon-Based and Modified Surfaces

Under the optimised conditions, the determination of aminonaphthalenes was performed by DPV at bare carbon surfaces–GCE, BDDE and CFE. Further, the effect of the modification of the GCE surface with Nafion or multiwalled carbon nanotubes for 1-AN measurement was tested and analytical parameters were compared.

#### *3.2.1 Determination at Bare and Modified GCE*

Calibration curves for 1-AN and 2-AN measured under the optimized conditions in the concentration range from 2 to 100 μmol L$^{-1}$ using a GCE as working electrode

  

Table 1. Analytical parameters from linear dependences for the determination of 1-AN and 2-AN by DPV at different types of electrodes in BR buffer pH 2.0.

| Electrode | Linear dynamic range ($\mu mol\,L^{-1}$) | Sensitivity ($nA\,\mu mol^{-1}\,L\,cm^{-2}$) | Correlation coefficient | *LOD* ($\mu mol\,L^{-1}$) | Pretreatment | *RSD* [a] (%) |
|---|---|---|---|---|---|---|
| **1-AN** | | | | | | |
| BDD | 2–20 | 282 | 0.9981 | 1.4 | electrochemical | 3.8 |
| CFE | 2–20 | 80 | 0.9914 | 3.1 | without | 16.0 |
| GCE | 2–100 | 257 | 0.9998 | 1.6 | mechanical | 4.3 |
| Nafion/GCE | 0.2–20 | 302 | 0.9998 | 0.4 | without | 9.8 |
| MWCNT/GCE | 10–100 | 229 | 0.9947 | 11.6 | without | 12.9 |
| **2-AN** | | | | | | |
| GCE | 2–100 | 358 | 0.9998 | 2.0 | mechanical | 4.4 |

[a] repeatability of peak height expressed by relative standard deviation, $c = 20\,\mu mol\,L^{-1}$, $n = 4$.

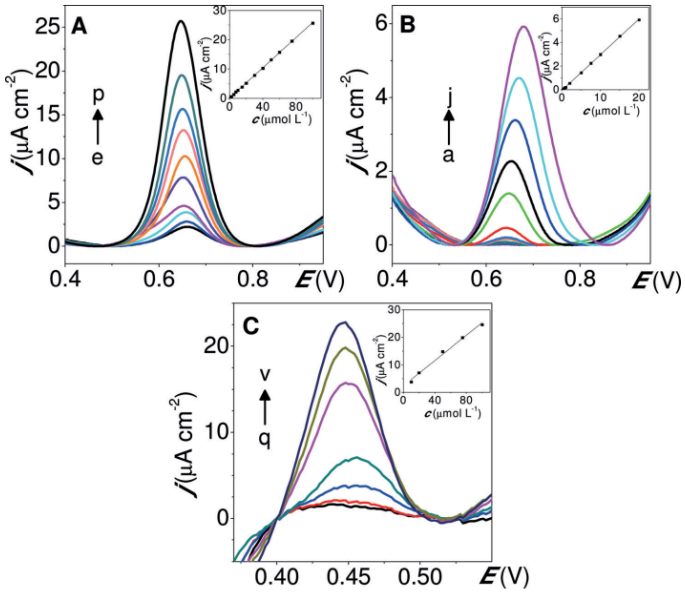


Fig. 4. DP voltammograms of 1-AN at bare GCE (A), Nafion/GCE (B), and MWCNT/GCE (C) in BR buffer pH 2.0; concentration of 1-AN: (A, B) 0.2 (a), 0.5 (b), 0.75 (c), 1.0 (d), 2.0 (e), 5.0 (f), 7.5 (g), 10.0 (h), 15.0 (i), 20.0 (j), 30.0 (k), 40.0 (l), 50.0 (m), 60.0 (n), 75.0 (o), 100.0 (p); (C) 2.0 (q), 5.0 (r), 10.0 (s), 20.0 (t), 50.0 (u), 75.0 (u), 100.0 (v) $\mu mol\,L^{-1}$, subtracted baselines. Insets: Linear dependences of 1-AN concentration on peak current density.

showed a linear dependence over the whole concentration range. The calibration parameters are presented in Table 1 and the linear dependence for 1-AN measured at bare GCE is depicted in Figure 4A. Micromolar limits of detection were obtained, specifically 1.6 $\mu mol\,L^{-1}$ for 1-AN and 2.0 $\mu mol\,L^{-1}$ for 2-AN.

In order to increase the response towards 1-AN, two different strategies were then investigated: modification of the glassy carbon surface with Nafion permselective membrane or with multiwalled carbon nanotubes. Selected analytical parameters from calibration dependences are shown in Table 1 and a comparison of DP voltammograms of all investigated bare and modified surfaces is depicted in Figure 5. In the case of Nafion modified GCE (Nafion/GCE), the calibration dependence is linear in the range from 0.2 to 20 $\mu mol\,L^{-1}$ (Figure 4B). For GCE modified by MWCNT (MWCNT/GCE), the calibration dependence is linear in the range from 10 to 100 $\mu mol\,L^{-1}$ (Figure 4C) and the considerable shift of peak potential to a less positive value $E_p = +450\,mV$ is evident

  

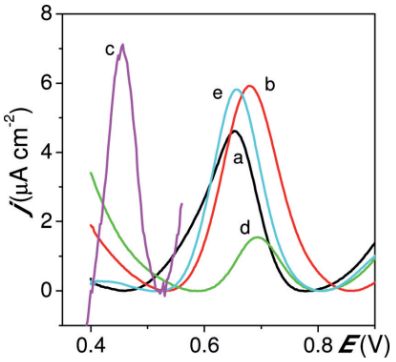


Fig. 5. DP voltammograms, after baseline subtraction, of 20 μmol L$^{-1}$ 1-AN at bare GCE (a), Nafion/GCE (b), MWCNT/GCE (c), CFE (d), and BDDE (e) in BR buffer pH 2.0.

(Figure 5) attributable to the electrocatalytic properties of MWCNT. The sensitivity at MWCNT/GCE decreased (229 nA μM$^{-1}$ cm$^{-2}$) and at Nafion/GCE increased (302 nA μM$^{-1}$ cm$^{-2}$) compared to bare GCE (257 nA μM$^{-1}$ cm$^{-2}$). Also, regarding the other characteristics, Nafion/GCE performed better than either bare GCE or MWCNT/GCE, i.e. linear dynamic range over two orders of magnitude of concentration, low noise and submicromolar *LOD* of 0.4 μmol L$^{-1}$. Another advantage of both modified surfaces is no necessity to clean the electrode surface between measurements.

*3.2.2 Determination at Different Electrode Surfaces*

Beside GCE, 1-AN was investigated at other carbon-based bare surfaces, namely carbon film electrodes obtained from electrical resistors and boron doped diamond film electrodes. DP voltammograms in 20 μmol L$^{-1}$ 1-AN for all investigated surfaces are depicted in Figure 5 and a comparison of analytical figures of merit is given in Table 1. 1-AN exhibited one peak at a similar potential for BDDE (+655 mV) and GCE (+657 mV), and was slightly more positive for CFE (+690 mV). The calibration dependences at BDDE and CFE were linear in a shorter range than at GCE (2–20 μmol L$^{-1}$ compared with 2–100 μmol L$^{-1}$). The detection limits for BDDE and GCE are comparable (ca. 1.5 μmol L$^{-1}$), the higher *LOD* for CFE (3.1 μmol L$^{-1}$) being explained by the lower sensitivity of this electrode material.

Blocking of the electrode surface was a problem for all types of bare electrode surface. However, this could be overcome by mechanical polishing at GCE or by anodic pre-treatment of BDDE. Thus, bare electrodes, after mechanical or electrochemical cleaning, exhibit better peak height repeatability than modified electrodes which do not require any cleaning if a slightly higher *RSD* can be accepted.

It can be concluded that Nafion/GCE is the most sensitive electrode material of those tested, with the lowest *LOD*, and with simple handling. However, highly reproducible responses, with easy recovery of the electrode surface can be obtained at unmodified GCE and this electrode exhibited a wider linear range, which is more suitable for practical applications.

**3.3 EIS Characterisation of 1-AN and 2-AN**

Electrochemical impedance spectroscopy measurements were carried out in BR buffer pH 2.0 and with addition of 50 μmol L$^{-1}$ 1-AN and 2-AN at GCE at different potentials, and comparison with BDDE was also performed for 1-AN. The potentials used were 0.0 V, where no reaction occurs, +0.65 V and +0.74 V, where oxidation of 1-AN and 2-AN, respectively, take place. Complex plane impedance spectra of 1-AN and 2-AN are shown in Figure 6.

The spectra were fitted with the same equivalent circuit, consisting of a cell resistance, $R_\Omega$, in series with a parallel combination of a constant phase element, CPE$_1$ and a resistance, $R_1$, this last being in series with another parallel combination of a double layer constant phase element, CPE$_{dl}$ and a charge transfer resistance, $R_{ct}$. The CPE are modelled as non-ideal capacitors, described by $CPE = -(i\omega C)^{-\alpha}$, where $\omega$ is the angular frequency and the $\alpha$ exponent reflects a non-uniform surface. The CPE$_1$ and $R_1$ are associated with the film formed at the electrode surface due to the adsorption of 1-AN or 2-AN. Data from the equivalent circuit fittings are presented in Table 2.

All spectra show similar behaviour with the addition of analyte in the supporting electrolyte, namely at 0.0 V almost no differences in the spectra were obtained, while at +0.65 V and +0.74 V, respectively, the values of the impedance significantly decreased in the presence of 1-AN or 2-AN, meaning that electron transfer occurs at this potentials. The values of cell resistance were 20 Ω cm$^2$ for GCE$_1$, 30 Ω cm$^2$ for GCE$_2$ and 60 Ω cm$^2$ for BDDE. The differences in the values are due to the different types of electrode used, and this is valid for all the other circuit elements. For BDDE, the values of $\alpha_{dl}$ are closer to 1.0 and lower values for CPE$_{dl}$ were obtained compared to GCE, showing that this electrode is more capacitive than GCE. The most significant alteration is observed for the charge transfer resistance, consistent with easier electron transfer in the presence of analyte (1$^{st}$ spectra). The process at GCE was faster than at BDDE, as reflected by the lower $R_{ct}$ values. When recording again the spectra in the presence of analyte after a short period, the value of the charge transfer resistance increases further (2$^{nd}$ spectra), showing that the aminonaphthalenes adsorb on the surface of the electrode, hindering electron transfer, in agreement with cyclic voltammetry.

  

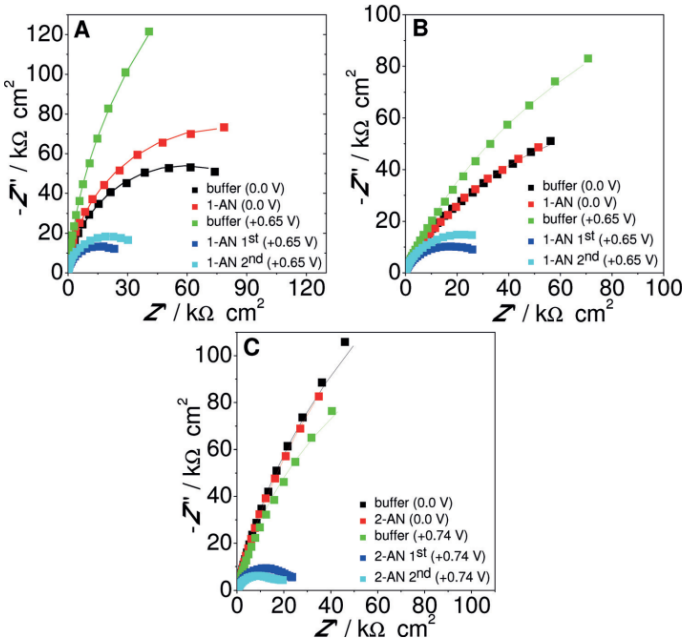


Fig. 6. Complex plane impedance spectra for 1-AN at BDDE (A) and GCE (B) and for 2-AN at GCE (C) in BR buffer pH 2.0 at different potentials. Lines indicate equivalent circuit fitting.

Table 2. Data obtained from equivalent circuit fitting of the impedance spectra at GCE for 1-AN and 2-AN and at BDD for 1-AN in BR buffer at pH 2.0 ($c = 50\ \mu mol\,L^{-1}$ for 1-AN and 2-AN).

| Electrode | Potential (mV) | Analyte | $R_1$ (kΩ cm²) | $CPE_1$ (μF cm$^{-2}$ s$^{\alpha-1}$) | $\alpha_1$ | $R_{ct}$ (kΩ cm²) | $CPE_{dl}$ (μF cm$^{-2}$ s$^{\alpha-1}$) | $\alpha_{dl}$ |
|---|---|---|---|---|---|---|---|---|
| $GCE_2$ | 0 | buffer | 12.5 | 5.81 | 0.89 | 209 | 10.6 | 0.56 |
| | | 1-AN | 11.5 | 6.09 | 0.89 | 185 | 11.5 | 0.60 |
| | 650 | buffer | 11.8 | 4.82 | 0.91 | 332 | 7.04 | 0.64 |
| | | 1-AN 1st | 10.3 | 4.53 | 0.91 | 24.9 | 13.1 | 0.65 |
| | | 1-AN 2nd | 12.5 | 3.53 | 0.92 | 33.5 | 8.89 | 0.64 |
| BDD | 0 | buffer | 0.143 | 5.95 | 0.96 | 111 | 3.78 | 0.97 |
| | | 1-AN | 0.092 | 6.32 | 0.95 | 149 | 3.43 | 0.99 |
| | 650 | buffer | 0.195 | 8.53 | 0.93 | 522 | 2.55 | 1.0 |
| | | 1-AN 1st | 0.151 | 8.69 | 0.92 | 31.1 | 2.92 | 1.0 |
| | | 1-AN 2nd | 0.130 | 7.08 | 0.94 | 40.9 | 4.12 | 0.98 |
| $GCE_1$ | 0 | buffer | 0.051 | 6.77 | 0.72 | 971 | 5.88 | 0.93 |
| | | 2-AN | 0.050 | 5.21 | 0.71 | 849 | 11.3 | 0.88 |
| | 740 | buffer | 0.053 | 7.65 | 0.70 | 508 | 5.86 | 0.93 |
| | | 2-AN 1st | 0.066 | 15.1 | 0.59 | 20.9 | 5.47 | 0.93 |
| | | 2-AN 2nd | 0.062 | 9.36 | 0.63 | 27.3 | 6.18 | 0.90 |

### 3.4 Simultaneous Determination of 1-AN and 2-AN and Recovery in Water Samples

On the basis of the presence of one peak and the difference of peak potentials of 1-AN ($E_p = +658$ mV) and 2-AN ($E_p = +726$ mV) at GCE, DPV was used for the simultaneous determination of the two analytes in a mixture in BR buffer pH 2.0 as supporting electrolyte. Each aminonaphthalene was measured by increasing its concentration in the range from 2 to 10 $\mu mol\,L^{-1}$, while keeping the concentration of the other aminonaphthalene at a constant value of 10 $\mu mol\,L^{-1}$. The corresponding DPV are

  

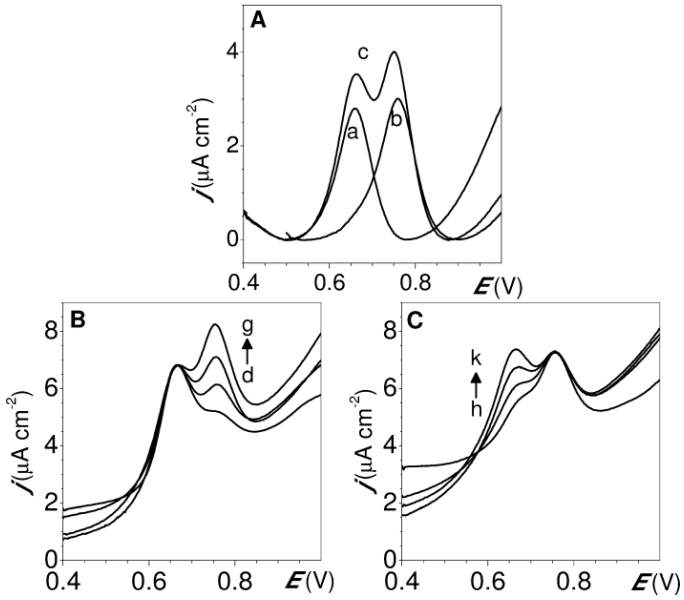


Fig. 7. (A) DP voltammograms of 1-AN (a), 2-AN (b) and mixture of 1-AN and 2-AN (c) ($c = 10\ \mu mol\ L^{-1}$ of each) at GCE in BR buffer pH 2.0; (B) and (C) DP voltammograms of mixture of 1-AN and 2-AN; (B) constant concentration of 1-AN ($10\ \mu mol\ L^{-1}$) and different concentrations of 2-AN: 2 (d), 5 (e), 7.5 (f), and 10 (g) $\mu mol\ L^{-1}$; (C) constant concentration of 2-AN ($10\ \mu mol\ L^{-1}$) and different concentrations of 1-AN: 2 (h), 5 (i), 7.5 (j), and 10 (k) $\mu mol\ L^{-1}$.

Table 3. Recovery of 1-AN and 2-AN in model samples of river water, $n = 5$, measured at GCE.

| Analyte | Concentration added ($\mu mol\ L^{-1}$) | Concentration found ($\mu mol\ L^{-1}$) | Recovery (%) |
|---|---|---|---|
| 1-AN | 50 | $51 \pm 1.9$ | 98–106 |
| | 100 | $95 \pm 4.1$ | 91–99 |
| 2-AN | 50 | $46 \pm 2.0$ | 88–96 |
| | 100 | $91 \pm 3.7$ | 87–95 |

shown in Figure 7. The responses showed linear dependences in this range and micromolar limits of detection were obtained, namely 1.9 and 1.6 $\mu mol\ L^{-1}$ for 1-AN and 2-AN, respectively.

The practical applicability of the proposed method was tested by the determination of 1-AN and 2-AN in model samples of river water (Table 3). The model samples were prepared as described in section 2.3, testing concentrations of 50 and 100 $\mu mol\ L^{-1}$ for each analyte. For 1-AN, recoveries between 91 and 106% were obtained and for 2-AN, the recoveries ranged from 87 to 96%, the relative standard deviation for 5 successive measurements, being $< 5\%$.

## 4 Conclusions

A comparison of bare carbon-based surfaces, namely glassy carbon, carbon film and boron doped diamond, with a GCE surface modified by Nafion permselective membrane and multiwalled carbon nanotubes for the electroanalysis of 1- and 2-aminonaphthalene was performed. Blocking of the electrode surface by reaction by-products occurred on all types of electrode surfaces. For 1-AN, similar detection limits were achieved for bare surfaces: at BDDE 1.4 $\mu mol\ L^{-1}$, at GCE 1.6 $\mu mol\ L^{-1}$ and at CFE 3.1 $\mu mol\ L^{-1}$, for the last electrode the sensitivity was markedly less than with the other electrode materials. Even though it was expected that there would be an increase in sensitivity as reported in many studies for MWCNT/GCE [23–25], no such effect was observed for the compounds studied here. Nafion/GCE offers the lowest limit of detection of 1-AN (0.4 $\mu mol\ L^{-1}$), and thus is useful only for lower concentrations range (0.2–20 $\mu mol\ L^{-1}$).

  

**Acknowledgements**

Financial support from *Fundação para a Ciência e a Tecnologia* (*FCT*), Portugal PTDC/QUI-QUI/116091/2009, POCH, POFC-QREN (co-financed by *FSE* and *European Community FEDER* Funds through the program *COMPETE* and *FCT* Project PEst-C/EME/UI0285/2013) is gratefully acknowledged. M. E. G. thanks *FCT* for a postdoctoral fellowship SFRH/BPD/36930/2007. The research was also supported by the *Grant Agency of the Czech Republic* (Projects P206/12/G151). J. Z thanks to *Specific University Research* (SVV260084) and the *European Commission* (grant under the *Erasmus* student exchange programme) for financial support.

## References

[1] IARC Working Group on the Evaluation of Carcinogenic Risks to Humans, *IARC Monographs on the Evaluation of Carcinogenic Risks to Humans*, Vol. 99, *Some Aromatic Amines, Organic Dyes, and Related Exposures*, IARC, Lyon, France **2010**.
[2] Y. Cheung, D. F. V. Lewis, T. I. Ridd, T. J. B. Gray, C. Ioannides, *Toxicology* **1997**, *118*, 115.
[3] Y. Masuda, D. Hoffmann, *Anal. Chem.* **1969**, *41*, 650.
[4] J. Zavazalova, H. Dejmkova, J. Barek, K. Peckova, *Electroanalysis* **2013**, *25*, 253.
[5] J. Barek, K. Jandova, K. Peckova, J. Zima, *Talanta* **2007**, *74*, 421.
[6] K. Cizek, J. Barek, J. Fischer, K. Peckova, J. Zima, *Electroanalysis* **2007**, *19*, 1295.
[7] V. Vyskocil, J. Barek, *Curr. Org. Chem.* **2011**, *15*, 3059.
[8] E. T. Seo, R. F. Nelson, J. M. Fritsch, L. S. Marcoux, D. W. Leedy, R. N. Adams, *J. Am. Chem. Soc.* **1966**, *88*, 3498.
[9] K. Peckova, J. Musilova, J. Barek, *Crit. Rev. Anal. Chem.* **2009**, *39*, 148.
[10] S. George, H. K. Lee, *Anal. Meth.* **2010**, *2*, 326.
[11] A. Ferancova, E. Korgova, J. Labuda, J. Zima, J. Barek, *Electroanalysis* **2002**, *14*, 1668.
[12] L. J. Felice, R. E. Schirmer, D. L. Springer, C. V. Veverka, *J. Chromatogr.* **1986**, *354*, 442.
[13] L. Maixnerova, J. Barek, K. Peckova, *Electroanalysis* **2012**, *24*, 649.
[14] D. C. Shin, D. A. Tryk, A. Fujishima, A. Muck, G. Chen, J. Wang, *Electrophoresis* **2004**, *25*, 3017.
[15] K. Peckova, V. Mocko, F. Opekar, G. M. Swain, J. Zima, J. Barek, *Chem. Listy* **2006**, *100*, 124.
[16] E. T. G. Cavalheiro, C. M. A. Brett, A. M. Oliveira-Brett, O. Fatibello-Filho, *Bioanal. Rev.* **2012**, *4*, 31.
[17] G. A. Rivas, M. D. Rubianes, M. C. Rodriguez, N. E. Ferreyra, G. L. Luque, M. L. Pedano, S. A. Miscoria, C. Parrado, *Talanta* **2007**, *74*, 291.
[18] C. Gouveia-Caridade, R. Pauliukaite, C. M. A. Brett, *Electrochim. Acta* **2008**, *53*, 6732.
[19] Q. Gao, M. Sun, P. Peng, H. L. Qi, C. X. Zhang, *Microchim. Acta* **2010**, *168*, 299.
[20] P. Yanez-Sedeno, J. Riu, J. M. Pingarron, F. X. Rius, *Trac – Trends Anal. Chem.* **2010**, *29*, 939.
[21] C. E. Banks, T. J. Davies, G. G. Wildgoose, R. G. Compton, *Chem. Commun.* **2005**, 829.
[22] H. J. Dai, *Accounts Chem. Res.* **2002**, *35*, 1035.
[23] R. Pauliukaite, M. E. Ghica, O. Fatibello, C. M. A. Brett, *Comb. Chem. High Throughput Screen.* **2010**, *13*, 590.
[24] S. L. Yang, R. Yang, G. Li, L. B. Qu, J. J. Li, L. L. Yu, *J. Electroanal. Chem.* **2010**, *639*, 77.
[25] X. L. Wang, C. C. Cheng, R. R. Dong, J. C. Hao, *J. Solid State Electrochem.* **2012**, *16*, 2815.
[26] M. E. Ghica, R. Pauliukaite, O. Fatibello-Filho, C. M. A. Brett, *Sens. Actuators B, Chem.* **2009**, *142*, 308.
[27] K. Balasubramanian, M. Burghard, *Anal. Bioanal. Chem.* **2006**, *385*, 452.
[28] J. Wang, *Electroanalysis* **2005**, *17*, 7.
[29] C. Heitner-Wirguin, *J. Membr. Sci.* **1996**, *120*, 1.
[30] A. Economou, P. R. Fielden, *Analyst* **2003**, *128*, 205.
[31] C. M. A. Brett, D. A. Fungaro, J. M. Morgado, M. H. Gil, *J. Electroanal. Chem.* **1999**, *468*, 26.
[32] C. M. A. Brett, D. A. Fungaro, *Talanta* **2000**, *50*, 1223.
[33] C. M. A. Brett, L. Angnes, H. D. Liess, *Electroanalysis* **2001**, *13*, 765.
[34] C. Gouveia-Caridade, C. M. A. Brett, *Electroanalysis* **2005**, *17*, 549.
[35] J. Barek, J. Fischer, T. Navratil, K. Peckova, B. Yosypchuk, J. Zima, *Electroanalysis* **2007**, *19*, 2003.
[36] A. E. Fischer, Y. Show, G. M. Swain, *Anal. Chem.* **2004**, *76*, 2553.
[37] D. Kul, M. E. Ghica, R. Pauliukaite, C. M. A. Brett, *Talanta* **2013**, *111*, 76.
[38] J. N. Miller, J. C. Miller, *Statistics and Chemometrics for Analytical Chemistry*, 5th ed., Pearson Education, Harlow **2005**.
[39] R. S. Deinhammer, M. Ho, J. W. Anderegg, M. D. Porter, *Langmuir* **1994**, *10*, 1306.
[40] J. Zavazalova, H. Dejmkova, J. Barek, K. Peckova, *Electroanalysis* **2014**, *26*, 687.

Received: December 10, 2014
Accepted: January 26, 2015
Published online: April 17, 2015

  

# *Appendix VI*

*Publication 6*

ANALYTICAL LETTERS
2015, VOL. 49, NO. 1, 80–91
http://dx.doi.org/10.1080/00032719.2014.1003425

Taylor & Francis
Taylor & Francis Group

ELECTROCHEMISTRY

## Boron-doped Diamond Electrodes for Voltammetric Determination of Benzophenone-3

Jaroslava Zavazalova, Katerina Prochazkova and Karolina Schwarzova-Peckova

Charles University in Prague, Faculty of Science, University Center of Excellence "Supramolecular Chemistry," Department of Analytical Chemistry, UNESCO Laboratory of Environmental Electrochemistry, Prague, Czech Republic

**ABSTRACT**
The goal of this study was to determine benzophenone-3 at the boron-doped diamond electrode and in the presence of cetyltrimethylammonium bromide by adsorptive stripping voltammetry. The oxidation of benzophenone-3 was irreversible by differential pulse voltammetry. The peak height increased with boron concentration in the electrode film deposited as 500–8000 parts per million boron/carbon. Limits of detection of 1.5, 1.9, and 0.8 micromoles per liter were obtained for 2000, 4000, and 8000 parts per million films in Britton-Robinson buffer at pH 12.0. Positive effect of cetyltrimethylammonium bromide on the determination of benzophenone-3 includes higher sensitivity, a shift of the peak potential to less positive values, and an improved limit of detection by an order of magnitude to 0.1 micromole per liter.

**ARTICLE HISTORY**
Received 31 October 2014
Accepted 20 December 2014

**KEYWORDS**
Adsorptive stripping voltammetry; benzophenone-3; boron-doped diamond electrode; cetyltrimethylammonium bromide

### Introduction

Benzophenone-3 (BP-3; 2-hydroxy-4-methoxybenzophenone or oxybenzone) is one of the most widely used ultraviolet filters in sunscreens and various consumer products (Gonzalez et al. 2006). The Scientific Committee on Consumer Products (SCCP) of the European Commission believes that the use of benzophenone-3 in concentrations up to 6% in cosmetic sunscreens and up to 0.5% in all types of cosmetic products to protect the formulation does not pose a risk to the health of the consumer except for its contact allergenic and photoallergenic potential [SCCP (Scientific Committee on Consumer Products) 2008].

Widespread use of these products can lead to contamination of the environment by benzophenone-3. As an endocrine disruptor, benzophenone-3 can negatively influence living organisms by disturbing hormonal equilibrium, as confirmed in studies with fish *Danio rerio* (Bluthgen, Zucchi, and Fent 2012) or *Oryzias latipes* (Kim et al. 2014). Further studies dealing with antiandrogenic and estrogenic activity of benzophenone and its derivatives were performed on cell cultures and rats (Suzuki et al. 2005; Molina-Molina et al. 2008). The occurrence, toxicity, and ecological risks of benzophenone-3 are summarized in a review by Kim and Choi (2014).

**CONTACT** Karolina Schwarzova-Peckova kpeckova@natur.cuni.cz Charles University in Prague, Faculty of Science, University Center of Excellence "Supramolecular Chemistry," Department of Analytical Chemistry, UNESCO Laboratory of Environmental Electrochemistry, Albertov 6, CZ-128 43, Prague 2, Czech Republic.
This paper is part of a special issue of papers presented at the Modern Electrochemical Methods XXXIV (in Jetřichovice, Czech Republic)/47th Heyrovský Discussion (in Třešť, Czech Republic) Conferences.

Benzophenone-3 is an electrochemically active compound and can be easily determined by modern voltammetric techniques, based on its reduction at the carbon nanoparticle modified carbon electrode (Vidal et al. 2008), dropping mercury electrode (Razak, Gazy, and Wahbi 2002), hanging mercury drop electrode (Cardoso et al. 2008), and boron doped diamond (BDD) electrode (Laranjeira et al. 2011). This electrode material has been widely used in past twenty years due to its wide potential window (especially in the anodic region), mechanical and chemical stability, low residual current, possibility of miniaturization, and biocompatibility (Fujishima et al. 2005; Peckova et al. 2006; Peckova, Musilova, and Barek 2009; Peckova and Barek 2011).

The morphology, conductivity and electrochemical properties are substantially influenced by the boron content of BDD film (Holt et al. 2004; Zivcova et al. 2013). While films with doping levels below $10^{19}$ boron atoms per $cm^{-3}$ exhibit clear valence bands, concentrations up to $2 \times 10^{20}$ per cubic centimeter lead to semiconductivity. A semiconducting/metallic transition has been predicted by Williams, Lightowlers, and Collins (1970) to occur at $[B] = 2 \times 10^{20}$ per cubic centimeter. Nevertheless, the estimation of exact concentration directly in the film is problematic and boron-doping level is usually given by the B/C ratio, where B and C refer to diborane or trimethylboron and methane concentrations in the gaseous phase for chemical vapor deposition procedure. These values are usually from 100 to 15,000 parts per million and experimental values for semiconducting/metallic transition of conductivity are ca. 1000–2000 parts per million (Hutton et al. 2013; Schwarzová-Pecková et al. submitted).

The benefits of surfactants for the determination of organic compounds at surfaces such as pencil graphite or glassy carbon electrodes are well-known (Levent, Yardim, and Senturk 2009; Yardim and Senturk 2011; Levent et al. 2014). Originally used for adsorptive electroanalytical techniques at BDD electrodes for the determination of organic analytes, this approach has not been employed because of the low propensity of the BDD surface to adsorption at the hydrophobic, hydrogen-terminated surface (Peckova, Musilova, and Barek 2009). This concept was disproved by the adsorptive transfer stripping voltammetric determination of the polyphenol chlorogenic acid (Yardim 2012). Furthermore, it was shown that the presence of surfactant may have a positive influence on selectivity and sensitivity of voltammetry due to the enhanced adsorption of the analyte in the presence of surfactant at the BDD surface. Cationic surfactants succeeded as shown in the oxidation of benzo[*a*]pyrene (Yardim et al. 2011), capsaicin (Yardim 2011), and ambroxol (Levent, Yardim, and Senturk 2014), and the reduction of benzophenone-3 (Laranjeira et al. 2011).

According to our best knowledge, an electroanalytical method based on the oxidation of benzophenone-3 has not been reported. In this study, a new method for the determination of benzophenone-3 at the BDD film electrode was developed using differential pulse voltammetry in Britton-Robinson buffer in the presence and absence of cetyltrimethylammonium bromide (CTAB). The effect of the B/C ratio in the BDD films was investigated upon the signal of the analyte.

## Experimental

### *Reagents*

A $1 \times 10^{-3}$ moles per liter stock solution of benzophenone-3 (98%, Aldrich) was prepared by dissolving the compound in 0.01 moles per liter aqueous sodium hydroxide (p.a., Penta,

Czech Republic). A $1 \times 10^{-2}$ moles per liter stock solution of cetyltrimethylammonium bromide (98%, Fluka) was prepared by dissolving the compound in deionized water (Millipore Q-Plus System, Millipore, USA). All stock solutions were kept in the dark at laboratory temperature. Britton-Robinson (BR) buffers were prepared by mixing a solution of phosphoric, acetic, and boric acid (concentration of each 0.04 moles per liter, all p.a., Lach-Ner, Czech Republic) with an appropriate volume of 0.2 mole per liter sodium hydroxide. Other chemicals included concentrated sulfuric acid, methanol (all p.a., Penta, Czech Republic), acetonitrile (isocratic grade for liquid chromatography, Merck, Germany), ethyl acetate, sodium hydroxide, and concentrated nitric acid (all p.a., Lach-Ner, Neratovice, Czech Republic).

### Apparatus

Voltammetric measurements were carried out using a computer controlled Eco-Tribo Polarograph with PolarPro software (version 5.1, Polaro-Sensors, Czech Republic). All electrochemical measurements were performed in a three-electrode arrangement, using a silver-silver chloride reference electrode (Ag|AgCl, 3 moles per liter KCl) and a platinum wire auxiliary electrode (both Elektrochemické detektory, Turnov, Czech Republic). Two types of boron-doped diamond electrodes were used as working electrodes. For voltammetric determination of benzophenone-3 in the absence of surfactant, boron-doped diamond films prepared at the Institute of Physics of the ASCR, v. v. i. in the Department of Functional Materials were used. They were deposited on silicon wafers by microwave plasma-assisted chemical vapor deposition of 99.0% $H_2$/1.0% $CH_4$ and trimethylboron gas with variable B/C ratio in the gas phase 500, 1000, 2000, 4000, and 8000 parts per million. Obtained BDD films at Si wafers were placed in a Teflon electrode body constructed in our laboratory (Cizek et al. 2007) with geometric surface area of 10.2 square millimeters. These electrodes were designated as $BDD_A$ in this work with specification of boron content in the BDD film. For optimization of differential pulse voltammetry, $BDD_A$ with B/C ratio 2000 parts per million was utilized. For voltammetric determination of benzophenone-3 in the presence of surfactant, commercially available boron-doped diamond electrodes with a diameter of 3.0 millimeters (geometric area 7.1 square millimeters, Windsor Scientific, UK; further marked as $BDD_B$) were used. All measurements were carried out at laboratory temperature.

### Procedures

For differential pulse voltammetry, a pulse height of +50 millivolts, pulse width of 100 milliseconds, and scan rate of 20 millivolts per second were employed. For cyclic voltammetry, a scan rate of 100 millivolts per second was used.

The working electrodes $BDD_A$ and $BDD_B$ were activated at the beginning of each working day in 0.5 mole per liter aqueous sulfuric acid by oxidation at +2.4 volts for 60 seconds. The working electrode $BDD_A$ used in the absence of surfactant was activated between individual measurements by stirring and applying potentials of +3, −3, +3, −3 volts, and +3, each for 10 seconds in 0.5 mole per liter aqueous sulfuric acid. Mechanical cleaning of $BDD_B$ electrode surface using a polishing pad and alumina (Elektrochemické detektory, Turnov, Czech Republic) with a subsequent rinse by deionized water was applied after each scan when working with surfactant containing solutions.

The solutions for measurements were prepared with benzophenone-3 stock solution and diluted with Britton-Robinson buffer of the required pH or 0.01 mole per liter NaOH. The peak heights ($I_p$) were measured from the straight line connecting minima on both sides of the peak. All calibration curves were measured in triplicate. The calibration dependences were processed using linear regression. For voltammetric measurements, the limits of detection (LOD) were calculated as the concentration of the analyte which gave a signal equal to three times the standard deviation of the peak height estimated from seven consecutive measurements of the lowest measurable concentration.

## Results and discussion

### Optimization of conditions for determination of benzophenone-3

#### Activation of the surface of the $BDD_A$

Preliminary experiments revealed that the oxidation of benzophenone-3 caused passivation of electrode surface independent of the pH and composition of the supporting electrolyte. Attempts to renew the electrode surface using very positive potentials in the region of water decomposition reaction directly in measured solutions, which is a common strategy at BDD electrodes (Fujishima et al. 2005; Peckova, Musilova, and Barek 2009; Zavazalova et al. 2013), previously succeeded in the reactivation of the surface by the oxidation of phenol (Iniesta et al. 2001). However, this approach was unsuccessful, and hence ex-situ electrochemical activation in 0.5 mole per liter aqueous sulfuric acid was tested with stirring. Consecutive voltammograms of $1 \times 10^{-4}$ moles per liter benzophenone-3 were measured in the Britton-Robinson buffer at pH 6.0 using different activation programs between individual scans. Employed activation programs are summarized in Table 1 and corresponding differential pulse voltammograms are shown in Figure 1. The activation program had a significant influence on the peak height and repeatability of benzophenone-3. The programs *a–e* were inefficient due to lower peak heights (from 388 to 655 nanoamperes) and poor repeatability. When the program *f* was used, the peak height of benzophenone-3 was several times higher (1624 nanoamperes) and the background current was lower compared to the other activation protocols. The relative standard deviation of the benzophenone-3 peak height, when using an activation program *f*, was 4.8%. For these reasons and the relatively short time needed for electrochemical activation, the electrode surface of $BDD_A$ was activated ex-situ by the program *f* before each benzophenone-3 measurement. This activation required two minutes as described in program *f*.

**Table 1.** Activation programs for the $BDD_A$ electrode surface in 0.5 mole per liter sulfuric acid.

| Program step | Activation program | Peak height of benzophenone-3 (nanoampere) |
|---|---|---|
| *a* | Potential +3 volts for five minutes | 655 |
| *b* | Potential +3 volts for one minute | 581 |
| *c* | Potential +3 volts for forty seconds | 388 |
| *d* | Switch of potentials +3, −3, +3 volts, each for two minutes | 469 |
| *e* | Switch of potentials +3, −3, +3 volts, each for one minute | 554 |
| *f* | Switch of potentials +3, −3, +3, −3, +3 volts, each for ten seconds | 1624 |

*Note*: Differential pulse voltammograms of $1 \cdot 10^{-4}$ mole per liter benzophenone-3 in Britton-Robinson buffer at pH 6.0 were measured directly after electrochemical activation of the electrode surface.

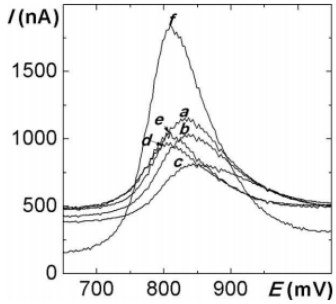


**Figure 1.** Differential pulse voltammograms of $1 \times 10^{-4}$ mole per liter benzophenone-3 at the $BDD_A$ electrode in Britton-Robinson buffer at pH 6.0 after application of activation programs a–f described in Table 1.

### *Influence of pH on differential pulse voltammograms of benzophenone-3*

The effect of pH on the current and peak potential of benzophenone-3 was measured at the $BDD_A$ (2000 parts per million) in Britton Robinson buffer with values from 2.0 to 12.0. Selected differential pulse voltammograms of $1 \times 10^{-4}$ moles per liter benzophenone-3 at various pH values are shown in Figure 2. At low pH, a gradual shift in the oxidation peak with peak potential toward more positive values was present. The slope for peak potential vs. pH dependence is 55 millivolts per pH unit, which is close to the theoretical value of 59 millivolts for the equivalent proton and electron number involved in the oxidation prior to the rate determining step. It is assumed that this oxidation corresponds to the one electron-one proton oxidation of the –OH group to the phenoxy–O· radical, which is a typical anodic process for phenolics at BDD electrodes as proposed for chlorophenols (Muna, Tasheva, and Swain 2004) or $\beta$-naphtol (Panizza and Cerisola 2003). Phenoxy radicals are responsible for the formation of a polymeric film during oxidation of phenolics due to radical-radical coupling and consequent reactions, as proposed for polymerization of the oxidation of phenol (Gattrell and Kirk 1993; Lund and Hammerich 2001). The highest peak current was observed at pH 12.0 and this value was used for further determinations.

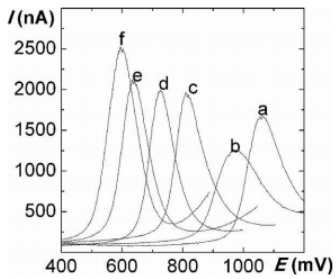


**Figure 2.** Differential pulse voltammograms of $1 \times 10^{-4}$ mole per liter benzophenone-3 at the $BDD_A$ (B/C ratio of 2000 parts per million) in Britton-Robinson buffer at pH (a) 2.0, (b) 4.0, (c) 6.0, (d) 8.0, (e) 10.0, and (f) 12.0.

### Influence of methanol and acetonitrile

Benzophenone-3 is water insoluble, but soluble in organic solvents, and thus its determination in daily care products requires dissolution with an organic solvent (Vidal et al. 2008; Laranjeira et al. 2011). The influences of methanol and acetonitrile on the peak height and peak position of benzophenone-3 were investigated. Two sets of benzophenone-3 solutions ($c = 1 \times 10^{-4}$ moles per liter) in Britton-Robinson buffer at pH 12.0 containing 1, 2, 10, 20, 50, 70, and 80% (*v/v*) of methanol and acetonitrile were prepared and measured by differential pulse voltammetry at the $BDD_A$ (2000 parts per million). The shift of peak potential toward less positive values (*ca.* 50–100 millivolts) was observed in 1% organic solvent and was independent of the concentration of methanol and acetonitrile while the peak height of benzophenone-3 decreased. With lower concentrations of methanol or acetonitrile, the decrease in peak height was approximately 10% (ca. 150 nanoamperes). In 50% methanol and 80% acetonitrile, the decrease of peak height was approximately 50%. The background current increased by ca. 250 nanoamperes from the initial value of 250 nanoamperes when the concentration of methanol was 50% or higher, and by ca. 385 nanoamperes from the initial value of 250 nanoamperes when the content of acetonitrile was 80% and more. Thus, in practical applications, the concentration of organic solvents should be minimized and hence were not employed in subsequent measurements.

### Boron concentration

A set of $BDD_A$ films with boron concentrations of 500, 1000, 2000, 4000, and 8000 parts per million were compared. The boron concentration in BDD films, given as number of boron atoms per cubic centimeter, influences the conductivity of the electrode (Holt et al. 2004; Zivcova et al. 2013). Raman spectroscopy has shown the absence of $sp^2$ impurities in the 1533 per centimeter region. Simultaneously, the symmetric Lorentzian band of the diamond phonon at 1332 per centimeter shifted to an asymmetric Fano-like lineshape and decreased to 1290 per centimeter with increasing boron concentration. Atomic force microscopy and scanning electron microscopy has shown the nanocrystallinity of the BDD film surface is independent of the boron-doping level (Vosáhlová, Zavázalová, and Schwarzová-Pecková 2014; Schwarzová-Pecková et al. submitted). Our previous study (Schwarzová-Pecková et al. submitted) revealed that for these electrodes, the limit is between films with 1000 parts per million boron exhibiting semiconductive properties and 2000 parts per million with metallic type conductivity. This is confirmed by differential pulse voltammograms of benzophenone-3, as the peak height increased with increasing boron concentration (Figure 3). For 500 and 1000 parts per million $BDD_A$, i.e., semiconductive films, the peak of benzophenone-3 was not fully developed. Films containing 2000 parts per million boron and higher had symmetric and well-shaped peaks. The peak potential of benzophenone-3 shifted to less positive values as the concentration of boron increased, similarly as reported previously with aminobiphenyls (Schwarzová-Pecková et al. submitted).

### Influence of cetyltrimethylammonium bromide

The influence of cetyltrimethylammonium bromide concentration on the benzophenone-3 peak height at $BDD_B$ electrode in Britton-Robinson buffer at pH 9.0 was studied. Figure 4A shows that the surfactant influences the shape, height, and position of the oxidation due to electrostatic interaction with benzophenone-3 in the anionic form at pH 9.0 ($pK_{a,BP\text{-}3}$

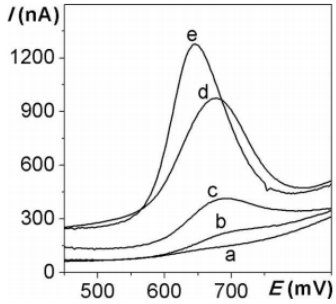


**Figure 3.** Differential pulse voltammograms of $1 \times 10^{-4}$ mole per liter benzophenone-3 at the $BDD_A$ in Britton-Robinson buffer at pH 12.0 with boron concentrations of (a) 500, (b) 1000, (c) 2000, (d) 4000, and (e) 8000 parts per million.

value 7.56). The potential shift is advantageous because the oxidation of benzophenone-3 was relatively close to the onset of supporting electrolyte in the absence of surfactant.

Because fouling of $BDD_B$ surface was observable, it was mechanically polished by alumina before each scan to provide good repeatability. The relative standard deviation was 5.0% at $1 \times 10^{-4}$ moles per liter benzophenone-3. The positive effect on the BDD electrode is evident from cyclic voltammograms (Figure 5) of a surface-sensitive redox marker $[Fe(CN)_6]^{3-/4-}$. The difference between the anodic and cathodic peak potentials $\Delta E_p$ prior and after alumina polishing decreased from 397 to 206 millivolts. Further repetitive polishing (four times for three minutes) resulted in a further decrease of $\Delta E_p$ to 114 millivolts. This positive effect of polishing on the reversibility of $[Fe(CN)_6]^{3-/4-}$ has been reported previously (McEvoy and Foord 2005; Hutton et al. 2013). A difference of 65 millivolts was reported for alumina polished microcrystalline BDD with $[B] = 1.9 \times 10^{20}$ per cubic centimeter (Hutton et al. 2013).

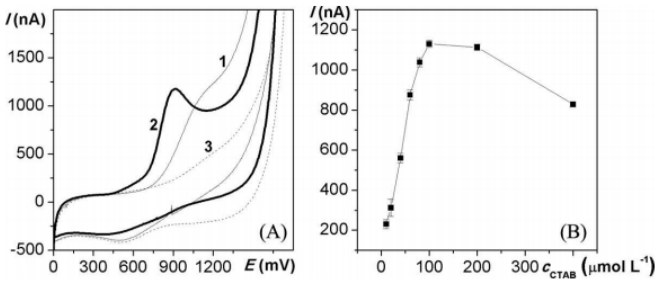


**Figure 4.** (A) Cyclic voltammograms at a scan rate of 100 milllivolts per second for $5 \times 10^{-5}$ mole per liter benzophenone-3 in the absence of surfactant (thin line 1) and in the presence of (bold 2) $1 \times 10^{-3}$ mole per liter cetyltrimethylammonium bromide at the $BDD_B$ electrode in Britton-Robinson buffer at pH 9.0 (dashed 3). (B) Dependence of peak height of $5 \times 10^{-5}$ mole per liter benzophenone-3 on the concentration of cetyltrimethylammonium bromide by differential pulse voltammetry at the $BDD_B$ electrode in 0.01 mole per liter NaOH. The error bars represent the standard deviation of the peak height of benzophenone-3.

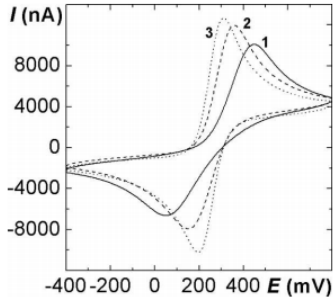


**Figure 5.** Selected cyclic voltammograms of 1 millimole per liter $[Fe(CN)_6]^{3-/4-}$ in 1 mole per liter KCl measured at the $BDD_B$ electrode at a scan rate of 100 millivolts per second. Preparation time by alumina polishing: (1) zero minutes; (2) three minutes, and (3) fifteen minutes. The third cycle is depicted.

The dependence of benzophenone-3 peak height on the concentration of cetyltrimethylammonium bromide was investigated. Differential pulse voltammograms of $5 \times 10^{-5}$ moles per liter benzophenone-3 in the presence of $1 \times 10^{-5}$ to $4 \times 10^{-4}$ moles per liter cetyltrimethylammonium bromide were measured at the $BDD_B$ electrode in 0.01 mole per liter NaOH. As shown in Figure 4B, the largest benzophenone-3 peak was obtained with $1 \times 10^{-4}$ mole per liter cetyltrimethylammonium bromide.

### *Effect of concentration*

The calibration of 1–100 micromoles per liter benzophenone-3 in the absence of surfactant was measured at the $BDD_A$ with boron concentrations of 2000, 4000, and 8000 parts per million. For 500 and 1000 parts per million BDD films, the lowest detectable concentration was 100 micromoles per liter and these preparations were not analytically useful. At the higher boron concentrations, a linear calibration range was observed. Differential pulse

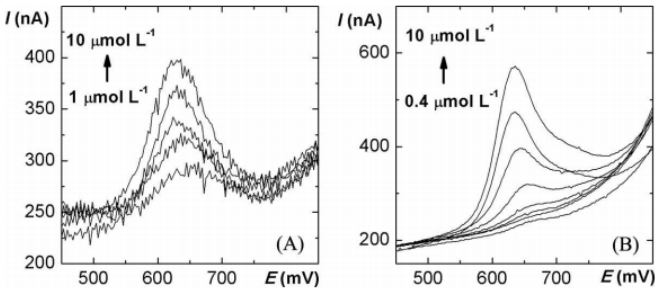


**Figure 6.** (A) Differential pulse voltammograms of benzophenone-3 at the $BDD_A$ electrode (2000 parts per million boron) in Britton-Robinson buffer at pH 12.0 in the absence of cetyltrimethylammonium bromide. Concentrations of benzophenone-3: 1.0, 2.5, 5.0, 7.5, and 10 micromoles per liter. (B) Differential pulse voltammograms of benzophenone-3 at the $BDD_B$ electrode in 0.01 micromole per liter NaOH in the presence of $1 \times 10^{-4}$ mole per liter cetyltrimethylammonium bromide. Concentration of benzophenone-3: 0.4, 0.6, 0.8, 1.0, 2.5, 5.0, 7.5, and 10 micromoles per liter.

**Table 2.** Analytical figures of merit for benzophenone-3 at the BDD electrodes by differential pulse voltammetry.

| Electrode | Linear dynamic range (micromole per liter) | Slope (nanoampere per micromole liter) | Intercept (nanoampere) | Correlation coefficient | Limit of detection (micromole per liter) |
|---|---|---|---|---|---|
| $BDD_A$ 2000 parts per million | 1–100 | 13.48 | 20.57 | 0.9981 | 1.5 |
| $BDD_A$ 4000 parts per million | 1–100 | 5.90 | 12.28 | 0.9980 | 1.9 |
| $BDD_A$ 8000 parts per million | 2.5–100 | 9.34 | 6.19 | 0.9976 | 0.8 |
| $BDD_B$ (+CTAB) | 10–75 | 18.98 | 129.65 | 0.9956 | – |
| | 0.8–10 | 29.85 | −19.44 | 0.9982 | – |
| | 0.4–0.8 | 13.29 | −1.35 | 0.9995 | 0.1 |

voltammograms are depicted in Figure 6A and calibration parameters are in Table 2. The limits of detection were 1.5, 1.9, and 0.8 micromoles per liter for 2000, 4000, and 8000 parts per million boron at the $BDD_A$ electrode, respectively.

The dependence of benzophenone-3 in the presence of $1 \times 10^{-4}$ moles per liter cetyltrimethylammonium bromide was measured at the $BDD_B$ from 0.4 to 100 micromoles per liter with a sigmoidal shape with three linear concentration ranges: 0.4–0.8, 0.8–10, and 10–75 micromoles per liter. These parameters are summarized in Table 2 and differential pulse voltammograms are shown in Figure 6B. A limit of detection of 0.1 micromoles per liter was obtained. The sigmoidal shape of calibration dependence has been previously reported for other compounds at the electrode surface (Peckova et al. 2007), demonstrating the adsorption of the benzophenone 3 associated with cetyltrimethylammonium bromide by electrostatic interaction.

## Conclusions

The influence of boron concentration in BDD films on anodic oxidation of benzophenone 3 and possibilities to influence its electroanalytical performance by the presence of cationic surfactant cetyltrimethylammonium bromide were investigated in this study. The oxidation of benzophenone-3 led to passivation of the electrode surface, as expected for phenolic species due to the formation of polymeric films. Thus, ex-situ anodic activation in acidic media or mechanical polishing by alumina was applied to ensure repeatability of the signals. Using differential pulse voltammetry in Britton-Robinson buffer at pH 12.0., the peak height of benzophenone-3 increased with boron concentration in the BDD films (deposited at 500–8000 parts per million B/C ratio in gaseous phase), and limits of detection of 1.5, 1.9, and 0.8 micromoles per liter were achieved for 2000, 4000, and 8000 parts per million boron. Semiconductive 500 and 1000 parts per million boron BDD films exhibited insufficient sensitivity for electroanalytical purposes.

Cetyltrimethylammonium bromide had a positive effect on the determination of benzophenone-3 due to the mutual electrostatic based interaction and increased adsorption at the electrode surface. The sensitivity was increased, the peak potential shifted to less positive values, and the limit of detection was 0.1 micromoles per liter: roughly an order of magnitude smaller than without a surfactant. To conclude, this study confirms that the boron concentration and the presence of cationic surfactant significantly influenced the analytical oxidation of benzophenone-3. The results of this study will be used for the

analysis of urine, wastewater, and sunscreen with sample preparation by solid phase extraction high-performance liquid chromatography prior to electroanalytical determination.

## Acknowledgments

The authors acknowledge Dr. Václav Petrák from Institute of Physics of the ASCR, v. v. i., Department of Functional Materials for providing boron-doped diamond films.

## Funding

The research was financially supported by the Grant Agency of the Charles University in Prague (Project GAUK 684213) and Charles University in Prague (project SVV).

## References

Bluthgen, N., S. Zucchi, and K. Fent. 2012. Effects of the UV filter benzophenone-3 (oxybenzone) at low concentrations in zebrafish (*Danio rerio*). *Toxicology and Applied Pharmacology* 263: 184–94. doi:10.1016/j.taap.2012.06.008

Cardoso, J. C., B. M. L. Armondes, J. B. Galindo, and V. S. Ferreira. 2008. Simultaneous electrochemical determination of three sunscreens using cetyltrimethylammonium bromide. *Colloids and Surfaces B: Biointerfaces* 63: 34–40. doi:10.1016/j.colsurfb.2007.11.001

Cizek, K., J. Barek, J. Fischer, K. Peckova, and J. Zima. 2007. Voltammetric determination of 3-nitrofluoranthene and 3-aminofluoranthene at boron doped diamond thin-film electrode. *Electroanalysis* 19: 1295–99. doi:10.1002/elan.200603851

Fujishima, A., Y. Einaga, T. N. Rao, and D. A. Tryk. 2005. *Diamond electrochemistry*. Amsterdam, The Netherlands: Elsevier.

Gattrell, M., and D. W. Kirk. 1993. A study of the oxidation of phenol at platinum and preoxidized platinum surfaces. *Journal of The Electrochemical Society* 140: 1534–40. doi:10.1149/1.2221598

Gonzalez, H., A. Farbrot, O. Larko, and A.-M. Wennberg. 2006. Percutaneous absorption of the sunscreen benzophenone-3 after repeated whole-body applications, with and without ultraviolet irradiation. *British Journal of Dermatology* 154: 337–40. doi:10.1111/j.1365–2133.2005.07007.x

Holt, K. B., A. J. Bard, Y. Show, and G. M. Swain. 2004. Scanning electrochemical microscopy and conductive probe atomic force microscopy studies of hydrogen-terminated boron-doped diamond electrodes with different doping levels. *The Journal of Physical Chemistry B* 108: 15117–27. doi:10.1021/jp048222x

Hutton, L. A., J. G. Iacobini, E. Bitziou, R. B. Channon, M. E. Newton, and J. V. Macpherson. 2013. Examination of the factors affecting the electrochemical performance of oxygen-terminated polycrystalline boron-doped diamond electrodes. *Analytical Chemistry* 85: 7230–40. doi:10.1021/ac401042 t

Iniesta, J., P. A. Michaud, M. Panizza, G. Cerisola, A. Aldaz, and C. Comninellis. 2001. Electrochemical oxidation of phenol at boron-doped diamond electrode. *Electrochimica Acta* 46: 3573–78. doi:10.1016/S0013-4686(01)00630-2

Kim, S., and K. Choi. 2014. Occurrences, toxicities, and ecological risks of benzophenone-3, a common component of organic sunscreen products: a mini-review. *Environment International* 70: 143–57. doi:10.1016/j.envint.2014.05.015

Kim, S., D. Jung, Y. Kho, and K. Choi. 2014. Effects of benzophenone-3 exposure on endocrine disruption and reproduction of Japanese medaka (*Oryzias latipes*) – a two generation exposure study. *Aquatic Toxicology* 155: 244–52. doi:10.1016/j.aquatox.2014.07.004

Laranjeira, M. T., F. de Lima, S. C. de Oliveira, V. S. Ferreira, and R. T. S. de Oliveira. 2011. Analytical determination of benzophenone-3 in sunscreen preparations using boron-doped diamond electrodes. *American Journal of Analytical Chemistry* 2: 383–91. doi:10.4236/ajac.2011.23047

Levent, A., A. Altun, Y. Yardim, and Z. Senturk. 2014. Sensitive voltammetric determination of testosterone in pharmaceuticals and human urine using a glassy carbon electrode in the presence of cationic surfactant. *Electrochimica Acta* 128: 54–60. doi:10.1016/j.electacta.2013.10.024

Levent, A., Y. Yardim, and Z. Senturk. 2009. Voltammetric behavior of nicotine at pencil graphite electrode and its enhancement determination in the presence of anionic surfactant. *Electrochimica Acta* 55: 190–95. doi:10.1016/j.electacta.2009.08.035

Levent, A., Y. Yardim, and Z. Senturk. 2014. Electrochemical performance of boron-doped diamond electrode in surfactant-containing media for ambroxol determination. *Sensors and Actuators B: Chemical* 203: 517–26.

Lund, H., and O. Hammerich. 2001. *Organic electrochemistry, fourth edition, revised and expanded*. New York, NY: Marcel Dekker.

McEvoy, J. P., and J. S. Foord. 2005. Direct electrochemistry of blue copper proteins at boron-doped diamond electrodes. *Electrochimica Acta* 50: 2933–41. doi:10.1016/j.electacta.2004.11.043

Molina-Molina, J.-M., A. Escande, A. Pillon, E. Gomez, F. Pakdel, V. Cavailles, N. Olea, S. Ait-Aissa, and P. Balaguer. 2008. Profiling of benzophenone derivatives using fish and human estrogen receptor-specific in vitro bioassays. *Toxicology and Applied Pharmacology* 232: 384–95. doi:10.1016/j.taap.2008.07.017

Muna, G. W., N. Tasheva, and G. M. Swain. 2004. Electro-oxidation and amperometric detection of chlorinated phenols at boron-doped diamond electrodes: a comparison of microcrystalline and nanocrystalline thin films. *Environmental Science & Technology* 38: 3674–82. doi:10.1021/es034656e

Panizza, M., and G. Cerisola. 2003. Influence of anode material on the electrochemical oxidation of 2-naphthol: part 1. Cyclic voltammetry and potential step experiments. *Electrochimica Acta* 48: 3491–97. doi:10.1016/S0013-4686(03)00468-7

Peckova, K., F. H. Ayyildiz, M. Topkafa, H. Kara, M. Ersoz, and J. Barek. 2007. Polarographic and voltammetric determination of trace amounts of 2-aminoanthraquinone. *Chemia Analyticzna (Warsaw)* 52: 989–1001.

Peckova, K., and J. Barek. 2011. Boron doped diamond microelectrodes and microelectrode arrays in organic electrochemistry. *Current Organic Chemistry* 15: 3014–28. doi:10.2174/138527211798357164

Peckova, K., V. Mocko, F. Opekar, G. M. Swain, J. Zima, and J. Barek. 2006. Miniaturized amperometric detectors for HPLC and capillary zone electrophoresis. *Chemicke Listy* 100: 124–32.

Peckova, K., J. Musilova, and J. Barek. 2009. Boron-doped diamond film electrodes – new tool for voltammetric determination of organic substances. *Critical Reviews in Analytical Chemistry* 39: 148–72. doi:10.1080/10408340903011812

Razak, O. A., A. A. Gazy, and A. M. Wahbi. 2002. Polarographic determination of phenytoin and benzophenone (as impurity) in pharmaceutical preparations. *Journal of Pharmaceutical and Biomedical Analysis* 28: 613–19. doi:10.1016/S0731-7085(01)00669-0

SCCP (Scientific Committee on Consumer Products). 2008. Opinion on benzophenone-3. 16 December. http://ec.europa.eu/health/ph_risk/committees/04_sccp/docs/sccp_o_159.pdf (accessed October 28, 2014).

Schwarzová-Pecková, K., J. Zavazalová, J. Vosáhlová, I. Šloufová, E. Pawlova, and V. Petrák. Submitted. Influence of boron concentration on spectral and electroanalytical characteristics of anodically oxidized boron-doped diamond electrodes. *Electrochimica Acta*.

Suzuki, T., S. Kitamura, R. Khota, K. Sugihara, N. Fujimoto, and S. Ohta. 2005. Estrogenic and anti-androgenic activities of 17 benzophenone derivatives used as UV stabilizers and sunscreens. *Toxicology and Applied Pharmacology* 203: 9–17. doi:10.1016/j.taap.2004.07.005

Vidal, L., A. Chisvert, A. Canals, E. Psillakis, A. Lapkin, F. Acosta, K. J. Edler, J. A. Holdaway, and F. Marken. 2008. Chemically surface-modified carbon nanoparticle carrier for phenolic pollutants: extraction and electrochemical determination of benzophenone-3 and triclosan. *Analytica Chimica Acta* 616: 28–35. doi:10.1016/j.aca.2008.04.011

Vosáhlová, J., J. Zavázalová, and K. Schwarzová-Pecková. 2014. Boron doped diamond electrode: influence of boron concentration on determination of 2-aminobiphenyl. *Chemicke Listy* 108: s270–73.

Williams, A. W. S., E. C. Lightowlers, and A. T. Collins. 1970. Impurity conduction in synthetic semiconducting diamond. *Journal of Physics C: Solid State Physics* 3: 1727–35. doi:10.1088/0022–3719/3/8/011

Yardim, Y. 2011. Sensitive detection of capsaicin by adsorptive stripping voltammetry at a boron-doped diamond electrode in the presence of sodium dodecylsulfate. *Electroanalysis* 23: 2491–97. doi:10.1002/elan.201100275

Yardim, Y. 2012. Electrochemical behavior of chlorogenic acid at a boron-doped diamond electrode and estimation of the antioxidant capacity in the coffee samples based on its oxidation peak. *Journal of Food Science* 77: C408–C413. doi:10.1111/j.1750–3841.2011.02609.x

Yardim, Y., A. Levent, E. Keskin, and Z. Senturk. 2011. Voltammetric behavior of benzo[a]pyrene at boron-doped diamond electrode: a study of its determination by adsorptive transfer stripping voltammetry based on the enhancement effect of anionic surfactant, sodium dodecylsulfate. *Talanta* 85: 441–48. doi:10.1016/j.talanta.2011.04.005

Yardim, Y., and Z. Senturk. 2011. Voltammetric behavior of indole-3-acetic acid and kinetin at pencil-lead graphite electrode and their simultaneous determination in the presence of anionic surfactant. *Turkish Journal of Chemistry* 35: 413–26. doi:10.3906/kim-1011-805

Zavazalova, J., H. Dejmkova, J. Barek, and K. Peckova. 2013. Voltammetric and amperometric determination of mixtures of aminobiphenyls and aminonaphthalenes using boron doped diamond electrode. *Electroanalysis* 25: 253–62. doi:10.1002/elan.201200424

Zivcova, Z. V., O. Frank, V. Petrak, H. Tarabkova, J. Vacik, M. Nesladek, and L. Kavan. 2013. Electrochemistry and in situ raman spectroelectrochemistry of low and high quality boron doped diamond layers in aqueous electrolyte solution. *Electrochimica Acta* 87: 518–25. doi:10.1016/j.electacta.2012.09.031

# Appendix VII

*Publication 7*

Monatsh Chem (2016) 147:21–29
DOI 10.1007/s00706-015-1621-6

ORIGINAL PAPER

## Factors influencing voltammetric reduction of 5-nitroquinoline at boron-doped diamond electrodes

**Jana Vosáhlová[1] · Jaroslava Zavázalová[1] · Václav Petrák[2,3] · Karolina Schwarzová-Pecková[1]**

Received: 17 September 2015 / Accepted: 24 November 2015 / Published online: 14 December 2015


**Abstract** The voltammetric signal of 5-nitroquinoline with reducible nitro and quinoline moieties largely depends on the pH of the indifferent electrolyte, electrode pretreatment, activation between individual scans, and boron concentration of the BDD film electrode. Anodic pretreatment at +2.4 V for 5 min in 0.5 mol $dm^{-3}$ $H_2SO_4$ and 20 s stirring between individual scans assured repeatable signals of nitro group in the whole pH range 2.0–12.0; in acetate buffer pH 5.0 limit of detection is $2 \times 10^{-7}$ mol $dm^{-3}$ for differential pulse voltammetry. The reduction of quinoline skeleton is visible in the pH range of 6.0–11.0. Presence of oxygen in the measured solutions led to slight increase of peak heights and acceptable increase of its relative standard deviation. BDD films with metallic type of conductivity deposited at B/C ratio 2000–8000 ppm exhibit faster electron transfer at lower potential for nitro group reduction than semiconductive films 500 and 1000 ppm.

✉ Karolina Schwarzová-Pecková
kpeckova@natur.cuni.cz

1 Charles University in Prague, Faculty of Science, Department of Analytical Chemistry, UNESCO Laboratory of Environmental Electrochemistry, Albertov 6, CZ-12843 Prague 2, Czech Republic

2 Department of Functional Materials, Institute of Physics ASCR, v.v.i., Na Slovance 2, 18221 Prague 8, Czech Republic

3 Faculty of Biomedical Engineering, Czech Technical University in Prague, Sítná 3105, 272 01 Kladno, Czech Republic

*Graphical abstract*

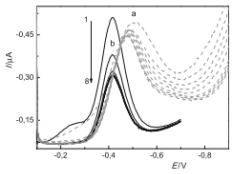


**Keywords** Voltammetry · Boron-doped diamond electrode · Boron concentration · Reduction · Electrochemistry

### Introduction

Boron doped diamond introduced for electroanalysis in 1992 [1] gained a deserved popularity especially for electrooxidation of organic compounds of biological, pharmaceutical, and environmental significance [2–5]. Its mechanical and electrochemical properties are among others significantly influenced by morphology of the BDD films, boron concentration, and electrode pretreatment, when high positive/negative current densities or potentials (Correctly ≥±2.0 V) in the region of water decomposition reactions are applied for few seconds to minutes. As results of this anodic/cathodic pretreatment, oxygen-terminated (O-BDD) or hydrogen-terminated (H-BDD) surfaces are produced, very often with different capabilities of prevention of surface passivation, enhancement of the voltammetric signals, and ensuring of repeatable and reproducible response of particular analytes [6–9].

Boron-doping level plays crucial role in basic electrochemical characteristics, e.g., electrical conductivity of the BDD film and kinetics of electron transfer [1, 7, 10]. The few studies concerned with influence of boron concentration on electroanalytical parameters for organic compounds [11, 12] including our reports on oxidation of benzophenone-3 [13] and 2-aminonaphthalene [14] report that semiconductive films exhibit more sluggish kinetics for surface-sensitive redox marker $[Fe(CN)_6]^{3-/4-}$ as well as decreased sensitivity towards mentioned analytes than metallic films. The predicted threshold for the semiconductive/metallic transition is at $\sim 2 \times 10^{20}$ boron atoms per $cm^3$ [15] (theoretical value), i.e. $\sim$1000–2000 ppm (experimental values) [14, 16, 17], which is the B/C ratio in the gaseous phase during the chemical vapour deposition of BDD films.

It can be traced in reviews [2–4] and monographs [5, 9] devoted to electroanalysis of organic compounds by means of BDD-based electrodes that lower attention has been paid to their utilization for electrochemical reductions despite the favorable characteristic for such applications: relatively wide potential window in the cathodic region and low sensitivity towards oxygen evolution [18, 19]. Among organic reducible compounds, substances containing nitro group at the aromatic skeleton represent an extensive group, where pharmaceuticals, agrochemicals, and environmental pollutants are present. Most of them are toxic, probably due to a reactive nitro-radical in their metabolic pathway [20, 21].

The few determinations based on nitro group reduction at BDD-based materials were suggested for some nitrophenols [22–26] and aminonitrophenols [27], and nitrogroup containing pesticides (methylparathion [28]), drugs (chloramphenicol [29], nitrofurazone [30, 31], selected benzazepines [32]), and derivatives of polycyclic aromatic hydrocarbons (1-nitropyrene [33], 3-nitrofluoranthene [35]).The reduction of nitro group has been investigated among the first electrochemical processes of organic compounds at dropping mercury and other mercury electrodes [20, 35, 36], later on it was extended on solid electrodes including carbon and amalgam based electrodes [20, 37]. In aqueous acidic and neutral media, independently on the electrode material, the first step of the reduction relies on the four-electron reduction of nitro group to the hydroxylamino group [Eq. (1)]. In acidic media, further two-electron reduction to amine may occur (Eq. 2) [35, 36, 40].

$$ArNO_2 + 4e^- + 4H^+ \rightarrow ArNHOH + H_2O \quad (1)$$

$$ArNHOH + 2e^- + 2H^+ \rightarrow ArNH_2 + H_2O \quad (2)$$

At mercury-based electrodes and solid electrodes, in the alkaline or non-aqueous media the lack of protons may lead to a split of the original four-electron reduction described in Eq. (1) and two reductive signals corresponding to Eqs. (3) and (4), also leading to hydroxylamine as the final product can be observed [36, 37, 40].

$$ArNO_2 + e^- \leftrightarrow ArNO_2^- \quad (3)$$

$$ArNO_2^- + 3e^- + 4H^+ \rightarrow ArNHOH + H_2O \quad (4)$$

Compared to the reduction of the nitro group, the reduction of the quinoline skeleton proceeds at more negative potentials, close to the onset of supporting electrolyte [38, 39]. Quinoline (Q) itself is polarographically reducible in two steps in alkaline media according to Eq. (5) and (6) yielding dihydroquinoline ($QH_2$) in the first step [Eq. (5)] and tetrahydroquinoline ($QH_4$) in the second one [Eq. (6)] [38, 41]:

$$Q + 2e^- + 2H^+ \rightarrow QH_2 \quad (5)$$

$$QH_2 + 2e^- + 2H^+ \rightarrow QH_4 \quad (6)$$

Also electrooxidation of the quinoline skeleton is relatively hardly achievable [42, 43] and thus there are not many studies devoted to utilization of these processes in voltammetry. Modification of electrode surface [42, 43] or presence of surfactant [39] was tested to afford results utilizable in electroanalysis.

The aim of this study is to extend the knowledge on the electro reduction of aromatic nitro group and quinoline skeleton at BDD electrodes. For this purpose, an environmental pollutant, formed as product of incomplete combustion of fossil fuels, 5-nitroquinoline was selected as model compound [38, 45]. It was previously studied in our laboratory at mercury, amalgam-based and carbon film electrodes, as obvious from the overview in Table 1 summarizing voltammetric methods used for determination of 5-nitroquinoline [38, 44, 45]. In this study, special attention has been paid to the influence of BDD electrode pretreatment, boron-doping level, and oxygen presence on voltammetric signal of 5-nitroquinoline to present the variety of specific factors influencing voltammetric analysis at BDD electrodes.

## Results and discussion

### Mechanism of reduction of 5-nitroquinoline

The mechanism of reduction of 5-nitroquinoline was studied using pH dependence in BR buffer of pH 2.0–12.0 using DC and DP voltammetry and further by cyclic voltammetric experiments. As relatively extended literature exists on the mechanism of reduction of nitro group at aromatic skeleton at liquid mercury and solid electrodes

**Table 1** Overview of voltammetric methods for the determination of 5-nitroquinoline

| Electrode | LOQ/μmol dm$^{-3}$ | LDR/μmol dm $^{-3}$ | Method | pH, medium | References |
|---|---|---|---|---|---|
| m-AgSAE | 0.3 | 0.2–100 | DPV | pH 9.0; 0.05 mol dm$^{-3}$ borate buffer | [46] |
| | 0.5 | 0.4–100 | DCV | | |
| Carbon film | 0.5 | –[a] | DPV | pH 11.0, BR buffer | [44] |
| DME | 0.9 | –[a] | DCTP | pH 3.0, BR buffer | [45] |
| | 0.09 | –[a] | DPP | pH 3.0, BR buffer | |
| | 0.01 | –[a] | DPP | 0.2 mol dm$^{-3}$ NaOH | |
| HMDE | 0.02 | –[a] | DPV | 0.2 mol dm$^{-3}$ NaOH | |

*DCTP* direct current tast polarography, *DCV* direct current voltammetry, *DPV/P* differential pulse voltammetry/polarography, *DME* dropping mercury electrode, *HMDE* hanging mercury drop electrode, *m-AgSAE* mercury meniscus-modified silver solid amalgam electrode, *LDR* linear dynamic range, *LOQ* limit of quantification

[a] Not given

[20, 35–37], analogies and differences could be found in the behavior of the studied compound.

### DP and DC voltammetry–influence of pH

Figure 1a, b represents pH-dependence of DC and DP voltammograms of 5-nitroquinoline. Relatively well-shaped main reduction signal can be traced in the whole pH range tested (2.0–12.0), with the slope of the peak potential $E_p$ vs. pH dependence of −83.52 mV between pH 2.0–5.0. It corresponds to the nitro group reduction to hydroxylamine according to Eq. (1). This signal is accompanied by indistinctive signals at more negative potential at pH values 6.0–12.0, as obvious from peak potential $E_p$ vs. pH dependence at Fig. 2a. These are of different origins:

1. For the most alkaline media 11.0 and 12.0 the splitting of the nitro-group reduction into two steps according to Eqs. (3) and (4) is foreseen, the reduction peaks of both processes lay within a narrow potential region of 250 mV. Thus, the first, pH-independent step corresponds to a fast one electron reduction of the nitro group to a nitro radical [Eq. (3)] and the second step

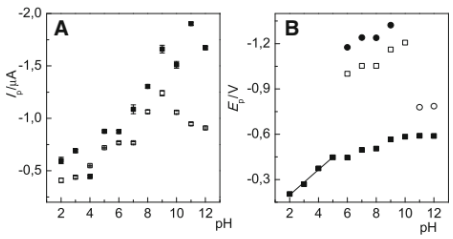


**Fig. 2** Dependence of the **a** peak currents ($I_p$) of the first cathodic peak in the presence (*closed square*) and absence (*open square*) of oxygen and dependence of the **b** peak potentials ($E_p$) on pH. Measured for 5-nitroquinoline ($c = 1\times10^{-4}$ mol dm$^{-3}$) using DP voltammetry. The *error bars* are constructed as standard deviations ($n = 5$)

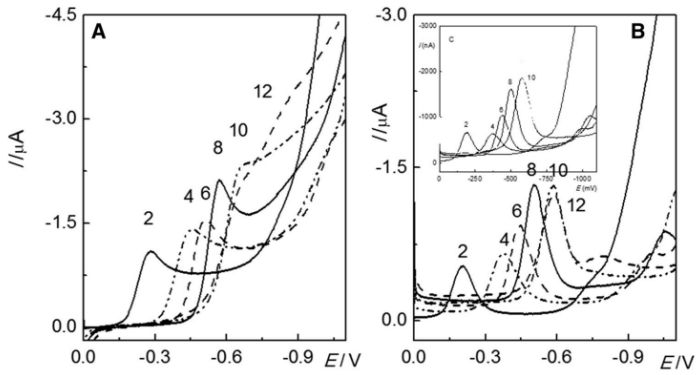


**Fig. 1** Selected **a** DC, **b** DP voltammograms of 5-nitroquinoline ($c = 1 \times 10^{-4}$ mol dm$^{-3}$) at BDD electrode ($B/C = 4000$ ppm) in BR buffer pH 2.0–12.0; the pH values are noted by the curves. The *inset* (**c**) in (**b**) shows DP voltammograms in the presence of oxygen. Scan rate for DPV is 20 mV s$^{-1}$ and for DCV is 50 mV s$^{-1}$

corresponds to the three electron reduction of the nitro radical to the hydroxylamine [Eq. (4)]. This type of splitting of the main reduction peak was described for example for reduction of 5-nitroquinoline and 6-nitroquinoline [38] and nitronaphtalenes [37] at amalgam electrodes. Generally it occurs when the transfer of the second electron in the overall four-electron reduction [Eq. (1)] is inhibited, as e.g., in non-aqueous media or surfactant containing media at mercury electrodes [20, 36] or at solid electrodes in alkaline media [37], including BDD electrode [30, 31], where the rate of electron transfer is diminished by the solid character of the electrode surface and simultaneously the lack of protons influences the reaction pathway. Clearly the surface of BDD electrodes has the same inhibiting effect on nitro group reduction of 5-nitroquinoline in alkaline media as other solid electrode materials. Nevertheless, this reduction splitting of aromatic nitro group cannot be assessed as general rule at BDD electrodes, because in previous reports on reduction of 3-nitrofluoranthene [34], formation of $ArNO_2^{\bullet -}$ was not reported and its stabilization is obviously connected to boron-doping level and other factors influencing electrochemical properties of BDD surface, and further content of organic cosolvent, and structure of the aromatic compound itself [30, 31].

2. In BR buffer pH 5.0–10.0 two pH-dependent signals at far negative potentials of ca −1000 to −1250 mV were observed. To confirm whether these signals can be assigned to the reduction of the quinoline skeleton, the reduction of quinoline has been investigated under the same conditions. An example of DP voltammogram of quinoline in BR buffer pH 9.0 is given in Fig. 3. It shows one reduction peak at the potential of −1183 mV while the curve of 5-nitroquinoline shows two steps reduction at the potentials of −1117 and −1255 mV, presumably corresponding to processes described in Eqs. (2) and (5): The reduction of the quinoline skeleton [Eq. (5)] is preceded by reduction of the hydroxylamino derivative to 5-aminoquinoline [Eq. (2)]. The latter reaction is enabled by stabilization of the product of dehydration of the hydroxylamine intermediate through resonance structures involving heterocyclic nitrogen. This pathway was found for several heterocyclic nitro derivatives [36, 40], nevertheless is not common for nitro derivatives of polycyclic aromatic hydrocarbons, which undergo reduction to the amino derivative only in acidic media [36]. The peak corresponding to reduction of the quinoline skeleton is characterized by $dE_p/dpH$ value of 52.2 mV in pH range 6.0–10.0, which is close to the theoretical value of 59 mV for an electrochemical reaction with equal number of protons and electrons, in accordance with Eq. (5). At these pH values the quinoline skeleton is not protonized ($pK_A$ of 5-nitroquinoline is 2.73) [46]. The reduction of quinoline skeleton does not appear in the range of pH 2.0–5.0 of BR buffer at BDD electrode probably due to shorter potential window in acidic media for BDD electrode.

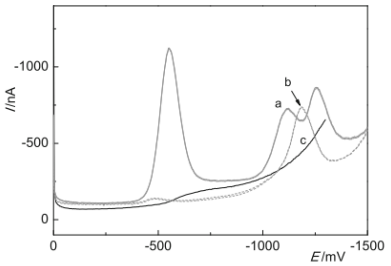


**Fig. 3** DP voltammograms (scan rate 20 mV $s^{-1}$) of 5-nitroquinoline (**a**) and quinoline (**b**) (for both $c = 1 \times 10^{-4}$ mol $dm^{-3}$) in BR buffer medium pH 9.0 (**c**)

These two reduction peaks at the end of potential window appeared also in voltammograms of 5-nitroquinoline at meniscus modified silver solid amalgam electrode in pH range 7.0–12.0 [38].

Furthermore, the influence of oxygen presence on the peak height and repeatability of 5-nitroquinoline reduction was investigated in solutions open to air in all pH range tested. Obviously oxygen reduction is inhibited at BDD electrode and the potential of the first cathodic reduction peak is in the range from ca −450 mV to −750 mV, i.e. in the region of reduction of 5-nitroquinoline. As expected, the DP voltammograms (Fig. 1b) of oxygen-free solution exhibit of about 10–30 % lower current response in the presence of 5-nitroquinoline than these when oxygen is present (DP voltammograms at Fig. 1c, evaluation of peak heights at Fig. 2a). This effect is mostly pronounced in alkaline media, but importantly, the peak height repeatability is not affected and remains acceptable for all investigated media, mostly in the range from 0.7 to 3.3 % for DPV with oxygen, and from 0.8 to 4.5 % for DPV without oxygen. For DCV higher values with maximum of 7.1 % with oxygen and 6.5 % without oxygen were achieved (relative standard deviation evaluated from five measurements). These results are promising for determination of electrochemically reducible organic compounds by means of BDD-based sensors in the presence of oxygen. This could be very advantageous from the analytical point of view because oxygen removal from solutions might be problematic and its traces cause problems e.g. when using electrochemical detection at mercury-based electrochemical sensors in liquid flow techniques [38, 47, 48].

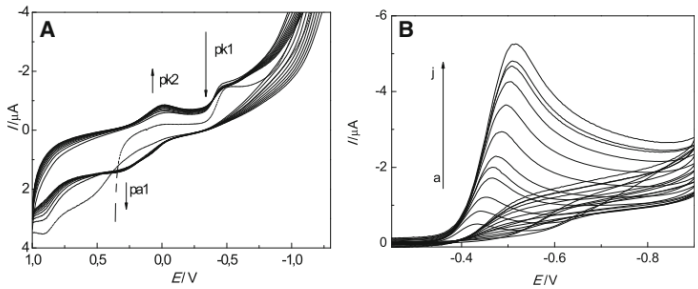


**Fig. 4** Cyclic voltammograms of 5-nitroquinoline ($c = 1 \times 10^{-4}$ mol dm$^{-3}$) in 0.1 mol dm$^{-3}$ acetate buffer pH 5.0: **a** ten consecutive cycles from +1.0 V to −1.3 V with the first cathodic scan starting at +0.36 V (*dashed line*), scan rate 100 mV s$^{-1}$, and **b** the first cycle for scan rates (mV s$^{-1}$): 5 (*a*), 10 (*b*), 20 (*c*), 40 (*d*), 80 (*e*), 160 (*f*), 320 (*g*), 640 (*h*), 1280 (*ch*), 2560 (*i*), 5120 (*j*)

Further measurements were performed in 0.1 mol dm$^{-3}$ acetate buffer pH 5.0; in this media only the main reduction signal corresponding to Eq. (1) is present.

### Cyclic voltammetry

Cyclic voltammograms in 0.1 mol dm$^{-3}$ acetate buffer pH 5.0 exhibited features typical for electrochemical reduction of aromatic nitro group (Fig. 4a). It is the main irreversible cathodic peak $p_{k1}$, corresponding to nitro group reduction to hydroxylamine [Eq. (1)], followed by the pair of peaks $p_{a1}$ and $p_{k2}$ in the reversed anodic/second cathodic scan at the potentials of ca +300 and 0 mV, corresponding to quasireversible oxidation/reduction of the pair hydroxylamino/nitroso derivative [Eq. (7); $p_{a1}$ and $p_{k2}$ in Fig. 4a]. This suggestion is confirmed by the fact that the cathodic peak $p_{k2}$ is absent in the first cathodic scan, similarly, the anodic peak $p_{a1}$ is absent when starting the scan at 0 V in positive direction. The behavior is in agreement with literature [40].

$$\mathrm{ArNHOH} \leftrightarrow \mathrm{ArNO} + 2e^- + 2H^+ \quad (7)$$

Further cycling leads to decrease of $p_{k1}$ and increase of $p_{a1}$ and $p_{k2}$ as result of surface passivation ($p_{k1}$) and formation of reaction products ($p_{a1}$ and $p_{k2}$). The main reaction–reduction of nitro group to hydroxylamine [Eq. (1)] is controlled by diffusion as proved by linear course of the peak current $I_p$ vs. scan rate $v^{1/2}$ dependence in the range from 10 to 80 mV s$^{-1}$ characterized by the regression line: $I_p/\mathrm{nA} = -257.3v^{1/2}/(\mathrm{mV\ s^{-1}}) + 2.8$ ($R = 0.996$); corresponding voltammograms are depicted at Fig. 4b.

### Pretreatment of BDD electrode and calibration dependences of 5-nitroquinoline

Optimal combination of electrode pretreatment and activation between individual scans was tested in 0.1 mol dm$^{-3}$ acetate buffer pH 5.0 with BDD electrode

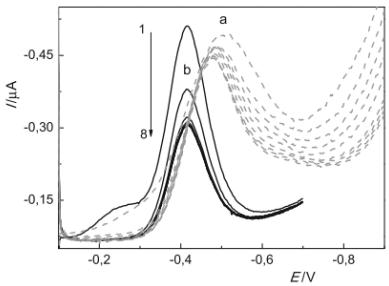


**Fig. 5** Eight differential pulse voltammograms of 5-nitroquinoline ($c = 1 \times 10^{-4}$ mol dm$^{-3}$) in 0.1 mol dm$^{-3}$ pH 5.0 acetate buffer using different pretreatment of the electrode in 0.5 mol dm$^{-3}$ sulfuric acid with positive or negative potential: **a** anodic pretreatment (5 min, +2.4 V), **b** cathodic pretreatment (10 min, −2.4 V). The scan rate was 20 mV s$^{-1}$

(B/C 4000 ppm). Anodic pretreatment at the potential of +2.4 V for 5 min and cathodic pretreatment at the potential of −2.4 V for 10 min in 0.5 mol dm$^{-3}$ sulfuric acid and three types of activation between individual scans directly in the measured solution were tested: anodic activation, cathodic activation, and stirring without application of potential. It was necessary because without any activation the signal height of 5-nitroquinoline is decreasing as obvious from Fig. 5: For eight consecutive scans, anodic pretreatment exhibits faster stabilization of electrode response and ca 100 mV more negative peak potential than the cathodic pretreatment with a fast decline in peak height for the first three scans. This decline is caused by instability of the H-terminated surface resulting from cathodic pretreatment; that surface is known to be relatively unstable not only in solutions, but also in air [49].

Thus, the activation between individual scans was also necessary. For all activation modes relative stability of electrode response was achieved, but as the application of cathodic or anodic potential had no explicitly positive

**Table 2** Parameters of the calibration straight lines and limits of detection and quantification for the reductive determination of 5-nitroquinoline using DC and DP voltammetry with anodic ($E = +2.4$ V, $t = 5$ min) or cathodic ($E = -2.4$ V, $t = 10$ min) pretreated BDD electrode (B/C 4000 ppm)

| BDD pretreatment | LDR/μmol dm$^{-3}$ | $R$ | Slope/nA dm$^3$ μmol$^{-1}$ | Intercept/nA | RSD (%)[a] | LOQ/μmol dm$^{-3}$ | LOD/μmol dm$^{-3}$ |
|---|---|---|---|---|---|---|---|
| DPV | | | | | | | |
| Anodic | 0.5–100 | 0.988 | −6.02 ± 0.06 | −4.1 ± 0.2 | 6.5 | 0.66 | 0.20 |
| Cathodic | 0.5–75 | 0.996 | −4.59 ± 0.05 | −10.4 ± 0.7 | 12 | 1.68 | 0.50 |
| DCV | | | | | | | |
| Anodic | 10–100 | 0.997 | −9.73 ± 0.12 | 24.1 ± 6.4 | 10 | 8.9 | 2.7 |
| Cathodic | 7.5–75 | 0.998 | −7.61 ± 0.14 | −31.1 ± 1.1 | 13 | 15.7 | 4.7 |

Supporting electrolyte was 0.1 mol dm$^{-3}$ acetate buffer pH 5.0, 20 s stirring between individual scans applied

*LOQ* limit of quantification, *LOD* limit of detection, *R* correlation coefficient

[a] Relative standard deviation (RSD) of ten times repeated measurement at the lowest concentration of LDR (linear dynamic range)

**Table 3** Peak potentials $E_p$, peak heights $I_p$ and their relative standard deviations (RSD) evaluated from DC and DP voltammograms of 5-nitroquinoline ($c = 1 \times 10^{-4}$ mol dm$^{-3}$) in 0.1 mol dm$^{-3}$ acetate buffer pH 5.0. Measured by BDD electrodes with B/C ratio in the range of 500–8000 ppm

| B/C ratio/ppm | DPV | | | DCV | | |
|---|---|---|---|---|---|---|
| | $E_p$/mV | $I_p$/nA | RSD/% | $E_p$/mV | $I_p$/nA | RSD/% |
| 500 | −561 | −579 ± 15 | 2.7 | −797 | −2502 ± 84 | 3.4 |
| 1000 | −498 | −255 ± 13 | 5.2 | −536 | −691 ± 53 | 7.2 |
| 2000 | −388 | −2065 ± 38 | 1.8 | −443 | −3616 ± 57 | 1.6 |
| 4000 | −438 | −1630 ± 40 | 2.5 | −510 | −3720 ± 52 | 1.4 |
| 8000 | −442 | −1589 ± 18 | 1.2 | −519 | −3581 ± 83 | 2.3 |

effect and RSD values of peak height were comparable with these when using stirring between individual scans, only stirring for 20 s was used to assure repeatable signals. For DC and DP voltammetry the RSD values of peak height were 6.5 and 0.5 % for cathodic pretreatment and 2.1 and 4.6 % for anodic pretreatment ($c = 1 \times 10^{-4}$ mol dm$^{-3}$, $n = 10$), respectively. For shorter times instability of electrode response was observed for all activation modes.

Parameters of the calibration straight lines for both types of pretreatment are given in Table 2. Better limits of detection in the $10^{-7}$ and $10^{-6}$ mol dm$^{-3}$ concentration range for DPV and DCV was obtained using anodic pretreatment, which is given by lower values of peak height repeatability for the lowest measurable concentration and higher value of the slope, i.e., parameters used for calculation of detection limit. Anodic pretreatment compared to cathodic one should be also preferred with respect to the extent of the linear dynamic range.

## Boron-doping level of BDD

Boron-doping level significantly affects the height of the peak and its potential, as summarized in Table 3 and shown in Fig. 6, where are depicted DC and DP voltammograms of $1 \times 10^{-4}$ mol dm$^{-3}$ solution of 5-nitroquinoline in 0.1 mol dm$^{-3}$ acetate buffer pH 5.0. Obviously, the peak height for electrodes with metallic type of conductivity (2000, 4000, and 8000 ppm) is comparable and significantly higher than for semiconductive BDD electrodes (500 ppm and 1000 ppm). Simultaneously, their peak potential is shifted to more positive values confirming the easier reduction of nitro group using 2000–8000 ppm electrodes. Further, favorable repeatability of peak height with RSD values ≤2.5 % for this set of electrodes was achieved. Among them, the 2000 ppm electrode exhibits additional favorable characteristics: low background current and negative shift in onset of supporting electrolyte caused by hydrogen evolution, which enables visualization of the reduction of the quinoline skeleton at the potential of about −910 mV; at the 4000 and 8000 ppm electrodes this signal is only insinuated.

Obviously, the electrodes with metallic type of conductivity perform similarly as in oxidation of benzophenone-3 [13], where the 2000 ppm electrode exhibited the highest slope of the linear calibration dependence. This electrode with the boron-doping level just above the semiconductive/metallic conductivity threshold seems favorable in terms of electroanalytical performance.

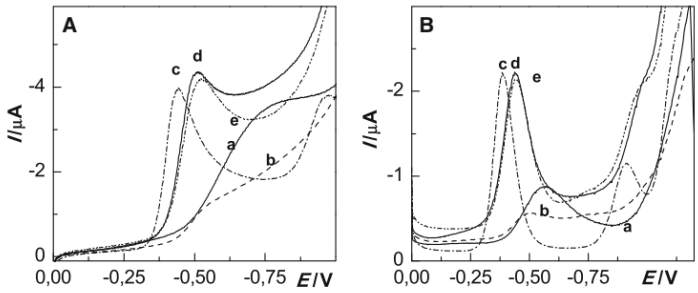


**Fig. 6** **A** DC and **B** DP voltammograms of 5-nitroquinoline ($c = 1 \times 10^{-4}$ mol dm$^{-3}$) in 0.1 mol dm$^{-3}$ acetate buffer pH 5.0 measured with BDD electrodes with different boron concentration (B/C ratio): (*a*) 500 ppm, (*b*) 1000 ppm, (*c*) 2000 ppm, (*d*) 4000 ppm, (*e*) 8000 ppm. Scan rate for DPV is 20 mV s$^{-1}$ and for DCV is 50 mV s$^{-1}$

## Conclusion

The voltammetric reduction of 5-nitroquinoline was elucidated at boron doped diamond (BDD) electrode in aqueous media of pH 2.0–12.0. The signal of the nitro group largely depends on the pH of the indifferent electrolyte, electrode pretreatment, activation between individual scans, and boron concentration of the BDD film electrode. In alkaline media, the four-electron reduction of the nitro to the hydroxylamino group occurs in two separated steps with the first one being a one electron reduction of the nitro group to the nitro-radical anion—a mechanism pathway previously recognized for 5-nitroquinoline at amalgam [38] electrodes or other nitro group containing aromatics at BDD electrodes [30]. Presence of oxygen in the measured solutions led to slight increase of peak heights and acceptable increase of its relative standard deviation. The detection limit for DPV achieved using optimized protocol, i.e. anodic pretreatment at +2.4 V for 5 min in 0.5 mol dm$^{-3}$ $H_2SO_4$ and 20 s stirring between individual scans assured limit of detection in the $10^{-7}$ mol dm$^{-3}$ concentration range, which is comparable with detection limits obtained at other solid electrode materials (compare in Table 1) including amalgam [38] and carbon film [44] electrodes. The nitro group reduction results in well-developed, observable signals at BDD films with metallic type of conductivity deposited at B/C ratio 2000–8000 ppm, but not using semiconductive films 500 and 1000 ppm. On the other hand, the reduction of the quinoline skeleton close to the onset of supporting electrolyte is well observable only at the 2000 ppm electrode. This might be connected with the increasing content of $sp^2$ impurities, existence of boron clusters [17, 50] and other factors influencing electron transfer and processes limiting the potential window when increasing boron-doping level.

To conclude, BDD electrodes seem to be good analytical alternative to determinations based on reduction of aromatic nitro group. For this purpose, highly doped BDD films are recommendable. The experimental data might be used for the development HPLC-ED method enabling separation and detection of nitro group containing aromatic compounds.

## Experimental

Stock solution of 5-nitroquinoline (99 %, Sigma-Aldrich, Czech Republic) was prepared by dissolving exact quantity in deionized water for final concentration of $1 \times 10^{-3}$ mol dm$^{-3}$. The experiments were carried out in Britton-Robinson (BR) buffer or 0.1 mol dm$^{-3}$ acetate buffer (pH 5.0) at laboratory temperature. BR buffers were prepared by mixing a solution of phosphoric, acetic and boric acid (concentration of each 0.04 mol dm$^{-3}$, all p.a., Lach-Ner, Czech Republic) with an appropriate amount of 0.2 mol dm$^{-3}$ sodium hydroxide solution. All solutions were prepared in deionized water (Millipore, Billerica, MA, USA). Other used chemicals were: acetic acid (Lach-Ner, Neratovice, Czech Republic), quinoline (Merck, Czech Republic). All measurements were performed using computer controlled Eco-Tribo Polarograph with PolarPro software (version 5.1, Eco-Trend Plus, Prague, Czech Republic) in a three electrode arrangement involving platinum wire auxiliary electrode and silver–silver chloride reference electrode (Ag|AgCl, 3 mol dm$^{-3}$ KCl) (both Elektrochemické detektory, Turnov, Czech Republic). As working electrodes served boron doped diamond electrodes with boron-doping level 500, 1000, 2000, 4000, and 8000 ppm (B/C ratio during microwave-plasma assisted chemical vapor procedure described in [13]).Obtained BDD films at Si wafers were placed in Teflon electrode body constructed in our laboratory [32] with geometric surface area of 5.72 mm$^2$ (disk diameter 2.7 mm). If not otherwise stated, the 4000 ppm films and 0.1 mol dm$^{-3}$ acetate buffer pH 5.0 as supporting electrolyte was used.

Differential pulse voltammetry was performed using the scan rate of 20 mV s$^{-1}$ with pulse amplitude −50 mV for 80 ms. Scan rate 50 mV s$^{-1}$ was used for DC voltammetry

and 100 mV $s^{-1}$ for cyclic voltammetry, if not otherwise stated.

The BDD electrode was pretreated in 0.5 mol $dm^{-3}$ sulfuric acid for 5 min with potential + 2.4 V before the measurement every day. During DP and DC voltammetry was BDD electrode activated for 20 s between each scan.

The influence of boron content was tested at 500–8000 ppm electrodes after anodic pretreatment or 5 min in 0.5 mol $dm^{-3}$ sulfuric acid at the potential of +2.4 V, 20 s stirring between individual voltammetric scans was applied. All measurements were carried out at laboratory temperature. The pH measurements were carried out by digital pH Meter 3510 (Jenway, UK) with combined glass electrode.

The solutions for measurements were prepared in 10 $cm^3$ volumetric flasks by measuring of proper volume of the 5-nitroquinoline stock solution and filling by BR buffer of the required pH or 0.1 mol $dm^{-3}$ acetate buffer pH 5.0 up to the mark. For DPV, the peak heights ($I_p$) were measured from the straight line connecting minima on both sides of the peak. In DCV they were measured from the line prolonging the voltammetric curve before the onset of the voltammetric signal of 5-nitroquinoline.

All calibration curves were measured in triplicate. The calibration dependences were processed using linear regression method. For voltammetric measurements, limits of detection (LOD) were calculated as the concentration of the analyte, which gave the signal equal to three times the standard deviation of peak heights estimated from ten consecutive measurements of the lowest measurable concentration.

**Acknowledgments** The research was financially supported by the Grant Agency of the Charles University in Prague (Project GAUK 684213) and Charles University in Prague (Project SVV).

## References

1. Fujishima A, Einaga Y, Rao TN, Tryk DA (2005) Diamond Electrochemistry. Elsevier, Amsterdam
2. Peckova K, Musilova J, Barek J (2009) Crit Rev Anal Chem 39:148
3. Musilova J, Barek J, Peckova K (2009) Chem Listy 103:469
4. Peckova K, Barek J (2011) Curr Org Chem 15:3014
5. Peckova-Schwarzova K, Zima J, Barek J (2015) Determination of Aromatic Hydrocarbons and Their Derivatives. In: Moretto LM, Kalcher K (eds) Electrochemical Analysis by Electrochemical Sensors and Biosensors. Springer, New York, p 931
6. Holt KB, Bard AJ, Show Y, Swain GM (2004) J Phys Chem B 108:15117
7. Hutton LA, Iacobini JG, Bitziou E, Channon RB, Newton ME, Macpherson JV (2013) Anal Chem 85:7230
8. Suffredini HB, Pedrosa VA, Codognoto L, Machado SAS, Rocha-Filho RC, Avaca LA (2004) Electrochim Acta 49:4021
9. Zavazalova J, Barek J, Peckova K (2013/2014) Boron Doped Diamond Electrodes in Voltammetry: New Designs and Applications (an Overview). In: Kalcher K, Metelka R, Švancara I, Vytřas K (eds), Sensing in Electroanalysis. University Press Centre, University of Pardubice, Pardubice, p 21
10. Zivcova ZV, Frank O, Petrak V, Tarabkova H, Vacik J, Nesladek M, Kavan L (2013) Electrochim Acta 87:518
11. Trouillon R, O'Hare D, Einaga Y (2011) Phys Chem Chem Phys 13:5422
12. Guinea E, Garrido JA, Rodriguez RM, Cabot PL, Arias C, Centellas F, Brillas E (2010) Electrochim Acta 55:2101
13. Zavazalova J, Prochazkova K, Schwarzova-Peckova K (2016) Anal Lett 49:80
14. Vosahlova J, Zavazalova J, Schwarzova-Peckova K (2014) Chem Listy 108:s270
15. Williams AW, Lightowl EC, Collins AT (1970) J Phys C: Solid State Phys 3:1727
16. Harfield JC, Toghill KE, Batchelor-McAuley C, Downing C, Compton RG (2011) Electroanalysis 23:931
17. Bernard M, Baron C, Deneuville A (2004) Diam Relat Mat 13:896
18. Yano T, Tryk DA, Hashimoto K, Fujishima A (1998) J Electrochem Soc 145:1870
19. Ernst S, Aldous L, Compton RG (2011) J Electroanal Chem 663:108
20. Vyskocil V, Barek J (2011) Curr Org Chem 15:3059
21. World Health Organization (2003) Selected Nitro- and Nitro-Oxy-Polycyclic Aromatic Hydrocarbons. WHO, Geneva
22. Musilova J, Barek J, Peckova K (2011) Electroanalysis 23:1236
23. Garbellini GS, Salazar-Banda GR, Avaca LA (2007) J Braz Chem Soc 18:1095
24. Pedrosa VA, Codognoto L, Machado SAS, Avaca LA (2004) J Electroanal Chem 573:11
25. Pedrosa VA, Suffredini HB, Codognoto L, Tanimoto ST, Machado SAS, Avaca LA (2005) Anal Lett 38:1115
26. Karaova J, Barek J, Schwarzova-Peckova K (2016) Anal Lett 49:66
27. Dejmkova H, Barek J, Zima J (2011) Int J Electrochem Sci 6:3550
28. Garbellini GS, Salazar-Banda GR, Avaca LA (2009) Food Chem 116:1029
29. Chuanuwatanakul S, Chailapakul O, Motomizu S (2008) Anal Sci 24:493
30. Juliao MSD, Almeida EC, La Scalea MA, Ferreira NG, Compton RG, Serrano SHP (2005) Electroanalysis 17:269
31. Juliao MSD, Ferreira EI, Ferreira NG, Serrano SHP (2006) Electrochim Acta 51:5080
32. Martins I, Canaes LD, Doretto KM, Rath S (2010) Electroanalysis 22:455
33. Yosypchuk O, Barek J, Vyskocil V (2012) Anal Lett 45:449
34. Cizek K, Barek J, Fischer J, Peckova K, Zima J (2007) Electroanalysis 19:1295
35. Laviron E, Vallat A, Meunier-Prest R (1994) J Electroanal Chem 379:427
36. Zuman P, Fijalek Z, Dumanovic D, Suznjevic D (1992) Electroanalysis 4:783
37. Peckova K, Barek J, Navratil T, Yosypchuk B, Zima J (2009) Anal Lett 42:2339
38. Jiranek I, Peckova K, Kralova Z, Moreira JC, Barek J (2009) Electrochim Acta 54:1939
39. Dar RA, Brahman PK, Tiwari S, Pitre KS (2012) Colloid Surf B-Biointerfaces 98:72
40. Gal M, Hromadova M, Pospisil L, Hives J, Sokolova R, Kolivoska V, Bulickova J (2010) Bioelectrochemistry 78:118
41. Pech J (1934) Collect Czech Chem Commun 6:126
42. Zhan XM, Liu LH, Gao ZN (2011) J Solid State Electrochem 15:1185

43. Geto A, Amare M, Tessema M, Admassie S (2012) Anal Bioanal Chem 404:525
44. Jiranek I, Rumlova T, Barek J (2010) Voltammetric Determination of 5-nitroquinoline at a Carbon Film Electrode. In: Navrátil T, Barek J (eds) XXX Modern Electrochemical Methods. BEST Servis, Usti nad Labem, Jetřichovice, p 93
45. Vyskocil V, Jiranek I, Danhel A, Zima J, Barek J, Wang J, Peckova K (2011) Collect Czech Chem Commun 76:1991
46. Armarego WL (1962) J Chem Soc:4094
47. Peckova K, Vrzalova L, Bencko V, Barek J (2009) Collect Czech Chem Commun 74:1697
48. Yosypchuk O, Karasek J, Vyskocil V, Barek J, Peckova K (2012) Sci World J, ID 231986
49. Salazar-Banda GR, Andrade LS, Nascente PAP, Pizani PS, Rocha RC, Avaca LA (2006) Electrochim Acta 51:4612
50. Azevedo AF, Baldan MR, Ferreira NG (2013) J Phys Chem Solids 74:599

## *Appendix VIII*

## Confirmation of participation

**1. Zavázalová J.**, Barek J., Pecková K.: Boron doped diamond electrodes in voltammetry: New designs and applications. An overview. In *Sensing in Electroanalysis*. Kalcher K., Metelka R., Švancara I., Vytřas K. (Eds.), **8** (2014) pp. 21-34, University Press Centre, Pardubice, Czech Republic.

Participation of Mgr. J. Zavázalová **~30 %**.

**2.** Schwarzová-Pecková K., Vosáhlová J., Barek J., Šloufová I., Pavlova E., Petrák V., **Zavázalová J.**: Influence of boron content on the morphological, spectral, and electroanalytical characteristic of anodically oxidized boron-doped diamond electrodes. *Electrochimica Acta* **243** (2017) 170-182.

Impact factor **5.116** (2017); participation of Mgr. J. Zavázalová **~50 %**.

**3.** Vosáhlová J., **Zavázalová J.**, Schwarzová-Pecková K.: Boron doped diamond electrodes: Effect of boron concentration on the determination of 2-aminobiphenyl. *Chemické Listy* **108** (2014) s270-s273.

Impact factor 0.272 (2014); participation of Mgr. J. Zavázalová **~30 %**.

**4. Zavázalová J.**, Dejmková H., Barek J., Pecková K.: Voltammetric and amperometric determination of mixtures of aminobiphenyls and aminonaphthalenes using boron doped diamond electrode. *Electroanalysis* **25** (2013) 253-262.

Impact factor 2.502 (2013); participation of Mgr. J. Zavázalová **~75 %**.

**5. Zavazalova J.**, Ghica M. E., Schwarzova-Peckova K., Barek J., Brett C. M. A.: Carbon-based electrodes for sensitive electroanalytical determination of aminonaphthalenes. *Electroanalysis* **27** (2015) 1556-1564.

Impact factor 2.471 (2015); participation of Mgr. J. Zavázalová **~75 %**.

**6. Zavazalova J.**, Prochazkova K., Schwarzova-Peckova K.: Boron-doped diamond electrodes for voltammetric determination of benzophenone-3. *Analytical Letters* **49** (2015) 80-91.

Impact factor 1.088 (2015); participation of Mgr. J. Zavázalová **~60 %**.

**7.** Vosáhlová J., **Zavázalová J.**, Petrák V., Schwarzová-Pecková K.: Factors influencing voltammetric reduction of 5-nitroquinoline at boron-doped diamond electrodes. *Monatshefte für Chemie* **147** (2016) 21-29.

Impact factor 1.282 (2016); participation of Mgr. J. Zavázalová **~20 %**.

I declare that the percentage of participation of Mgr. Jaroslava Zavázalová at the above given papers corresponds to the above given numbers.

Prague …….....

RNDr. Karolina Schwarzová, Ph.D.

## *Appendix IX*

## List of publications, presentations, achievements and grants

*Theses*

[1] **Zavazalova J.**: Amperometric detection in HPLC determination of oxidizable derivatives of polycyclic aromatic hydrocarbons. *Bachelor Thesis*, Charles University, Faculty of Science, Department of Analytical Chemistry, Prague 2009.

[2] **Zavazalova J.**: The electrochemical detection of amino derivatives of naphthalene and biphenyl using platinum electrodes. *Diploma Thesis*, Charles University, Faculty of Science, Department of Analytical Chemistry, Prague 2011.

*Journal publications*

[1] **Zavazalova J.**, Dejmkova H., Barek J., Peckova K.: Amperometric and spectrophotometric detection of aminobiphenyl and aminonaphthalene in HPLC. *Chemicke Listy* **105** (2011) S87-S89.

[2] **Zavazalova J.**, Dejmkova H., Barek J., Peckova K.: Voltammetric and amperometric determination of mixtures of aminobiphenyls and aminonaphthalenes using boron doped diamond electrode. *Electroanalysis* **25** (2013) 253-262.

[3] **Zavazalova J.**, Dejmkova H., Barek J., Peckova K.: Tubular and microcylindrical platinum electrodes for amperometric detection of aminobiphenyls and aminonaphthalenes in HPLC. *Electroanalysis* **26** (2014) 687-696.

[4] Vosahlova J., **Zavazalova J.**, Schwarzova-Peckova K.: Boron doped diamond electrodes: Effect of boron concentration on the determination of 2-aminobiphenyl. *Chemicke Listy* **108** (2014) S270-S273.

[5] **Zavazalova J.**, Ghica M. E., Schwarzova-Peckova K., Barek J., Brett C. M. A.: Carbon-based electrodes for sensitive electroanalytical determination of aminonaphthalenes. *Electroanalysis* **27** (2015) 1556-1564.

[6] **Zavazalova J.**, Prochazkova K., Schwarzova-Peckova K.: Boron-doped diamond electrodes for voltammetric determination of benzophenone-3. *Analytical Letters* **49** (2016) 80-91.

[7] Vosahlova J., **Zavazalova J.**, Petrak V., Schwarzova-Peckova K.: Factors influencing voltammetric reduction of 5-nitroquinoline at boron-doped diamond electrodes. *Monatshefte Fur Chemie* **147** (2016) 21-29.

[8] Schwarzova-Peckova K., Vosahlova J., Barek J., Sloufova I., Pavlova E., Petrak V., **Zavazalova J.**: Influence of boron content on the morphological, spectral, and electroanalytical characteristics of anodically oxidized boron-doped diamond electrodes. *Electrochimica Acta* **243** (2017) 170-182.

*Chapters in books*

[1] **Zavazalova J.**, Dejmkova H., Ramesova S., Barek J., Peckova K.: Amperometric and spectrophotometric detection of aminobiphenyls and aminonaphthalenes in HPLC. In *Sensing in Electroanalysis*. Vytřas K., Kalcher K. and Švancara I. (Eds.), **5** (2010) pp. 163-173, University of Pardubice, Pardubice.

[2] **Zavazalova J.**, Houskova L., Barek J., Zima J., Dejmkova H.: Determination of pesticide chlortoluron using HPLC with amperometric detection at a carbon paste electrode. In *Sensing in Electroanalysis*. Kalcher K., Metelka R., Švancara I. and Vytřas K. (Eds.), **7** (2012) pp. 293-300, University Press Centre, Pardubice, Czech Republic.

[3] **Zavazalova J.**, Barek J., Peckova K.: Boron doped diamond electrodes in voltammetry: New designs and applications. An overview. In *Sensing in Electroanalysis*. Kalcher K., Metelka R., Švancara I. and Vytřas K. (Eds.), **8** (2014) pp. 21-34, University Press Centre, Pardubice, Czech Republic.

*Oral presentations*

[1] Peckova K., Dejmkova H., **Zavazalova J.**, Barek J.: Arrangements of platinum electrodes in amperometric detectors for detection of hydroxy and amino derivatives of polycyclic aromatic hydrocarbons. *Modern Electrochemical Methods 2009*. Barek J. and Nesměrák K. (Eds.), **103** (2009) pp. s272-s272, Česká společnost chemická – Chemické listy, Prague, Czech Republic.

[2] Dejmkova H., Vysoka M., **Zavazalova J.**, Zima J., Barek J.: Electrochemical determination of propyl gallate on carbon paste electrode. *XXX. Modern Electrochemical Methods*. Navratil T. and Barek J. (Eds.), (2010) pp. 26-29, BEST Servis Ústí nad Labem, Jetřichovice, Czech Republic.

[3] Dejmkova H., Barek J., Dedik J., Janovcova M., Maixnerova L., Ramesova S., **Zavazalova J.**, Peckova K.: Nové možnosti amperometrické detekce aminoderivátů polycyklických aromatických uhlovodíků v HPLC. *63$^{th}$ Chemical Congress*, **7** (2011) pp. 71-72, Slovenská chemická spolocnost – ChemZi, Tatry, Slovakia.

[4] **Zavazalova J.**, Dejmkova H., Barek J., Peckova K.: Voltammetric determination of amino derivatives of naphthalenes using boron-doped diamond film electrode. *XXXII. Modern Electrochemical Methods*. Navratil T. and Fojta M. (Eds.), (2012) pp. 159-162, BEST Servis Ústí nad Labem, Jetřichovice, Czech Republic.

[5] **Zavazalova J.**, Barek J., Peckova K.: Utilization of boron-doped diamond thin film electrode in electroanalysis of selected derivatives of amino derivatives of polycyclic aromatic hydrocarbons. *8$^{th}$ International Student Conference 'Modern Analytical Chemistry'*. Nesměrák K. (Ed.), (2012) pp. 41-44, Charles University in Prague, Prague, Czech Republic.

[6] **Zavazalova J.**, Ghica M. E., Barek J., Peckova K., Brett C. M. A.: Voltammetric determination of selected aminonaphthalenes at different electrode surfaces. *9th International Students Conference 'Modern Analytical Chemistry'*. Nesměrák K. (Ed.), (2013) pp. 115-116, Charles University in Prague, Prague, Czech Republic.

[7] Vosahlova J., **Zavazalova J.**, Peckova K.: Vliv koncentrace bóru na elektrochemické vlastnosti bórem dopovaných diamantových elektrod pro elektroanalýzu. *15th Student Scientific Conference*. Hornacek M. (Ed.), (2013) pp. 88-89, Slovak University of Technology, Bratislava, Slovakia.

[8] Vosahlova J., **Zavazalova J.**, Peckova K.: Bórem dopované diamantové elektrody: Vliv koncentrace bóru na stanovení 2-aminobifenylu. *17th annual competition "O cenu firmy Merck 2014"*. Barek J. and Vyskocil V. (Eds.), (2014) pp. 161-167, Česká společnost chemická – Chemické listy, Pardubice, Czech Republic.

[9] Nezbedova M., **Zavazalova J.**: Studium vlastností borem dopované diamantové elektrody v přítomnosti vybraných surfaktantů. *Studentská vědecká konference – Jsem mladý vědec!* (2014), Národní technická knihovna v Praze, Praha, Česká republika.

[10] **Zavazalova J.**, Prochazkova K., Nezbedova M., Peckova K.: Voltammetric determination of benzophenone-3 at boron-doped diamond electrode. *XXXIV. Modern Electrochemical Methods*. Navratil T., Fojta M. and Peckova K. (Eds.), (2014) pp. 242-245, Srsenova Lenka-Best Servis Ústí nad Labem, Jetřichovice, Czech Republic.

[11] Benesova L., Hammer P., Vosahlova J., **Zavazalova J.**, Peckova K.: Electrochemical behavior of oxygen-terminated boron-doped diamond electrodes in different electrolyte media. *XXXIV. Modern Electrochemical Methods*. Navratil T., Fojta M. and Peckova K. (Eds.), (2014) pp. 19-22, Srsenova Lenka-Best Servis Ústí nad Labem, Jetřichovice, Czech Republic.

[12] Peckova K., **Zavazalova J.**, Benesova L., Sloufova I., Vosahlova J., Barek J.: Oxygen-terminated boron-doped diamond electrodes in electroanalysis of biologically active organic compounds. *15th International Conference on Electroanalysis – ESEAC 2014*, (2014) p. 79, International Conference on Electroanalysis, Malmo, Sweden.

[13] **Zavazalova J.**, Prochazkova K., Nezbedova M., Peckova K.: Utilization of boron-doped diamond electrode in electroanalysis of benzophenone-3. *10th International Student Conference 'Modern Analytical Chemistry'*. Nesměrák K. (Ed.), (2014) pp. 54-55, Charles University in Prague, Prague, Czech Republic.

[14] Prochazkova K., **Zavazalova J.**, Schwarzova K.: Stanovení benzofenonu-3 na borem dopované diamantové filmové elektrodě. *16th Student Scientific Conference*. Bakosova M., Hornacek M. and Oravec J. (Eds.), (2014) pp. 17-18, Slovak University of Technology Bratislava, Slovakia.

[15] Vosahlova J., **Zavazalova J.**, Petrak V., Schwarzova-Peckova K.: Boron-doped diamond electrodes in electroanalysis of reducible organic compounds. *XXXV. Modern Electrochemical Methods*. Navratil T., Fojta M. and Schwarzova K. (Eds.), (2015)

pp. 275-279, Srsenova Lenka-Best Servis Ústí nad Labem, Jetřichovice, Czech Republic.

*Poster presentation*

[1] Dejmkova H., Maixnerova L., **Zavazalova J.**, Barek J., Peckova K.: Ampérometrická detekce genotoxických aminoderivátů polycyklických aromatických uhlovodíků s využitím platinových a bórem dopovaných diamantových elektrod. *62th Chemical Congress*, **104** (2010) p. 460, Česká společnost chemická – Chemické listy, Pardubice, Czech Republic.

[2] Dejmkova H., **Zavazalova J.**, Barek J., Peckova K.: Determination of aminobiphenyles and aminonaphtalenes using HPLC with amperometric detection on platinum tubular electrode. *Electrochem 2010: Electrochemistry and Sustainability*, (2010) p. 12, Society of Chemical Industry, Telford, United Kingdom.

[3] **Zavazalova J.**, Dejmkova H., Barek J., Ramesova S., Peckova K.: Ampérometrická detekce genotoxických aminoderivátů polycyklických aromatických uhlovodíků v HPLC s využitím platinového mikrocylindrického detektoru. *63th Chemical Congress*, **7** (2011) p. 174, Slovenská chemická spolocnost – ChemZi, Tatry, Slovakia.

[4] **Zavazalova J.**, Dejmkova H., Barek J., Peckova K.: Voltammetric and amperometric determination of mixtures of aminobiphenyls and aminonaphthalenes using boron-doped diamond film electrodes. *14th International Conference on Electroanalysis – ESEAC 2012,* (2012) p. 175, National Institute of Chemistry, Portorož, Slovenia.

[5] **Zavazalova J.**, Houskova L., Zima J., Barek J., Dejmkova H.: The application of HPLC with electrochemical detection for the determination of pesticide chlorotoluron. *4th EuCheMS Chemistry Congress*, **106** (2012) p. s1158, Česká společnost chemická – Chemické listy, Prague, Czech Republic.

[6] Vosahlova J., Fahnrichova B., **Zavazalova J.**, Petrak V., Sloufova I., Barek J., Peckova K.: Effect of doping level on electrochemical performance of boron-doped diamond electrodes in electroanalysis of organic compounds. *The XVII European Conference on Analytical Chemistry EUROANALYSIS,* (2013), Warsaw, Poland.

[7] Vosahlova J., **Zavazalova J.**, Sloufova I., Petrak V., Barek J., Peckova K.: Influence of boron concentration on electroanalytical performance of anodically oxidized boron-doped diamond electrodes. *International Conference on Diamond and Carbon Materials,* (2013), Riva del Garda, Italy.

[8] **Zavazalova J.**, Vosahlova J., Hammer P., Peckova K.: Boron Doped Diamond Electrode: Influence of Boron Doping Level on Potential Window and Determination of Oxidizable Organic Compound. *15th International Conference on Electroanalysis – ESEAC 2014,* (2014) p. 240, International Conference on Electroanalysis, Malmo, Sweden.

[9] Benesova L., Hammer P., **Zavazalova J.**, Peckova K.: Elektrochemická oxidace vybraných fytosterolů na bórem dopovaných diamantových elektrodách. *XIII. konferencia s medzinárodnou účasťou Súčasný stav a perspektívy analytickej chemie v praxi*. Hrouzkova S. and Majek P. (Eds.), (2014) pp. 118-119, Slovak University of Technology Bratislava, Slovakia.

[10] **Zavazalova J.**, Vosahlova J., Prochazkova K., Sloufova I., Schwarzova-Peckova K.: Comparison of electrochemical and spectral characteristics of laboratory-made and commercially available boron-doped diamond electrodes with different boron content. *The XVIII European Conference on Analytical Chemistry EUROANALYSIS*, (2015) p. 226, Bordeaux, France.